



Norwegian University of
Science and Technology

Long Span Network Arch Bridges in Timber

Morten Eilertsen
Dag Erik Haddal

Civil and Environmental Engineering (2 year)

Submission date: June 2016

Supervisor: Kjell A Malo, KT

Co-supervisor: Johannes Veie, Statens Vegvesen
Anna W Ostrycharczyk, KT

Norwegian University of Science and Technology
Department of Structural Engineering

Pretext

This master thesis is the final assignment after a two-year master's degree programme in Civil and Environmental Engineering. The thesis is the result of 20 weeks of work and is rewarded with 30 ECTS credits to each student. The thesis is written for the Department of Structural Engineering at the Norwegian University of Science and Technology (NTNU), and in cooperation with the Norwegian Public Roads Administration (NPRA)

The authors had no previous experience with designing bridges and had previously not modelled anything more than a cantilever beam in Abaqus. Therefore, most of the time has been spent on immersing our self in literature and bridge standards, and the design of the bridges in Abaqus.

We would like to express our deepest thanks and sincere appreciation to our principal supervisor Prof. Kjell A. Malo from the department of structural engineering at NTNU, for all the advice and support during the study.

We would like to express our gratitude to our advisor Johannes Veie from the NPRA, for taking his time to help us, and for supplying us with much of the data needed to carry out the research.

Acknowledgement goes out to Anna W. Ostrycharczyk, for all her previous work with the numerical model and giving us a running start with Abaqus.

Finally we would like to direct our gratitude to all of the participants from the construction industry that has provided us with cost estimates and useful information.

Abstract

For years, the reduction in greenhouse gas emissions have been a global goal, and in the recent years this has led to an increased focus on emissions from the construction industry as well. With timber being an environmental-friendly building material, the focus on the environment has led to the construction of a number of minor timber bridges in Norway the past years.

This master thesis looks at the possibility of constructing long span network arch bridges in glue-laminated timber. The thesis presents two structural alternatives and compare these with a network arch bridge in steel and concrete, Driva Bridge. The primary focus has been on the structures stability, cost and feasibility. The bridge span is 111 meters for all three bridges.

Alternative 1: A network arch bridge without wind bracing between arches. Instead, the bridge has hangers with an out-of-plane angle relative to the arch to create sideways stability. One of the reasons for this is to avoid connections on the side of the arches, which are more vulnerable for weather damage. The arches have a massive glulam cross-section with moment resistant splice joints. The arches cross-section is $1600 \times 850 \text{ mm}^2$. The hangers are connected to the transverse beams, thus having an equidistant distribution on the lower chord. The transverse steel beams support the stress laminated timber deck. The bridge has no ties, and is therefore relying on the foundation to absorb the horizontal forces at the support.

Alternative 2: A network arch bridge with the same design as Driva Bridge. The bridge has glue-laminated K-shaped wind bracings for sideways stability. The arches have a massive glulam cross-section varying from $1100 \times 1100 \text{ mm}^2$ to $850 \times 850 \text{ mm}^2$. The bridge deck is the same as for alternative 1. The transverse beams and the hangers are connected to box-profile steel ties. The hangers have an equidistant distribution on the arch.

Structural analyses has been carried out on numerical models in the FEM-software Abaqus CAE, and Focus Konstruksjoner. Design checks have been carried out after relevant Eurocodes and design manuals.

Rough cost estimates have been made on the bridge alternatives to find out if they are cost competitive with Driva Bridge. The cost data used are based on previous projects, actual costs on Driva Bridge and budget prices provided from manufacturers.

Sammendrag

I årevis har det vært et globalt fokus på klimagassutslipp, og dette har ført til et stadig økt fokus på utslipp også fra bygge bransjen. Tre er et miljø- og klimavennlig byggemateriale, noe som har ført til at en hel rekke mindre trebroer har blitt bygget i Norge de senere årene.

I denne masteroppgaven er det sett på muligheten for å bygge nettverksbuebruer i limtre ved lengre spenn. Denne oppgaven presenterer to konstruktive løsninger, og sammenligner disse opp mot en nettverksbuebru i stål og betong, Driva bru. Oppgavens hovedfokus omhandler strukturell stabilitet, kostnad og gjennomførbarhet. Bruspennet på bruene er 111 meter.

Alternativ 1: En nettverksbuebru uten vindfagverk mellom buene. I stedet for vindfagverk har bruene hengestag med vinkler orientert ut av planet som sørger for sideveis stabilitet. Med denne løsningen unngår man innfestninger på buenes sider, som er et utsatt punkt for fuktinntrengninger på trebruer. Buene er av massivt limtre med en dimensjon på 1600x850 mm², og sammensatt med momentstive skjøter. Hengerstagene er festet til tverrbjelkene slik at avstanden er jevnt fordelt nede ved dekket. Tverrbjelker danner opplegg for ett spennlaminert limtredekke. Konstruksjonen har ikke strekkbånd mellom buenes ender, og er derfor avhengig av at fundamentene tar horisontale krefter.

Alternativ 2: En nettverksbuebru med samme utforming som Driva bru. Brua har K-fagverk av limtre som for sideveis stabilitet. Buene er av massivt limtre med et tverrsnitt som varierer fra 1100x1100 mm² til 850x850 mm². Brudekket er utført som ved alternativ 1. Tverrbjelker og hengestag er festet til strekkbåndene utformet som bokstverrsnitt spent mellom buenes ender. Hengerstagene er festet med fast avstand langs buene.

Konstruksjonsanalyser er utført på numeriske modeller i FEM-programmet Abaqus CAE, og Focus Konstruksjon. Prosjektering er utført etter relevante Eurokoder og håndbøker.

Grove kostnadsoverslag er utført for å undersøke om alternativene er prismessig konkurransedyktig, sammenlignet med Driva bru. De estimerte prisene er basert på tidligere prosjekter, anbudspriser på Driva bru og tilsendt pristilbud fra leverandører.

Index

PRETEXT	I
ABSTRACT	III
SAMMENDRAG	V
INDEX	7
LIST OF FIGURES	11
LIST OF TABLES	15
1 INTRODUCTION	1
1.1 Background.....	1
1.2 Purpose and thesis question	2
1.3 Limitations.....	2
2 THEORY	3
2.1 The network arch.....	3
2.1.1 Hanger arrangement.....	4
2.2 Timber in network arch bridges.....	5
2.3 Vibration.....	6
3 DESCRIPTION OF DRIVA BRIDGE	7
4 BRIDGE ALTERNATIVES	9
4.1 Bridge alternative 1.....	9
4.1.1 General.....	9
4.1.2 Glulam arch	10
4.1.3 Boundary conditions and joints.....	10
4.1.4 Hangers.....	13
4.1.5 Bridge deck.....	14
4.1.6 Wearing pavement.....	17
4.1.7 Transverse beams.....	18
4.1.8 Guardrail	19
4.1.9 Weather protection.....	20
4.2 Bridge alternative 2.....	22
4.2.1 General.....	22
4.2.2 Glulam arch	22
4.2.3 Wind Bracing	23
4.2.4 Boundary conditions and joints.....	23
4.2.5 Hangers.....	25
4.2.6 Bridge deck.....	26

4.2.7	<i>Wearing pavement</i>	26
4.2.8	<i>Tie</i>	26
4.2.9	<i>Transverse beam</i>	27
4.2.10	<i>Guardrail</i>	27
4.2.11	<i>Weather protection</i>	28
5	FINITE ELEMENT ANALYSIS	28
5.1	Shell elements	28
5.2	Beam elements	29
5.3	Truss elements	29
5.4	Material properties.....	29
5.5	Results from Abaqus.....	30
6	LOADS	31
6.1	Dead load.....	31
6.1.1	<i>Super dead load</i>	32
6.2	Variable loads	33
6.2.1	<i>Temperature load</i>	33
6.2.2	<i>Wind load</i>	34
6.2.3	<i>Traffic load</i>	35
6.2.4	<i>Earthquake</i>	37
6.2.5	<i>Load events for hangers</i>	38
6.3	Load models	40
6.3.1	<i>Ultimate limit state</i>	40
6.3.2	<i>Service limit state</i>	40
6.3.3	<i>Progressive limit state</i>	42
7	COST	42
8	FEASIBILITY	43
8.1	Construction of Driva Bridge	44
8.2	Other ways of erecting the network arch	45
8.3	Construction of Bridge 1.....	47
8.4	Construction of Bridge 2.....	48
9	RESULTS.....	48
9.1	Service Limit State	48
9.2	Stability.....	50
9.2.1	<i>Driva Bridge</i>	51
9.2.2	<i>Bridge 1</i>	53
9.2.3	<i>Bridge 2</i>	64
9.3	Utilization results.....	70

9.3.1	<i>Bridge 1</i>	71
9.3.2	<i>Bridge 2</i>	79
9.4	Hanger Relaxation	91
9.5	Cost results	92
10	REMEDIES	94
10.1	Bridge 1	94
10.1.1	<i>U-shape stiffening frame</i>	94
10.1.2	<i>Lowered arch rise</i>	95
10.1.3	<i>Increasing joint stiffness</i>	97
10.1.4	<i>Trusses between arches in the top</i>	97
10.2	Bridge 2	98
11	DISCUSSION	99
11.1	Stability	99
11.2	Cost	100
11.3	Feasibility	100
12	CONCLUSION	101
13	FURTHER WORK	102
	CITATIONS	103
	APPENDIX	1

List of figures

Figure 1.1 Driva Bridge [4]..... 2

Figure 2.1 Tied arch with network configuration of hangers [7] 3

Figure 2.2 Example of optimal hanger arrangement [13] 5

Figure 2.3 Steien Bridge [3] 6

Figure 3.1: Driva Bridge [18]..... 7

Figure 3.2 Hanger arrangement on Driva Bridge [18] 7

Figure 3.3 Arch dimensions. Driva Bridge 8

Figure 3.4 Transverse beam and concrete deck. Driva Bridge [18]..... 8

Figure 4.1 Bridge alternative 1 9

Figure 4.2 Moment resisting arch splice joint..... 11

Figure 4.3 End support, impost hinge. 12

Figure 4.4 Boundary conditions. Bridge 1 12

Figure 4.5 Arch-hanger connection. Bridge 1 13

Figure 4.6 Hanger angles. Bridge 1 14

Figure 4.7 Bridge deck 14

Figure 4.8 Vertical displacement on deck. LM1 Eq 1b 15

Figure 4.9 Largest strain in the deck. LM1 Eq 1b..... 15

Figure 4.10 Tensioning system, bridge deck..... 16

Figure 4.11 Bridge deck end support [16]..... 16

Figure 4.12 Solution on membrane layer at height transition 18

Figure 4.13 Transverse steel beam 19

Figure 4.14 Side mounted guardrail 20

Figure 4.15 Structural weather protection on the arch [24] 21

Figure 4.16 Bridge alternative 2..... 22

Figure 4.17 Rotation of the arch relative to a vertical plane. Bridge 2 23

Figure 4.18 Boundary conditions. Bridge 2 24

Figure 4.19 Arch support connection. Bridge 2 24

Figure 4.20 Hanger arrangement. Bridge 2..... 25

Figure 4.21 Arch-hanger connection. Bridge 2..... 25

Figure 4.22 Tie-hanger connection. Bridge 2 26

Figure 4.23 Steel tie dimensions. Bridge 2 26

Figure 4.24 Transverse beam. Bridge 2 27

Figure 4.25 Cladding on top surfaces [16]	28
Figure 5.1 Euler buckling load, combined with global buckling factor.....	31
Figure 6.1 Dead load. Bridge 1	32
Figure 6.2 Dead load. Bridge 2	32
Figure 6.3 Maximum and minimum temperature with a return period of 50 year [39].....	33
Figure 6.4 Design temperature	34
Figure 6.5 LM1 traffic load distribution. From appendix C.	35
Figure 6.6 Placement and load magnitude of LM1 [42]	36
Figure 6.7 Axle load placement LM2. [42].....	37
Figure 6.8 Seismic zones, south Norway (a_{g40Hz}) [43].....	38
Figure 6.9 Traffic load during hanger change.....	39
Figure 6.10 Removed hangers on Bridge 1	39
Figure 6.11 Removed hangers on Bridge 2.....	40
Figure 8.1 Transport of Driva Bridge [46].....	45
Figure 8.2 Åkvik Sound Bridge lifted in place by a floating crane [47].....	46
Figure 8.3 Erection procedure for a network arch using pontoon [9].....	46
Figure 8.4 Erection of the arches with mobile cranes [47]	47
Figure 8.5 Erection of the arches with mobile cranes on temporary fillings [47].....	47
Figure 9.1 The first four modes of free vibration. Bridge 1	49
Figure 9.2 The first four modes of free vibration. Bridge 2.....	50
Figure 9.3 Buckling analysis, ULS gravity. Driva Bridge[18]	51
Figure 9.4 Buckling analysis, ULS gravity and UDL. Driva Bridge [18].	52
Figure 9.5 Buckling analysis, ULS gravity. Bridge 1	53
Figure 9.6 Buckling analysis, ULS LM1 Eq 1b. Bridge 1	54
Figure 9.7 Buckling analysis, ULS LM1 Eq 1a, half load. Bridge 1	55
Figure 9.8 Buckling analysis, PLS gravity, removed hangers. Bridge 1	56
Figure 9.9 Buckling analysis, PLS LM1, removed hangers. Bridge 1.....	57
Figure 9.10 Buckling analysis, ULS gravity, hanger change. Bridge 1	58
Figure 9.11 Buckling analysis, ULS LM1 Eq 1a, hanger change. Bridge 1	59
Figure 9.12 Buckling analysis, ULS gravity, with wind trusses. Bridge 1	60
Figure 9.13 Buckling analysis, ULS LM1 Eq 1b, with wind trusses. Bridge 1	61
Figure 9.14 Buckling analysis, ULS gravity, 14m rise of arch. Bridge 1	62
Figure 9.15 Buckling analysis, ULS LM1 Eq 1b. Bridge 1, 14m rise of arch.....	63
Figure 9.16 Buckling analysis, ULS gravity. Bridge 2	64

Figure 9.17 Buckling analysis, ULS LM4 Eq 4b. Bridge 2	65
Figure 9.18 Buckling analysis, ULS LM4 Eq 4b, half load. Bridge 2	66
Figure 9.19 Buckling analysis, ULS LM1 Eq 1a, hanger change. Bridge 2	67
Figure 9.20 Buckling analysis, PLS LM1 Eq 1a, removed hangers. Bridge 2	68
Figure 9.21 Buckling analysis, ULS Gravity, removed wind bracing. Bridge 2	69
Figure 9.22 Utilization plot arch 1, full load. Bridge 1	71
Figure 9.23 Utilization plot arch 2, full load. Bridge 1	72
Figure 9.24 Utilization plot arch 1, half load. Bridge 1	73
Figure 9.25 Utilization plot arch 2, half load. Bridge 1	74
Figure 9.26 Utilization plot arch 1, hanger change. Bridge 1	75
Figure 9.27 Utilization plot arch 2, hanger change. Bridge 1	76
Figure 9.28 Utilization plot arch 1, hanger removal. Bridge 1	77
Figure 9.29 Utilization plot arch 2, hanger removal. Bridge 1	78
Figure 9.30 Utilization plot arch 1, full load. Bridge 2	79
Figure 9.31 Utilization plot arch 2, full load. Bridge 2	80
Figure 9.32 Utilization plot tie 2, full load. Bridge 2	81
Figure 9.33 Utilization plot arch 1, half load. Bridge 2	82
Figure 9.34 Utilization plot arch 2, half load. Bridge 2	83
Figure 9.35 Utilization plot Tie 2, half load. Bridge 2	84
Figure 9.36 Utilization plot Arch 1, hanger change. Bridge 2	85
Figure 9.37 Utilization plot Arch 2, hanger change. Bridge 2	86
Figure 9.38 Utilization plot Tie 2, hanger change. Bridge 2	87
Figure 9.39 Utilization plot Arch 1, hanger removal. Bridge 2	88
Figure 9.40 Utilization plot Arch 2, hanger removal. Bridge 2	89
Figure 9.41 Utilization plot Tie 1, hanger removal. Bridge 2	90
Figure 9.42 The lowest occurring hanger forces with half load. Bridge 1	91
Figure 9.43 The lowest occurring hanger forces with half load. Bridge 2	91
Figure 10.1 U-frame illustration	95
Figure 10.2 U-frame. Comparison in out-of-plane stability	95
Figure 10.3 Wind trusses. Bridge 1	97

List of tables

Table 4.1 Transverse beam, displacement and utilization 19

Table 5.1 Material properties for timber parts 30

Table 5.2 Material properties for the remaining parts..... 30

Table 6.1 Super dead loads 33

Table 6.2 Characteristic wind load..... 35

Table 6.3 Load models for ULS STR/GEO - set B..... 41

Table 6.4 Load models for SLS - frequent load..... 41

Table 6.5 load models for PLS - accidental load 42

Table 7.1 Hanger parameters used for cost estimates 43

Table 8.1 Self-weight for parts and assemblies..... 44

Table 9.1 Results from vertical and horizontal displacement analyses..... 49

Table 9.2 Description of equations used in design check for glulam parts..... 70

Table 9.3 Utilization arch 1, full load. Bridge 1 71

Table 9.4 Utilization arch 2, full load. Bridge 1 72

Table 9.5 Utilization arch 1, half load. Bridge 1 73

Table 9.6 Utilization arch 2, half load. Bridge 1 74

Table 9.7 Utilization arch 1, hanger change. Bridge 1 75

Table 9.8 Utilization arch 2, hanger change. Bridge 1 76

Table 9.9 Utilization arch 1, hanger removal. Bridge 1 77

Table 9.10 Utilization arch 2, hanger removal. Bridge 1 78

Table 9.11 Utilization arch 1, full load. Bridge 2 79

Table 9.12 Utilization arch 2, full load. Bridge 2 80

Table 9.13 Utilization Tie 1 & 2, full load. Bridge 2..... 80

Table 9.14 Utilization K-Truss diagonal, full load. Bridge 2 81

Table 9.15 Utilization K-Truss transverse, full load. Bridge 2 81

Table 9.16 Utilization arch 1, half load. Bridge 2..... 82

Table 9.17 Utilization arch 2, half load. Bridge 2..... 83

Table 9.18 Utilization Tie 1 & 2, half load. Bridge 2 83

Table 9.19 Utilization K-Truss diagonal, half load. Bridge 2..... 84

Table 9.20 Utilization K-Truss transverse, half load. Bridge 2 84

Table 9.21 Utilization Arch 1, hanger change. Bridge 2..... 85

Table 9.22 Utilization Arch 2, hanger change. Bridge 2..... 86

Table 9.23 Utilization Tie 1 & 2, hanger change. Bridge 2 87

Table 9.24 Utilization K-Truss diagonal, hanger change. Bridge 2.....	87
Table 9.25 Utilization K-Truss transverse, hanger change. Bridge 2	87
Table 9.26 Utilization Arch 1, hanger removal. Bridge 2.....	88
Table 9.27 Utilization Arch 2, hanger removal. Bridge 2.....	89
Table 9.28 Utilization Tie 1&2, hanger removal. Bridge 2	89
Table 9.29 Utilization K-Truss diagonal, hanger removal. Bridge 2.....	90
Table 9.30 Utilization K-Truss transverse, hanger removal. Bridge 2	90
Table 9.31 cost estimate - bridge deck.....	92
Table 9.32 cost estimate - network arch - bridge 1	92
Table 9.33 Cost estimate - network arch - Bridge 2.....	93
Table 10.1 Effects of reduced rise of arch, LM1 Eq b.....	96
Table 10.2 Effects of reduced rise of arch, Gravity	96
Table 10.3 Effects of increased joint stiffness	97
Table 10.4 Effects of wind trusses on bridge 1	98
Table 10.5 Results after removing four K-shaped wind trusses	99

1 Introduction

1.1 Background

For years, the reduction in greenhouse gas emissions have been a global goal, and in the recent years this has led to an increased focus on emissions from the construction industry as well. It is well known that the production of steel and concrete contribute to large emissions of CO₂ and other greenhouse gases, which has led to an increased focus on timber as a building material. Timber is an environmental-friendly building material which Norway have good access to, and the increased usage of this resource will create employment and increased activity across the country [1].

As a result of an increased focus on green materials, the Norwegian Public Road Administration (NPRA) have decided to use timber constructions on a number of bridge projects during the recent years [2]. This have led to the following question:

“How does glulam Network Arch Bridges perform with long spans”

At the same time, The Norwegian University of Science and Technology (NTNU) has an ongoing research project regarding glulam network arch bridges. A new structural concept, which has not yet been compared in performance against other bridges.

This thesis is a result of the collaboration between the department of structural engineering at NTNU and NPRA.

1.2 Purpose and thesis question

In order to say something about the performance of glulam bridges with long spans, and continue the work on the concept bridge, the thesis will compare two glulam bridges with Driva Bridge, see Figure 1.1. Driva Bridge is a network arch bridge in steel and concrete. The span is 111 meters, 25% longer than the longest main span on a timber bridge today [3].



Figure 1.1 Driva Bridge [4]

The two bridge alternatives will be designed after Eurocodes and the manuals developed by the NPRA. After the two bridges are designed, they will be compared against Driva Bridge in:

- Stability
- Cost
- Feasibility

Will the timber bridges be as stable as the one in steel and concrete when the span is increased to 111 meters? Will the timber bridges be competitive when it comes to cost? Are the timber bridges possible to construct in a practical way, and create a robust structure? These questions will be covered and answered throughout the thesis.

1.3 Limitations

Because of the relative short time available, the thesis does not include design of foundations or end supports, or the possibility of settlements. Instead, boundary conditions are assumed, and simple sketches are provided that show the intention or ideas of the design.

Detailed joint design on the arches are also excluded, because the type of arch splice joint described later on is under development and is still undergoing experiments in the lab. Joint design on the wind bracing is excluded as well.

Connections between the deck and the transverse beam, fatigue and dynamic analyses are not covered. Design checks on the end-beams has not been carried out in this thesis.

2 Theory

2.1 The network arch

Network arch bridges are tied arches with inclined hangers. The hangers need to cross at least two other hangers that are inclined in the opposite direction, for it to be called a network arch [5]. Compared with conventional bridges, the network arch bridge usually saves more than half the amount of steel weight [6].

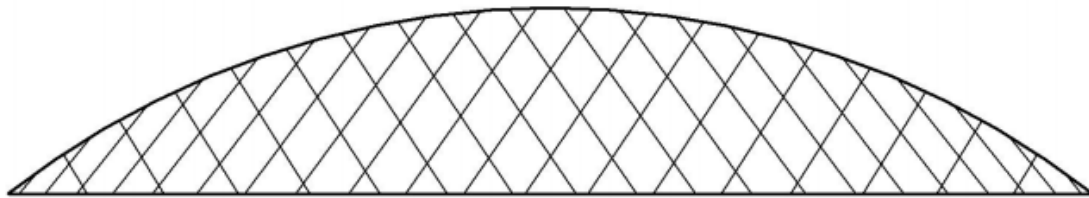


Figure 2.1 Tied arch with network configuration of hangers [7]

The network arch works as a simply supported beam, where the arch is the compressive flange, the tie the tensile flange and the hangers are the web. The characteristic hanger orientation connect the arch and tie at small intervals, leading to small bending moments [8].

The axial force in the arch and tie are inversely proportional with the distance between them. In tied arches, aesthetic reasons limit this distance, but what is considered aesthetic varies from country to country [9]. German arch bridges are usually built with a rise of the arch about 15% of the span, two American bridges have a rise of 20% and most Japanese network arches lie in between [10].

Modern arches are slender and light, and offer the opportunity of graceful arch forms. The disadvantage to slenderness and lightness is that the arch by itself, if not restrained, is usually not sufficiently stable under the required design loads. Because the arch is under high compression, it is prone to buckling in both in-plan and out-of-plane directions [11]. In the network arch, the hangers, being spread so evenly along the arch, offers great in-plane stiffness. Provided transversal stiffening is in place, usually in form of bracing between the arches [11], the buckling stress in the network arch is high [8]. The described reduction of local moments combined with a high buckling safety, opens the door for the design of extremely slender structures [5].

Live load placed on one side of the span can make hangers relax, causing significant increase in bending moments. Effectively, the result of multiple relaxed hangers, is that part of the bridge will now act as a tied arch with one set of hangers [8]. However, with moderate loading, the maximum stress will be smaller, because the axial force from partial loading is smaller. Tveit [8] showed that in order to get the same maximum stress in the arch with a partly loaded span, the live load had to equal 61% of the dead load. Bell [12] expresses another concern about relaxed hangers. “hanger buckling” caused by noticeable shortening can cause hangers to “flap” with unacceptable amplitudes. The best way to prevent this is to “pre-stress” the hangers, with the self-weight of the bridge deck.

2.1.1 Hanger arrangement

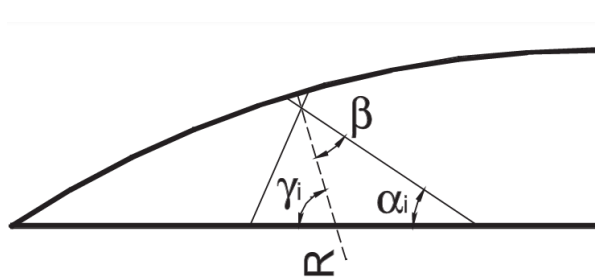
To use the static advantages of the network arch, the arrangement of the hangers is very important [13]. The optimal arrangement is dependent on several parameters [9, 13]:

- Span of the bridge
- Number of hangers and the associated distance between them
- Rise of the arch
- Slope of the hangers
- Ratio of live load to dead load
- Size of concentrated load compared to size of evenly distributed live load,
- Length of concentrated live load
- Curvature of the arch.

With a smaller angle between the hanger and the lower chord, the hanger’s tendency to relax is reduced, and thus bending due to relaxation is reduced. The smaller angle with the chords would however, increase bending due to concentrated loads [8].

Hangers distributed evenly along the arch, will in a normal network arch, give the smallest buckling length in the arch and the smallest bending moments due to curvature of the arch.

Given a bridge span between 100 meters and 125 meters, with the number of hangers ranging from 36 to 48 placed equidistant along the arch, Teich [13] found the optimal hanger arrangement to be one with a radial distribution. Meaning that each hanger has a fixed angle β , to the arch radius, see Figure 2.2.



α_i .. Hanger slope $\alpha_i = \gamma - \beta$

β .. Angle between arch radius and hanger

γ .. Angle between arch radius and deck

$\gamma_i = (180^\circ - \delta) / 2 + (j + 0.5) * \delta / (n + 1)$

R.. Arch radius; δ .. Arch angle

n.. Number of hangers

j.. Hanger number in relation to all hangers

i.. Hanger number in relation to its hanger set

Figure 2.2 Example of optimal hanger arrangement [13]

2.2 Timber in network arch bridges

In the last decades, many glulam bridges have been built in Norway. The ones with the largest main span are: Tretten Bridge (truss bridge) [14], Flisa Bridge (truss bridge) [15], and Tynset Bridge (tied arch bridge) [12]. All three bridges have a main span around 70 meters.

Several theses and papers deal with the possibility of using timber in network arches. However, the only glulam network arch bridge to be built so far is Steien Bridge in Norway, see Figure 2.3. Steien Bridge will have the longest span for timber bridges in Norway, with a total length of 88,2 meters [3]. The bridge is a good example of the pragmatic approach when choosing structural materials for timber bridges in Norway. One of the characteristics of Norwegian timber bridges is the combination of different materials, using the most advantageous material for the different parts of the bridge [16]. Hangers and transverse beams have consistently been of steel, the deck in concrete, and the overlying construction in timber. In this way timber bridges in Norway, as far as you can call it a timber bridge, are cost competitive with steel and concrete bridges [16].



Figure 2.3 Steien Bridge [3]

When it comes to using timber for the bridge deck in network arch bridges, Bell [12] concluded that the popular stress laminated timber deck would be too light for the network arch bridge. The total weight of the deck would be too low to effectively pre-stress the hangers and prevent relaxation. In addition the NPRA [16] does not recommend using stress laminated timber deck on bridges with more than 5000 annual average daily traffic (AADT), because there is not enough data confirming the long term performance.

2.3 Vibration

Vibration from pedestrians may resonate with the bridge's frequency and create unwanted oscillations. A simple design strategy to ensure structural safety and comfort, is to avoid the frequency range that might lead to resonance between the fundamental frequency of the structure, and the first or second harmonic load amplitude of the loads induced by walking [17]. It is recommended that the fundamental frequency f_0 should not fall in the following ranges [17]:

$$1,6 \text{ Hz} \leq f_0 \leq 2,4 \text{ Hz}$$

$$3,5 \text{ Hz} \leq f_0 \leq 4,5 \text{ Hz}$$

3 Description of Driva Bridge

Driva Bridge is a network arch bridge. It has a span of 111 meters, and the rise of the arch is 18 meters, 16% of the span. The arches are connected together with wind trusses to provide out-of-plane stability for the structure. There are ties connecting the arch ends together and taking the longitudinal forces at the supports.

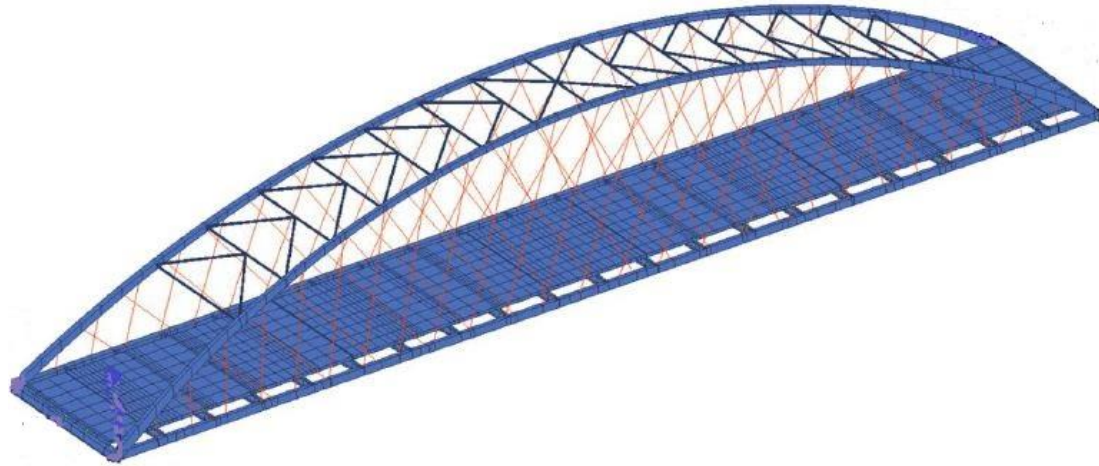


Figure 3.1: Driva Bridge [18]

The hangers are evenly distributed along the arch with a linearly varying angle from 40 to 87 degrees to the steel ties where they are connected. Each arch has two sets of 21 hangers that creates the network. In total, the bridge has 84 hangers; 45 mm full locked coil ropes.

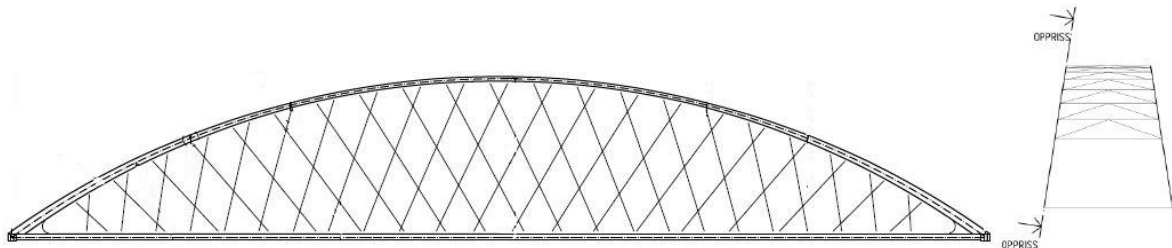
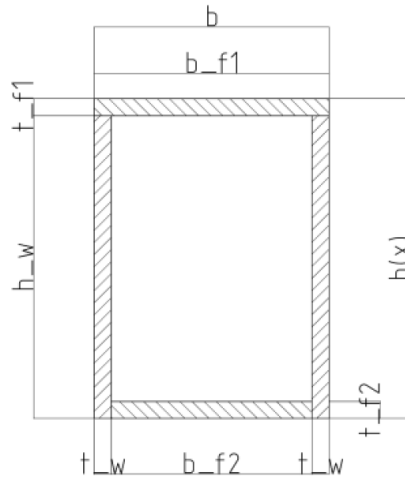


Figure 3.2 Hanger arrangement on Driva Bridge [18]

The wind trusses are rectangular hollow sections (RHS). The arches and ties are made from steel box cross-sections. The ties have constant cross-section along the length of the bridge and the arches have a varying cross-section height and material thickness. Dimensions for the arch are shown in Figure 3.3.



Width	$b=550$ mm
Height (varies)	$h=1200$ mm \rightarrow 550 mm
Thickness top flange (varies)	$t_{f1}= 40$ mm \rightarrow 30 mm
Thickness bottom flange (varies)	$t_{f2}= 40$ mm \rightarrow 30 mm
Thickness web (varies)	$t_w= 40$ mm \rightarrow 30 mm

Figure 3.3 Arch dimensions. Driva Bridge

Transverse beams span between the ties. The transverse beams are welded to the ties; this gives the beams a little spring stiffness at the supports [18]. The beams also works as composite beams, interacting with the concrete by shear studs on the top flange, increasing the bending stiffness. These two interactions makes it possible to choose a relatively slender beam cross-section with a low height.

The bridge deck is 12.95 meters wide, and consist of two traffic lanes and a pedestrian lane. The deck is made of reinforced concrete with a thickness of 350 mm in the traffic lane and 540 mm in the pedestrian lane. The required cross-slope for the deck is constructed by a varying height of the transverse beam, see Figure 3.4. In this way, the concrete deck can be cast with a constant thickness. Only having to increase the thickness at the pedestrian lane because the requirements of 200 mm height difference between a traffic lane and a pedestrian lane [19].

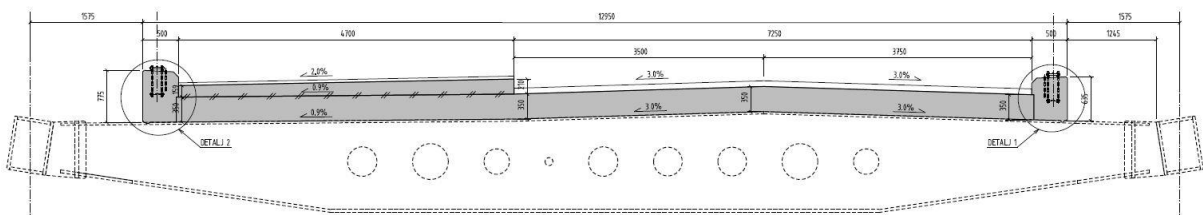


Figure 3.4 Transverse beam and concrete deck. Driva Bridge [18]

4 Bridge alternatives

This thesis presents two designed alternatives to Driva Bridge. Both alternatives have glulam arches and deck, but the layout and design of the bridges are different. The following sub chapters will deal with the proposed solutions. Explaining the design and the assumptions that were made.

The global analyses on both bridges was performed in Abaqus CAE [20]. Chapter 5 and 6 will explain more about the software, how the numerical models was built and what load models were used.

4.1 Bridge alternative 1

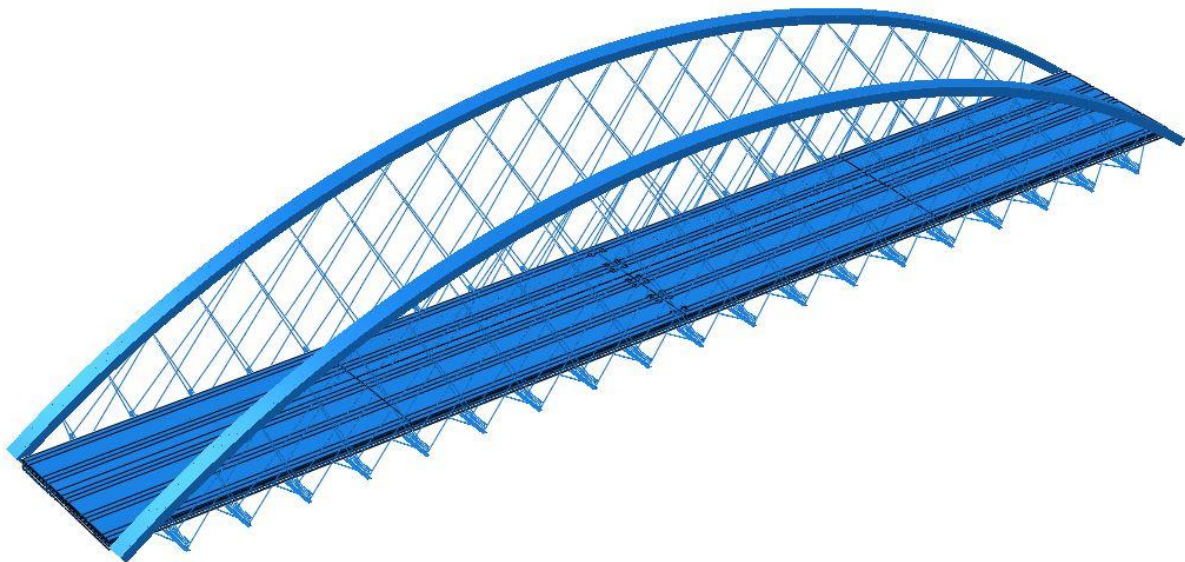


Figure 4.1 Bridge alternative 1

4.1.1 General

Alternative 1 is similar to the network arch bridge that PhD student Anna W Ostrycharczyk is currently working on in her dissertation, and have been the topics on several previous master theses [21-23] at NTNU. Previously this type of bridge have been designed with a span up to 100 meters. This time the span is increased to 111 meters, and the most interesting part is no longer if it is possible, but whether if it holds up compared to steel and concrete bridges like Driva Bridge.

This network arch bridge has no bracing between the arches, and are depending on four sets of hanger on each arch, with an angle out of the arch's plane. This provides out-of-plane stability when the hangers are loaded with the self-weight of the structure. Of course, the arch's own bending stiffness out-of-plane contribute to the stability as well. One of reasons behind the idea

of not using wind bracing is to avoid all connections and discontinuities on the sides of the glulam arches. Experience show that these connections are one of the vulnerabilities for timber bridges when it comes to moisture damage [24]. Timber bridges like all other bridges in Norway are designed for 100 years life expectancy. Therefore, it is important to design robust solutions that can stand the test of time. With all connections placed underneath the arches, the bridge is considered more durable when it comes to climate protection. This is deemed extra important on bridge alternative 1 and 2 since they will not have any chemical protection like Cu-salts or creosote.

The reason for choosing structural protection over chemical, is because the only chemical with a lasting effect like creosote is a highly toxic substance [16, 25]. It can be expected that structures treated with creosote will “sweat” out creosote oil on warm days, for as long as 10 to 30 years after construction [26], creating a hazard for the surroundings. In terms of life cycle cost, timber treated with creosote is also considered as dangerous waste and will be more costly to dispose of [26].

4.1.2 Glulam arch

The arch will have a massive rectangular glulam cross-section. The chosen material strength for the arch is GL32h [27]. Cross-section dimensions has been selected based on results from global analyses done in Abaqus, and design calculations according to EC5-1-1 [28]. The selected cross-section is 1600x850 mm², and it is constant along the arch. This is a relatively wide cross-section, but was necessary to get the desired out of plane stability, without using wind bracing. Remedies used to try to decrease this cross-section and increase the out of plane stability will be treated in chapter 10.

The arch is split into four parts with an equal length of 30 meters. This is because of limitations on the length during transportation. If the arch had been split in three parts they would have a length of 39.5 meters and would be too long to transport. The parts will be assembled at the construction site. Design check of the arch can be found in Appendix G.1

4.1.3 Boundary conditions and joints

The suggestion for arch splice joint have been borrowed from an ongoing project at NTNU, that PhD candidate Martin Cepelka and master student Halvar Veium are experimenting on [29]. The idea is that threaded rods will be inserted with a 5-degree rod-to-grain angle, and with an embedded length equal to 1.2 to 1.8 meters. Other experiments on threaded steel rods with an 18 mm diameter shows that specimens with embedded length in the range 600 mm and

above will lead to ductile steel failure instead of withdrawal failure [30]. Threaded rods are inserted at the top, and at the bottom of the cross-section on both connecting members. Two and two rods will then be connected together with a special made circular hollow section (CHS). The CHS have two holes where the rods will be inserted. The rods will be tightened to the CHS with a bolt nut inside and outside the CHS. In this way the rods can also be pre-stressed, to avoid slack in the joints. The threaded rods transfer the tensile bending force. The axial force is transferred by direct contact between the glulam parts. The connection is illustrated in Figure 4.2.

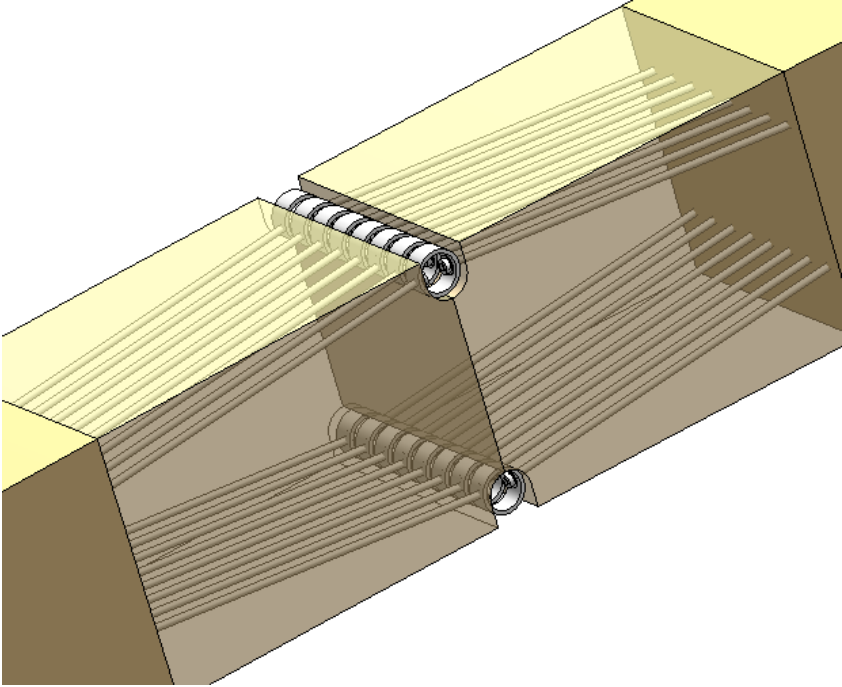


Figure 4.2 Moment resisting arch splice joint

The end connection at the arch supports will also be carried out using threaded rods in the same way as for the splice joint. These threaded rods, will secure connection between the arch and an impost hinge, with a rotational degree of freedom (RDOF) in the arch’s in-plane axis, see Figure 4.3. The impost hinge restrains out-of-plane rotation. The impost hinge should be as wide as the arch itself to ensure a moment resistant joint. The impost hinge in Figure 4.3 may be too narrow, but it shows the principle. It was considered having an even more rigid connection, restraining the in-plane RDOF as well. This would increase the stability of the arch, but also increase the bending forces, leading to a bigger cross-section and most likely a more expensive and labour intensive solution.

Since the hangers have an angle out of the arch-plane, the option to connect the hangers to the tie as on Driva Bridge, is no longer possible. Therefore, it was decided not to use ties on Bridge

1. With no tie connecting the arch ends in the longitudinal direction, the longitudinal forces has to be absorbed by the foundations. Figure 4.3 shows the impost hinge cast into a concrete foundation. No calculations has been made on the foundation or the steel joint.

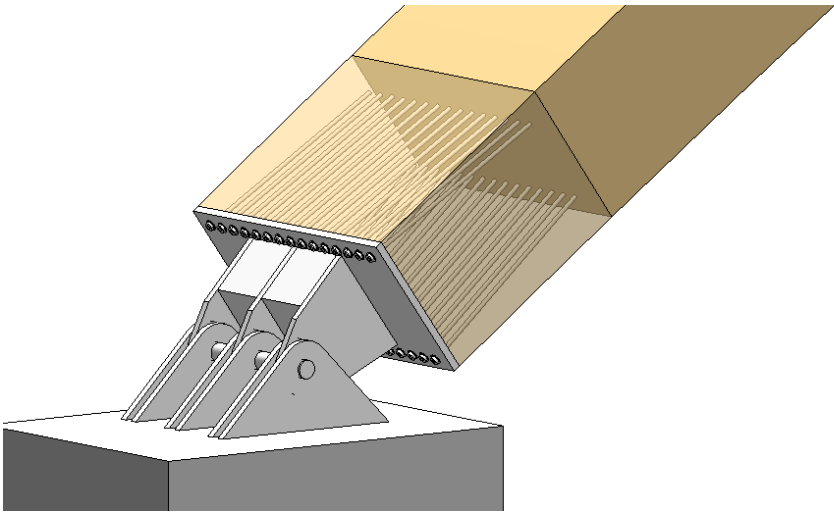


Figure 4.3 End support, impost hinge.

Not knowing the exact stiffness of the arch splice joints, a conservative approach was made to the joints in the FEM models; reducing the overall stiffness of the arch to half of the elastic modulus. The length of the reduced part depends on the cross-section of the joint. The distance from the joint was taken as:

$$L_{50\%} = \sqrt{height \times width}$$

The difference in the structural behaviour with the reduced stiffens in the connections compared to fixed connections (100% stiffness), is addressed in chapter 10.

Boundary conditions can be seen in Figure 4.4. The ends are restrained from lateral movements in all directions, and is only free to rotate about its in-plane axis.

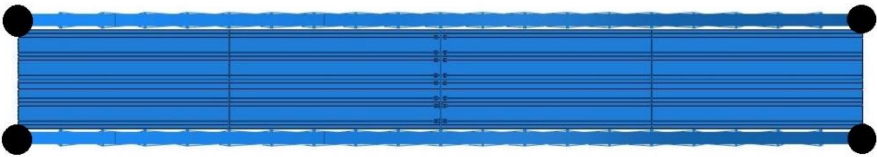


Figure 4.4 Boundary conditions. Bridge 1

4.1.4 Hangers

The hangers are connected to the arch with T-stubs. The T-stubs are connected to the arch with threaded rods like shown in Figure 4.5. The threaded rods are fitted with nuts on both sides of the base plate, this is to secure fastening of the t-stub, but also prevent moisture building up between the arch and the base plate, causing damage to the structure. The threaded rods are inserted with a length equal to 40-50 times the diameter of the rods, to ensure that the design value will be steel failure [30]. Design check on the T-stubs are given in appendix F.1.

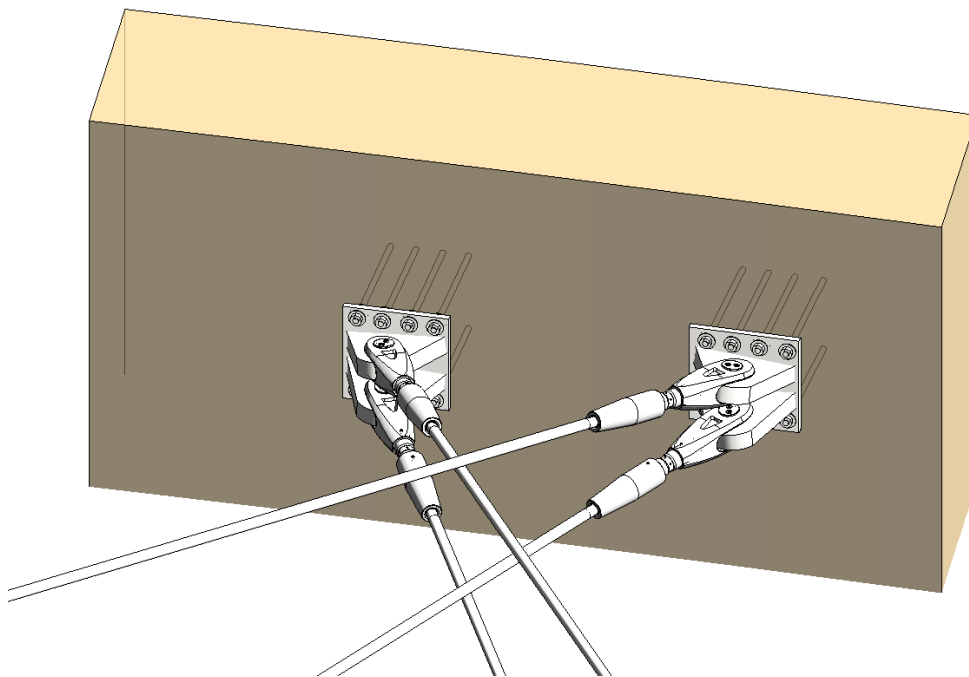


Figure 4.5 Arch-hanger connection. Bridge 1

Bridge model 1 is fitted with 152 out-of-plane inclined hangers with a diameter of 30 mm, distributed in four sets for each arch. The hangers are connected to the transverse beams, evenly distributed every 5.55 meters with a linearly varying in-plane angle: from 48 degrees oriented according to the deck, and rising to 69 degrees for the last hanger in each set.

The spacing between the hanger connections on the transverse beam is fixed to 2 meters. A fixed spacing on the beam causes the out-of-plane angles to vary with the rise of the arch: from 15 degrees for the shortest hangers connecting closest to the arch ends, and 3 degrees for the hangers connected closest to the top of the arch. The out-of-plane angle is illustrated in Figure 4.6.

The solution connecting the hangers to the transverse beams leads to an even distribution at the bottom chord, and a varying distribution on the arch. As mentioned in Hanger

arrangement 2.1.1, a more optimal hanger orientation, would be to have the hangers evenly distributed on the arch, which gives lower moments in the arch and a smaller buckling length.

The hangers are connected to the arch with T-stubs, and to the transverse beams by welded in-place mounting lugs. Calculations of welds, T-stubs and utilization on hangers are given in appendix F.

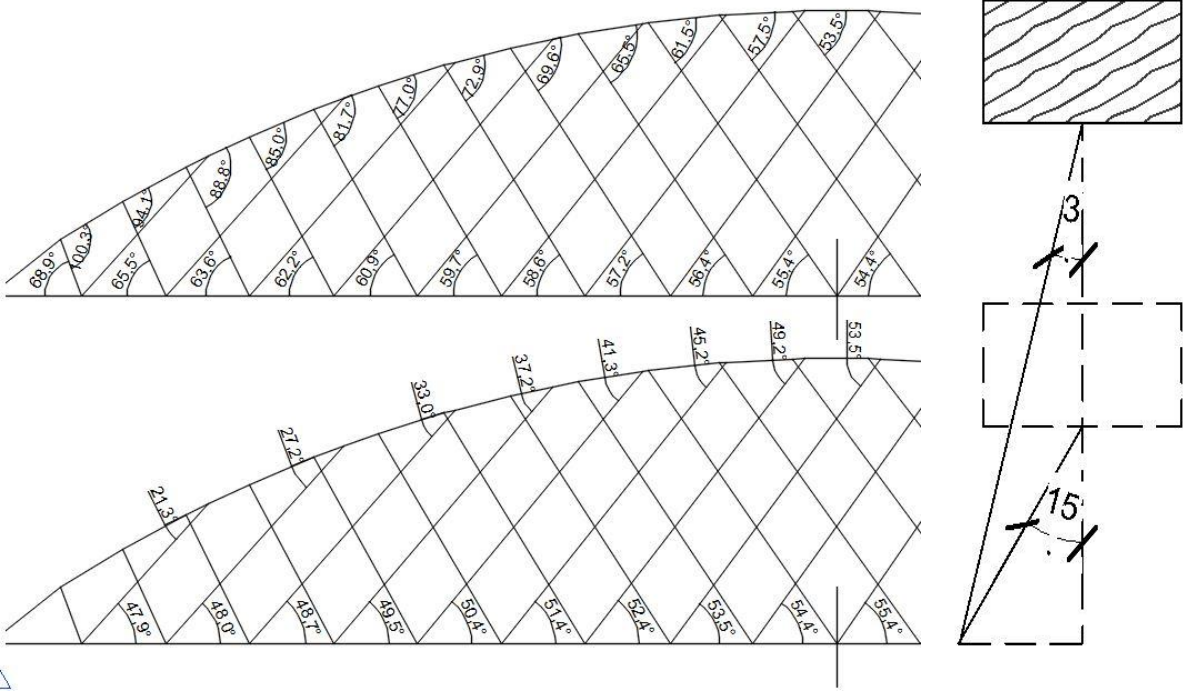


Figure 4.6 Hanger angles. Bridge 1

4.1.5 Bridge deck

The chosen bridge deck is a stress-laminated timber deck made of 115 mm wide glulam beams. The deck has a varying lamella height between the carriageway and the pedestrian lane. The carriageway has 600 mm height, and the pedestrian lane has a height of 800 mm.



Figure 4.7 Bridge deck

The dimensions were chosen on behalf of an analysis made in Abaqus. Design checks were made in service limit state for deflection, and ultimate limit state where utilization and strain requirements were controlled. $L/500$ as maximum deflection [28], and the strain requirement of 1.2 ‰ given in HB N400 [19] were checked directly in Abaqus, see Figure 4.8 and Figure

4.9 for the worst cases. The distance between the transverse beams is 5.5 meters, resulting in a maximum allowed deflection of 11 mm. The Abaqus model for the bridge deck can be found in appendix J. The elastic modulus for the bridge deck was reduced in the deck analyses, because of an empirical butt-joint factor for reduced system stiffness [19].

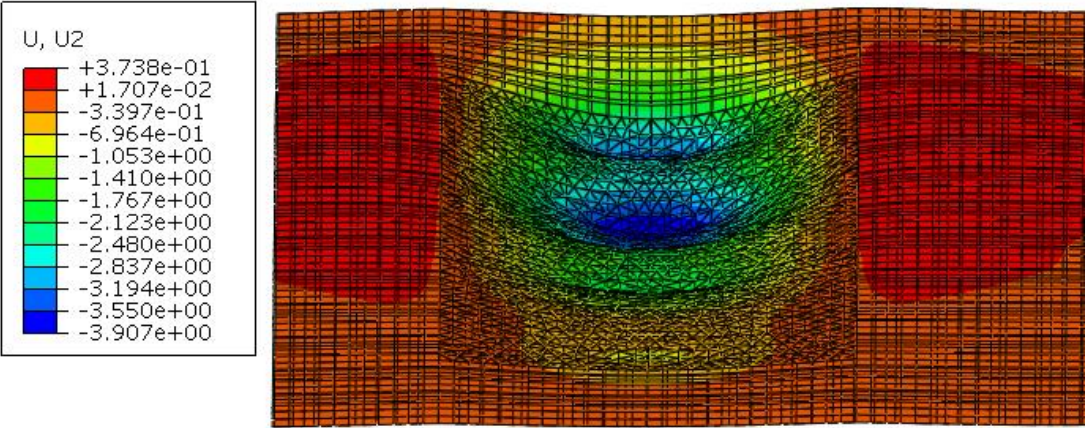


Figure 4.8 Vertical displacement on deck. LM1 Eq 1b

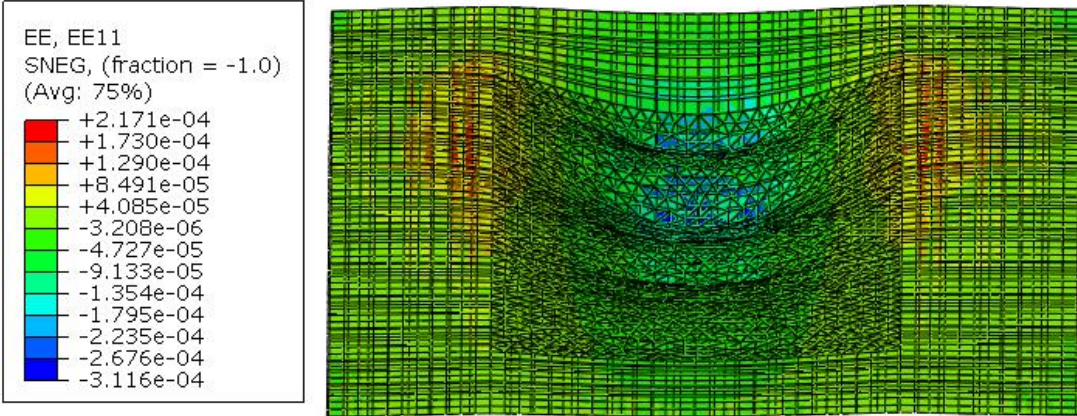


Figure 4.9 Largest strain in the deck. LM1 Eq 1b

The deck lamellas are held together by a tensioning system consisting of 28 mm “Dywidag” tension rods [31], going all the way through the deck with anchorage steel plates on each side. It is important to use a tensioning system with high steel strength to secure the highest possible extension, to minimise the effect of anchor losses and creep [16]. The stressed tension rod redistribute the forces to the anchor plates, which then forces the lamellas together. The size of the anchor plates are decided based on the glulam’s pressure capacity perpendicular to the grain. The tension force serves two purposes [16].

- Create friction that prevents the lamellas in the deck to slide relative to each other.
- Prevent cracks between the lamellas when transverse bending occurs.

The friction between the lamellas from the tension system is necessary for the deck to be able to transfer transverse shear forces. Figure 4.10 shows the distribution of the anchor plates on the side of the deck, and the placement of the pressure plate for the guardrail system in between. Design check for the stress laminated bridge deck are given in appendix [E.1].

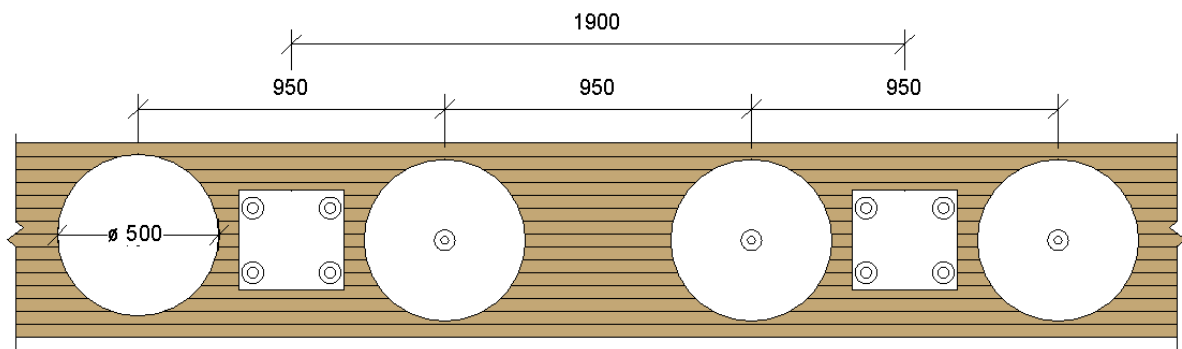


Figure 4.10 Tensioning system, bridge deck

Experiences from inspections on existing bridges have shown that it is difficult to provide a watertight sealing between the deck and the edge of the foundation, and in many cases very difficult or close to impossible to perform inspections from underneath the bridge. This has resulted in several new designs on timber deck supports [16]. The suggested design for the deck support solution is shown in Figure 4.11.

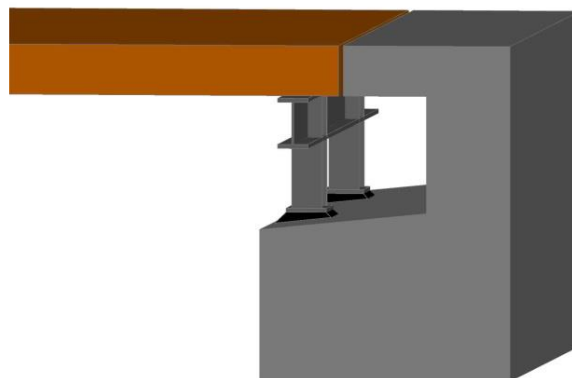


Figure 4.11 Bridge deck end support [16]

This solution has moved the transverse support beam a distance from the abutment, and fitted a concrete cantilever which extends towards the deck. The cantilever prevents rotation of the

timber deck edge, which would happen if the deck extended like a cantilever towards the back wall. This solution secures good drainage and provide easy access for inspections [16].

The end support has to be able to transfer forces from the deck down to the foundation. The longitudinal forces are transferred to the concrete cantilever, and the transverse forces has to be transferred to the support beam by a connection that restrains transverse movement. Sideway connection is suggested with recessed lateral supports in the deck, mounted on top of the support beam [16].

4.1.6 Wearing pavement

On road bridges where the traffic is not insignificant, the most appropriate choice is a wearing pavement of asphalt. The estimated future amount of traffic at the location of Driva Bridge has a magnitude larger than 6000 AADT, and asphalt is the correct choice. It is most common to use the same type of asphalt on the bridge as on the adjoining roads [16]. The basis for the selection of wearing pavement are given in Appendix M.

The asphalt is built up by two layers, base and wearing layer according to HB N200 [32]. The asphalt on the carriageway and pedestrian lane is laid with cross-slope to secure adequate water drainage. The cross-slope on the carriageway has a magnitude of three percent, and the pedestrian lane has a cross-slope with magnitude of two percent, shown in Figure 4.7.

The asphalt is not watertight. Therefore, an additional base layer has to be applied to secure water protection of the glulam deck. To weatherproof the topside of the deck a layer of Topeka 4s [33] is suggested. Topeka 4s is an elastic material and will move together with the temperature and moisture movement of the deck. The Topeka is applied in a warm liquid state, less than 190 °C. The moisture from the heated deck will evaporate through the liquid membrane. This minimises the possibility for blisters under the membrane later when the heated asphalt layer is applied on top of the membrane[16].

The transition between the carriageway and pedestrian lane have to be done in a manner which secure a continuously membrane layer. A suggestion to secure protection for height differences in wooden decks are presented in Figure 4.12 [24].

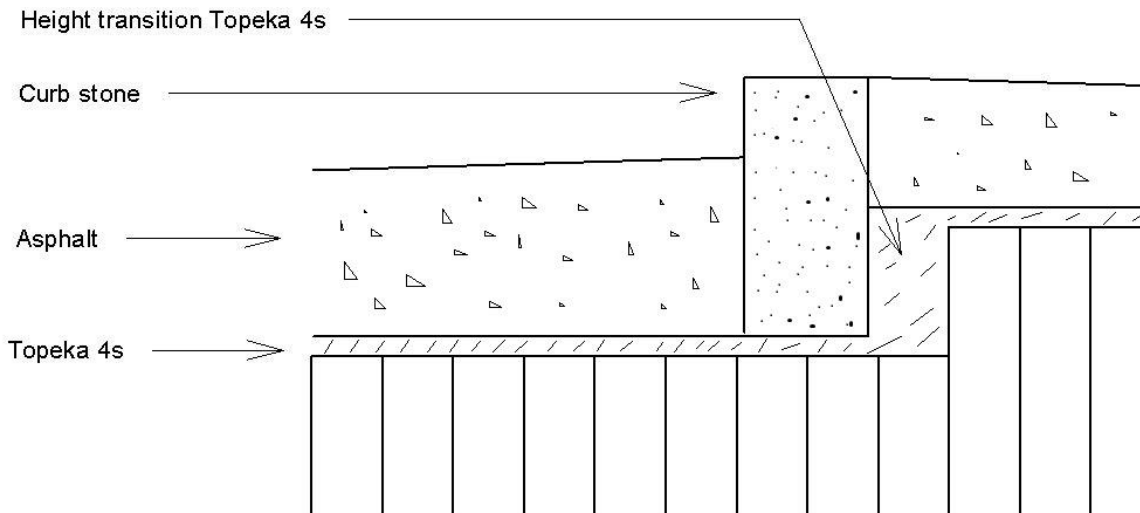


Figure 4.12 Solution on membrane layer at height transition

4.1.7 Transverse beams

The suggested solution of the transverse beam consists of an I-profile with underlying compression and tensile members, behaving much like a truss beam. On Driva bridge the transverse beam and the concrete deck interact via shear studs welded to the beams top flange, making it composite beam. With a timber deck we don't have this interaction, therefore the bridge deck is only considered as deadweight on top of the beam, not contributing to the beams bending stiffness. Without interaction, it was necessary to look for an alternative solution on the beam design, to reduce the self-weight of the beam. The proposed solution made it possible to make a lighter transverse beam than if only an I-beam profile was used.

Where the transverse beams are in direct contact with timber, there will be small or large cavities where condensation may collect. Stagnant water in cavities like this may create white rust on the zinc coating, which can lead to corrosion of the top flange. This is an area which is inaccessible for inspections [16]. In addition to a protective epoxy coating on the top flange to protect the transverse beam against corrosion, the I-profile is fitted with an oval top flange to ensure drainage and prevent stationary moisture, which would be damaging for the timber deck as well.

The beam was designed in Focus Konstruksjon [34], satisfying utilization and deflection requirements. Calculations can be found in appendix H.1. S355 is the material strength of the beam. There has not been done any calculations on the welds connecting the different parts together. Utilization and deflection from the load models that gave the highest values are presented in Table 4.1.

Focus Konstruksjon Transverse beam analysis		Bridge	
		1	2
Maximum allowed displacement		36	33
ULS_LM1_gr1a_Eq 1b	Utilization	0.88	0.78
SLS_LM1_gr1a	Deflection	35.9	26.9

Table 4.1 Transverse beam, displacement and utilization

The transverse beam are shown in Figure 4.13, with a list of the dimensions used on transverse beam solution 1 and 2.

I-beam	
Top flange	400 x 40 mm
Bottom flange	400 x 30 mm
Web	20 x 730 mm
Compression members	
RHS	250 X 250 X 6,3 mm
Tensile members	
Flat steel	250 x 50 mm

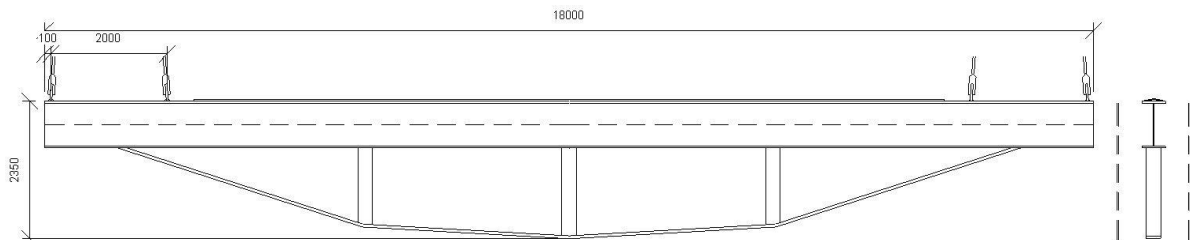


Figure 4.13 Transverse steel beam

4.1.8 Guardrail

The guardrail has been chosen to fulfil the requirements given in HB N101 [35]. All bridge railings must have a handrail with a minimum height of 1.2 meters above the deck, and it must be constructed in such a way that it is difficult to climb. The necessary strength class of the guardrail is decided based on the speed limit, amount of traffic and the roads side terrain. Because the consequence of a large vehicle breaking through the guardrail on a bridge, the strength class is H2. H2 is designed for large vehicles [35].

The suggested solution is developed by the Swedish company “AB VARMFORFORZINKING” and has the strength class H2.W2.A, which is sufficient for the traffic on Driva Bridge.

The guardrail is mounted to the side of the deck. To secure sufficient anchorage, four threaded rods are inserted into the side of the deck. The two top rods must be long enough to avoid withdrawal failure, and the bottom two can be shorter as they only transfers pressure force onto a pressure plate. The guardrail has two steel plates distanced with bolt nuts in order to adjust for irregularities in the bridge deck. Figure 4.10 shows the placement of the steel plate on the deck.

In case of an accident the threaded rods are the weakest link, and are designed to break between the two steel plates, this is to ensure easy replacement after breaking. If they were to break inside the deck, it would be near impossible to get them out. For design and dimensions of the guardrail, see appendix N.

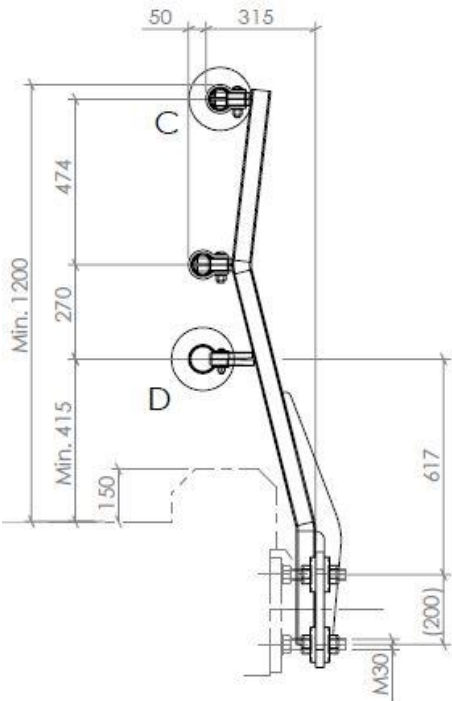


Figure 4.14 Side mounted guardrail

4.1.9 Weather protection

To prevent weather damage, the arches will have structural protection. The weather protection will be carried out with zinc cladding on the top of the arches, and the sides will be fitted with louvered timber cladding. The most used material for cladding on top of timber structures is copper. Copper is easy to work with and has several hundred years of durability. Moisture accumulating under the cladding is also less prone to cause rot, because of the positive effect of copper ions. The biggest downside to using copper is its high value as scrap metal. There are several cases where copper cladding has been stolen from timber bridges in Norway, leaving

the structure vulnerable [24]. Since the cladding on arch bridges are relatively accessible for thieves, copper was deemed an unfit choice for the bridge. Zinc is less valuable than copper and is considered as a good alternative. One of benefits with zinc, in addition to having a low value, is that the problem with copper ions wearing down the zinc protective coating on underlying structural steel is avoided. All cladding must be done in a manner that secure adequate ventilation of moisture. Figure 4.15 shows an example on this type of structural protection.



Figure 4.15 Structural weather protection on the arch [24]

As mentioned in chapter 4.1.6, the topside of the timber deck is protected with a layer of Topeka 4s. The sides of the bridge deck is fitted with flashing to secure that the surface water is directed away from the deck and the tensioning systems anchorage plates. The tensioning systems nuts can as an extra safety be fitted with protective caps filed with grease to prevent corrosion [24].

4.2 Bridge alternative 2



Figure 4.16 Bridge alternative 2

4.2.1 General

Bridge 2 is the second alternative timber bridge presented in this thesis. The layout of the bridge is identical to Driva Bridge, See Figure 1.1. It is of interests to see how the timber bridge will perform compared to the steel and concrete bridge when the geometry is otherwise the same.

Unlike bridge 1, bridge 2 has K-shaped wind trusses connecting the two arches to ensure lateral stability instead of using four sets of hangers on each arch. Bridge 2 is also fitted with steel ties and end-beams.

The choice to only have structural weather protection on bridge 2 is not as easy to defend, since the wind trusses will complicate the cladding considerably, and increase the risk for construction errors. Regardless, that is the chosen solution for this bridge.

4.2.2 Glulam arch

Like bridge 1, the network arch will have a rectangular massive glulam cross-section. The arch is split in four parts of equal length, which will be assembled on the construction site. The two end parts of the arch has a varying cross-section to accommodate the increased bending moments at the wind portal. The cross-section starts with $1100 \times 1100 \text{ mm}^2$ at the support and ending at $850 \times 850 \text{ mm}^2$ at the first joint. The two middle parts have a constant cross-section of $850 \times 850 \text{ mm}^2$.

Wind trusses connecting the two arches ensure good lateral stability. In addition, the arches are tilted towards each other with an 8-degree angle, see Figure 4.17. This reduces the bracing between the arches and the bending moments in the wind portal [9]. Design check of the arch can be found in Appendix G.2

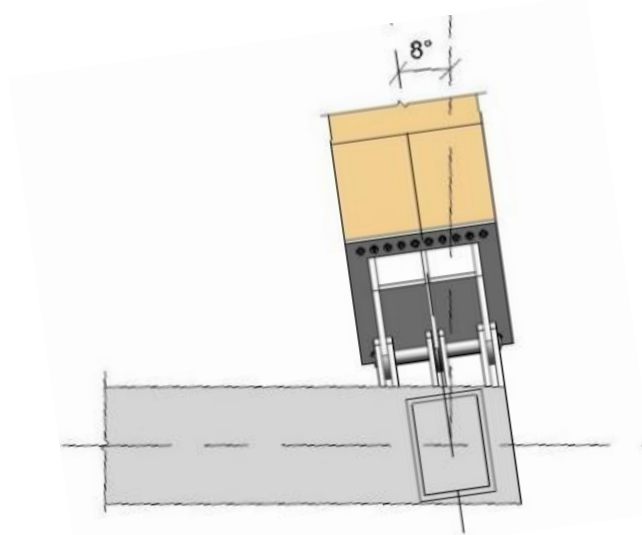


Figure 4.17 Rotation of the arch relative to a vertical plane. Bridge 2

4.2.3 Wind Bracing

The wind bracing is made of K-shaped trusses in glulam. The bracing is not modelled as trusses, but beams with 25% joint stiffness, resulting in a combination of compression/tensile forces, shear and bending moment in the trusses. The utilization in the wind bracing presented in chapter 9.3 is very low. This is because the cross-sections was chosen so that the wind bracing would not be the first parts to buckle in the buckling analyses, in order to get the desired buckling modes.

There are two different cross-sections for the K-shaped trusses: The diagonal trusses have a rectangular cross-section equal to $400 \times 400 \text{ mm}^2$ and the transverse trusses a rectangular cross-section equal to $300 \times 450 \text{ mm}^2$

Design check of the wind trusses are given in appendix L.

4.2.4 Boundary conditions and joints

Bridge 2 have the translational DOF shown in Figure 4.18. The arrows indicate where the end supports are free to move. This bridge can be viewed as a simply supported beam, unlike bridge

1 that has pinned supports. The ties and end-beams are holding the arches in place and as a result, the bridge is not as dependent on the foundation for stability.

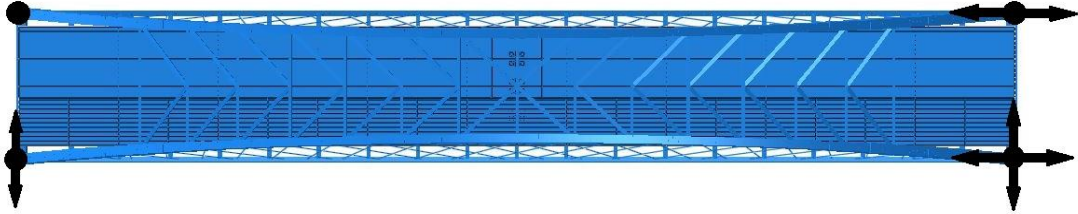


Figure 4.18 Boundary conditions. Bridge 2

As shown in Figure 4.19 the arches are free to rotate in its own plane, and is restrained from rotating out-of-plane. Clamping the arch and restraining RDOF in all directions will increase the stresses in the tie considerably near the arch. An impost hinge was therefore deemed more suitable. The tie is welded to the side of the end-beams and the arch's impost hinge is welded to the top. This was necessary to get enough place for the impost hinge. A negative consequence of this is that the centrelines of the three members; arch, tie and end-beam, does not intersect in the same point, creating eccentricity moments on the end-beam.

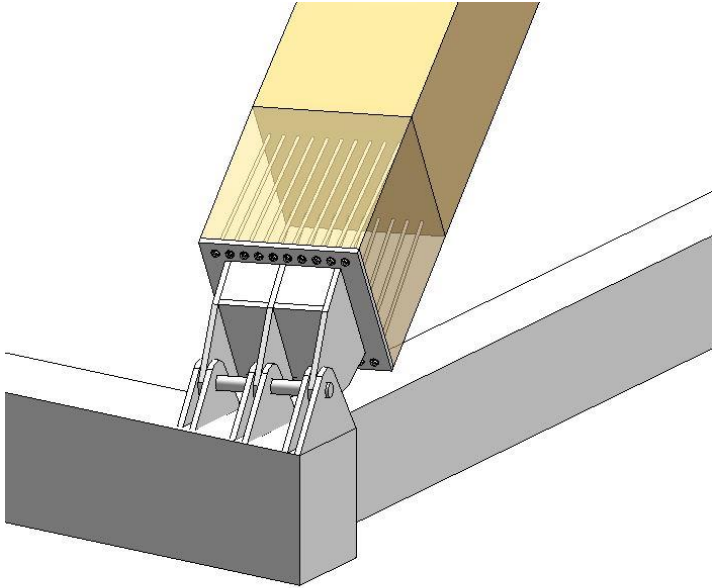


Figure 4.19 Arch support connection. Bridge 2

4.2.5 Hangers

The hanger arrangement is identical to Driva Bridge [18]. The hangers are placed systematically with two hanger sets on each arch, where every set consists of 21 hangers. The hangers are orientated with a linearly varying angle to the bottom chord, from 87 to 40 degrees, see Figure 4.20. The hangers have an equidistant distribution on the arch with 5 meter horizontal distance between each hanger. Since there are two sets of hangers on each arch the effective distance between the hangers is 2.5 meters.

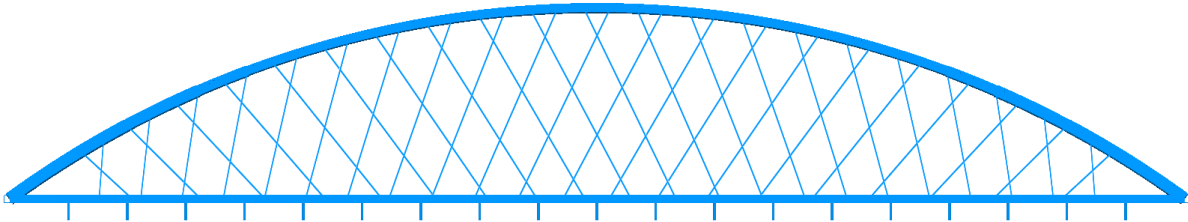


Figure 4.20 Hanger arrangement. Bridge 2

The hanger connections to the arch on Bridge 2 is similar to the connections on Bridge 1. The hangers are connected to T-stubs that are fastened to the arch with threaded rods. Since bridge 2 only has two sets of hangers on each arch, only one hanger are connected to each T-stub, see Figure 4.21.

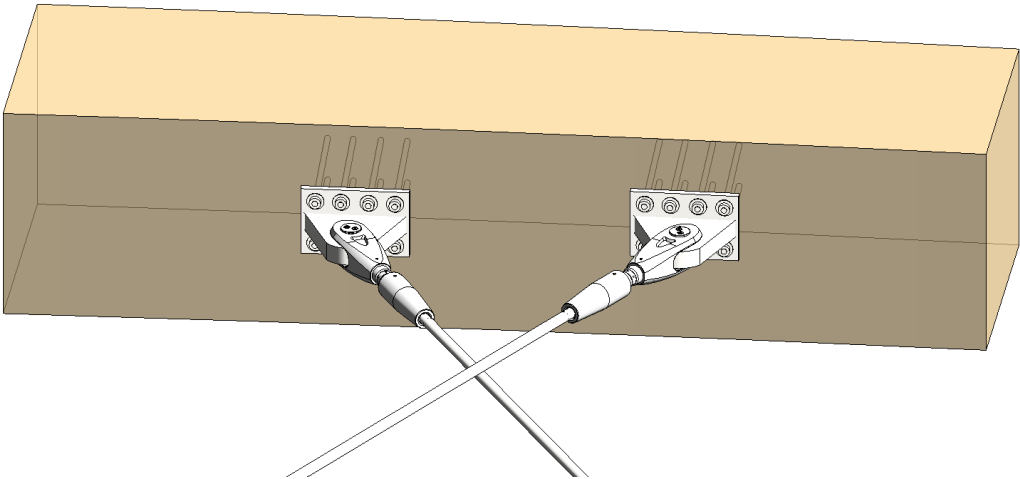


Figure 4.21 Arch-hanger connection. Bridge 2

As shown in Figure 4.20 the hangers are not connected to the transverse beams like on bridge 1, but are instead connected to the tie. The welded in-place mounting lugs on the tie are placed on top of the outer web of the tie. The eccentricity of the mounting lug creates a torque on the

tie that has to be included in the design check of the tie, see Figure 4.22. Design check on the T-stubs and mounting lug are given in appendix F.2.

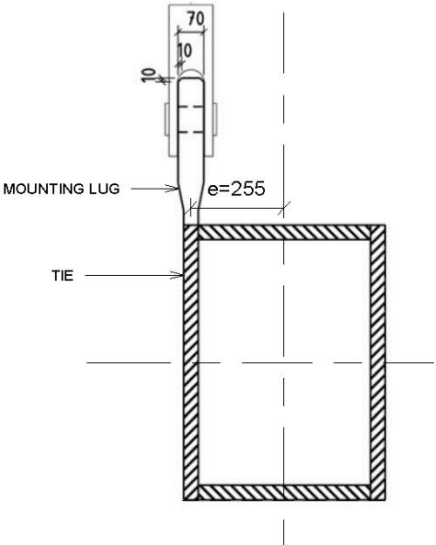


Figure 4.22 Tie-hanger connection. Bridge 2

4.2.6 Bridge deck

The Bridge deck is identical to Bridge 1, see Chapter 4.1.5.

4.2.7 Wearing pavement

The wearing pavement is identical to Bridge 1, see Chapter 4.1.6.

4.2.8 Tie

Bridge 2 has steel ties in the same way as Driva Bridge. The main focus in this thesis was to design the glulam parts of the bridge, therefore not much time was devoted to optimize the dimensions for the steel tie. The dimensions used in the analyses was the same as for Driva Bridge, see Figure 4.23. Figure 4.23 also shows the three sections of the tie controlled for maximum stresses. Design check of the tie are given in Appendix K.

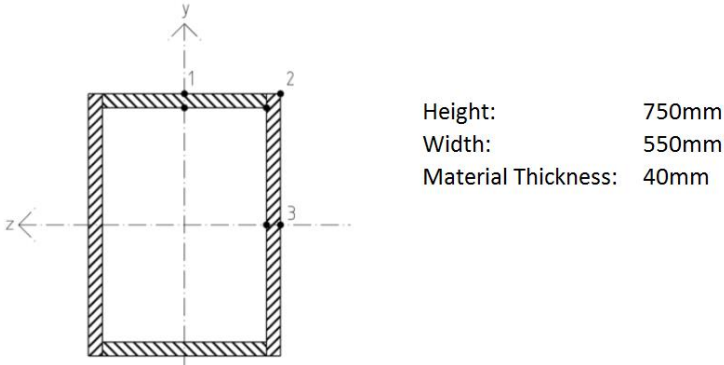


Figure 4.23 Steel tie dimensions. Bridge 2

The two ties are connected to several structural elements on the bridge. All the forces from the bridge deck, which lies on the transverse beams are transferred to the ties, and from the ties the forces are transferred to the arch via the hangers. The ties are not connected directly to the arches at the support, but are welded to the end-beams which are connected to the arches, see Figure 4.19.

The cross-section is rotated 8 degrees about its longitudinal axis in order to be orientated in the same plane as the arch.

4.2.9 Transverse beam

The transverse beam design on Bridge 2 is the same as for Bridge 1, see Figure 4.13 for cross-section dimensions and design details. However, there are some differences. The hangers are no longer connected to the transverse beam, this reduces the necessary length of the beam. The necessary length is based on requirements of spacing behind the guardrail in case of a traffic accident, and clearing between structural parts and traffic [19].

The transverse beams are welded to the side of the ties. The ties give the beams some rotational stiffness in their supports. This is not included in the calculations made in Focus Konstruksjoner [34]. The beam is modelled as a simply supported beam with 16.5 meter span, which is considered conservative. Calculations made in Focus Konstruksjoner are given in appendix H.1 and H.2. However, the spring stiffness is included in the Abaqus bridge model, as a normal consequence of the weld connection between the parts in the model.

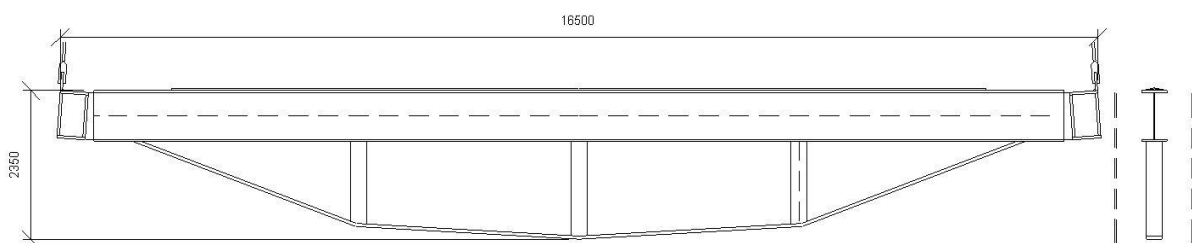


Figure 4.24 Transverse beam. Bridge 2

4.2.10 Guardrail

The guardrail is identical to Bridge 1, see Chapter 4.1.8

4.2.11 Weather protection

Bridge 2 has the same type of structural weather protection as Bridge 1, with zinc cladding on the top surface of the arches and louvered timber cladding on the sides. See Chapter 4.1.9 for more information.

The same solution of protection is chosen for the wind trusses as well. Figure 4.25 shows how the cladding can lead surface water away from the connections. Note that the sketch does not include the timber cladding on the sides.

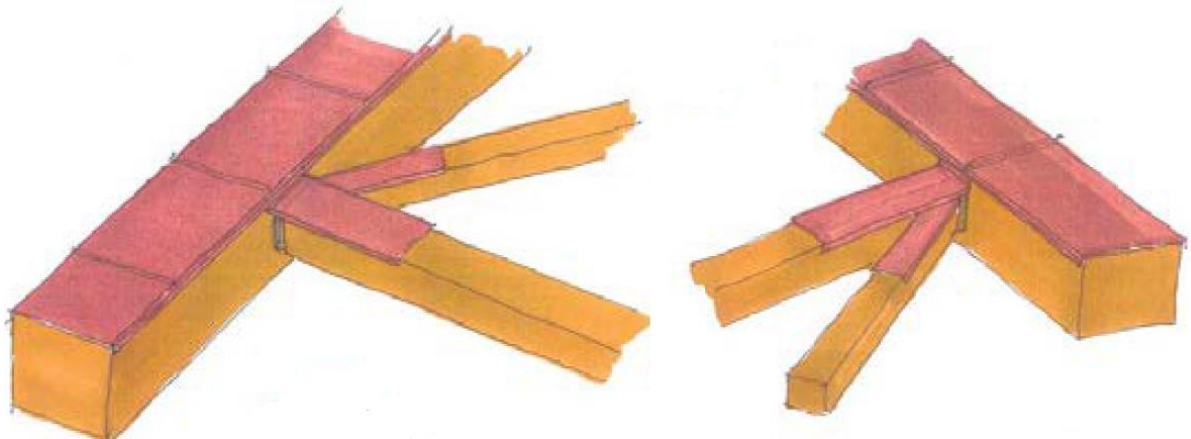


Figure 4.25 Cladding on top surfaces [16]

5 Finite element analysis

All global analyses was performed in Abaqus CAE, an interactive environment used to create finite element models, submit Abaqus analyses, monitor and diagnose jobs, and evaluate results [20]. This chapter will explain how the two bridges are discretized in Abaqus and which kind of results are extracted from the analyses. The numerical Abaqus models can be found in Appendix J.

5.1 Shell elements

The bridge deck and the asphalt layer are modelled as three-dimensional general-purpose shell elements, named S3R and S4R in Abaqus. The general-purpose shell element is neither a thin shell element (Kirchhoff shell theory) or a thick shell element (shear flexible Mindlin shell theory), but a combination that can provide robust and accurate solutions to both thin and thick shell problems [20].

All traffic loads are placed on the asphalt shell element surface. Vertical traffic loads are placed directly on the surface, but the horizontal braking loads are first applied to a “virtual beam”

along the asphalt in the longitudinal and transverse direction. This virtual beam has no mass and its only purpose is to transfer the braking load to the asphalt layer. The bottom surface of the asphalt is tied to the top surface of the timber deck. A tie constraint can be explained as two surfaces being glued together, with an infinitely strong glue.

The bridge deck is pointwise connected to the transverse beam by connector elements, every 500 mm. A connector element is a 2-node wire feature connecting two nodes on different parts in the model together, applying constraints and creating interaction between the parts. The consequence of using connector elements on shell surfaces, is that there will be high concentrated stresses at the connector points. In reality, the connection between the beam and deck is continuous; therefore, these high stresses are ignored.

5.2 Beam elements

The arch, tie, transverse beam, end beam, and wind bracing are modelled as beam elements. The beam elements, named B31 in Abaqus, is a 2-node linear beam in space. These elements in Abaqus are formulated so that they are efficient for thin beams, where Euler-Bernoulli theory is accurate, as well as for Timoshenko thick beam theory: because of this they are the most effective beam elements in Abaqus [20].

All connections in the model are weld connections, coupling all DOF on the connected parts. To account for less stiff connections, the elastic modulus of the material is reduced in the area of the connection.

5.3 Truss elements

The hangers are modelled as truss elements. One-dimensional bars or rods that are assumed to deform by axial stretching only. They are pin jointed at their nodes, and so only translational displacements at each node are used in the discretization [20].

The hangers can only take tensile forces, but the analysis does not converge if the trusses are set to tensile only. A remedy for this is to model “virtual hangers” overlapping the “real hangers” to take compressive forces. These virtual hangers have such a low density and low elastic modulus, see Table 5.2, that they will not be able to affect the bridge in any way, but the analysis will converge.

5.4 Material properties

All parts in the models are designated their own material properties, including mass density, elastic modulus, poisson’s ratio, shear modulus and a thermal expansion coefficient. Table 5.1

shows the material properties for the glulam timber parts used in Abaqus, Table 5.2 show the material properties for the remaining parts in the model.

	Materiaial	Mass Density kg/m ³	E1 N/mm ²	E2 N/mm ²	E3 N/mm ²	p12	p13	p23	G12 N/mm ²	G13 N/mm ²	G23 N/mm ²	Expansion coeff
Arch	GL32h	4,90E-10	14200	300	300	0,42	0,48	0,5	650	650	65	5,00E-06
Arch joint	GL32h	4,90E-10	7100	150	150	0,42	0,48	0,5	650	650	65	5,00E-06
Wind-Truss	GL32h	4,90E-10	14200	300	300	0,42	0,48	0,5	650	650	65	5,00E-06
Wind-Truss joint	GL32h	4,90E-10	3550	75	75	0,42	0,48	0,5	650	650	65	5,00E-06
Bridge deck	GL24c	4,00E-10	11000	300	300	0,42	0,48	0,5	650	650	65	5,00E-06

Table 5.1 Material properties for timber parts

The material strength are sourced from NS-EN 14080:2013 [27]. The poisson’s ratios are average values from several researches performed on various spruce species [36].

	Mass Density kg/m ³	Young's Modulus N/mm ²	Poisson's Ratio	Expansion Coeff
Asphalt layer	2,50E-09	100	0,35	5,00E-06
Transverse beam	7,80E-09	210000	0,3	1,20E-05
Tie	7,80E-09	210000	0,3	1,20E-05
Hanger	7,80E-09	160000	0,3	1,20E-05
Virtual Hanger	7,80E-20	1000	0,3	1,20E-05

Table 5.2 Material properties for the remaining parts

The elastic modulus for hangers is acquired from the producers brochure [37].

5.5 Results from Abaqus

Three types of analysis was performed in Abaqus: Static analysis, buckling analysis and frequency analysis. Static analysis was carried out for all load models in SLS and ULS. Buckling analysis was carried out for all load models in ULS.

The static analysis produces results including stresses, strains, displacement and forces for all elements in the model. These output variables are printed out and used in the design checks, in accordance to the appropriate Eurocode.

The Buckling analysis is performed by using a global load factor (buckling factor), increasing all active loading until the structure buckle. By watching the buckling mode, it is possible to see whether the structure’s buckling mode represents buckling in-plane or out-of-plane, relevant to the network arch. The buckling factor is then used in a version of the classic formula for Euler buckling load, Figure 5.1, to determine the arch’s in-plane or out-of-plane buckling length. The buckling lengths is finally used in the design check of the arches. This method of

calculating the arch buckling length was also used in the design of Steien Bridge [38], and it is also given in [16].

$$N_{critical} := N_{Ed} \cdot \lambda \qquad l_{buckling} := \sqrt{\frac{\pi^2 \cdot E_{0.05} \cdot I}{N_{critical}}}$$

Figure 5.1 Euler buckling load, combined with global buckling factor

For some buckling modes in Abaqus, the buckling factor can come out as negative. This means that the structure would buckle if the loads were applied in the opposite direction. These modes has no practical value for the bridge analysis and is disregarded, because the traffic load and gravity can never be applied in the opposite direction, pulling the bridge towards the sky.

Frequency analysis was performed to find the bridges fundamental frequency, to control that it lies outside the range of the first or second harmonic load amplitude of pedestrian loading [17]. The structures first fundamental frequency is also used to find the structures natural oscillation period, to decide whether dynamic wind loading needs to be considered or not, see Chapter 6.2.2.

6 Loads

6.1 Dead load

The dead load for the structural elements in numerical modelled are calculated by Abaqus. The user defines cross-sections, density and gravity acceleration when creating the model . The dead load has also been manually calculated to use in the cost and feasibility chapters.

The dead load for the material used in the bridge structures have been listed in Figure 6.1 and Figure 6.2.

Bridge 1						
Structural element	Quantity	Length [m]	cross sectional [m ²][m ³]	density [kN/m ³]	Total weight [kN]	Weight per meter bridge [kN/m]
Arch	2	118,6	1,36	4,81	1550,05	13,96
Transverse beam	19	18,0	0,06	78,50	1478,46	13,32
Hangers	-	2510,0	6,48E-04	84,75	137,84	1,24
T-stub/hanger connections	76	-	0,02	78,50	124,09	1,12
Deck	-	111,0	8,81	3,92	3836,34	34,56
Self weight, deck structure*					5314,8	47,9
Total weight					7126,8	64,2

*The deck structure include transverse beam and glulam deck

Figure 6.1 Dead load. Bridge 1

Bridge 2						
Structural element	Quantity	Total length [m]	cross sectional [m ²][m ³]	density [kN/m ³]	Total weight [kN]	Weight per meter bridge [kN/m]
Tie	2	111,0	0,10	78,50	1700,88	15,32
wind trusses, transverse	-	164,0	0,14	4,81	106,38	0,96
wind trusses, diagonal	-	220,0	0,16	4,81	169,14	1,52
Arch	2	118,6	0,84	4,81	957,39	8,63
Transverse beam	19	16,5	0,06	78,50	1455,67	13,11
End beam	2	18,0	0,15	78,50	413,73	3,73
Hangers	-	1181,5	1,13E-03	84,56	112,40	1,01
T-stub/hanger connections	84		0,01	78,50	72,53	0,65
Deck	-	111,0	8,81	3,92	3836,34	34,56
Self weight, deck structural*					7406,6	66,7
Total weight					8824,4	79,5

*The deck structure include tie, end beams, transverse beam and glulam deck

Figure 6.2 Dead load. Bridge 2

6.1.1 Super dead load

Super dead loads listed in Table 6.1, except asphalt, are added as uniform distributed loads in the numerical model.

Bridge 1 and 2	Total length [m]	cross sectional area [m ²]	density [kN/m ³]	Total weight [kN]	Weight per meter bridge [kN/m]
Asphalt (AgB)	111	1,885	25	5230,9	47,1
Asphalt(Ag)	111	0,658	25	1826,0	16,5
Topeka 4s	111			493,6	4,4
Railing	222		-	111,0	0,5
Water pipe	111		-	333,0	3,0
Total weight				7994,4	71,5

Table 6.1 Super dead loads

6.2 Variable loads

6.2.1 Temperature load

Temperature loads, changes in the structures average temperature and temperature difference for the height above sea level, are calculated according to HB N400 [19] and EC1-1-5 [39]. Values for upper and lower maximum air temperature for Sunndal municipality is selected from Figure 6.3.

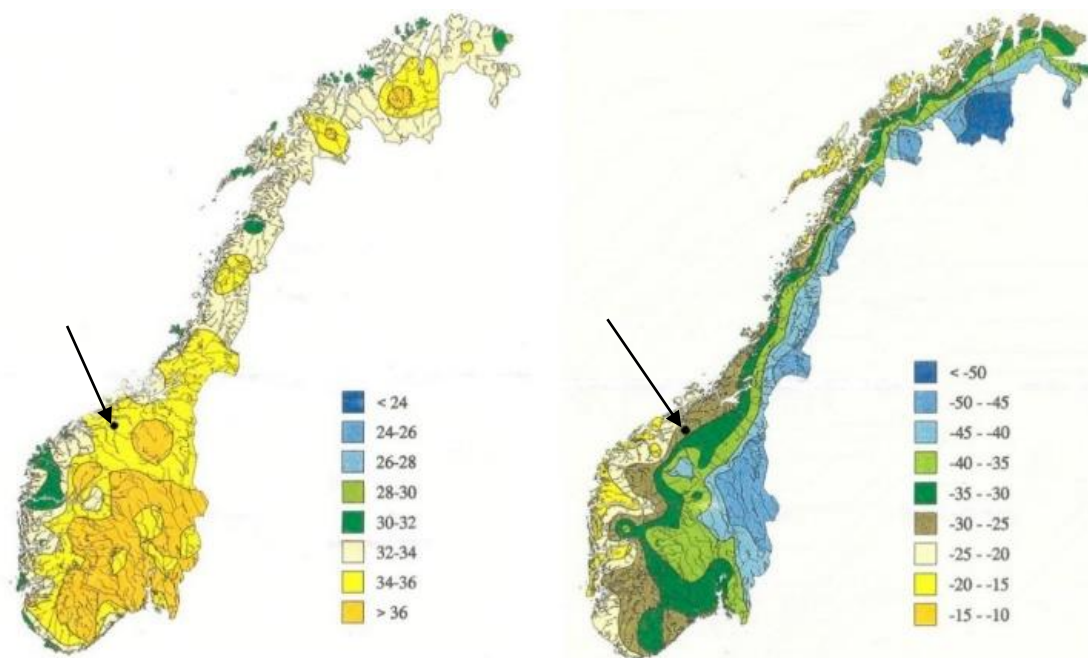


Figure 6.3 Maximum and minimum temperature with a return period of 50 year [39].

The main components of the Bridge 1 and Bridge 2 consists of glulam timber. The standard does not cover the temperature loads of timber bridges. According to the report “*Kepp, et.al; Thermal Action on Timber Bridges*” [40] it is sufficient to let the difference between the highest

and lowest daily mean temperature be the design temperature difference. The expansion temperature difference shown in Figure 6.4, was used in the analyses.

The contraction and expansion of the timber material is only taken into account longitudinal to the grain. The following temperature expansion coefficient for wood and steel have been used:

$$\alpha_{glulam} = 0.005 \text{ mm/m} \times K$$

$$\alpha_{Steel} = 0.012 \text{ mm/m} \times K$$

$T_{max}=35^{\circ}C$	Upper representative air temperature	
$T_{min}=-30^{\circ}C$	Lower representative air temperature	
$T_0=10^{\circ}C$	Initial temperature	
$\Delta T_{N.con}=T_0-T_{MIN}$	$=40^{\circ}C$	(Contraction)
$\Delta T_{N.exp}=T_{max}-T_0$	$=25^{\circ}C$	(Expansion)
$\Delta T_N=T_{MAX}-T_{MIN}$	$=65^{\circ}C$	(Total temperature difference)

Figure 6.4 Design temperature

6.2.2 Wind load

Wind load is calculated according to HB N400 [19] and EC1-1-4 [41]. The relevant structures belong to wind load Class 1: bridge structures with negligible dynamic load effect from wind. Wind Class 1 includes all bridges where the lowest natural oscillation period T is less than 2 seconds. Analyses of natural oscillation periods was carried out in Abaqus.

$$Bridge\ 1 : T = \frac{1}{f} = \frac{1}{0.714} = 1.4\ s$$

$$Bridge\ 2 : T = \frac{1}{f} = \frac{1}{1.521} = 0.7\ s$$

The calculations use reference wind speed for Sunndal municipality, $v_{b,0} = 27\ m/s$. Load effects are calculated based on the peak velocity pressure for the individual structural component. The wind load should be reduced by up to 50% where this has an adverse effect on parts of the structure. Calculations of wind speed on the different components of the structure are given in appendix A.

The bridge structures have been controlled for wind without traffic load in both ultimate limit state and service limit state for a wind field with return period equal to 50 years.

Road bridges in wind class 1 shall also be checked in SLS and ULS with simultaneous wind and traffic loads. Wind loads are calculated with a wind field where the peak wind velocity at the highest point of the deck is equal to 35 m/s, or with a return period of 50 years if this gives a lower value.

Calculations from wind appendix	Bridge 1	Bridge 2
	Wind load Without traffic. $V_{b,0}=27\text{m/s}$	
Deck	$q_{y,Deck}= 11.024 \text{ kN/m}$	$q_{y,Deck}= 11.207 \text{ kN/m}$
	$q_{z,Deck}= 2.586 \text{ kN/m}$	$q_{z,Deck}= 3.615 \text{ kN/m}$
Arch	$q_{z,Arch}= 1.933 \text{ kN/m}$	$q_{z,Arch}= 2.809 \text{ kN/m}$
Hangers	$q_{z,Hanger}= 0.080 \text{ kN/m}$	$q_{z,Hanger}= 0.080 \text{ kN/m}$
	Wind load With traffic. $V_{b,0}^*=24.3\text{m/s}$	
Deck	$q_{y,Deck}^*= 7.717 \text{ kN/m}$	$q_{y,Deck}^*= 7.845 \text{ kN/m}$
	$q_{z,Deck}^*=2.534 \text{ kN/m}$	$q_{z,Deck}^*=3.545 \text{ kN/m}$
Arch	$q_{z,Arch}^*= 1.353 \text{ kN/m}$	$q_{z,Arch}^*= 1.967 \text{ kN/m}$
Hangers	$q_{z,Hanger}^*= 0,056 \text{ kN/m}$	$q_{z,Hanger}^*= 0,056 \text{ kN/m}$

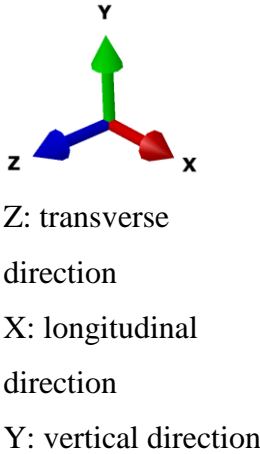


Table 6.2 Characteristic wind load

6.2.3 Traffic load

Traffic Loads are calculated according to EC1-2 [42] . The road bridges are designed for three different traffic load models LM1, LM2 and LM4. LM3, which includes special vehicles is not covered in this thesis. The bridge deck is divided into 4 different traffic lanes, with different combinations of load placement. The load placements used Abaqus and Focus Konstruksjoner are shown in appendix C. Traffic load calculations are given in appendix B.

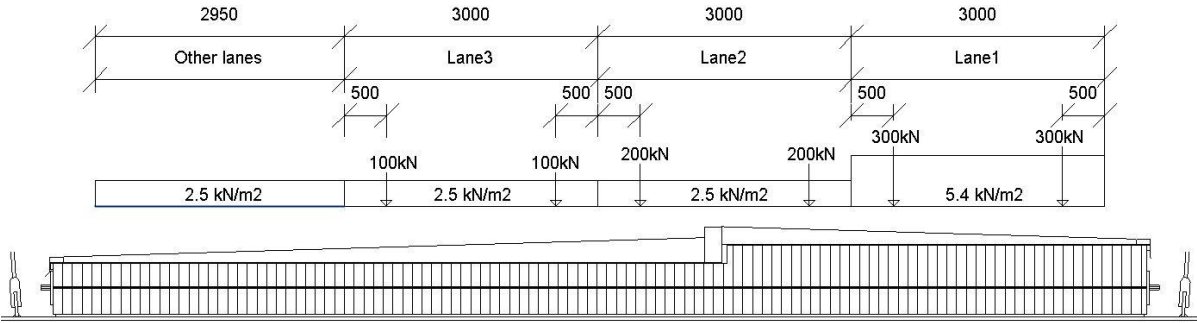


Figure 6.5 LM1 traffic load distribution. From appendix C.

6.2.3.1 Vertical traffic loads

Load Model 1 consists of double axel concentrated loads $\alpha_Q \times Q_k$, Tandem systems and uniformly distributed loads $\alpha_q \times q_k$, on the traffic Lanes. α_Q and α_q are adjustment factors selected depending on traffic, given in EC1-2 [42] in the national annex. No more than one

tandem system should be applied for each lane, traveling centrally along the lanes axis. The uniformly distributed loads should be applied only in the unfavourable parts of the lane [42]. The axle load are distributed over four quadratic load zones, 400x400 mm². The placement of the axle loads and uniformly distributed loads in the traffic lanes are shown in Figure 6.6.

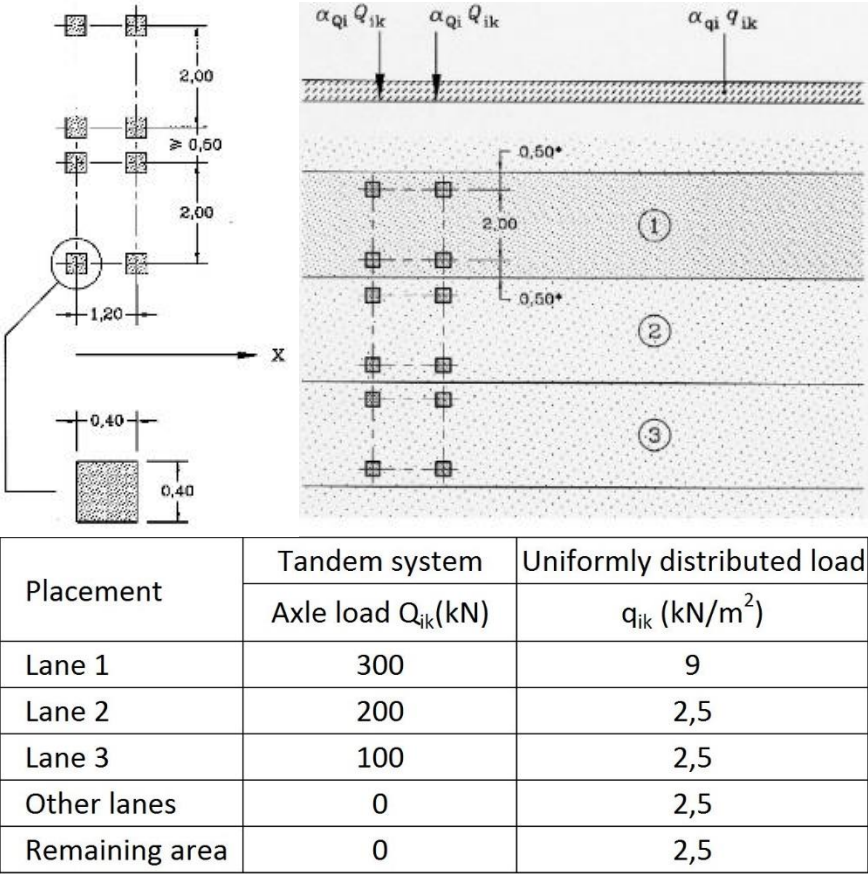


Figure 6.6 Placement and load magnitude of LM1 [42]

Load Model 2 (LM2), shall be used for local design of the bridge deck. LM2 consists of a single axle load ($\beta_Q \times Q_{ak}$), where Q_{ak} is 400 kN and the load factor β_Q is given for each country's national annex. The load should be place on the most unfavourable position on the bridge deck, with a minimum distance of 0.5 meters from the guardrail or other obstacles. The axle load is distributed on two square load zones of 350x600 mm², see Figure 6.7. When relevant, or unfavourable, a single wheel load of 200 kN should be used [42].

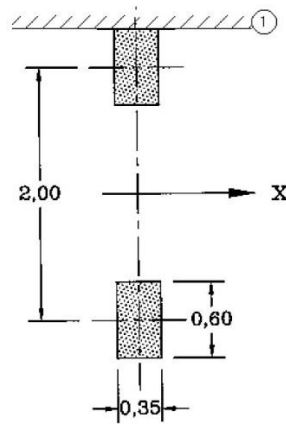


Figure 6.7 Axle load placement LM2. [42]

Load model 4 (LM4), apply for a gathering crowd on the road lanes. It is represented by an uniformly distributed load equal to 5 kN/m^2 . The load should be applied on all relevant parts of the length and width of the deck EC1-2 [42].

6.2.3.2 Horizontal traffic loads

Horizontal loads associated with braking forces and acceleration forces, shall be applied in the longitudinal and transverse direction. Forces are calculated according to EC1-2 [42]. Acceleration forces are in equal to braking forces, applied in the opposite direction [42]. Calculations on braking forces are given in appendix B.

6.2.4 Earthquake

Earthquake loads are calculated according to EC8-1[43]. Ground peak acceleration in the area is given by figure NA.3 (901), and has the value 0.4 m/s^2 with a return period equal to 475 years. The reference peak value for bedrock acceleration equals

$$a_{gR} = 0.8 \times a_{g40Hz} = 0.24 \text{ m/s}^2$$

Soil factor (S), depending ground conditions has to be selected from EC8-1 Table NA.3.3 [43]. Soil conditions have been set to be classification C [18], which leads to a soil factor, $S = 1.4$.

According to EC8-1 NA:3.2.1(5) [43] and EC8-2 NA.2.3.7(1) [44], the bridge construction can be dimensioned after regulations for low seismic actively if

$$a_g \times S = \gamma_I (0,8 \times a_{g40Hz}) S < 0,05 \times g$$

Seismic classification : II

$$\gamma_1 := 1.0$$

$$a_{g40Hz} := 0.4 \frac{m}{s^2}$$

$$S := 1.4$$

$$\gamma_1 \cdot (0.8 \cdot a_{g40Hz}) \cdot S = 0.448 \frac{m}{s^2}$$

$$0.448 \frac{m}{s^2} \leq 0.49 \frac{m}{s^2}$$

There are no requirements for analytical calculations

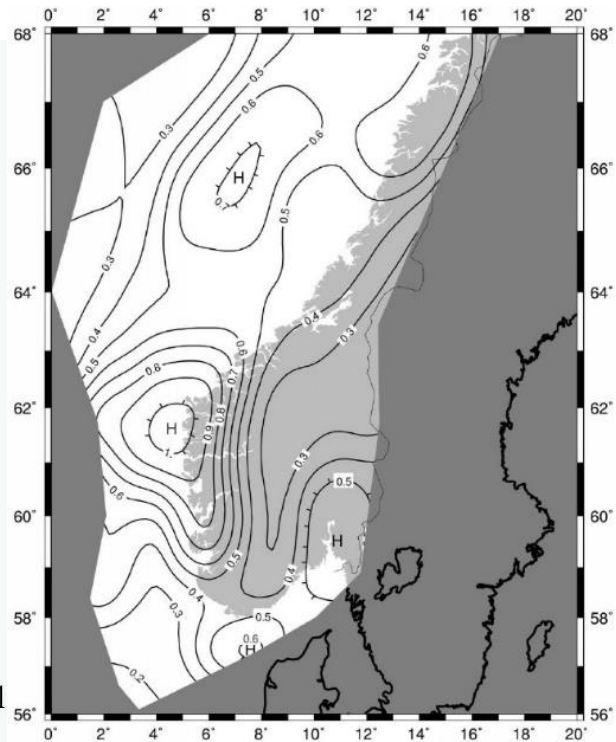


Figure 6.8 Seismic zones, south Norway (a_{g40Hz}) [43]

Calculations show that there are no need for a separate earthquake analysis. It is assumed that the forces from other horizontal loads, wind and traffic, will be adequate. The calculations regarding earthquake given in appendix D.

6.2.5 Load events for hangers

According to HB N400, 7.9.9 [19] the bridge has to be dimensioned for two possible events regarding the hangers.

1. Replacement of an arbitrary hanger. The situation has to be checked within the normal load situations, which is usually ULS traffic loads. In addition the area where the maintenance work will take place has to be loaded with loads from the scaffolding, crane and other pay loads necessary to perform the task.
2. Loss of an arbitrary hanger. The situation should be checked in the progressive limit state.

6.2.5.1 Replacement of hangers

The replacement of a hanger will be carried out while closing the traffic lane closest to the hanger, and the analyses will be performed with traffic load LM1 in the ultimate limit state. The load from the scaffolding, crane and other pay loads are simplified to two loads consisting

of 100 kN distributed over four areas of 400x400 mm². The traffic loads are applied like shown in figure 6.9.

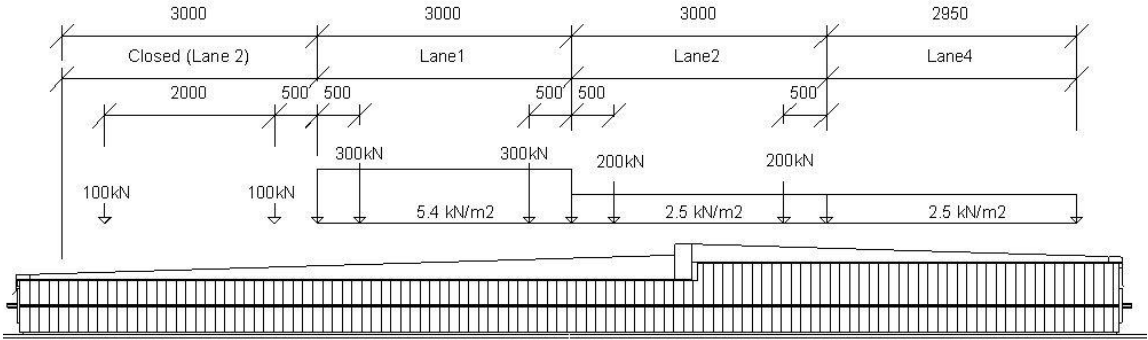


Figure 6.9 Traffic load during hanger change.

6.2.5.2 Loss of hangers

The possibility that the structure could experience loss of hangers have been treated by removing multiple hangers from the structure. The analysis with removed hangers have been conducted while applying the load models for progressive limit state. The hangers where removed below the part of the arches that where already experiencing the highest bending moments.

Figure 6.10 illustrates the removed hangers on Bridge 1. Only the hangers in the hanger-set closest to the roadway are removed, because these are the hangers most likely to be damaged in case of an accident. In total 8 hangers have been removed in the analysis.

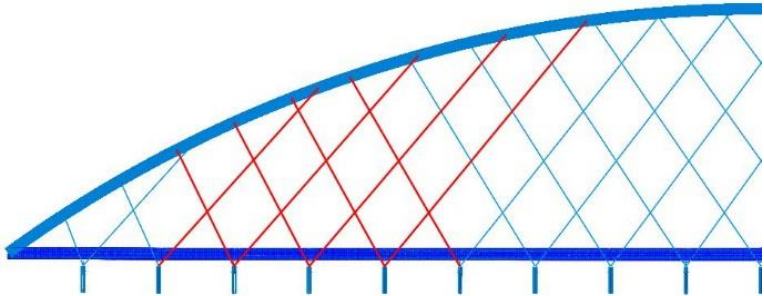


Figure 6.10 Removed hangers on Bridge 1

Figure 6.11 illustrates the removed hangers on Bridge 2. The hangers have been removed on both arches, so in total 8 hangers have been removed from in the analysis.

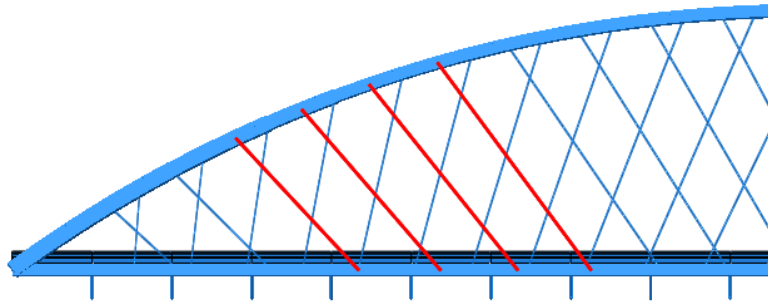


Figure 6.11 Removed hangers on Bridge 2

6.3 Load models

The bridge structure shall be checked in the ultimate limit state (ULS), service limit state (SLS), fatigue limit state (FLS) and progressive limit state (PLS).

6.3.1 Ultimate limit state

The ULS load models are made according to EC0 amendment A1 Table NA.A2.4 (B) [45]. The values in Table 6.3 shows the load factor (γ) multiplied by the combination factor (ψ). ULS loads are used for the design check of material strength and structural stability.

Load model Temperature 6b has been included in the analysis but the results always showed less stresses compared to LM1 1b, which is to be expected since the thermal expansion in timber is so small and the self-weight of the bridge is such a big part of the overall loading. Therefore, no design checks was performed with the loads from the temperature steps.

6.3.2 Service limit state

The SLS load models for frequent loads are made according to EC0 amendment A1 Table NA.A2.6 [45]. The values in Table 6.4 Load models for SLS - frequent loadTable 6.4 are the result of load factor (γ) multiplied by the combination factor (ψ). The load models are used in Abaqus to control vertical and horizontal displacements. It was also used in Focus Konstruksjon when designing the transverse beam. The requirements used for vertical and horizontal displacement w is:

$$w = \frac{L_{bridge}}{500}$$

ULS STR/GEO-set B	1a	1b	2a	2b	4a	4b	5a	5b	6b
Permanent loads	gr1a	gr1a	gr1b	gr1b	gr4	gr4	Wind without traffic	Wind without traffic	Temp.
Self weight	1,35	1,20	1,35	1,20	1,35	1,20	1,35	1,20	1,20
Variable loads	Variable loads with a favourable effect: 0,0								
Traffic, LM1	0,95	1,35	-	-	-	-	-	-	0,95
Traffic, pedestrian	0,95	1,35	-	-	0,95	1,35	-	-	0,95
Traffic, LM2	-	-	0,95	1,35	-	-	-	-	-
Traffic, LM4	-	-	-	-	0,95	1,35	-	-	-
Traffic, horizontal forces	0,95	1,35	-	-	-	-	-	-	0,95
Wind with traffic	1,12	1,12	1,12	1,12	1,12	1,12	-	-	1,12
Wind without traffic	-	-	-	-	-	-	1,12	1,6	-
Temperature	0,84	0,84	0,84	0,84	0,84	0,84	0,84	0,84	1,2

Table 6.3 Load models for ULS STR/GEO - set B

SLS	1	2	3	4	5	6
Frequent	gr1a	gr1b	gr3	Wind without traffic	Wind with traffic	Temp.
Permanent loads						
Self weight	1,00	1,00	1,00	1,00	1,00	1,00
Variable loads	Variable loads with a favourable effect: 0,0					
Traffic, LM1	0,70	-	-	-	0,20	0,20
Trafikk, pedestrian	0,70	-	0,70	-	0,20	0,20
Trafikk, LM2	-	0,70	-	-	-	-
Trafikk, LM4	-	-	0,70	-	-	-
Traffic, horizontal forces	0,70	-	-	-	0,20	0,20
Wind with traffic	0,60	0,60	0,60	-	0,60	0,60
Wind without traffic	-	-	-	0,60	-	-
Temperature	-	-	-	-	-	0,60

Table 6.4 Load models for SLS - frequent load

6.3.3 Progressive limit state

The load models for PLS have been made according to EC0, A1. Table 6.5 shows the load models and the load factors used in the analysis.

PLS		
Accidental load		
Variable loads	1	2
Self weight	1,00	1,00
Variable loads		
Traffic, LM1	0,20	0,20
Traffic, pedestrian	0,20	0,20
Traffic, LM2	0,20	0,20
Traffic, LM4	0,20	0,20
Traffic, horizontal forces	-	-
Wind with traffic	-	-
Wind without traffic	-	-
Temperature	-	-
Accidental load		
Collision	1,00	-
fracture in hangers	-	1,00

Table 6.5 load models for PLS - accidental load

7 Cost

In order to be a good and equal alternative to steel and concrete bridges, the timber bridges should also be competitive when it comes to cost. This is only a conceptual study. Therefore, no actual bid from a contractor exist to compare against the bids on Driva bridge. So in order to get a realistic cost estimate on the timber bridges, it was decided to only look at the cost of the main parts of the bridges, i.e. arches, wind truss, bridge deck, hangers, transverse beams and ties. All other costs associated with the construction of the bridge is assumed to be the same.

The cost of the timber parts is based on empirical data from previous and similar projects. The data was provided from the largest manufacturer of glulam timber in Norway, Moelven Industrier ASA. The prices include the cost for material, production and assembly.

Driva Bridge had six different contractors making bids on the project. The prices used for the cost estimates on the steel parts for Bridge 1 and 2 are the average prices from all the six contractors.

The hanger layout on Driva Bridge and Bridge 2 is identical, but Bridge 1 has twice the amount of hangers. Therefore, it was of great interest to see how this affected the total cost of the bridge. The necessary information for which the hanger cost is based, are given in Table 7.1.

	Bridge 1	Bridge 2
Hanger diameter	30mm	40mm
Average system length	17m	15m
Number of hangers	152	84

Table 7.1 Hanger parameters used for cost estimates

The hanger manufacturer contributed with cost estimates on the different hanger layouts. The actual prices are not open for general view and can only be found in the confidential appendix I.

8 Feasibility

One of the great advantages when it comes to using timber is its low weight to strength ratio, something that is relevant when it comes to the construction and erection of the glulam network arch. To consider the different possibilities of erection, the self-weight for the different parts and assemblies are presented in Table 8.1.

Bridge 1		Bridge 2	
Single Arch module	20 tonne	Single Arch module	12 tonne
Single Arch	80 tonne	Single Arch	49 tonne
Single Arch with hangers	94 tonne	Single Arch with hangers	58 tonne
Arches + Hangers + Transverse Beam	339 tonne	Single Arch + hangers + tie	145 tonne
Arches + Hangers + Transverse Beam + Deck	730 tonne	Arches + Hangers + ties + end beams + Wind Bracing	360 tonne
		Arches + Hangers + tie + end beams + Transverse Beams + Wind bracing	508 tonne
Final weight	1540 tonne	Arches + Hangers + tie + end beams + Transverse Beams + Wind bracing + deck	900 tonne
		Final weight	1715 tonne

Table 8.1 Self-weight for parts and assemblies

First, the method of construction used on Driva Bridge will be explained. Followed by other examples of erecting the network arch bridge. Then the feasibility of Bridge 1 and Bridge 2 are addressed, by looking at the possibility of building the bridges like Driva Bridge and in a more general perspective.

8.1 Construction of Driva Bridge

Driva Bridge was partly build off-site and moved to the bridge site after the steel skeleton was erected. Weighing around 800 tonne, the bridge was transported on multiwheelers placed under each arch end. The bridge was then moved over the river on two temporary fillings, with an opening for the water covered by two temporary bridges, see Figure 8.1 Transport of Driva BridgeFigure 8.1. The formwork and the most time demanding rebar for the concrete deck was in place, but because of the limiting strength of the two temporary bridges, most of the rebar would have to be installed after crossing the river.



Figure 8.1 Transport of Driva Bridge [46]

The bridge is then placed on temporary foundation next to the existing bridges, which it will be replacing. Here the rest of the construction on the deck will be done, and the bridge will take all traffic while they are dismantling the old bridges. Once the new and final foundation has been cast where the old bridges were, the new Driva Bridge, now weighing around 2000 tonne will be moved sideways up to its final foundation.

8.2 Other ways of erecting the network arch

Transporting and erecting the network arch bridge like Driva Bridge is just one out of many possibilities. Per Tveit, the father of network arch bridges, presents different ways of erecting and transporting the bridges in [47].

In big rivers and coastal areas, the network arch can be erected on shore and then lifted in place by floating cranes. The crane “Uglen” in Figure 8.2, has a lifting capacity of 600 tonne, 60 meters above the water [47]. For even heavier lifts, two cranes can be used like at Brandanger Bridge in Norway, where the main span weighed 1862 tonne. Brandanger Bridge was lifted by two big dutch floating cranes that could lift 1200 tonne each [9].



Figure 8.2 Åkvik Sound Bridge lifted in place by a floating crane [47]

Another example for big rivers, if the floating crane is not an option is to drag the erected bridge over the river using a pontoon. The bridge will be erected partly on shore and partly on temporary scaffolding in the river, depending on the how close to land the pontoon can get [47], see Figure 8.3.

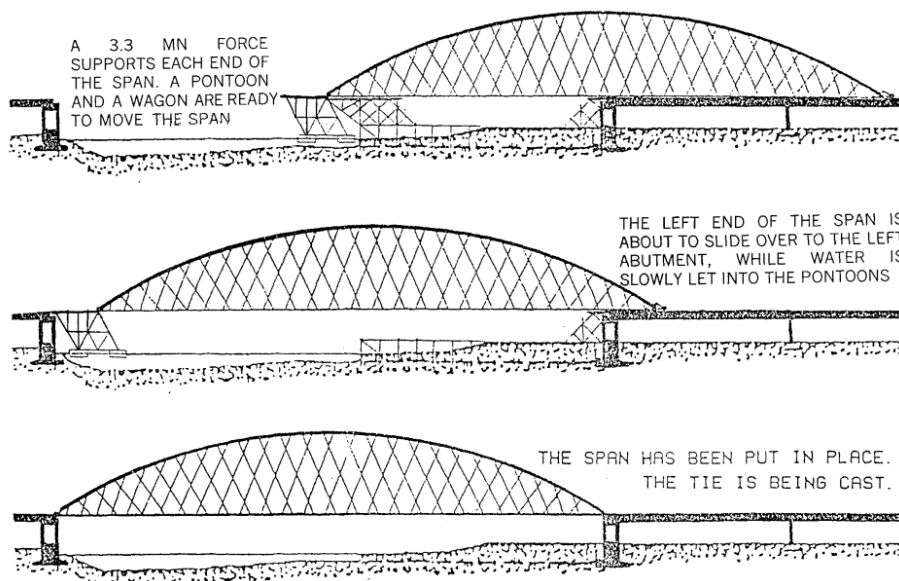


Figure 8.3 Erection procedure for a network arch using pontoon [9]

If the surrounding area allows it, mobile cranes can be used to erect the network arch over the river, and use temporary frame support under the deck until the hangers are installed, see Figure 8.4. If necessary temporary fillings in the river can be made for the mobile cranes, see Figure 8.5.



Figure 8.4 Erection of the arches with mobile cranes [47]



Figure 8.5 Erection of the arches with mobile cranes on temporary fillings [47]

8.3 Construction of Bridge 1

Without ties and transverse end-beams, Bridge 1 cannot be moved like Driva Bridge, because it is dependent on foundation to take its longitudinal forces. Therefore, without some kind of temporary stiff lower chord to take the longitudinal forces, and bracing or guying to keep the arches stable, the network arch would have to be erected on site. The arches would have to be installed on its foundations before loading the hangers with the weight of the transverse beams.

The arch consist of four parts, Trebruhåndboken [16] recommend assembling the arch lying on the ground and then lift the assembled arch in place using cranes, this may not be possible when the arch is as long as 118 meters. Since the proposed splice joint in this thesis is moment

resistant, see chapter 4.1.3, another solution is to assemble the arch in two parts first, and then mount the two parts together like a three-hinged arch. By doing so, the lifting weight and distance is reduced by half. If that proves difficult as well, one could install one part after another, placing temporary supports under the erected arch parts like shown in Figure 8.5.

Until the transverse beams have been installed with a temporary bracing between them, the arches would have to be guyed in order to have sideways stability. Possibly, the glulam deck would also have to be installed in order to have enough self-weight to be stable. This has not been investigated any further in this thesis.

8.4 Construction of Bridge 2

Bridge 2 can be erected in the same way as described for Bridge 1 and Driva Bridge. In addition, bridge 2 can be lifted as a whole or as different assemblies of parts, see Table 8.1, depending on the lifting capacity. In general, with the lightest skeleton weighing 360 tonne, dragging the bridge across the water on pontoons or using a floating crane will not be a problem.

9 Results

This chapter present the results from the analyses regarding

- Displacements in SLS
- Free vibration analyses
- Structural stability with buckling curves, buckling factor and the critical axial force for the load models with the highest utilization and the lowest stability of the structure.
- Utilization for all load models are tabulated, and a graph showing the utilization along the arch and tie. Only the worst case are displayed.
- Cost calculations presenting bridge alternative 1 and 2 compared to Driva Bridge.

9.1 Service Limit State

The displacement results from all SLS load models analysed in Abaqus, are presented in Table 9.1. The load models are described in chapter 6.3.2, and the placement and magnitude of the loads used in the analyses are presented in appendix B and C.

Load System	Bridge 1		Bridge 2	
	Vertical displacemen	Horizontal displacemen	Vertical displacemen	Horizontal displacemen
	U2 (mm)	U3 (mm)	U2 (mm)	U3 (mm)
Maximum allowed displacement	222	222	222	222
Gravity only	79	20	141	3
Gr1a LM1 (TS and UDL systems)	124	153	197	30
Gr1b LM2 (Single axle)	91	171	158	28
Gr3 Uniformly distributed load	85	134	187	28
Wind with traffic	94	138	160	28
Wind without traffic	83	182	147	39
Temperature	88	137	174	29

Table 9.1 Results from vertical and horizontal displacement analyses

Results from the free vibration analysis of Bridge 1 shows that the first four modes of free undamped vibration is outside the critical range for pedestrian traffic, stated in chapter 2.3.

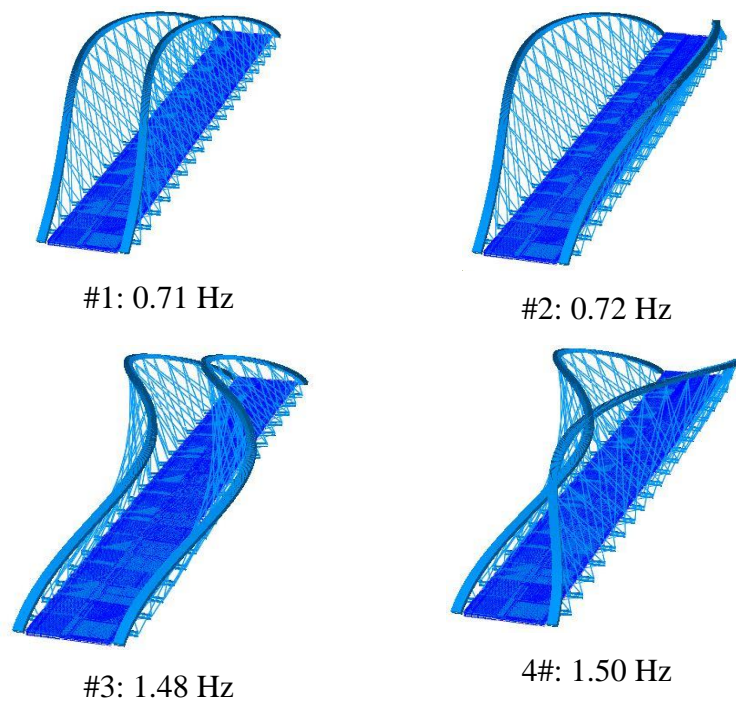


Figure 9.1 The first four modes of free vibration. Bridge 1

Results from the free vibration analysis of Bridge 2 shows that the first two modes of free undamped vibration is outside the critical range for pedestrian traffic stated in chapter 2.3.

However, mode 3 and 4 is not. Testing and analysis of the dynamic effect on Bridge 2 are recommended as further work.

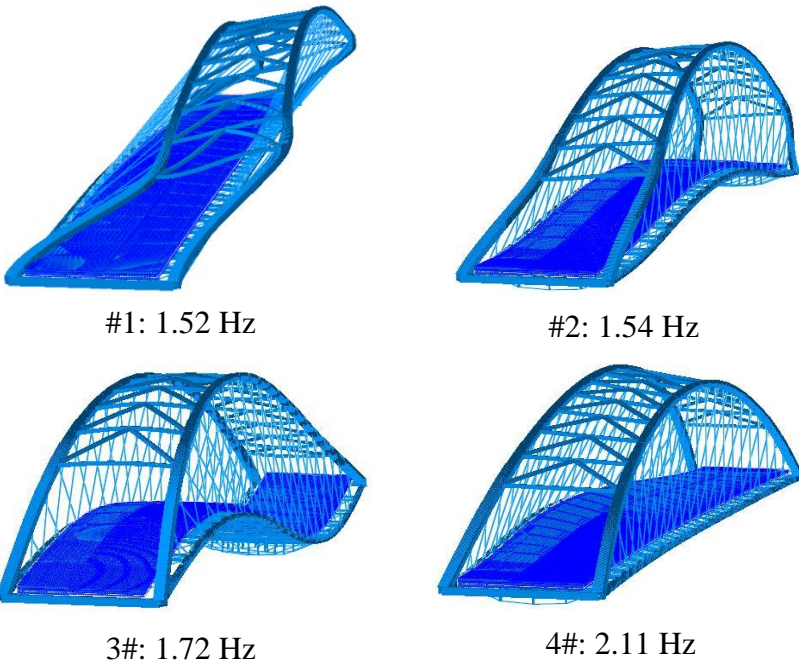


Figure 9.2 The first four modes of free vibration. Bridge 2

9.2 Stability

To be able to say anything about the stability of bridge 1 and 2 compared to Driva Bridge, several buckling analyses has been made in Abaqus

Global stability has been tested for various load situations in ULS. The results shown represent the cases with the lowest buckling factors in the following situations: gravity only, full load, half load, hanger change and removed hangers. In addition results from buckling analysis of Bridge 1 with 14 meters rise of the arch, and with wind bracing are shown. More information on these versions of Bridge 1 can be found in chapter 10.

For Bridge 1, some of the load models in the analyses only produced buckling modes out-of-plane and many negative buckling modes, see chapter 5.5. In these cases the highest buckling factor for the out-of-plane buckling was used in the calculation of in-plane buckling length. This is conservative since the real buckling factor for in-plane buckling would be higher, resulting in a shorter buckling length. To get the real buckling factor for in-plane buckling the analysis would have to run for days, which was considered as a waste of time since buckling out-of-plane has the highest utilization and is the biggest problem with Bridge 1.

9.2.1 Driva Bridge

Figure 9.3 shows the buckling modes along with its buckling factor and critical axial force, for the load model with gravity only [18].

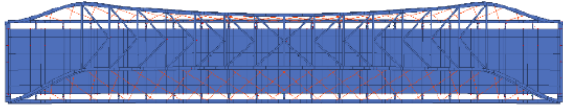
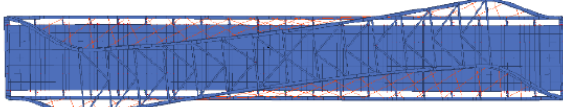
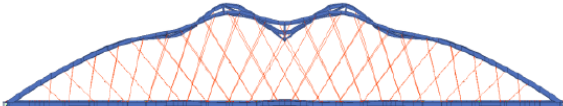

Mode		λ	$N_{cr} = \lambda \cdot N_x$
#1		3.459	35504
#2		5.417	55601
#3		8.972	92090
#4		9.128	93691

Figure 9.3 Buckling analysis, ULS gravity. Driva Bridge[18]

Figure 9.4 shows the buckling modes along with its buckling factor and critical axial force, for a load model with traffic and uniformly distributed load [18].

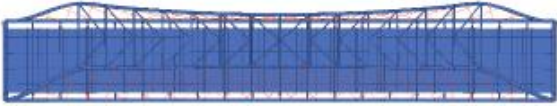


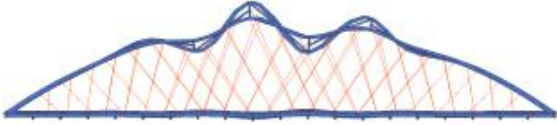
Mode		λ	$N_{cr} = \lambda \cdot N_x$
#1		2.787	35726
#2		4.345	55698
#3		7.037	90206
#4		7.155	91719

Figure 9.4 Buckling analysis, ULS gravity and UDL. Driva Bridge [18].

9.2.2 Bridge 1

Figure 9.5-9.15 shows the buckling modes along with its buckling factor and the critical axial force. Presenting the first four buckling modes out-of-plane and the first in-plane buckling mode, for the load situations described in 9.2.

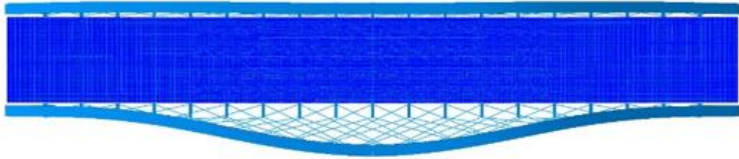
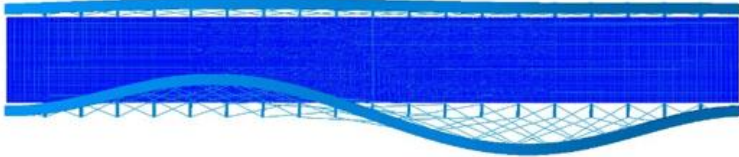
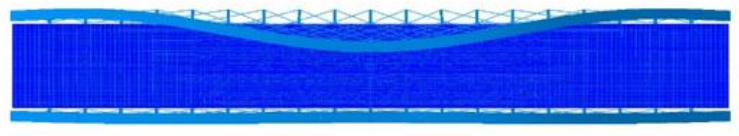
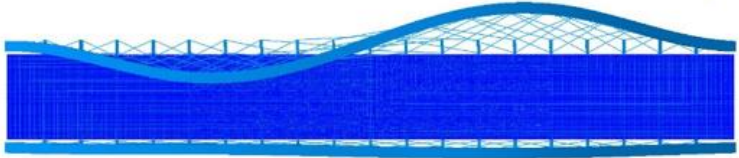

	Mode	λ	$N_{cr}=\lambda \cdot N_x$ (kN)
#1		2.476	21457
#2		2.588	22428
#3		2.765	23961
#4		2.895	25088
#6		6.865	59542

Figure 9.5 Buckling analysis, ULS gravity. Bridge 1

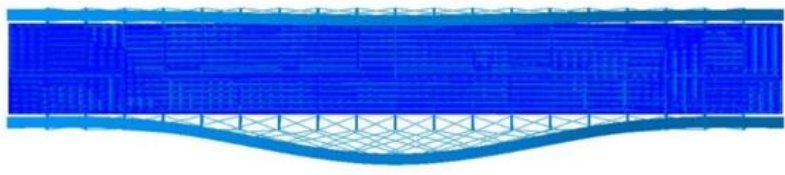
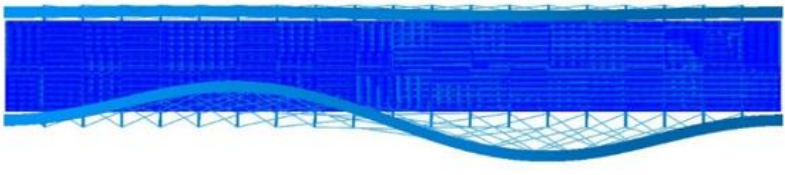
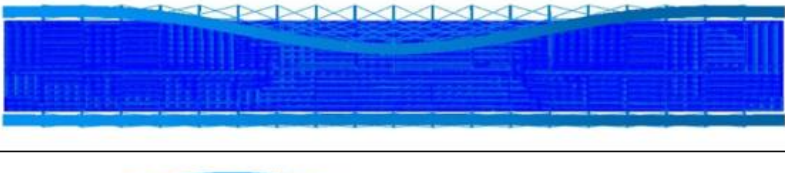
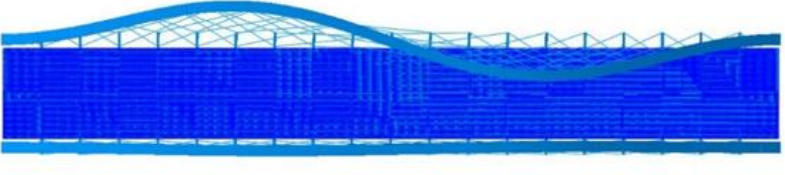
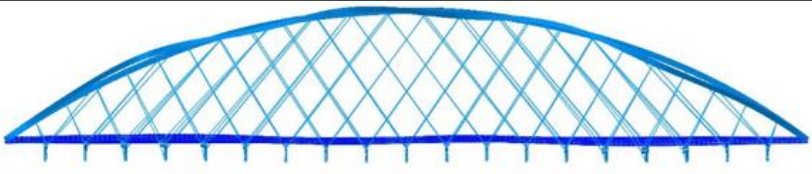
	Mode	λ	$N_{cr}=\lambda \cdot N_x$ (kN)
#1		1.764	21702
#2		1.816	22342
#3		2.039	25086
#4		2.092	25738
#6		4.868	59891

Figure 9.6 Buckling analysis, ULS LM1 Eq 1b. Bridge 1

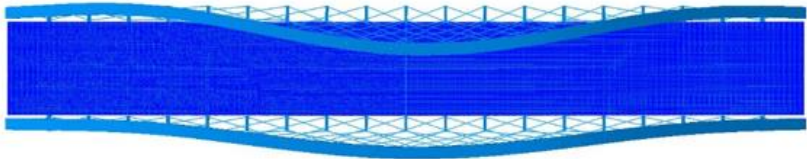
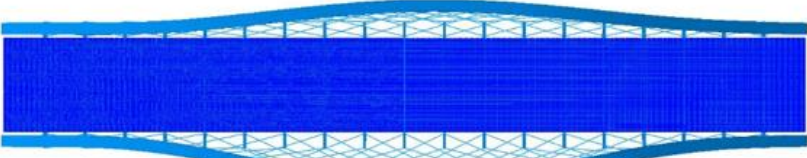
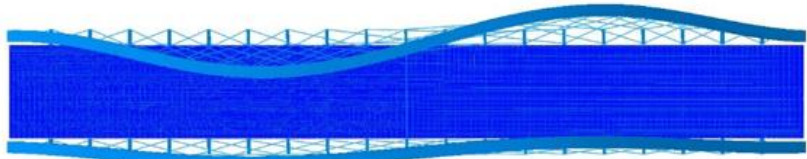
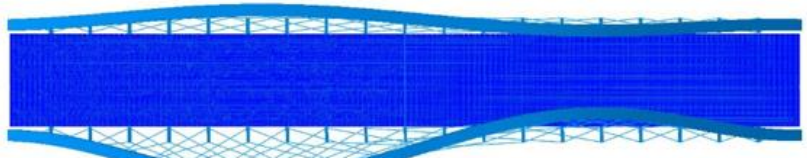
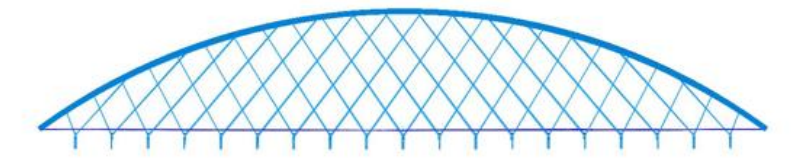
	Mode	λ	$N_{cr}=\lambda \cdot N_x$ (kN)
#1		2.047	22699
#2		2.095	23231
#3		2.157	23919
#4		2.192	24307
#5		5.398	59858

Figure 9.7 Buckling analysis, ULS LM1 Eq 1a, half load. Bridge 1

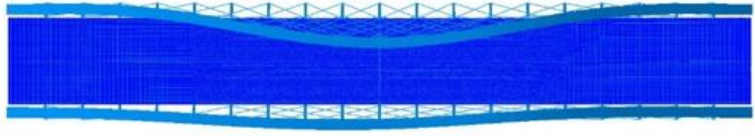
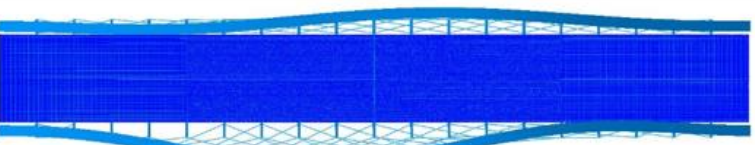
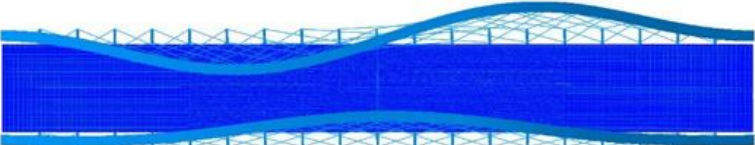
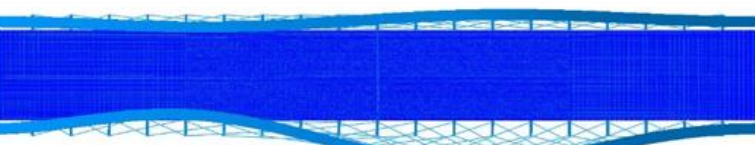
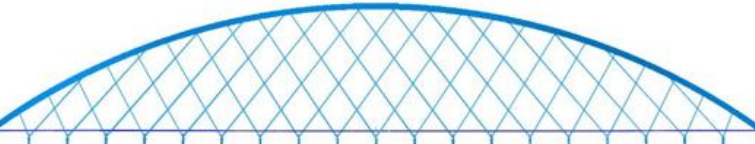
	Mode	λ	$N_{cr}=\lambda \cdot N_x$ (kN)
#1		3.280	21523
#2		3.380	22180
#3		3.454	22665
#4		3.546	23269
#5		8.649	56754

Figure 9.8 Buckling analysis, PLS gravity, removed hangers. Bridge 1

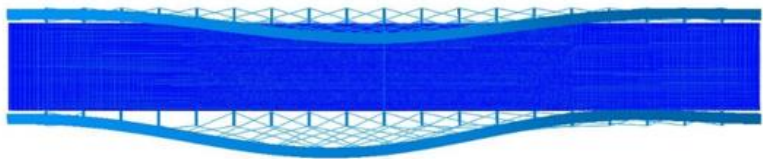
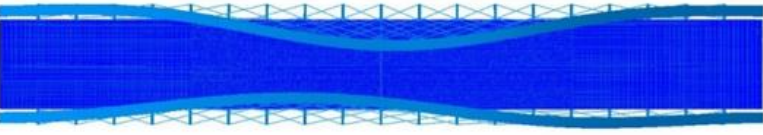
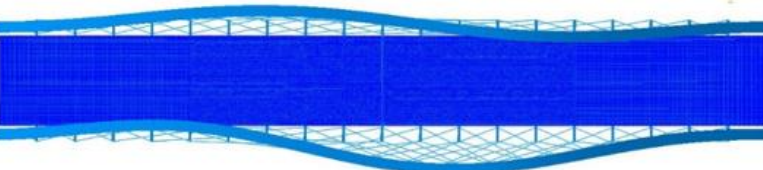
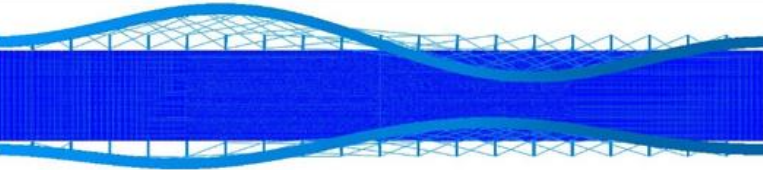
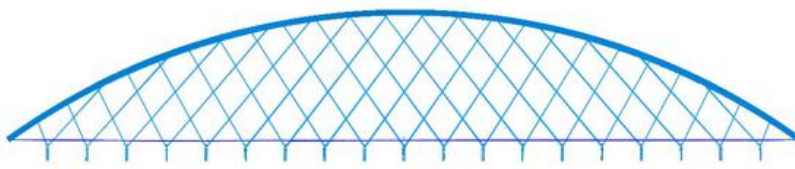
	Mode	λ	$N_{cr}=\lambda \cdot N_x$ (kN)
#1		3.003	22087
#2		3.063	22528
#3		3.157	23220
#4		3.197	23514
#5		8.084	59457

Figure 9.9 Buckling analysis, PLS LM1, removed hangers. Bridge 1

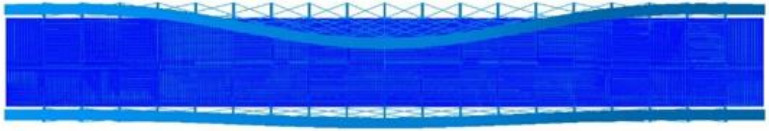
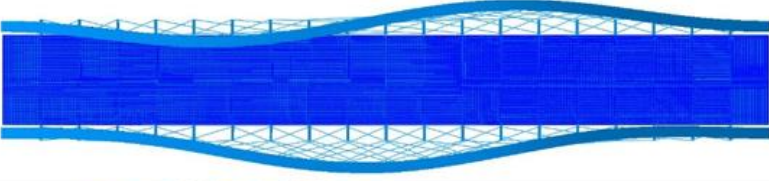
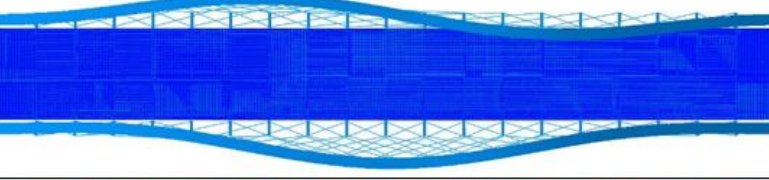
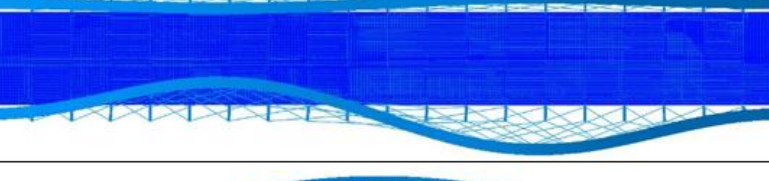
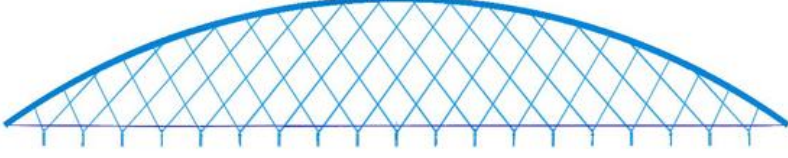
Mode		λ	$N_{cr} = \lambda \cdot N_x$ (kN)
#1		2.433	21412
#2		2.550	22442
#3		2.556	22495
#4		2.684	23621
#4		2.684	23621

Figure 9.10 Buckling analysis, ULS gravity, hanger change. Bridge 1

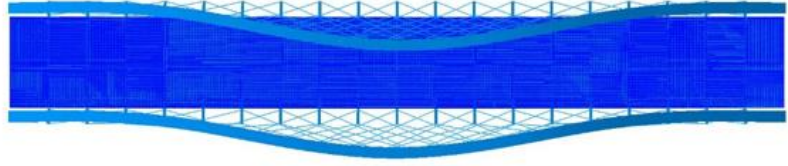
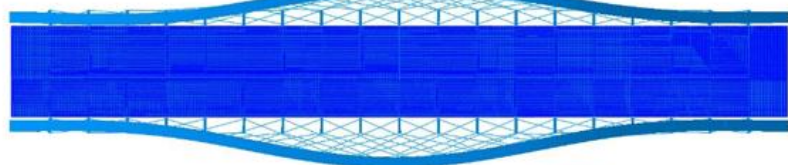
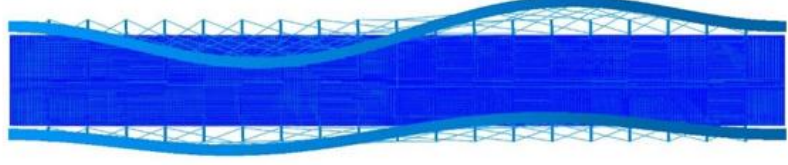
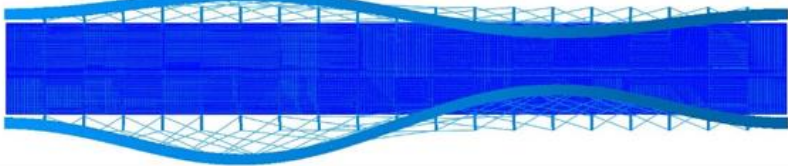
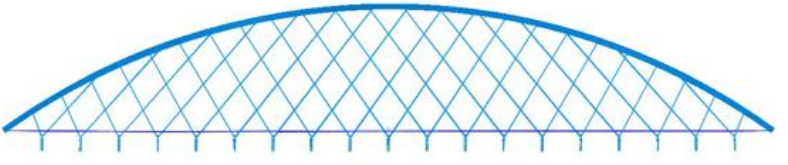
	Mode	λ	$N_{cr}=\lambda \cdot N_x$ (kN)
#1		1.953	22229
#2		1.993	22684
#3		2.047	23298
#4		2.086	23742
#5		2.086	23742

Figure 9.11 Buckling analysis, ULS LM1 Eq 1a, hanger change. Bridge 1


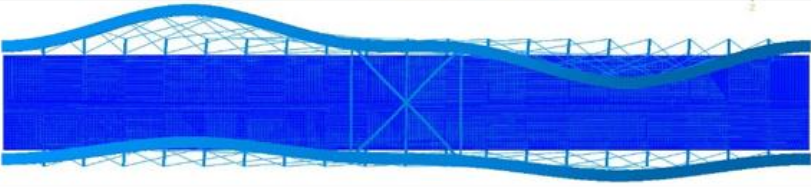
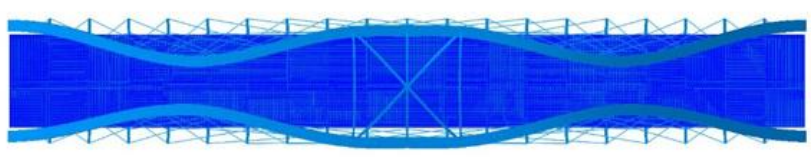
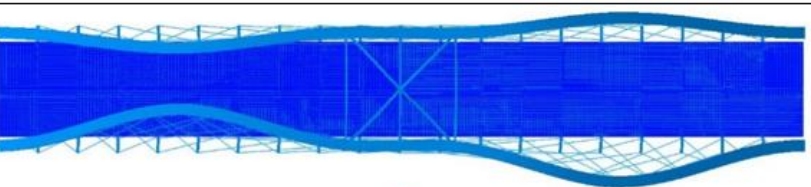
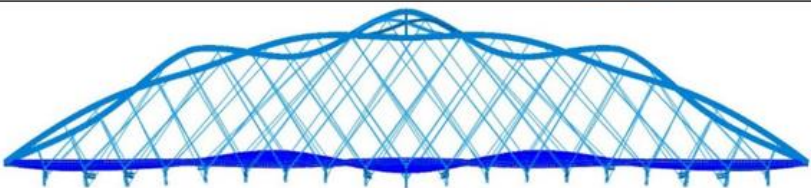
	Mode	λ	$N_{cr}=\lambda \cdot N_x$ (kN)
#1		3.543	31373
#2		5.632	49871
#3		5.913	52360
#4		6.064	53697
#5		7.837	69397

Figure 9.12 Buckling analysis, ULS gravity, with wind trusses. Bridge 1

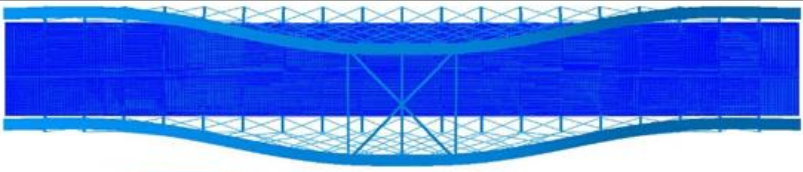
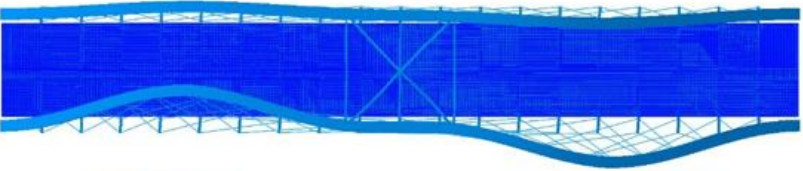
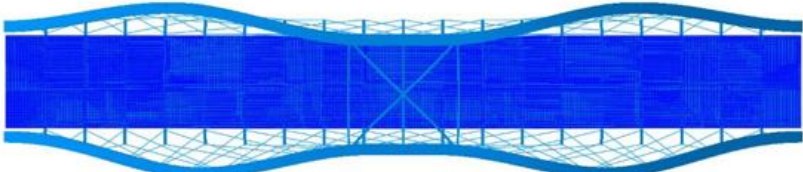
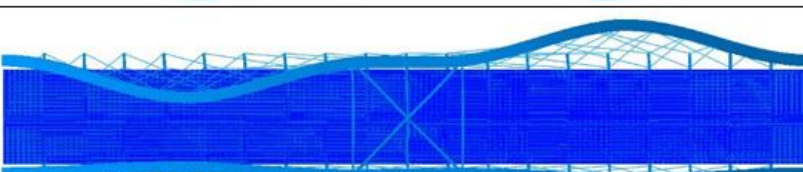

	Mode	λ	$N_{cr}=\lambda \cdot N_x$ (kN)
#1		2.706	32204
#2		4.144	49318
#3		4.463	53114
#4		4.738	56387
#5		5.977	71132

Figure 9.13 Buckling analysis, ULS LM1 Eq 1b, with wind trusses. Bridge 1

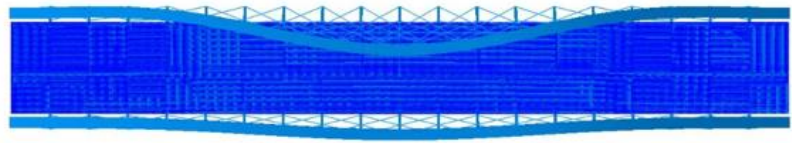
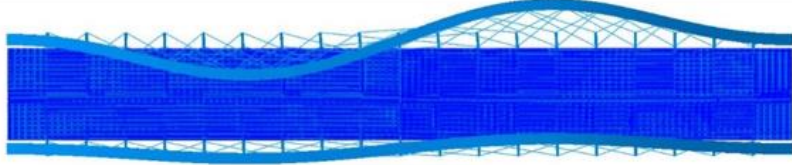
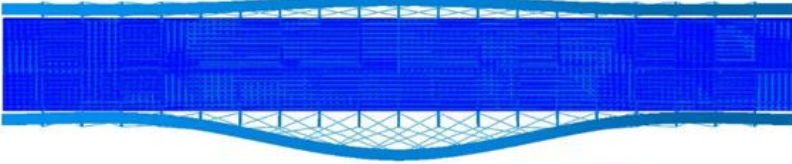
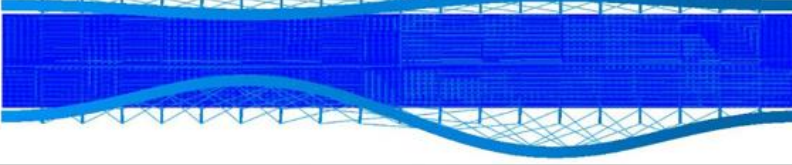

	Mode	λ	$N_{cr}=\lambda \cdot N_x$ (kN)
#1		2.590	27887
#2		2.644	28468
#3		2.750	29609
#4		2.809	30245
#5		6.152	66239

Figure 9.14 Buckling analysis, ULS gravity, 14m rise of arch. Bridge 1

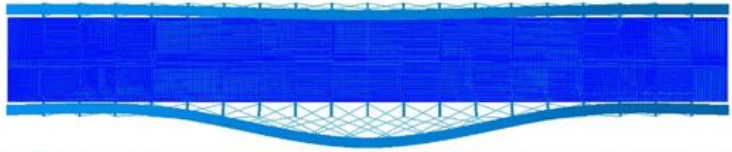
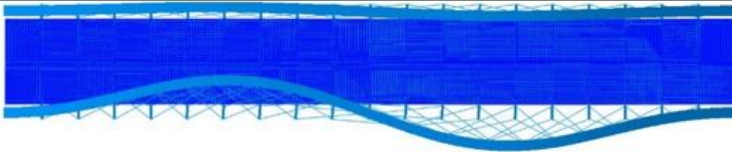
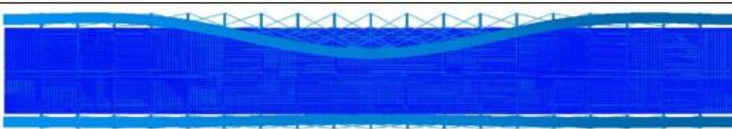
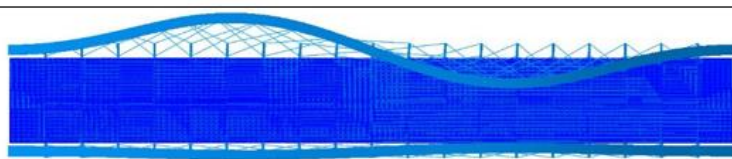
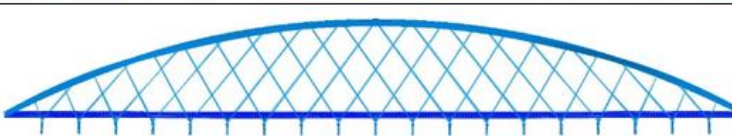
	Mode	λ	$N_{cr}=\lambda \cdot N_x$ (kN)
#1		1.872	28599
#2		1.888	28843
#3		2.124	32448
#4		2.141	32708
#5		4.497	68701

Figure 9.15 Buckling analysis, ULS LM1 Eq 1b. Bridge 1, 14m rise of arch

9.2.3 Bridge 2

Figure 9.16-9.21 shows the buckling modes along with its buckling factor and the critical axial force. Presenting the four buckling modes, for the load situations described in 9.2.

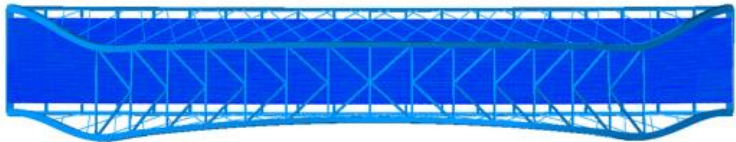
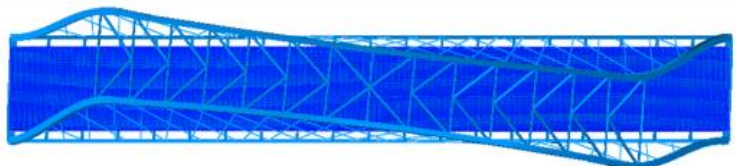


	Mode	λ	$N_{cr} = \lambda \cdot N_x$ (kN)
#1		6.605	61981
#2		6.838	64168
#3		8.339	78253
#4		9.129	85666

Figure 9.16 Buckling analysis, ULS gravity. Bridge 2

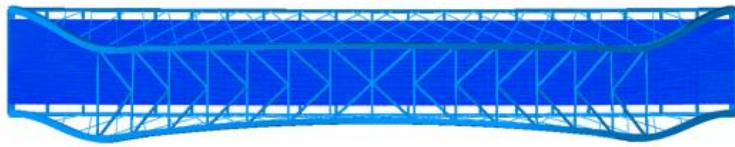
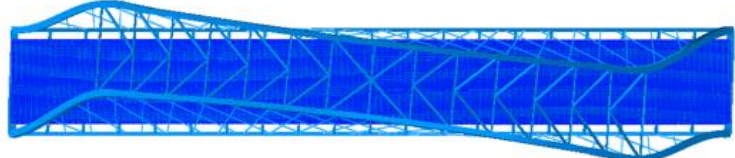
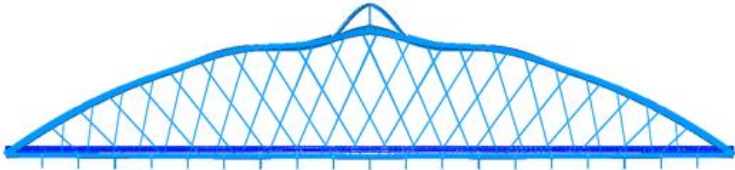

	Mode	λ	$N_{cr} = \lambda \cdot N_x$ (kN)
#1		5.130	62894
#2		5.275	64671
#3		6.460	79200
#4		7.052	86458

Figure 9.17 Buckling analysis, ULS LM4 Eq 4b. Bridge 2

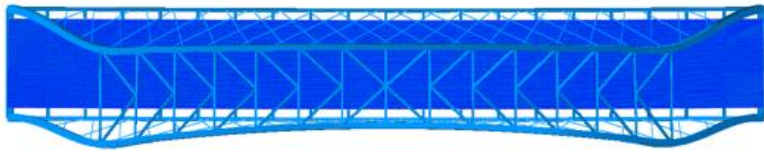
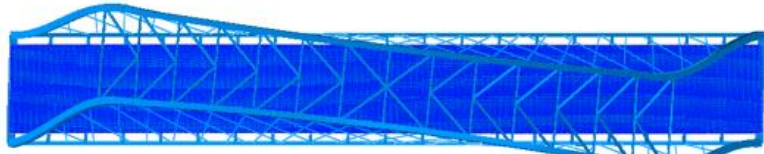


	Mode	λ	$N_{cr}=\lambda \cdot N_x$ (kN)
#1		5.865	64456
#2		6.660	73193
#3		7.708	84710
#4		8.397	92283

Figure 9.18 Buckling analysis, ULS LM4 Eq 4b, half load. Bridge 2

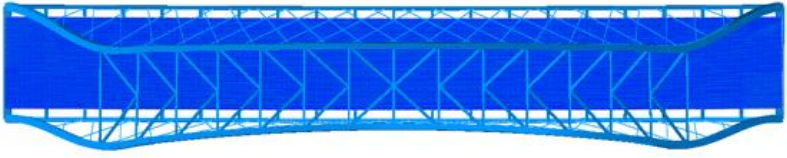
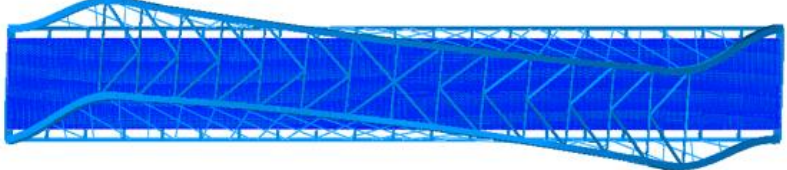
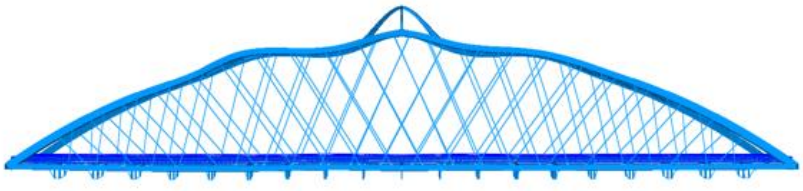
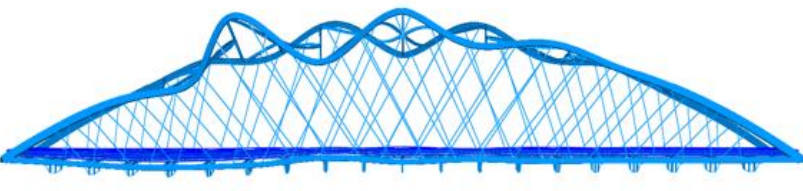
	Mode	λ	$N_{cr} = \lambda \cdot N_x$ (kN)
#1		5.333	61927
#2		5.624	65305
#3		6.770	78613
#4		7.212	83746

Figure 9.19 Buckling analysis, ULS LM1 Eq 1a, hanger change. Bridge 2

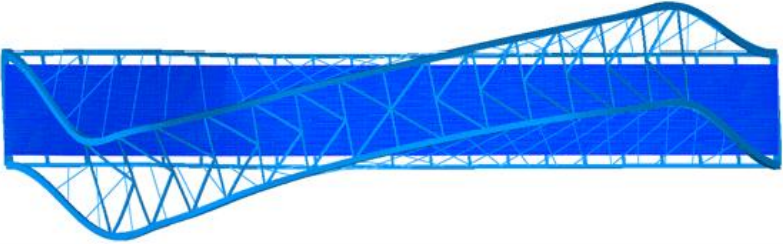
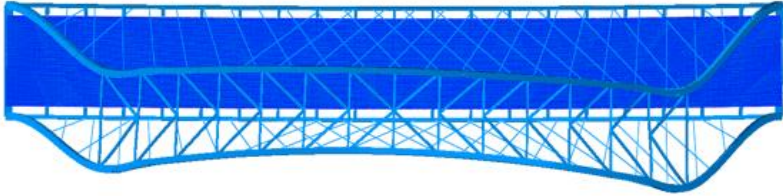
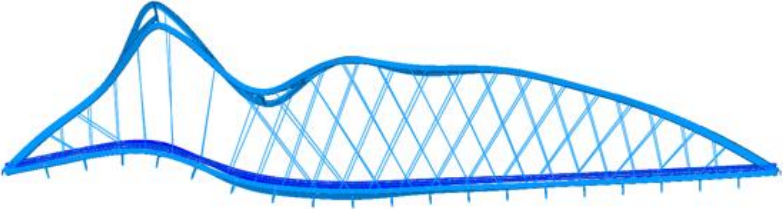

	Mode	λ	$N_{cr}=\lambda \cdot N_x$ (kN)
#1		7.521	57182
#2		8.109	61652
#3		9.496	72198
#4		10.467	79580

Figure 9.20 Buckling analysis, PLS LM1 Eq 1a, removed hangers. Bridge 2

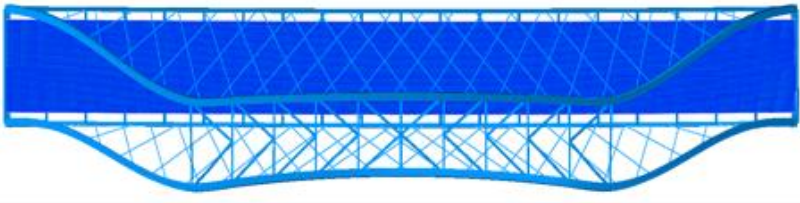
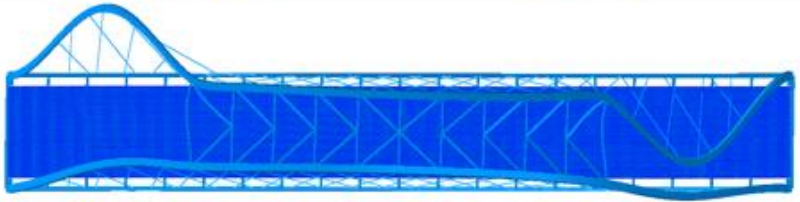
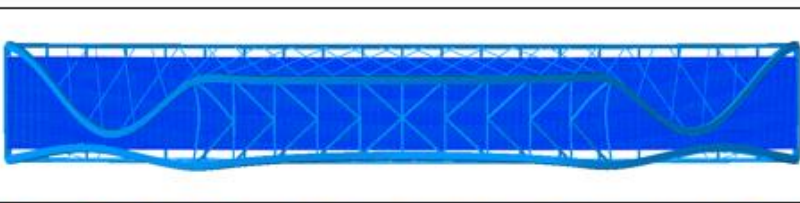
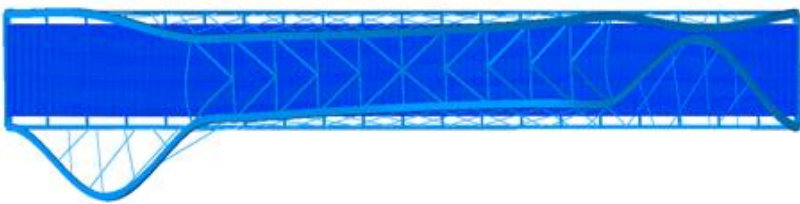
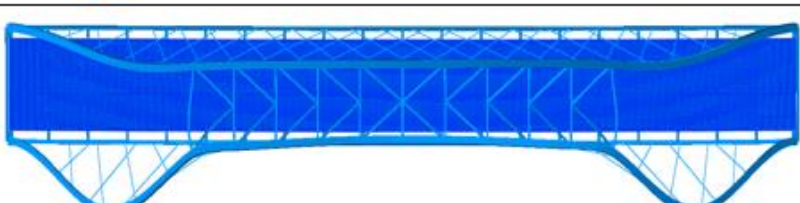

	Mode	λ	$N_{cr} = \lambda \cdot N_x$ (kN)
#1		3.824	36549
#2		5.996	57309
#3		6.081	58122
#4		6.528	62394
#5		6.337	60569
#6		6.643	63493

Figure 9.21 Buckling analysis, ULS Gravity, removed wind bracing. Bridge 2

9.3 Utilization results

The tables in this chapter shows the utilization results for load models in the following situations: gravity, full load, half load, removed hangers and hanger change. The graphic display shows the utilization along the arch and tie, of the load model with the highest utilization.

Design check for the arches for all load models are given in Appendix G. Design check for the wind trusses for all load models are given in Appendix L. A simplified check was performed to see if it was necessary to run load models without wind ($k_{mod}=0.9$). The design check for the load model with the highest utilization, full load LM1 Eq 1a for Bridge 1 see Table 9.3, did not fail when reducing the k_{mod} from 1.1 to 0.9. Therefore, load models without wind was considered unnecessary. The same procedure was carried out for Bridge 2, with the same conclusion.

Table 9.2 explains different equations used in the design checks of the arches and wind bracing.

Equations in Eurocode 5-1-1	
Eq 6.17	Combined bending and axial tension
Eq 6.18	Combined bending and axial tension
Eq 6.19	Combined bending and axial compression
Eq 6.20	Combined bending and axial compression
Eq 6.23	Columns subjected to either compression or combined compression and bending
Eq 6.24	Columns subjected to either compression or combined compression and bending
Eq 6.41	Apex bending stress in cambered beams
Eq 6.53	Combined tension perpendicular to grain and shear in cambered beams
Shear + Torsion	combined stresses from shear and torsion

Table 9.2 Description of equations used in design check for glulam parts

The utilization results for the ties in Bridge 2, are based on maximum von-mises stresses in three different sections of the box profile, see Figure 4.23.

9.3.1 Bridge 1

9.3.1.1 Full load

Arch1	Eq 6.19	Eq 6.20	Eq 6.23	Eq 6.24	Eq 6.41	Eq 6.53	Shear + Torsion
Gravity	0,26	0,24	0,88	0,97	0,02	0,24	0,20
LM1 gr1a Eq 1a	0,23	0,23	0,47	0,80	0,03	0,17	0,28
LM1 gr1a Eq 1b	0,20	0,21	0,44	0,78	0,03	0,17	0,30
LM2 gr1b Eq 2a	0,16	0,17	0,58	0,63	0,01	0,13	0,25
LM2 gr1b Eq 2b	0,15	0,16	0,55	0,61	0,01	0,12	0,23
LM4 gr4 Eq 4a	0,21	0,22	0,72	0,77	0,02	0,17	0,30
LM4 gr4 Eq 4b	0,21	0,22	0,73	0,77	0,02	0,18	0,31
Wind without traffic Eq a	0,26	0,28	0,56	0,58	0,02	0,19	0,36
Wind without traffic Eq b	0,28	0,30	0,55	0,60	0,02	0,18	0,42

Table 9.3 Utilization arch 1, full load. Bridge 1

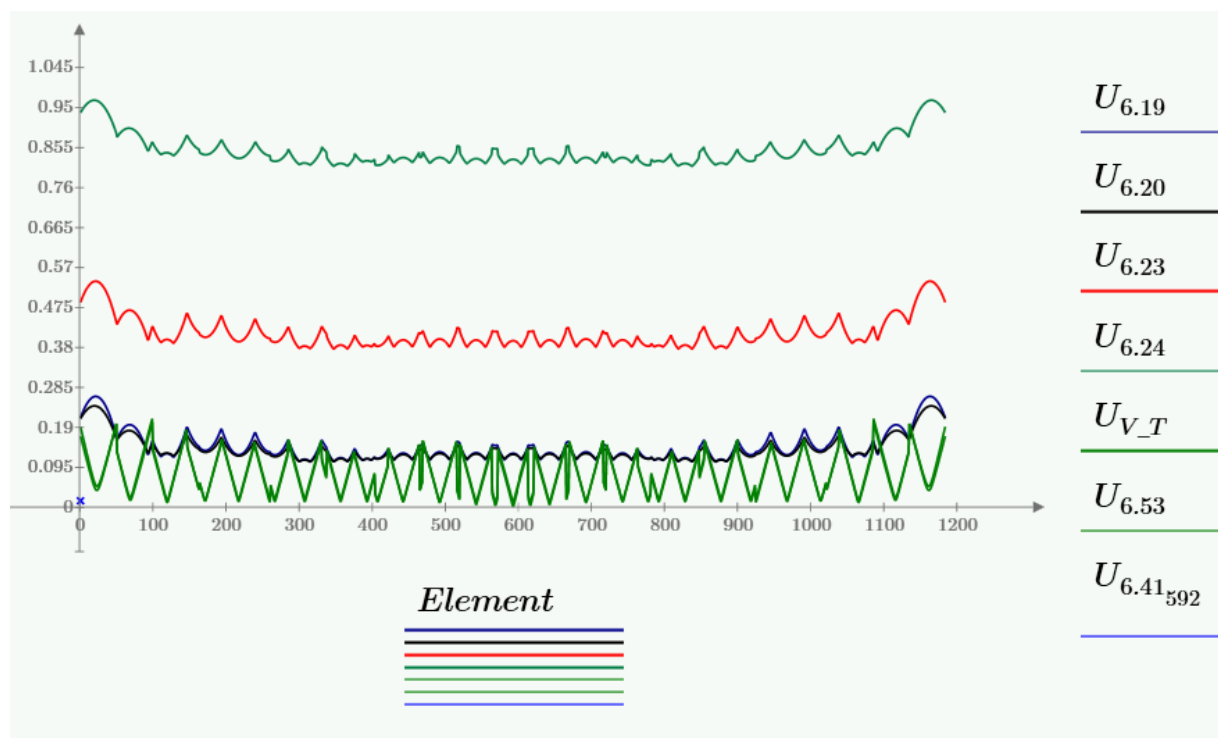


Figure 9.22 Utilization plot arch 1, full load. Bridge 1. Gravity, $k_{mod}=0.6$

Arch2	Eq 6.19	Eq 6.20	Eq 6.23	Eq 6.24	Eq 6.41	Eq 6.53	Shear + Torsion
Gravity	0,31	0,27	0,90	0,98	0,02	0,21	0,23
LM1 gr1a Eq 1a	0,19	0,19	0,44	0,74	0,04	0,19	0,28
LM1 gr1a Eq 1b	0,22	0,21	0,47	0,77	0,06	0,21	0,30
LM2 gr1b Eq 2a	0,14	0,15	0,56	0,60	0,02	0,14	0,23
LM2 gr1b Eq 2b	0,13	0,14	0,53	0,57	0,03	0,13	0,22
LM4 gr4 Eq 4a	0,19	0,20	0,69	0,74	0,01	0,17	0,27
LM4 gr4 Eq 4b	0,20	0,20	0,70	0,74	0,01	0,18	0,27
Wind without traffic Eq a	0,25	0,25	0,54	0,56	0,02	0,19	0,32
Wind without traffic Eq b	0,27	0,29	0,54	0,59	0,02	0,18	0,40

Table 9.4 Utilization arch 2, full load. Bridge 1

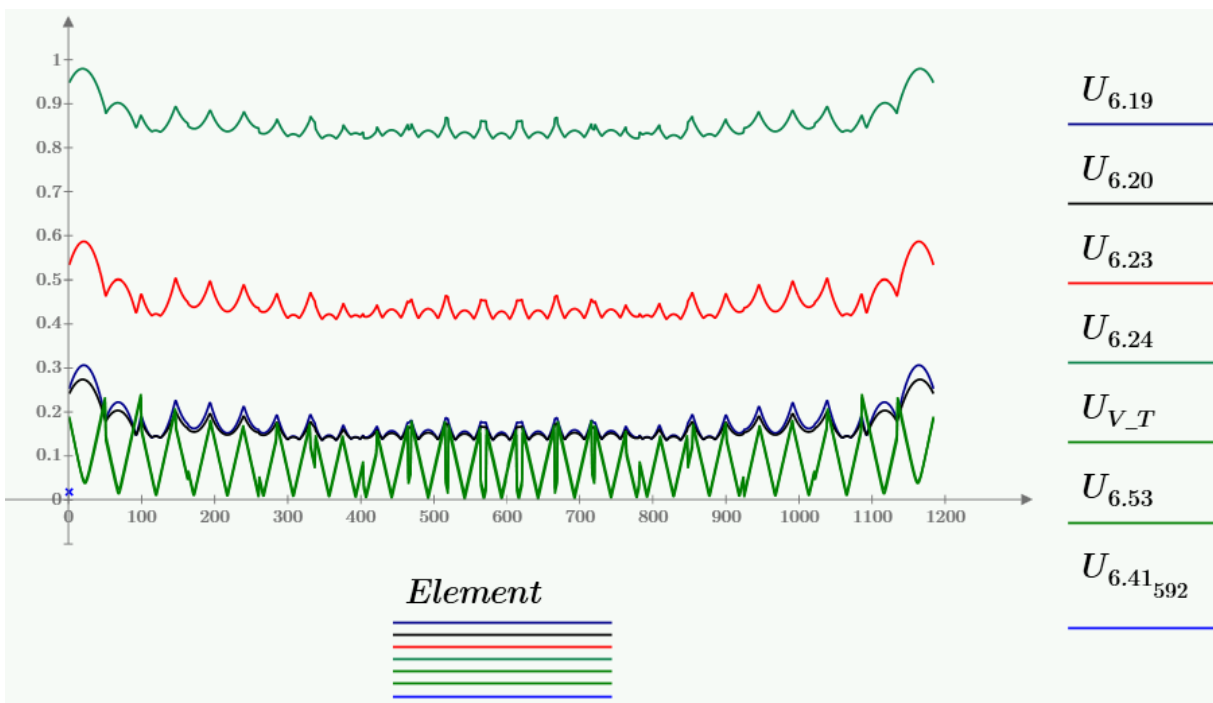


Figure 9.23 Utilization plot arch 2, full load. Bridge 1. Gravity, $k_{mod}=0.6$

9.3.1.2 Half load

Arch1	Eq 6.19	Eq 6.20	Eq 6.23	Eq 6.24	Eq 6.41	Eq 6.53	Shear + Torsion
LM1 gr1a Eq 1a	0,27	0,25	0,73	0,75	0,02	0,18	0,28
LM1 gr1a Eq 1b	0,29	0,25	0,72	0,73	0,02	0,18	0,30
LM2 gr1b Eq 2a	0,16	0,18	0,58	0,63	0,01	0,13	0,25
LM2 gr1b Eq 2b	0,15	0,16	0,55	0,60	0,01	0,12	0,23
LM4 gr4 Eq 4a	0,20	0,20	0,65	0,69	0,01	0,16	0,28
LM4 gr4 Eq 4b	0,21	0,20	0,65	0,69	0,01	0,16	0,28

Table 9.5 Utilization arch 1, half load. Bridge 1

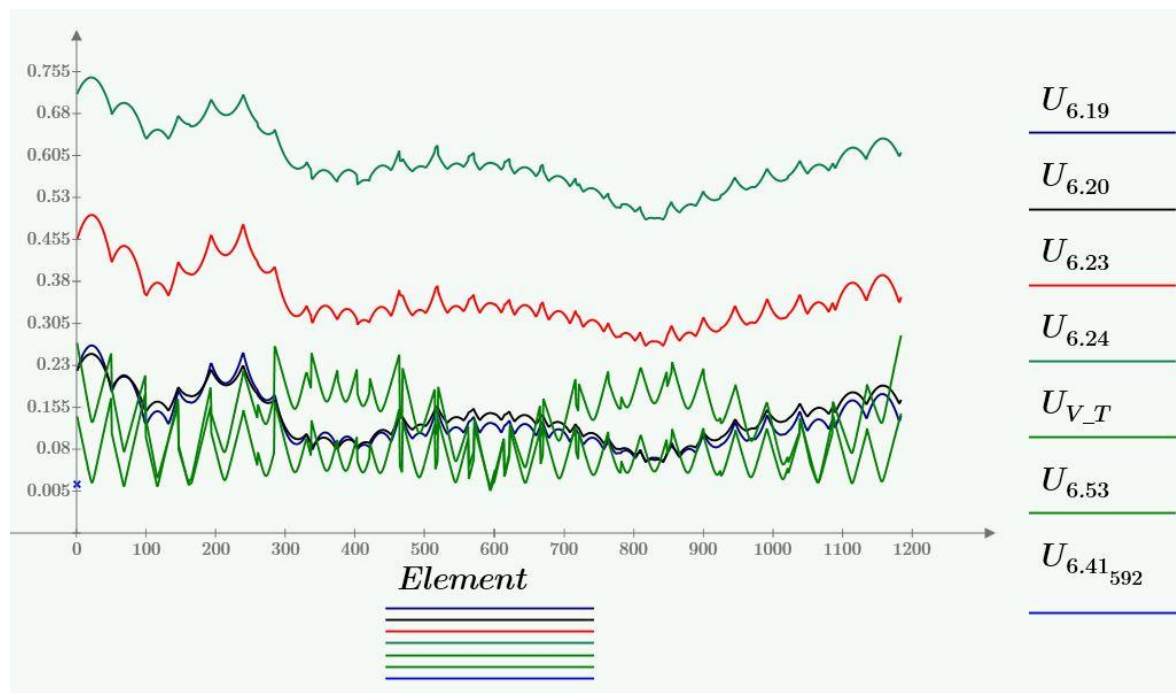


Figure 9.24 Utilization plot arch 1, half load. Bridge 1. LM1 Eq 1b, $k_{mod}=1.1$

Arch2	Eq 6.19	Eq 6.20	Eq 6.23	Eq 6.24	Eq 6.41	Eq 6.53	Shear + Torsion
LM1 gr1a Eq 1a	0,23	0,20	0,69	0,70	0,01	0,18	0,25
LM1 gr1a Eq 1b	0,20	0,19	0,64	0,67	0,01	0,16	0,25
LM2 gr1b Eq 2a	0,15	0,15	0,56	0,60	0,01	0,14	0,23
LM2 gr1b Eq 2b	0,15	0,15	0,54	0,58	0,01	0,13	0,23
LM4 gr4 Eq 4a	0,19	0,19	0,64	0,67	0,01	0,16	0,24
LM4 gr4 Eq 4b	0,19	0,19	0,64	0,68	0,01	0,16	0,24

Table 9.6 Utilization arch 2, half load. Bridge 1

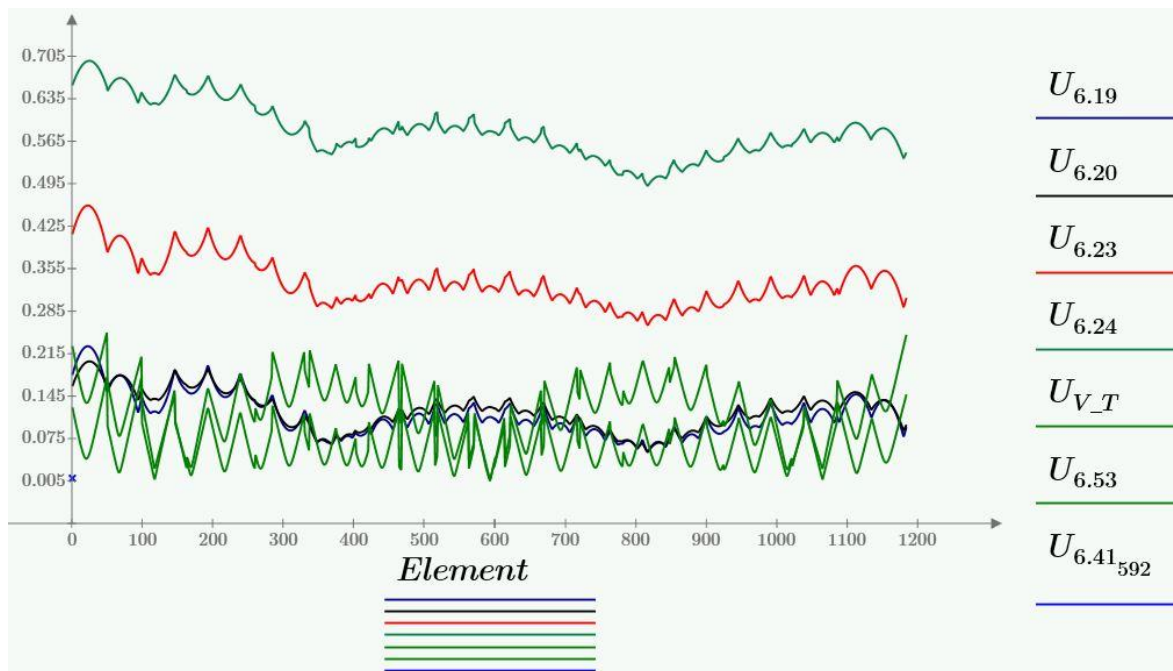


Figure 9.25 Utilization plot arch 2, half load. Bridge 1. LM1 Eq 1a, $k_{mod}=1.1$

9.3.1.3 Hanger change

Arch1	Eq 6.19	Eq 6.20	Eq 6.23	Eq 6.24	Eq 6.41	Eq 6.53	Shear + Torsion
Gravity	0,27	0,25	0,91	0,97	0,02	0,23	0,23
LM1 gr1a Eq 1a	0,26	0,25	0,74	0,76	0,02	0,18	0,29
LM1 gr1a Eq 1b	0,27	0,25	0,73	0,76	0,02	0,18	0,30

Table 9.7 Utilization arch 1, hanger change. Bridge 1

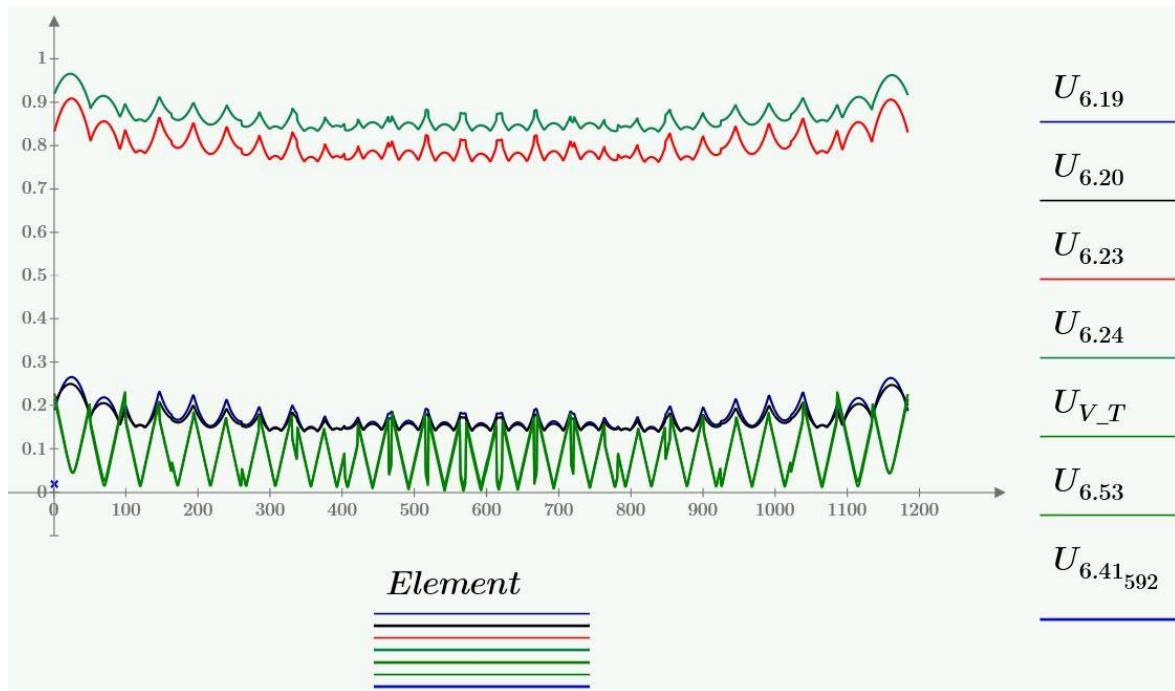


Figure 9.26 Utilization plot arch 1, hanger change. Bridge 1. Gravity, $k_{mod}=0.6$

Arch2	Eq 6.19	Eq 6.20	Eq 6.23	Eq 6.24	Eq 6.41	Eq 6.53	Shear + Torsion
Gravity	0,25	0,23	0,90	0,96	0,01	0,22	0,22
LM1 gr1a Eq 1a	0,22	0,25	0,74	0,76	0,00	0,16	0,29
LM1 gr1a Eq 1b	0,23	0,21	0,70	0,72	0,00	0,16	0,27

Table 9.8 Utilization arch 2, hanger change. Bridge 1

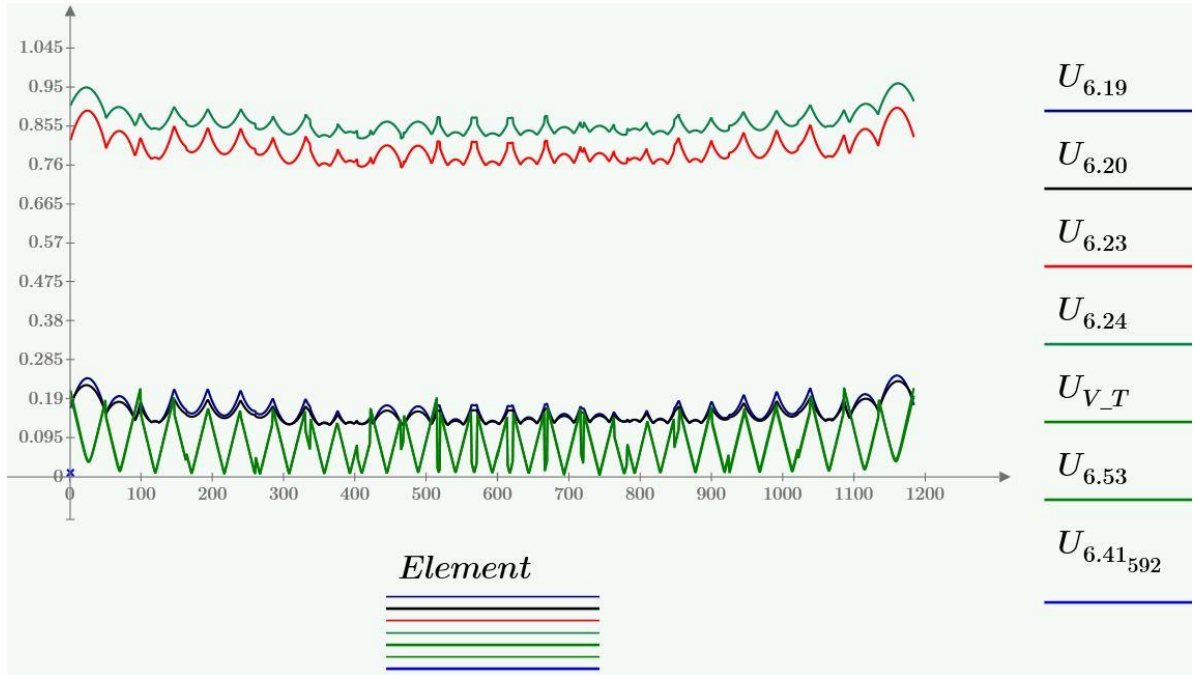


Figure 9.27 Utilization plot arch 2, hanger change. Bridge 1. Gravity, $k_{mod}=0.6$

9.3.1.4 Hanger removal

Arch1	Eq 6.19	Eq 6.20	Eq 6.23	Eq 6.24	Eq 6.41	Eq 6.53	Shear + Torsion
Gravity	0,17	0,16	0,68	0,72	0,01	0,17	0,17
LM1	0,11	0,11	0,51	0,50	0,01	0,13	0,13
LM2	0,10	0,10	0,47	0,49	0,01	0,12	0,12
LM4	0,11	0,10	0,50	0,52	0,01	0,13	0,13

Table 9.9 Utilization arch 1, hanger removal. Bridge 1

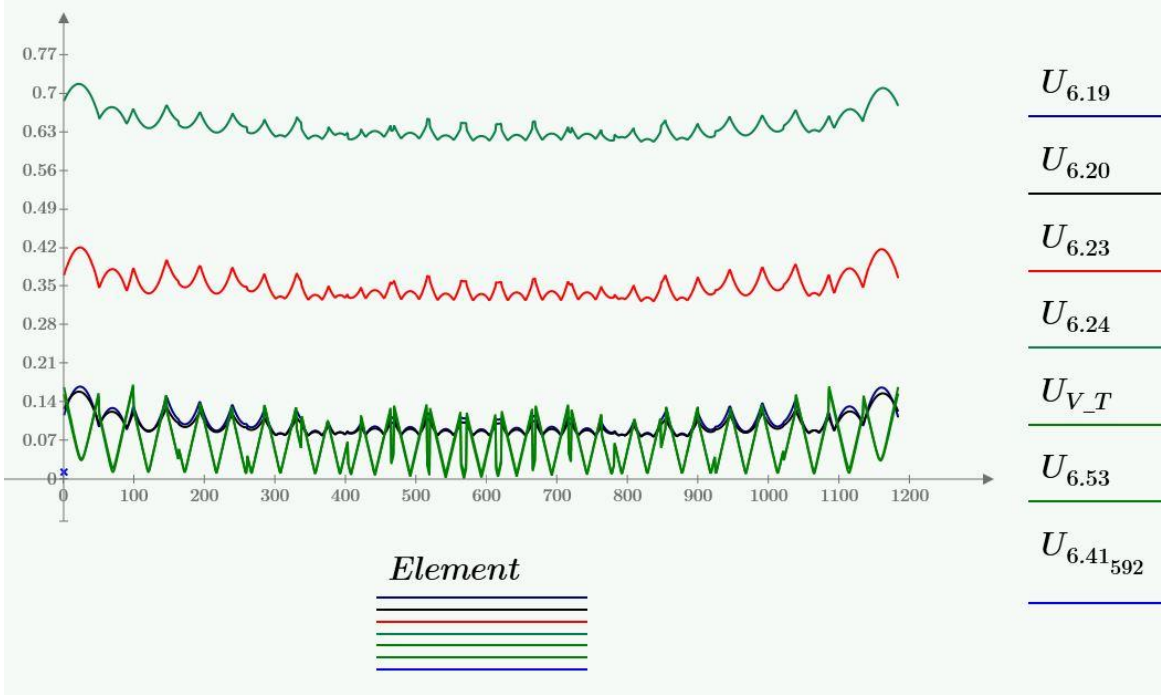


Figure 9.28 Utilization plot arch 1, hanger removal. Bridge 1. Gravity, $k_{mod}=0.6$

Arch2	Eq 6.19	Eq 6.20	Eq 6.23	Eq 6.24	Eq 6.41	Eq 6.53	Shear + Torsion
Gravity	0,21	0,21	0,73	0,77	0,01	0,18	0,22
LM1	0,15	0,15	0,54	0,55	0,01	0,15	0,17
LM2	0,14	0,14	0,51	0,53	0,01	0,13	0,16
LM4	0,16	0,15	0,54	0,57	0,01	0,14	0,17

Table 9.10 Utilization arch 2, hanger removal. Bridge 1

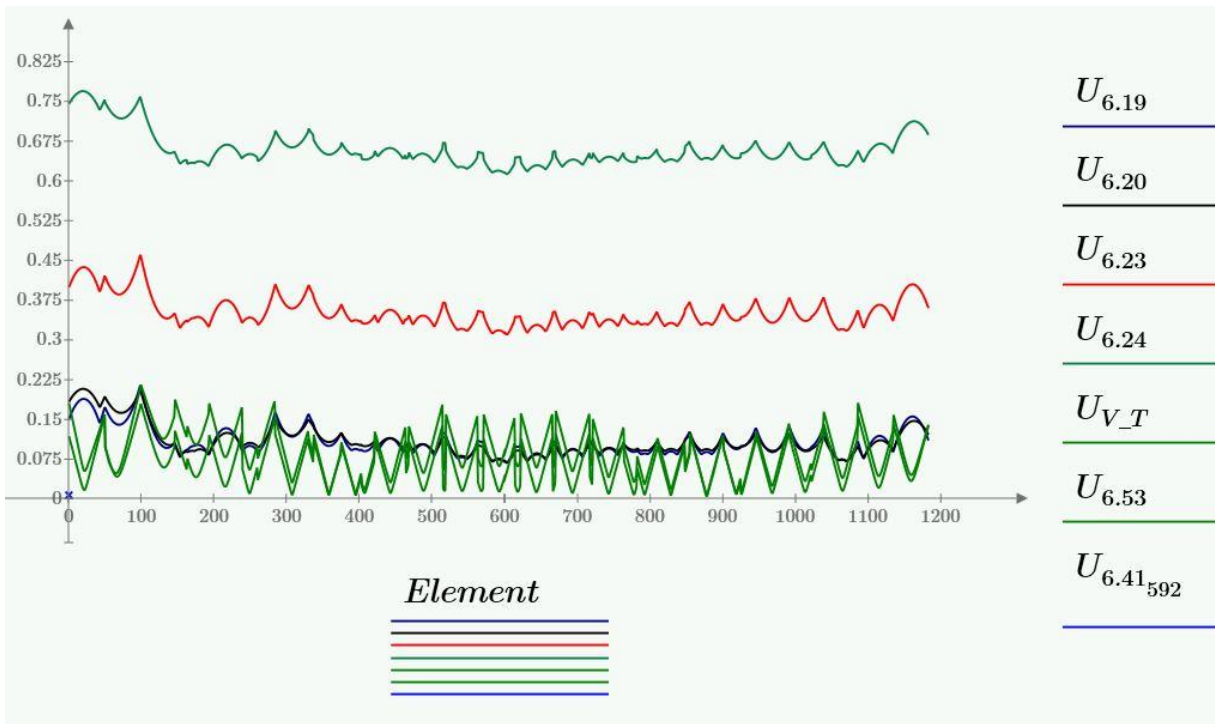


Figure 9.29 Utilization plot arch 2, hanger removal. Bridge 1. Gravity, $k_{mod}=0.6$

9.3.2 Bridge 2

9.3.2.1 Full Load

Arch1	Eq 6.19	Eq 6.20	Eq 6.23	Eq 6.24	Eq 6.41	Eq 6.53	Shear + Torsion
Gravity	0,65	0,63	0,86	0,86	0,006	0,58	0,49
LM1 gr1a Eq 1a	0,38	0,38	0,62	0,63	0,006	0,45	0,34
LM1 gr1a Eq 1b	0,37	0,38	0,61	0,62	0,008	0,47	0,34
LM2 gr1b Eq 2a	0,33	0,34	0,54	0,56	0,004	0,36	0,29
LM2 gr1b Eq 2b	0,30	0,33	0,50	0,52	0,005	0,35	0,27
LM4 gr4 Eq 4a	0,41	0,41	0,65	0,66	0,002	0,38	0,36
LM4 gr4 Eq 4b	0,41	0,41	0,65	0,66	0,002	0,38	0,37
Wind without traffic Eq a	0,38	0,40	0,59	0,63	0,002	0,38	0,31
Wind without traffic Eq b	0,42	0,48	0,62	0,68	0,002	0,30	0,33

Table 9.11 Utilization arch 1, full load. Bridge 2

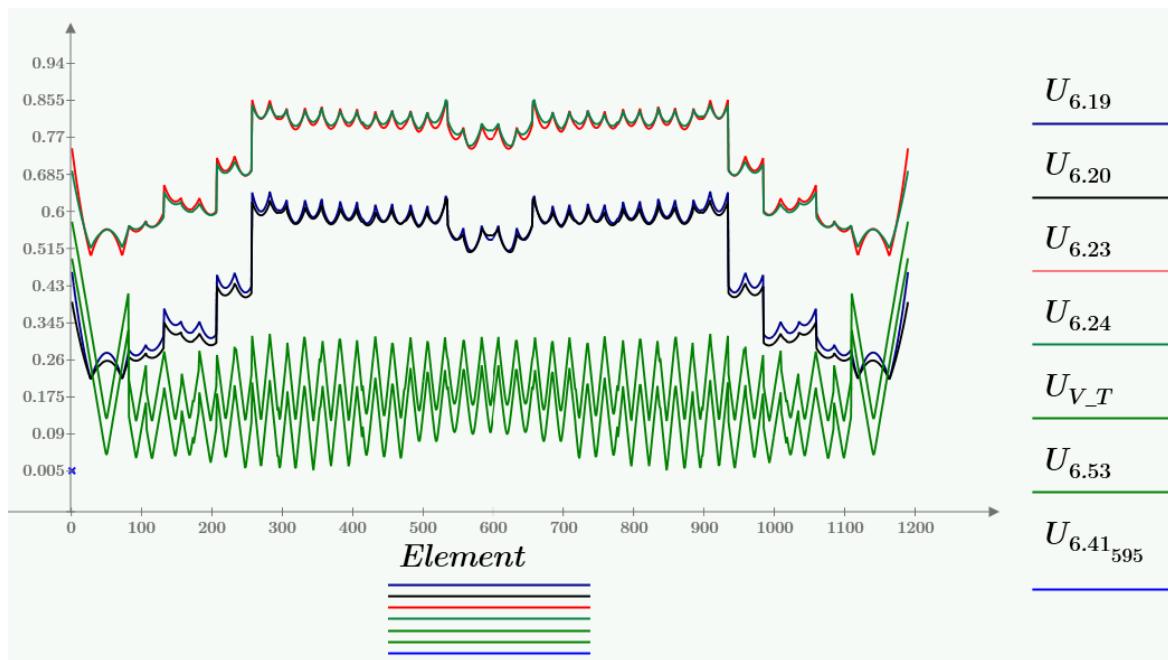


Figure 9.30 Utilization plot arch 1, full load. Bridge 2. Gravity, $k_{mod}=0.6$

Arch2	Eq 6.19	Eq 6.20	Eq 6.23	Eq 6.24	Eq 6.41	Eq 6.53	Shear + Torsion
Gravity	0,60	0,59	0,82	0,83	0,005	0,55	0,48
LM1 gr1a Eq 1a	0,38	0,38	0,63	0,63	0,010	0,54	0,40
LM1 gr1a Eq 1b	0,38	0,38	0,64	0,64	0,013	0,60	0,40
LM2 gr1b Eq 2a	0,32	0,32	0,54	0,55	0,008	0,45	0,34
LM2 gr1b Eq 2b	0,29	0,30	0,50	0,52	0,005	0,35	0,32
LM4 gr4 Eq 4a	0,39	0,38	0,63	0,64	0,003	0,40	0,40
LM4 gr4 Eq 4b	0,39	0,39	0,63	0,64	0,003	0,40	0,40
Wind without traffic Eq a	0,35	0,38	0,57	0,61	0,004	0,35	0,35
Wind without traffic Eq b	0,40	0,46	0,61	0,67	0,004	0,35	0,37

Table 9.12 Utilization arch 2, full load. Bridge 2

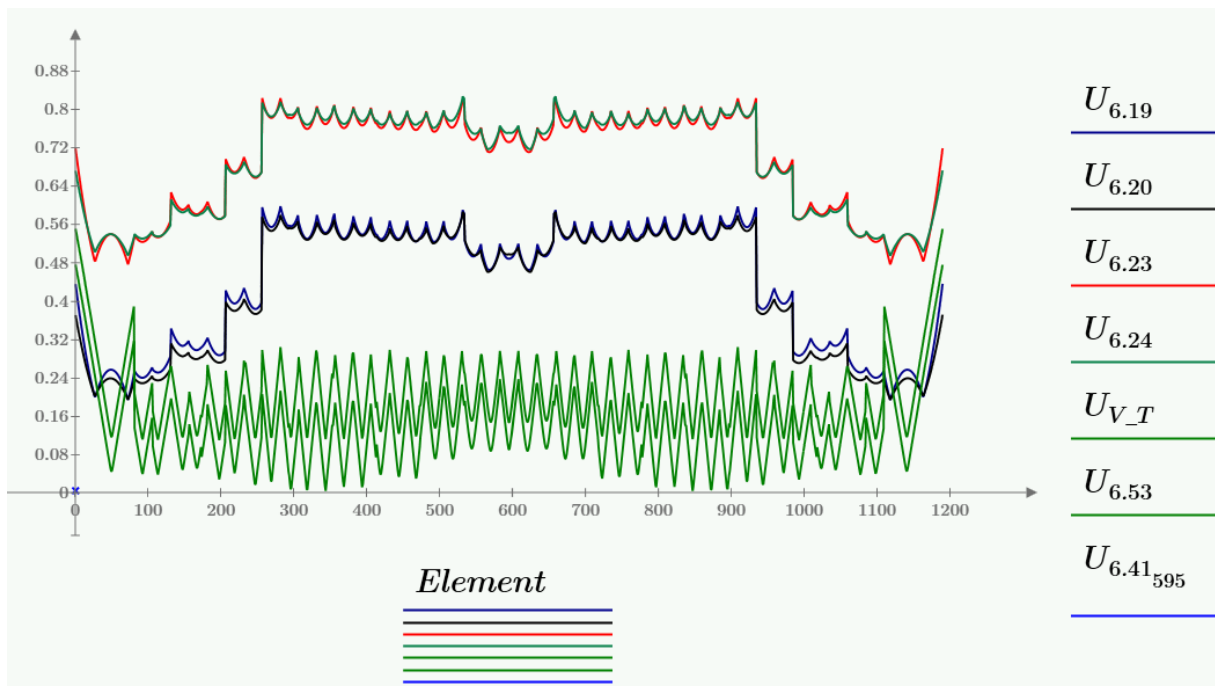


Figure 9.31 Utilization plot arch 2, full load. Bridge 2. Gravity, $k_{mod}=0.6$

Tie1	Elastic capacity	Tie2	Elastic capacity
LM1 gr1a Eq 1a	0,52	LM1 gr1a Eq 1a	0,60
LM1 gr1a Eq 1b	0,51	LM1 gr1a Eq 1b	0,61
LM2 gr1b Eq 2a	0,44	LM2 gr1b Eq 2a	0,50
LM2 gr1b Eq 2b	0,39	LM2 gr1b Eq 2b	0,47
LM4 gr4 Eq 4a	0,56	LM4 gr4 Eq 4a	0,61
LM4 gr4 Eq 4b	0,56	LM4 gr4 Eq 4b	0,61
Wind without traffic Eq a	0,44	Wind without traffic Eq a	0,50
Wind without traffic Eq b	0,39	Wind without traffic Eq b	0,47

Table 9.13 Utilization Tie 1 & 2, full load. Bridge 2

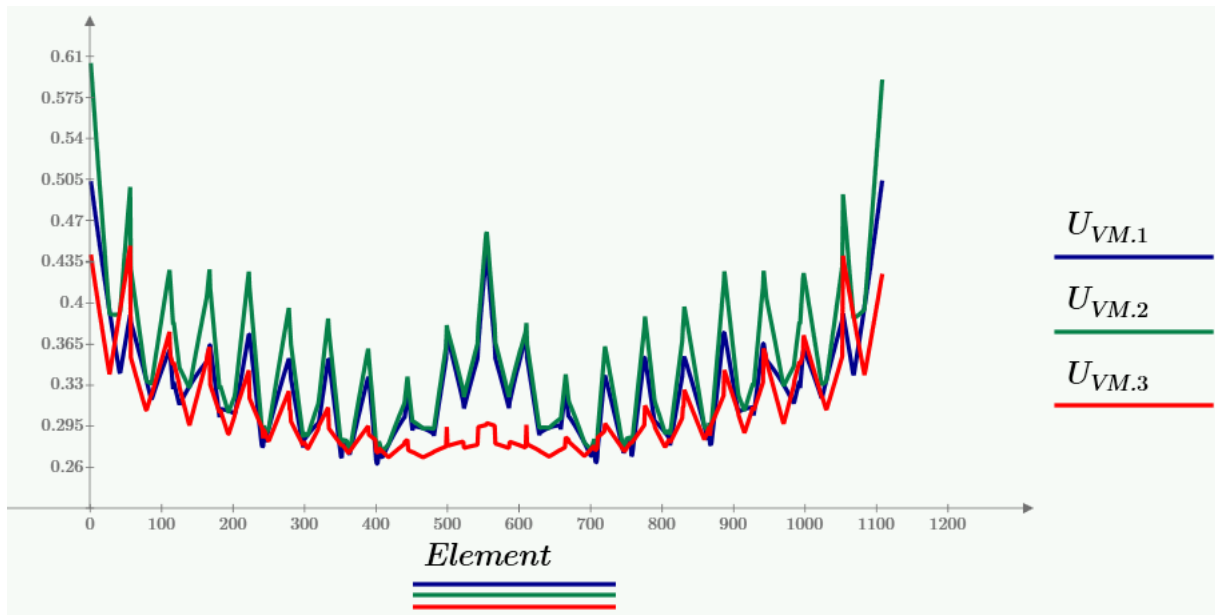


Figure 9.32 Utilization plot tie 2, full load. Bridge 2. LM1 Eq 1a

K-Truss diagonal	Eq 6.19	Eq 6.20	Eq 6.23	Eq 6.24	Shear + Torsion
Gravity	0,15	0,14	0,39	0,38	0,06
LM1 gr1a Eq 1a	0,07	0,06	0,21	0,21	0,03
LM1 gr1a Eq 1b	0,11	0,09	0,29	0,28	0,04
LM2 gr1b Eq 2a	0,08	0,07	0,24	0,23	0,03
LM2 gr1b Eq 2b	0,07	0,06	0,21	0,21	0,03
LM4 gr4 Eq 4a	0,11	0,09	0,29	0,27	0,04
LM4 gr4 Eq 4b	0,11	0,09	0,29	0,28	0,04
Wind without traffic Eq a	0,08	0,07	0,23	0,22	0,03
Wind without traffic Eq b	0,07	0,06	0,21	0,20	0,03

Table 9.14 Utilization K-Truss diagonal, full load. Bridge 2

K-Truss transverse	Eq 6.17	Eq 6.18	Eq 6.19	Eq 6.20	Eq 6.23	Eq 6.24	Shear + Torsion
Gravity	0,39	0,39	0,28	0,27	0,29	0,29	0,13
LM1 gr1a Eq 1a	0,25	0,26	0,21	0,17	0,30	0,48	0,11
LM1 gr1a Eq 1b	0,24	0,25	0,22	0,16	0,28	0,46	0,11
LM2 gr1b Eq 2a	0,23	0,23	0,16	0,16	0,29	0,47	0,08
LM2 gr1b Eq 2b	0,21	0,21	0,11	0,14	0,28	0,45	0,08
LM4 gr4 Eq 4a	0,25	0,26	0,21	0,17	0,30	0,48	0,11
LM4 gr4 Eq 4b	0,25	0,25	0,23	0,16	0,29	0,47	0,11
Wind without traffic Eq a	0,23	0,22	0,16	0,16	0,36	0,61	0,08
Wind without traffic Eq b	0,24	0,22	0,16	0,14	0,43	0,79	0,07

Table 9.15 Utilization K-Truss transverse, full load. Bridge 2

9.3.2.2 Half load

Arch1	Eq 6.19	Eq 6.20	Eq 6.23	Eq 6.24	Eq 6.41	Eq 6.53	Shear + Torsion
LM1 gr1a Eq 1a	0,38	0,38	0,61	0,63	0,000	0,31	0,33
LM1 gr1a Eq 1b	0,37	0,38	0,60	0,62	0,001	0,32	0,32
LM2 gr1b Eq 2a	0,33	0,34	0,54	0,57	0,001	0,29	0,29
LM2 gr1b Eq 2b	0,31	0,32	0,51	0,53	0,001	0,26	0,27
LM4 gr4 Eq 4a	0,38	0,38	0,61	0,62	0,003	0,37	0,33
LM4 gr4 Eq 4b	0,37	0,37	0,60	0,61	0,003	0,37	0,32

Table 9.16 Utilization arch 1, half load. Bridge 2

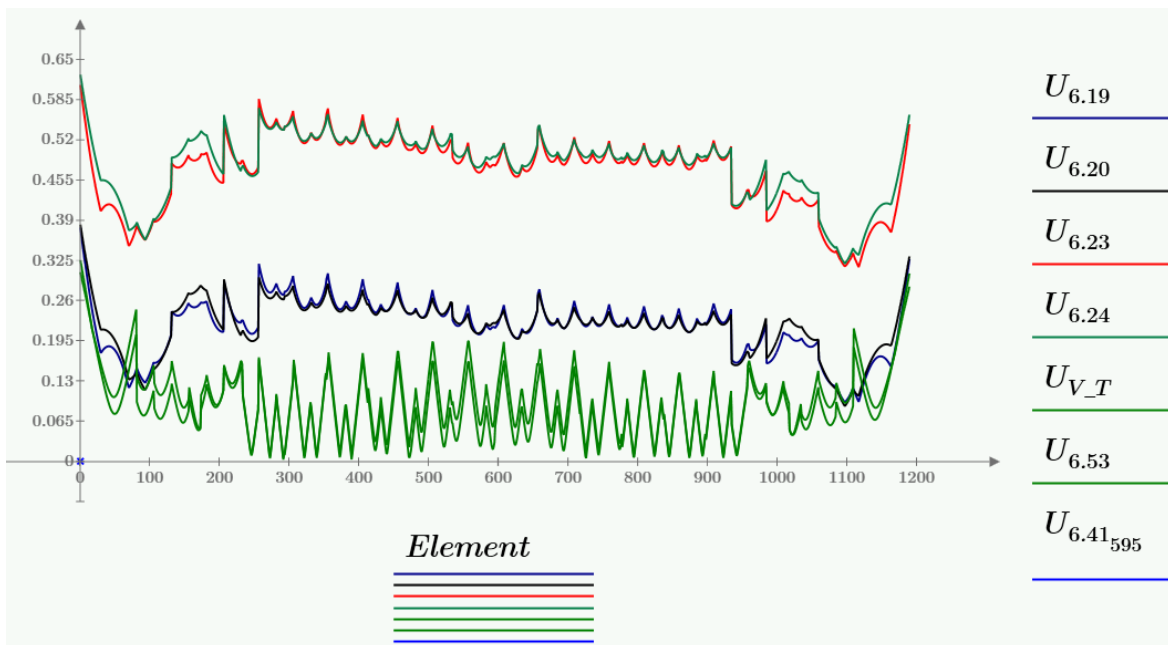


Figure 9.33 Utilization plot arch 1, half load. Bridge 2. LM1 Eq 1a, $k_{mod}=1.1$

Arch2	Eq 6.19	Eq 6.20	Eq 6.23	Eq 6.24	Eq 6.41	Eq 6.53	Shear + Torsion
LM1 gr1a Eq 1a	0,37	0,37	0,61	0,62	0,001	0,35	0,39
LM1 gr1a Eq 1b	0,37	0,38	0,64	0,63	0,003	0,39	0,39
LM2 gr1b Eq 2a	0,32	0,33	0,54	0,56	0,000	0,29	0,34
LM2 gr1b Eq 2b	0,30	0,31	0,51	0,53	0,002	0,31	0,32
LM4 gr4 Eq 4a	0,36	0,36	0,59	0,60	0,004	0,39	0,37
LM4 gr4 Eq 4b	0,35	0,35	0,58	0,59	0,004	0,39	0,36

Table 9.17 Utilization arch 2, half load. Bridge 2

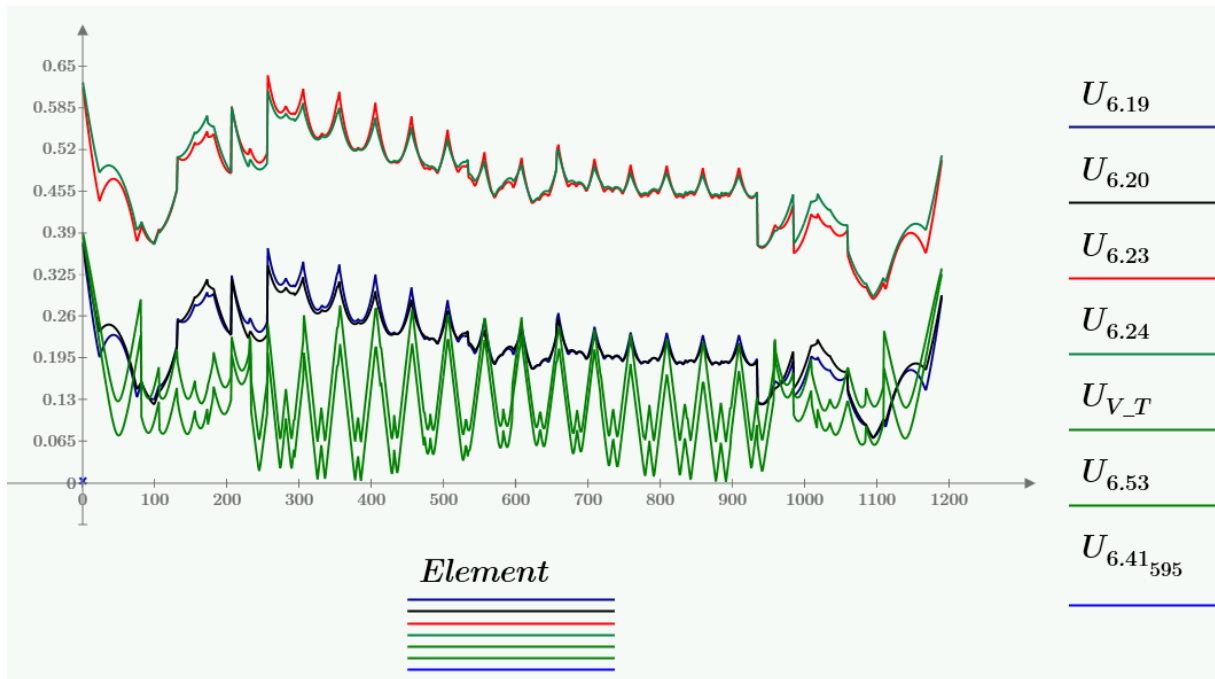


Figure 9.34 Utilization plot arch 2, half load. Bridge 2. LM1 Eq 1b, $k_{mod}=1.1$

Tie1	Elastic capacity	Tie2	Elastic capacity
LM1 gr1a Eq 1a	0,48	LM1 gr1a Eq 1a	0,59
LM1 gr1a Eq 1b	0,46	LM1 gr1a Eq 1b	0,50
LM2 gr1b Eq 2a	0,43	LM2 gr1b Eq 2a	0,43
LM2 gr1b Eq 2b	0,38	LM2 gr1b Eq 2b	0,49
LM4 gr4 Eq 4a	0,51	LM4 gr4 Eq 4a	0,56
LM4 gr4 Eq 4b	0,50	LM4 gr4 Eq 4b	0,56

Table 9.18 Utilization Tie 1 & 2, half load. Bridge 2

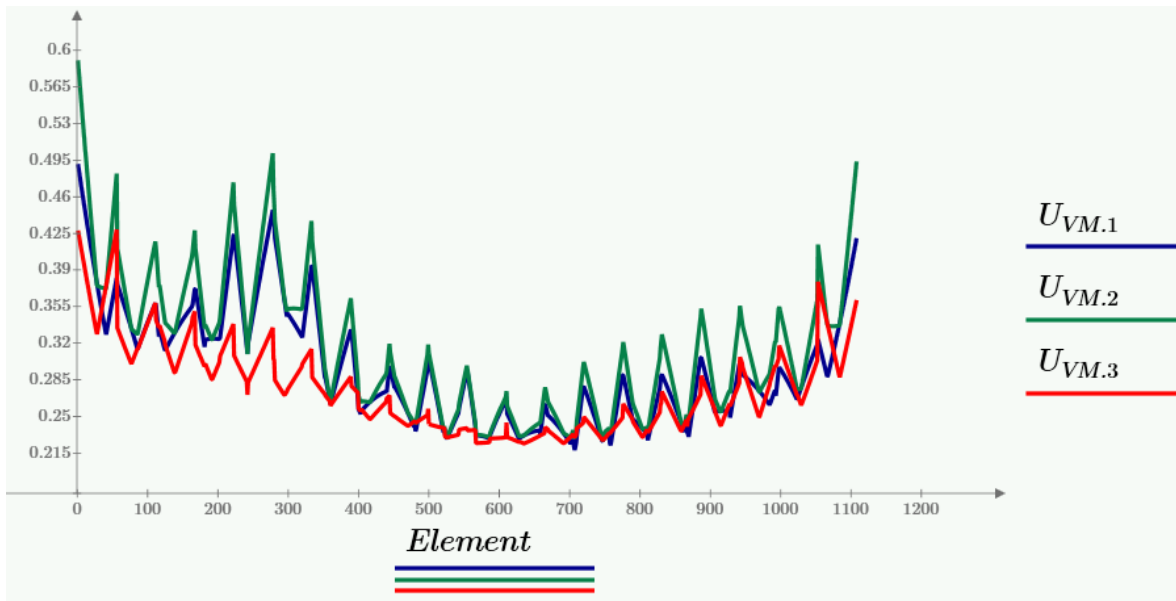


Figure 9.35 Utilization plot Tie 2, half load. Bridge 2. LM1 Eq 1a, $k_{mod}=1.1$

K-Truss diagonal	Eq 6.19	Eq 6.20	Eq 6.23	Eq 6.24	Shear + Torsion
LM1 gr1a Eq 1a	0,09	0,08	0,26	0,25	0,03
LM1 gr1a Eq 1b	0,09	0,08	0,25	0,24	0,03
LM2 gr1b Eq 2a	0,08	0,07	0,23	0,22	0,03
LM2 gr1b Eq 2b	0,07	0,06	0,22	0,21	0,03
LM4 gr4 Eq 4a	0,09	0,08	0,25	0,24	0,03
LM4 gr4 Eq 4b	0,08	0,07	0,24	0,23	0,03

Table 9.19 Utilization K-Truss diagonal, half load. Bridge 2

K-Truss transverse	Eq 6.17	Eq 6.18	Eq 6.19	Eq 6.20	Eq 6.23	Eq 6.24	Shear + Torsion
LM1 gr1a Eq 1a	0,24	0,24	0,17	0,16	0,31	0,50	0,09
LM1 gr1a Eq 1b	0,22	0,23	0,17	0,15	0,30	0,50	0,09
LM2 gr1b Eq 2a	0,23	0,23	0,16	0,16	0,31	0,49	0,08
LM2 gr1b Eq 2b	0,21	0,21	0,14	0,14	0,29	0,48	0,07
LM4 gr4 Eq 4a	0,24	0,24	0,17	0,16	0,30	0,48	0,09
LM4 gr4 Eq 4b	0,22	0,22	0,17	0,15	0,29	0,47	0,09

Table 9.20 Utilization K-Truss transverse, half load. Bridge 2

9.3.2.3 Hanger change

Arch1	Eq 6.19	Eq 6.20	Eq 6.23	Eq 6.24	Eq 6.41	Eq 6.53	Shear + Torsion
Gravity	0,62	0,61	0,84	0,84	0,004	0,54	0,49
LM1 gr1a Eq 1a	0,39	0,39	0,63	0,64	0,002	0,37	0,35
LM1 gr1a Eq 1b	0,39	0,39	0,63	0,64	0,004	0,40	0,35

Table 9.21 Utilization Arch 1, hanger change. Bridge 2

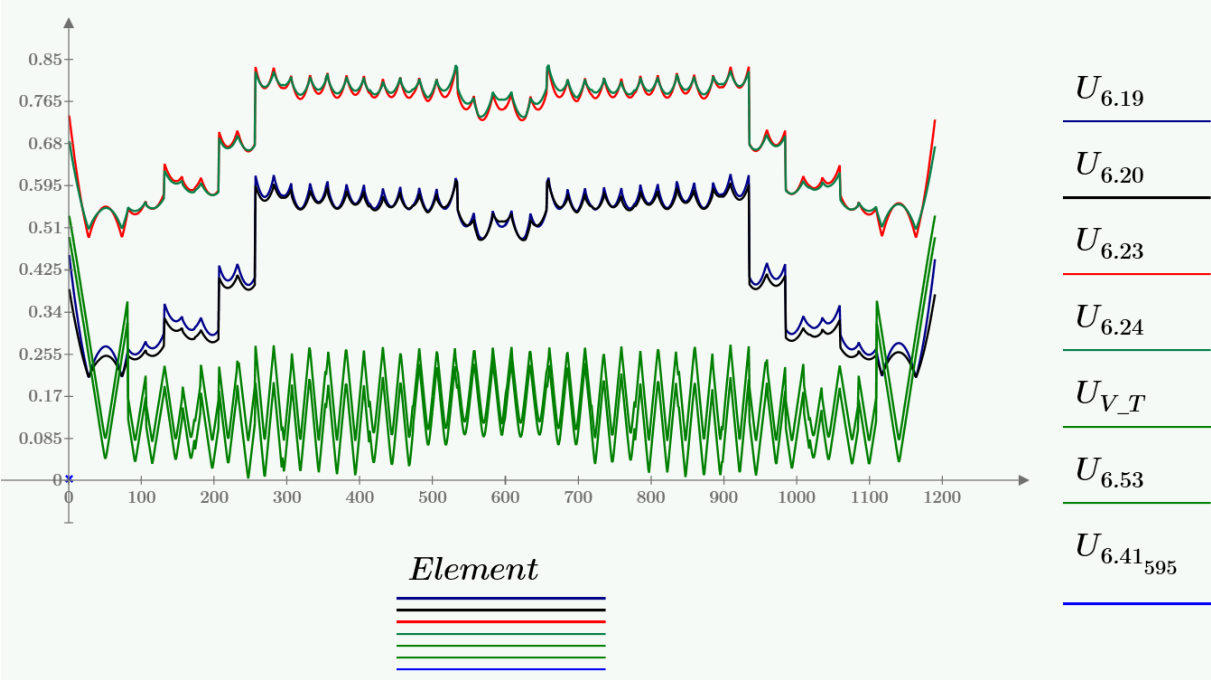


Figure 9.36 Utilization plot Arch 1, hanger change. Bridge 2. Gravity, k_{mod}=0.6

Arch2	Eq 6.19	Eq 6.20	Eq 6.23	Eq 6.24	Eq 6.41	Eq 6.53	Shear + Torsion
Gravity	0,68	0,64	0,92	0,89	0,003	0,49	0,47
LM1 gr1a Eq 1a	0,41	0,37	0,63	0,64	0,008	0,48	0,38
LM1 gr1a Eq 1b	0,41	0,37	0,68	0,65	0,010	0,54	0,38

Table 9.22 Utilization Arch 2, hanger change. Bridge 2

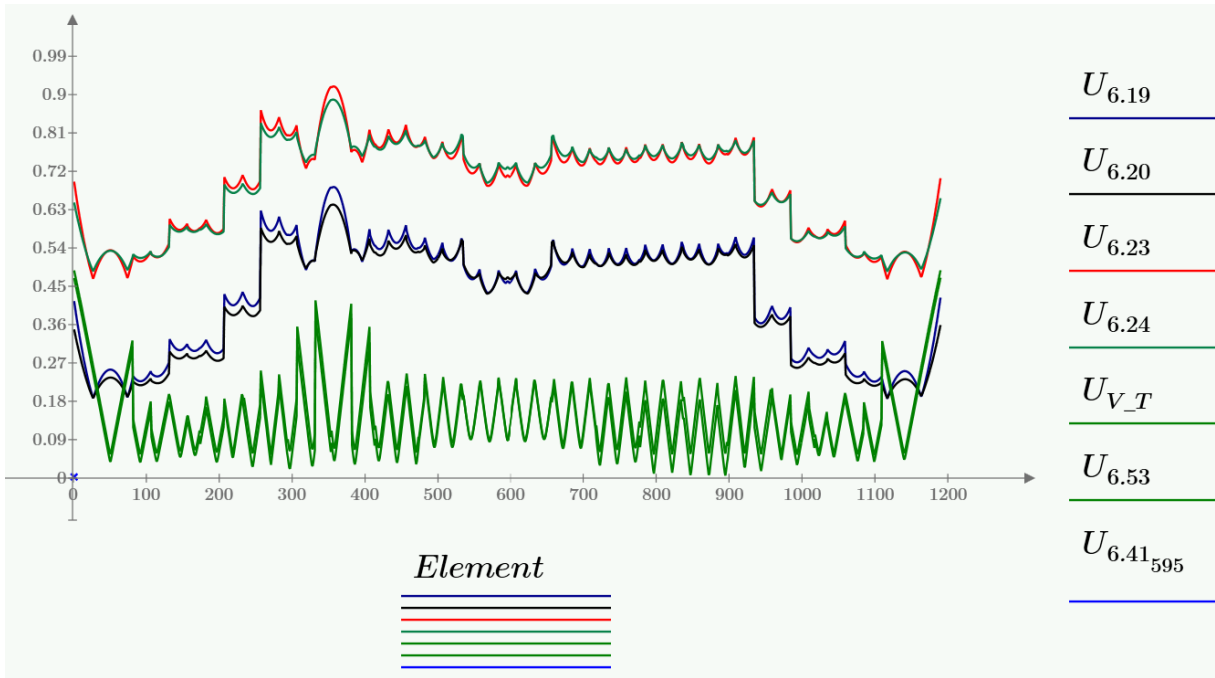


Figure 9.37 Utilization plot Arch 2, hanger change. Bridge 2. Gravity, $k_{mod}=0.6$

Tie1	Elastic capacity	Tie2	Elastic capacity
LM1 gr1a Eq 1a	0,54	LM1 gr1a Eq 1a	0,55
LM1 gr1a Eq 1b	0,53	LM1 gr1a Eq 1b	0,59

Table 9.23 Utilization Tie 1 & 2, hanger change. Bridge 2

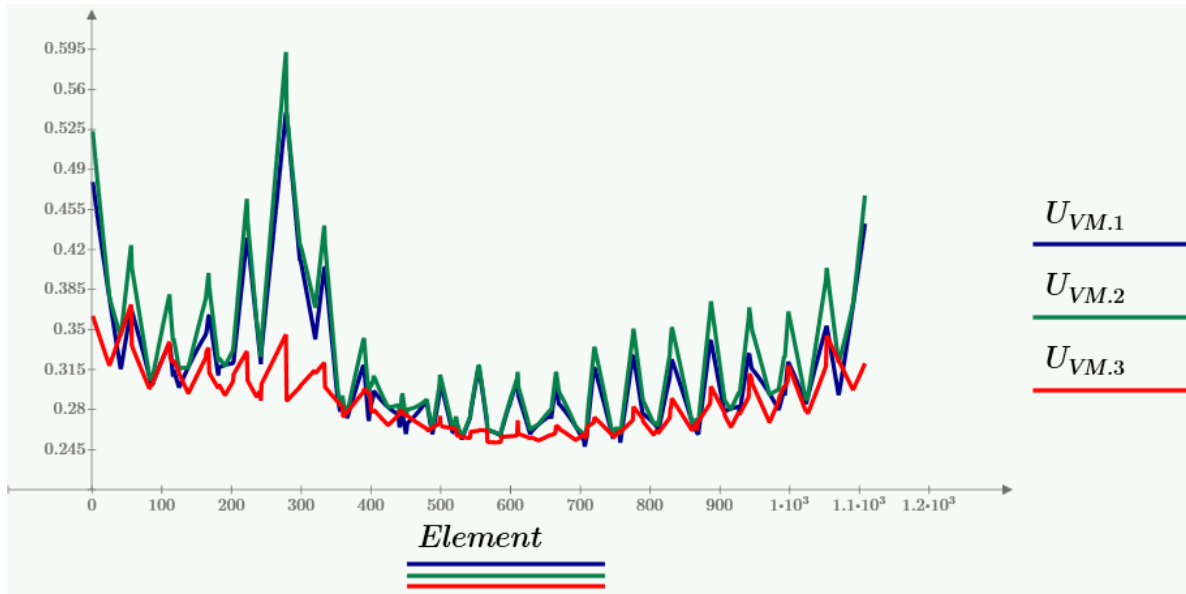


Figure 9.38 Utilization plot Tie 2, hanger change. Bridge 2. LM1 Eq 1b

K-Truss diagonal	Eq 6.19	Eq 6.20	Eq 6.23	Eq 6.24	Shear + Torsion
Gravity	0,15	0,14	0,39	0,38	0,06
LM1 gr1a Eq 1a	0,07	0,06	0,21	0,21	0,03
LM1 gr1a Eq 1b	0,11	0,09	0,29	0,28	0,04

Table 9.24 Utilization K-Truss diagonal, hanger change. Bridge 2

K-Truss transverse	Eq 6.17	Eq 6.18	Eq 6.19	Eq 6.20	Eq 6.23	Eq 6.24	Shear + Torsion
Gravity	0,39	0,39	0,28	0,27	0,29	0,29	0,13
LM1 gr1a Eq 1a	0,25	0,26	0,21	0,17	0,30	0,48	0,11
LM1 gr1a Eq 1b	0,24	0,25	0,22	0,16	0,28	0,46	0,11

Table 9.25 Utilization K-Truss transverse, hanger change. Bridge 2

9.3.2.4 Hanger removal

Arch1	Eq 6.19	Eq 6.20	Eq 6.23	Eq 6.24	Eq 6.41	Eq 6.53	Shear + Torsion
Gravity	0,72	0,61	0,99	0,88	0,000	0,43	0,43
LM1 gr1a Eq 1a	0,46	0,37	0,71	0,63	0,001	0,33	0,31
LM1 gr1a Eq 1b	0,47	0,48	0,73	0,74	0,001	0,39	0,39
LM2 gr1b Eq 2a	0,42	0,34	0,67	0,60	0,001	0,30	0,29
LM2 gr1b Eq 2b	0,42	0,35	0,67	0,60	0,001	0,31	0,29
LM4 gr4 Eq 4a	0,42	0,35	0,67	0,60	0,000	0,31	0,29
LM4 gr4 Eq 4b	0,48	0,39	0,73	0,66	0,000	0,32	0,32

Table 9.26 Utilization Arch 1, hanger removal. Bridge 2

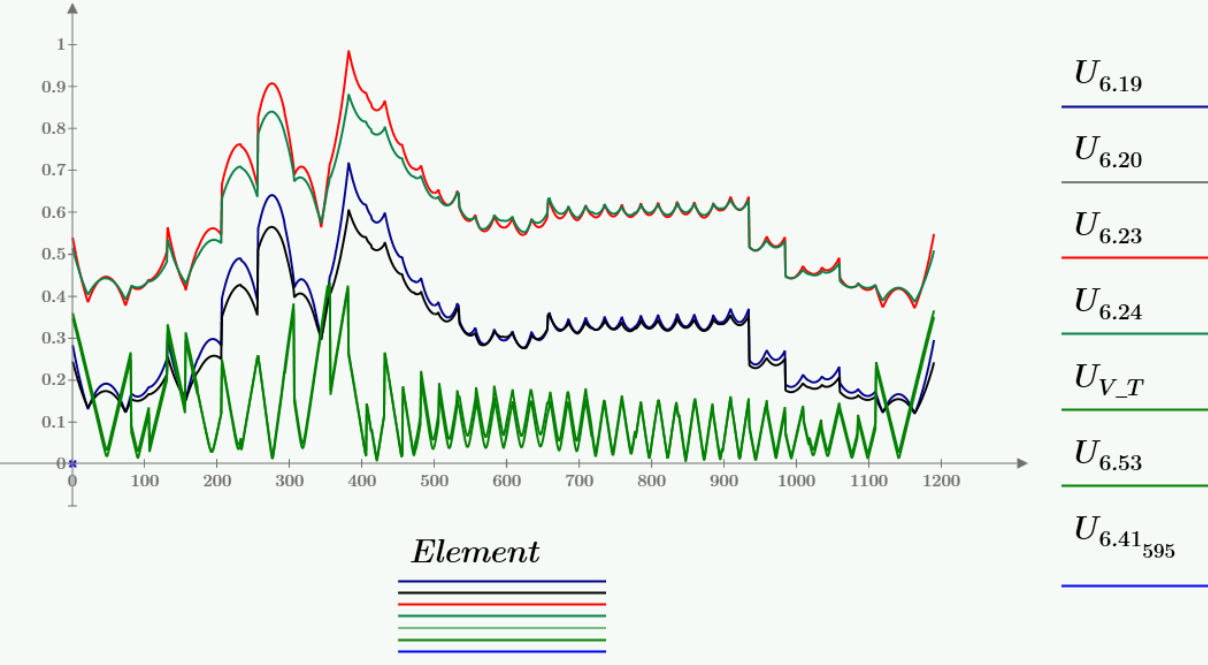


Figure 9.39 Utilization plot Arch 1, hanger removal. Bridge 2. Gravity, $k_{mod}=0.6$

Arch2	Eq 6.19	Eq 6.20	Eq 6.23	Eq 6.24	Eq 6.41	Eq 6.53	Shear + Torsion
Gravity	0,66	0,55	0,92	0,83	0,002	0,44	0,41
LM1 gr1a Eq 1a	0,43	0,36	0,68	0,61	0,003	0,36	0,30
LM1 gr1a Eq 1b	0,52	0,49	0,77	0,75	0,004	0,48	0,47
LM2 gr1b Eq 2a	0,40	0,32	0,64	0,57	0,003	0,33	0,28
LM2 gr1b Eq 2b	0,41	0,33	0,65	0,58	0,003	0,35	0,29
LM4 gr4 Eq 4a	0,42	0,34	0,67	0,60	0,001	0,31	0,30
LM4 gr4 Eq 4b	0,44	0,36	0,69	0,62	0,001	0,32	0,31

Table 9.27 Utilization Arch 2, hanger removal. Bridge 2

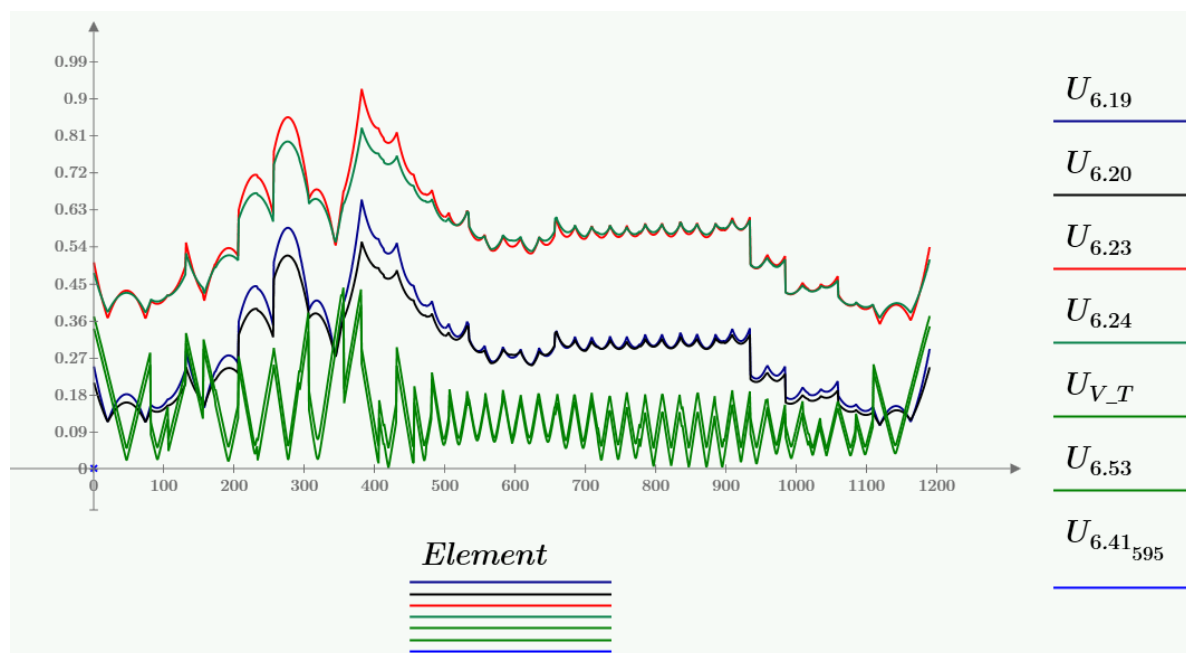


Figure 9.40 Utilization plot Arch 2, hanger removal. Bridge 2. Gravity, $k_{mod}=0.6$

Tie1	Elastic capacity	Tie2	Elastic capacity
LM1 gr1a Eq 1a	0,40	LM1 gr1a Eq 1a	0,37
LM1 gr1a Eq 1b	0,42	LM1 gr1a Eq 1b	0,38
LM2 gr1b Eq 2a	0,38	LM2 gr1b Eq 2a	0,35
LM2 gr1b Eq 2b	0,38	LM2 gr1b Eq 2b	0,35
LM4 gr4 Eq 4a	0,41	LM4 gr4 Eq 4a	0,37
LM4 gr4 Eq 4b	0,42	LM4 gr4 Eq 4b	0,38

Table 9.28 Utilization Tie 1&2, hanger removal. Bridge 2

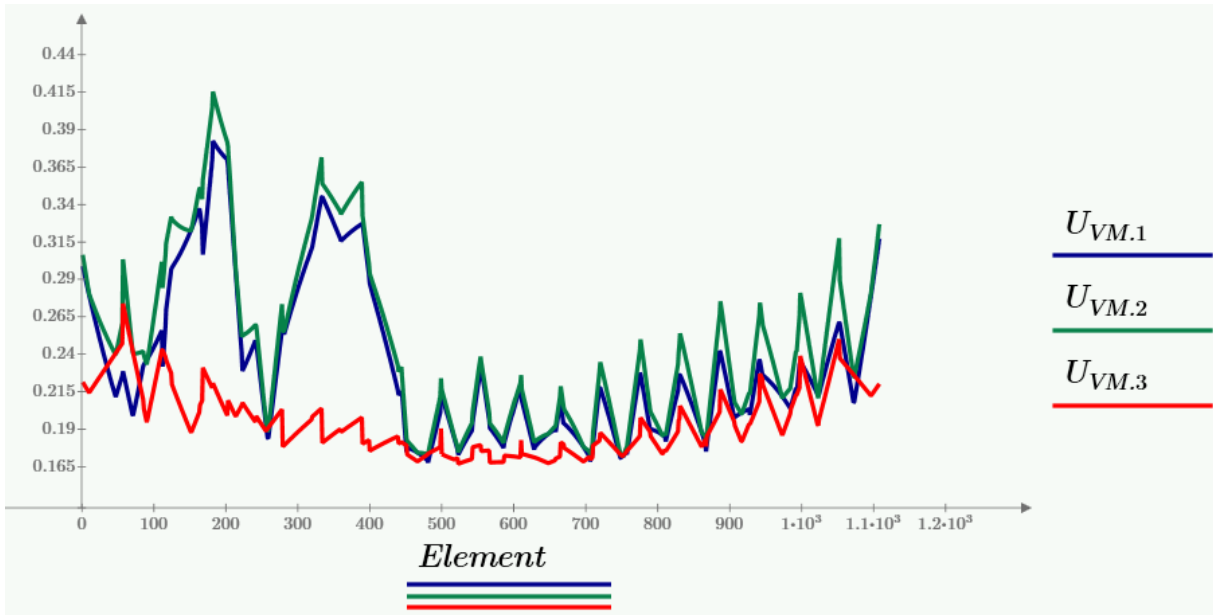


Figure 9.41 Utilization plot Tie 1, hanger removal. Bridge 2. LM1 Eq 1b

K-Truss diagonal	Eq 6.19	Eq 6.20	Eq 6.23	Eq 6.24	Shear + Torsion
Gravity	0,10	0,09	0,29	0,28	0,04
LM1 gr1a Eq 1a	0,06	0,05	0,17	0,17	0,02
LM1 gr1a Eq 1b	0,06	0,05	0,18	0,17	0,02
LM2 gr1b Eq 2a	0,05	0,04	0,16	0,16	0,02
LM2 gr1b Eq 2b	0,05	0,05	0,16	0,16	0,02
LM4 gr4 Eq 4a	0,06	0,05	0,17	0,17	0,02
LM4 gr4 Eq 4b	0,06	0,05	0,18	0,17	0,02

Table 9.29 Utilization K-Truss diagonal, hanger removal. Bridge 2

K-Truss transverse	Eq 6.17	Eq 6.18	Eq 6.19	Eq 6.20	Eq 6.23	Eq 6.24	Shear + Torsion
Gravity	0,30	0,29	0,22	0,20	0,22	0,23	0,11
LM1 gr1a Eq 1a	0,17	0,17	0,12	0,11	0,12	0,12	0,06
LM1 gr1a Eq 1b	0,17	0,17	0,12	0,11	0,12	0,12	0,06
LM2 gr1b Eq 2a	0,17	0,16	0,12	0,11	0,12	0,12	0,06
LM2 gr1b Eq 2b	0,17	0,16	0,12	0,11	0,12	0,11	0,06
LM4 gr4 Eq 4a	0,17	0,17	0,12	0,11	0,12	0,13	0,06
LM4 gr4 Eq 4b	0,17	0,17	0,12	0,12	0,12	0,13	0,06

Table 9.30 Utilization K-Truss transverse, hanger removal. Bridge 2

9.4 Hanger Relaxation

Hanger relaxation was controlled in LM1, LM2 and LM4 with traffic load on 50% of the bridge deck. The check was carried out with a load factor of 1.0 on self-weight, because the self-weight will pre-stress the hangers and help prevent relaxation. The load model with either the most relaxed hangers or with the lowest hanger force are presented for both bridges in Figure 9.42 and Figure 9.43.

Bridge 1 experienced relaxation of the hangers in multiple load models. The worst case was LM1 Equation b, having 10 relaxed hangers in one of the hanger sets. Figure 9.42 marks the relaxed hangers as blue.

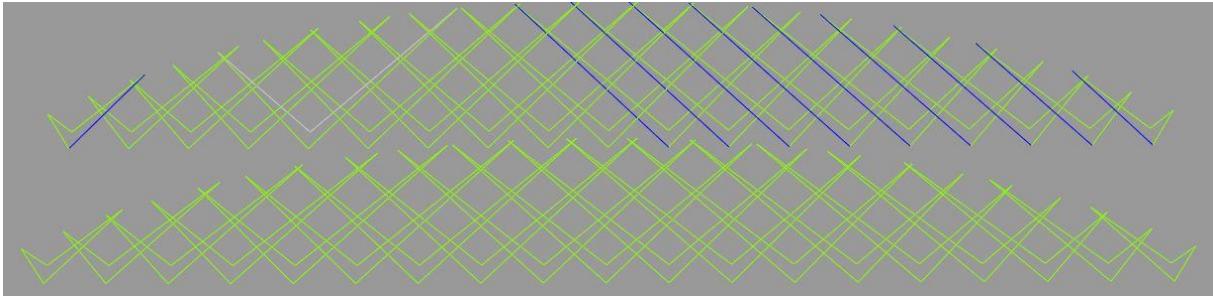


Figure 9.42 The lowest occurring hanger forces with half load. Bridge 1

Bridge 2 had the lowest occurring hanger forces in LM1 Equation b, but there was not any case of relaxed hangers.

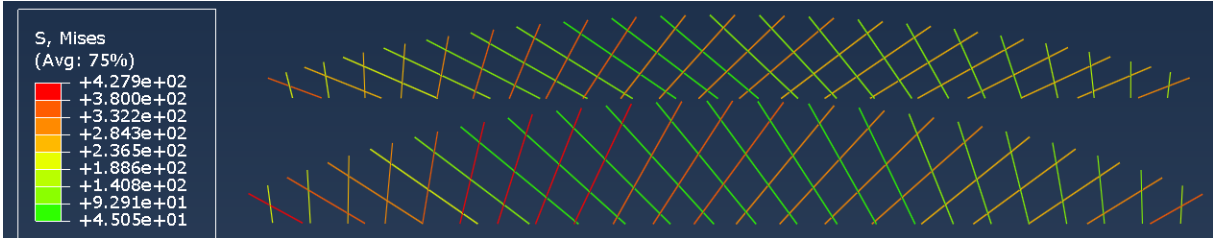


Figure 9.43 The lowest occurring hanger forces with half load. Bridge 2

9.5 Cost results

Cost estimate - report - Bridge deck	Unit	Quantity	Cost	Total
Stresslaminated timber deck, GL32c	m ³	978	kr 15 000,00	kr 14 667 000
Tensioning system	m ²	138	kr 3 100,00	kr 426 250
Flashings details	m ²	67	kr 3 000,00	kr 199 800
Bridge deck - Bridge alternative 1 and 2				kr 15 293 050
Bridge deck - Driva Bridge				kr 9 031 474
Difference				kr 6 261 576

Table 9.31 cost estimate - bridge deck

Cost estimate - report - Bridge 1	Unit	Quantity	Cost	Total
Arch, GL32h	m ³	323	kr 18 300,00	kr 5 903 580,00
Arch, GL32h - Assembly	m ³	323	kr 10 000,00	kr 3 226 000,00
Zinc flashings on top surface	m ²	380	kr 3 000,00	kr 1 138 500,00
Cladding and paint on side surface	m ²	403	kr 3 350,00	kr 1 350 720,00
Delivery of rolled steel for welding, transverse beams	tonne	151	kr 10 760,00	kr 1 624 760,00
Delivery of rolled steel for welding, hanger connections	tonne	13	kr 11 384,00	kr 147 992,00
Preliminary work for production*	RS	1	kr 170 600,00	kr 170 600,00
Processing rolled steel, transverse beams	tonne	151	kr 5 572,00	kr 841 372,00
Processing rolled steel, hanger connections	tonne	13	kr 8 920,00	kr 115 960,00
Welding, transverse beams	tonne	151	kr 6 880,00	kr 1 038 880,00
Welding, hanger connections	tonne	13	kr 7 440,00	kr 96 720,00
Qualification of work procedures	piece	4	kr 22 290,00	kr 89 160,00
Blast cleaning, transverse beams	m ²	1327	kr 130,00	kr 172 510,00
Blast cleaning, hanger connections	m ²	37	kr 130,00	kr 4 810,00
Metallization by thermal spray with zinc, transverse beams	m ²	1327	kr 283,00	kr 375 541,00
Metallization by thermal spray with zinc, hanger connections	m ²	37	kr 283,00	kr 10 471,00
Sealer/tie-coat on thermal sprayed zinc, transverse beams	m ²	1327	kr 62,00	kr 82 274,00
Sealer/tie-coat on thermal sprayed zinc, hanger connections	m ²	37	kr 62,00	kr 2 294,00
Epoxy mastic, transverse beams	m ²	1327	kr 106,00	kr 140 662,00
Epoxy mastic, hanger connections	m ²	37	kr 106,00	kr 3 922,00
Transportation of steel structures	tonne	164	kr 3 272,00	kr 536 608,00
Assembly of steel structures*	RS	1	kr 2 463 700,00	kr 2 463 700,00
Network arch - Bridge 1				kr 19 537 036,00
Network arch - Driva Bridge				kr 25 310 058,00
Difference				kr -5 773 022,00

*cost based on the amount of steel compared to Driva Bridge

Table 9.32 cost estimate - network arch - bridge 1

Cost estimate - report - Bridge 2	Unit	Quantity	Cost	Total
Arch, GL32h	m ³	199	kr 18 300,00	kr 3 645 360,00
Arch, GL32h - Assembly	m ³	199	kr 10 000,00	kr 1 992 000,00
Zink flashings on top surface	m ²	219	kr 3 000,00	kr 657 900,00
Cladding and paint on side surface	m ²	433	kr 3 350,00	kr 1 451 220,00
Truss work, GL32h	m ³	33	kr 18 300,00	kr 607 560,00
Truss work - Assembly	m ³	33	kr 10 000,00	kr 332 000,00
Zinc flashings on top surface, truss work	m ²	77	kr 3 000,00	kr 229 500,00
Cladding and paint on side surface, truss work	m ²	206	kr 3 350,00	kr 689 430,00
Delivery of rolled steel for welding, transverse beams	tonne	151	kr 10 760,00	kr 1 624 760,00
Delivery of rolled steel for welding, ties	tonne	174	kr 10 740,00	kr 1 868 760,00
Delivery of rolled steel for welding, end beams	tonne	42	kr 11 680,00	kr 490 560,00
Delivery of rolled steel for welding, hanger connections	tonne	6,5	kr 11 384,00	kr 73 996,00
Preliminary work for production*	RS	1	kr 398 040,00	kr 398 040,00
Processing rolled steel, transverse beams	tonne	151	kr 5 572,00	kr 841 372,00
Processing rolled steel, ties	tonne	174	kr 5 860,00	kr 1 019 640,00
Processing rolled steel, end beam	tonne	42	kr 5 572,00	kr 234 024,00
Processing rolled steel, hanger connections	tonne	6,5	kr 8 920,00	kr 57 980,00
Welding, transverse beams	tonne	151	kr 6 880,00	kr 1 038 880,00
Welding, ties	tonne	174	kr 6 690,00	kr 1 164 060,00
Welding, end beams	tonne	42	kr 6 880,00	kr 288 960,00
Welding, hanger connections	tonne	6,5	kr 7 440,00	kr 48 360,00
Qualification of work procedures	piece	4	kr 22 290,00	kr 89 160,00
Blast cleaning, transverse beams	m ²	1176	kr 130,00	kr 152 880,00
Blast cleaning, ties	m ²	577	kr 130,00	kr 75 010,00
Blast cleaning, end beams	m ²	138	kr 130,00	kr 17 940,00
Blast cleaning, hanger connections	m ²	37	kr 130,00	kr 4 810,00
Metallization by thermal spray with zinc, transverse beams	m ²	1176	kr 283,00	kr 332 808,00
Metallization by thermal spray with zinc, ties	m ²	577	kr 283,00	kr 163 291,00
Metallization by thermal spray with zinc, end beams	m ²	138	kr 283,00	kr 39 054,00
Metallization by thermal spray with zinc, hanger connections	m ²	37	kr 283,00	kr 10 471,00
Sealer/tie-coat on thermal sprayed zinc, transverse beams	m ²	1176	kr 62,00	kr 72 912,00
Sealer/tie-coat on thermal sprayed zinc, ties	m ²	577	kr 62,00	kr 35 774,00
Sealer/tie-coat on thermal sprayed zinc, end beams	m ²	138	kr 62,00	kr 8 556,00
Sealer/tie-coat on thermal sprayed zinc, hanger connections	m ²	37	kr 62,00	kr 2 294,00
Epoxy mastic, transverse beams	m ²	1327	kr 106,00	kr 140 662,00
Epoxy mastic, ties	m ²	577	kr 106,00	kr 61 162,00
Epoxy mastic, end beams	m ²	138	kr 106,00	kr 14 628,00
Epoxy mastic, hanger connections	m ²	37	kr 106,00	kr 3 922,00
Transportation of steel structures	tonne	164	kr 3 272,00	kr 536 608,00
Assembly of steel structures*	RS	1	kr 5 748 631,00	kr 5 748 631,00
Network arch Bridge 2				kr 26 264 935,00
Network arch Driva Bridge				kr 25 310 058,00
Difference				kr 954 877,00

*cost based on the amount of steel compared to Driva Bridge

Table 9.33 Cost estimate - network arch - Bridge 2

10 Remedies

10.1 Bridge 1

Bridge 1 has significantly lower critical axial force in the arch compared to Driva Bridge, only 60% in the gravity load model: see Figure 9.3 and Figure 9.5. To try and increase the stability of Bridge 1 to the level of Driva Bridge, several measures were tested to see their influence on the global stability. It was not desirable to increase the cross-section, because of aesthetic considerations.

10.1.1 U-shape stiffening frame

The first remedy tested was a U-shaped stiffening frame. This is a very common way to ensure out-of-plane stability for arch bridges, where the rise of the arch is too low to have wind trusses between the arches. Figure 10.1 shows an example of this U-frame used on a timber arch bridge.

The U-frame is a bending stiff connection between a transverse beam and the arch at one or several locations of the structure [16]. Because the rise of the arch is so high, there is a practical limit for how far into the bridge span we can place the U-frame. At the third transverse beam the necessary height of the U-frame was already 9.7 meters. This would demand a significant cross-section of the U-frame column to restrain the arch from transverse movement.

To see the effect of the U-frame, a 100% stiff frame was assumed at the third transverse beam at each end. The frame was modelled as a rolling support, restraining only transverse displacement out-of-plane. The placement and illustration of the U-frame are shown in Figure 10.1. The third transverse beam is also the only placement that would allow the placement of a U-frame below the arch without it colliding with the hangers. The U-frame solution at any other transverse beam would have to be done in a different manner, for example having the U-frame column going up on the outside of the hangers and connecting to the side of the arch.

The buckling analysis of the U-frame model did not provide any significant improvement in stability for the structure. A comparison of the out-of-plane stability is shown in Figure 10.2.

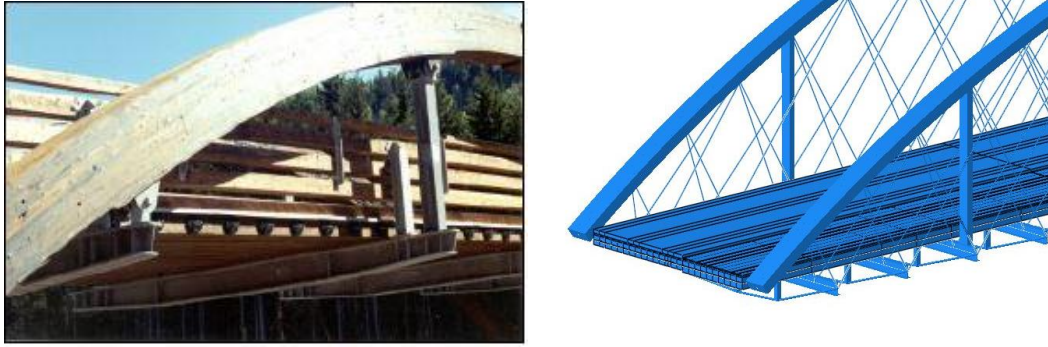


Figure 10.1 U-frame illustration



Load model		U-frame	Without U-frame
ULS-LM1-gr1a-Eq.b	Buckling factor	1.903	1.764
	Buckling mode 1		

Figure 10.2 U-frame. Comparison in out-of-plane stability

10.1.2 Lowered arch rise

The second method tested was to reduce the rise of the arch. The rise of the arch in bridge 1 and 2 is 18m, or 16.2% of the span, the same as for Driva Bridge. Since Bridge 1 is stabilized by the hanger’s out-of-plane angle, a reduction in the rise of the arch would increase that angle and thus increase the stability. Reducing the rise of the arch to 14 meters, 11.8% of the span, is considered low for a network arch, as mentioned in chapter 2.1 it is normal to lie between 15% and 20% of the span. Connecting the hangers at a wider distance to the transverse beam to increase the angle is not desirable, since the hangers already are connected with a wider distance than the width of the arch. Another positive effect is that the calculated wind load on the structure will decrease.

The axial forces in the arches increase with more than 25%, which combined with the increase in buckling factor reduces the buckling length both in- and out-of-plane, see Figure 5.1.

However, reducing the rise of the arch also leads to a significant increase in bending moments in the arch, which is unfavourable when it comes to buckling.

Table 10.1 and Table 10.2 show an overview of the changes in buckling factor (λ), axial force, bending moments, buckling length, buckling modes and utilization (%) for the load models with the highest utilization and the lowest out-of-plane stability.



Load model		Arch rise	
		14m	18m
ULS-LM1- gr1a-Eq.b	Buckling factor	1.87	1.764
	Axial force (MN)	13.46	10.73
	Buckling length out-of-plane (m)	29.9	42.3
	$M_{z.Ed}$ (kNm)	767	370
	$M_{y.Ed}$ (kNm)	873	1141
	$M_{x.Ed}$ (kNm)	72	158
	Utilization	0.78	0.78
	Buckling mode 1		

Table 10.1 Effects of reduced rise of arch, LM1 Eq b



Load model		Arch rise	
		14m	18m
Gravity	Buckling factor	2.59	2.48
	Axial force (MN)	10.77	7.75
	Buckling length out-of-plane (m)	35.6	42
	$M_{z.Ed}$ (kNm)	714	381
	$M_{y.Ed}$ (kNm)	344	322
	$M_{x.Ed}$ (kNm)	9	18
	Utilization	1.044	0.98
	Buckling mode 1		

Table 10.2 Effects of reduced rise of arch, Gravity

10.1.3 Increasing joint stiffness

The arch is divided into four parts and the assumed stiffness in the splice connections and the support connections are 50% of the arch material stiffness. Experiments done on the splice connection in bridge 1 and 2 shows that this is a conservative stiffness [29]. The results from the research of the joint stiffness is not published yet. Therefore, a simple approach was made to see how the joint stiffness would affect the structure. The joint stiffness was set to 100%, in other words: like there is no joint at all, and that the arch ends are fully clamped for sideways rotations.

The difference in global stability with 100% stiffness compared to the conservative approach with 50% stiffness was very small, see Table 10.3. Seeing the low increase of stability with the 100% stiff joint, shows that the conservative assumption of 50% stiffness does not skew the results of the bridge in any significant way.



Load model		Stiffness in joints and supports	
		50%	100%
ULS-LM1-gr1a-Eq.b	Buckling factor	1.764	1.866
	Buckling mode 1		

Table 10.3 Effects of increased joint stiffness

10.1.4 Trusses between arches in the top

The last remedy was wind trusses between the arches in the middle of the span, see Figure 10.3. Two K-shaped trusses like the ones used in Bridge 2, was used in the analysis, only changing the dimensions of the trusses.

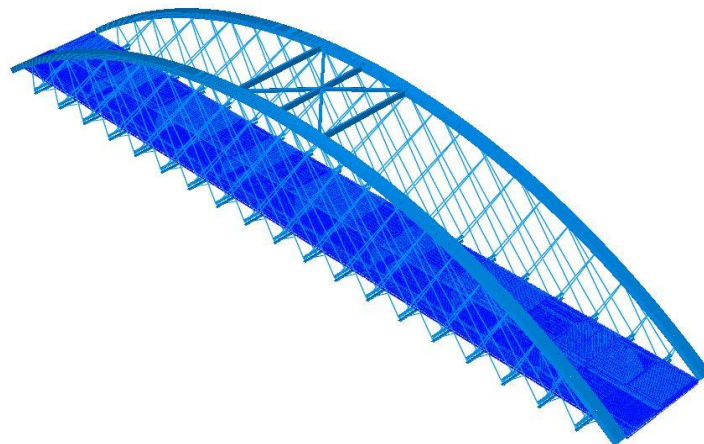


Figure 10.3 Wind trusses. Bridge 1

The dimension for the transverse trusses between the arches are 300x850 mm² and the diagonal trusses are 400x400 mm². The dimensions are chosen to increase the stiffness and global stability, and therefore the utilization in the wind-trusses are very low.

Results from the buckling analysis shows that by only placing two K-shaped wind trusses in the middle of the span, and keeping the original arch dimensions, results stability equal to Driva bridge. The results are presented in Table 10.4, show the increase in stability.





Load model		Wind trusses	
		Without	With
ULS-LM1-gr1a-Eq.b	Buckling factor	1.764	2.706
	Utilization	0.78	0.60
	Buckling curve		
ULS-Gravity	Buckling factor	2.48	3.54
	Utilization	0.98	0.72
	Buckling curve		

Table 10.4 Effects of wind trusses on bridge 1

10.2 Bridge 2

Bridge 2 has significantly higher critical axial force in the arch compared to Driva Bridge, 75% higher in the gravity load model, see Figure 9.3 and Figure 9.16. Since the stability of Bridge 2 was so high, it was decided to see how much of the wind bracing that could be removed, before the bridge was less stable than Driva Bridge. The idea of this was to reduce the number of unwanted connections on the sides of the arch.

Two K-shaped wind trusses were removed on each end of the bridge, and the arch cross-section is held constant with a width and height equal 1.1 meter. The results are presented in Table 10.5.

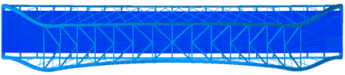
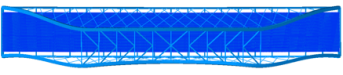

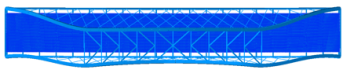
Load Model		Removed 4 K-shaped wind trusses + constant cross-section	
		Complete	Removed
ULS-LM4-gr4-Eq.b	Buckling factor	5.130	3.029
	Utilization	0.66	0.84
	Buckling mode 1		
ULS-Gravity	Buckling factor	6.605	3.824
	Utilization	0.86	0.83
	Buckling mode 1		

Table 10.5 Results after removing four K-shaped wind trusses

11 Discussion

11.1 Stability

The results from the buckling analyses in chapter 9.2.2 shows that Bridge 1 is considerably less stable compared to Driva Bridge. In order to be considered as an alternative to the steel and concrete bridge, the stability would have more or less the same. Especially if the bridges cost the same. The remedies tested to try to increase the stability did not show any significant improvement, except for the last remedy where wind trusses were placed between the arches in the middle of the span.

With wind trusses, the stability on Bridge 1 was equal to Driva Bridge, but the solution comes with a price. The wind trusses compromises the structural weather protection, and one of the main ideas of the bridge concept is to avoid connections that are exposed to rain. It is worth mentioning that the number of exposed connections is far less, compared to bridge 2 that only relies on wind trusses for sideways stability.

The aesthetic impression would also have to be considered, because the wind trusses will change the desired expression of the bridge, with two free and independent arches rising above the pavement. The wind trusses is placed approximately 16 meters above the bridge deck, so it might create such an oppressive feeling. No other thoughts have been given to this topic.

Bridge 2 offers great stability both in-plan and out-of-plane, compared to Driva Bridge. The results in chapter 9.2.1 and 9.2.3 shows that the critical axial load for out-of-plane buckling is 75% higher for Bridge 2 compared to Driva Bridge. This may be an indication that the design of bridge 2 is not the most efficient solution. The remedy with removing the two lower wind

trusses on each side and using a constant arch cross-section, shows results in stability equal to Driva Bridge. This solution also reduces the number of unfavourable connections on the sides of the arch, and may have the positive effect of creating a more open feeling.

11.2 Cost

The cost results in chapter 9.5 show that the stress laminated timber deck is 70% more expensive than the concrete deck. The uncertainty regarding the cost of the bridge deck is considered low. The cost are based on previous projects, and this thesis has not introduced any new approach to the deck solution, that would change the cost of production or assembly in any way. In addition, the deviation in price estimates on the concrete deck from the different contractors was negligible.

The asphalt layer has not been included in the cost estimate, but considering the solution using asphalt to create the cross-slope, the amount of asphalt needed is almost tripled, increasing the cost of the solution even more.

Bridge 1 has almost twice the amount of hangers as bridge 2. However, the prices given in Appendix I, shows that the price per hanger is reduced as the quantity increases, and also when the dimension of the hanger is reduced. This results in a negligible price difference between the two alternatives. Therefore, it can be said that the hanger cost alone, for Bridge 1, is not a reason to look for other alternatives.

The total cost of Bridge 1 and Bridge 2, excluding deck and hangers, presented in Table 9.32 and Table 9.33, shows that the estimated costs of the glulam bridges are competitive with Driva Bridge. However, there are some uncertainties in the cost estimates regarding the assembly cost of the network arch. The authors believe that the proposed connections in this thesis, is less complicated and labour-intensive than the standard dowel / slotted in steel plates connections the estimates are based on. With an easier solution the price should go down, given that the ongoing experiments shows that the solutions works as intended.

11.3 Feasibility

Bridge 1 offers less possibilities regarding erection of the network arch, since it has to be erected directly on its final foundation. For example, under the construction of Driva Bridge the traffic flow has to continue as normal during construction, and they want the new bridge to be placed on the same position as the old bridge. This is solved by erecting the new bridge at a temporary position and let the traffic run across it while the old bridge is demolished. This is impossible

with Bridge 1 without a temporary bottom chord to take the horizontal forces. Most likely, they would have to close the road for the entire demolition and construction period, because a temporary bridge or temporary road on fillings might be too expensive on such a wide river, compared to other alternatives.

Bridge 2 has the same possibilities as Driva Bridge regarding erection, not surprising, as the geometry is the same. In addition, since Bridge 2 has a lower self-weight than Driva Bridge it offers more opportunities with regards to transport of the bridge skeleton, in other situations. For example, using a floating crane to lift the complete skeleton without deck, weighing around 508 tonne.

The choice to only have structural weather protection is sufficient on both Bridge 1 and 2, given that the workmanship is done right. The report from the NRPA [24] shows many examples of poor workmanship resulting in premature deterioration of the timber structure. However, it is assumed in this thesis that the designing engineers has sufficient knowledge about timber structures, how to avoid water damage and conducts sufficient controls in the construction phase, to avoid unnecessary mistakes.

12 Conclusion

The conclusions are based on the comparison with Driva Bridge, but are also meant to be applicable for other situations, where timber bridges are considered.

Stability

For a 111 meter long span, Bridge 1 is too unstable with the chosen cross-section, 1600x850 mm². A remedy that solves the stabilization problem is to have wind bracing between the arches in the middle of the span. Bridge 2 is more than stable enough, and would be a good alternative for spans in this range.

Cost

Both alternatives are considered cost competitive with Driva Bridge.

Feasibility

Bridge 1 is possible to construct, but would need to be erected on its final foundations. This might limit the number of projects where the bridge solution would be considered. Bridge 2 is possible to construct and transport, and offers many different ways of construction.

13 Further work

Foundations have not been a topic in this thesis and is set to further work. Bridge 1 is 500 tonne lighter than Driva Bridge, but need more horizontal support from the foundation. Bridge 2 is 300 tonne lighter than Driva Bridge with the same support conditions. How will this effect the foundations?

Several research projects are ongoing at NTNU which are applicable for the two bridge alternatives. For instance, moment resistant splice joints, withdrawal strength and fatigue of threaded rods perpendicular to the grain, are being tested. In the case of using the proposed splice joints in massive glulam arches it is also necessary to run experiments on the joint capacity in bending out-of-plane.

If Bridge 1 with wind trusses is considered as an acceptable solution, more research should be made on this alternative.

Optimization of the steel parts in Bridge 2 is set as further work, because the authors know there are more to save here, for example using high strength steel, and approach the maximum stresses in the tie.

Introducing load trains in the model is set to further work. This should be used to find the correct stresses to use in the design check for fatigue, and find the worst load placement for hanger change. There may be a more suited software for this task, for example RM Bridge, which was used in the design of Driva Bridge.

The proposed solution for cross-slope on the deck requires a large amount of asphalt. Therefore another way of creating the cross-slope on such a wide stress laminated timber deck should be investigated. For example with skew cutting on the top of the lamellas.

Citations

1. Hansdatter A. *Tre KAN bli fremtidens byggemateriale*. 2012 [cited 2016 03.06]; Available from: <https://www.regjeringen.no/no/aktuelt/apningsinnlegg-tre-kan-bli-fremtidens-by/id698315/>.
2. Landbruks- og matdepartementet. *Trebroer for millioner*. 2014 [cited 2016 03.06]; Available from: <https://www.regjeringen.no/no/aktuelt/Trebroer-for-millioner/id764349/>.
3. Veie J. and Abrahamsen R.B., *Steien Network Arch Bridge*, in *2nd International Conference on Timber Bridges*. 2013: Las Vegas, Nevada USA.
4. Herksedal K. -*Dette gikk knakende godt!* 2016 [cited 2016 20.05.16]; Available from: <http://www.vareveger.no/artikler/dette-gikk-knakende-godt/277374>.
5. Pircher M., Stacha M., and Wagner J., *Stability of network arch bridges under traffic loading*. Proceedings of the Institution of Civil Engineers - Bridge Engineering, 2013. **166**(3): p. 186-192.
6. Tveit P., *An Introduction to the Network Arch*. 2006: <http://home.uia.no/pert/index.php/>.
7. Vlad M., et al., *A MODERN APPROACH TO TIED-ARCH BRIDGE ANALYSIS AND DESIGN*. Institutul Politehnic din Iasi. Buletinul. Sectia Constructii. Arhitectura, 2015. **61**(2): p. 75-75.
8. Tveit P., *Considerations for Design of Network Arches*. Journal of Structural Engineering, 1987. **113**(10): p. 2189-2207.
9. Tveit P., *The Network Arch. Bits of Manuscript in March 2014 after Lectures in 50+ Countries*. 2014.
10. Tveit P. *About the Network Arch*. 2011 [cited 2016 24.05.16]; 2nd:[Available from: http://home.uia.no/pert/index.php/My_Publications.
11. Tang Man-Chung, *The art of arches. Maintenance, Management, Life-Cycle Design and Performance*, 2015. **11**(4): p. 443-449.
12. Bell K., *Structural systems for glulam arch bridges*, in *International Conference on Timber Bridges*. 2010: Lillehammer, Norway.
13. Teich S., *Development of general design principles for the hanger arrangements of network arch bridges*. Stahlbau, 2011. **80**(2): p. 100-111.
14. Hårstad-Evjen J.A., *Tretten Bridge - Timber and Steel in Harmony*, in *2. International Conference on Timber Bridges 2013*: Las Vegas, Nevada USA.
15. Broer.no. *Flisa Bru*. [cited 2016 23.05.16]; Available from: <http://broer.no/bro/index.php?ID=63>.
16. Statens Vegvesen, *Trebruhåndboken*. 2016.
17. Kasperski M., *Vibration serviceability for pedestrian bridges*. Proceedings of the Institution of Civil Engineers - Structures and Buildings, 2006. **159**(5): p. 273-282.
18. johs.Holts as, *Fv. 62 DRIVA BRU, Beregningsrapport*. 2015.
19. Statens Vegvesen, *Håndbok N400: Bruprosjektering*. 2015.
20. 3DS SIMULIA. *Abaqus 6.14 Online Documentation*. 2014 [cited 2016; Available from: <http://129.97.46.200:2080/v6.14/books/usb/default.htm>.
21. Hovi S.B. and Skjerve E.K., *Prosjektering av nettverksbuebru i tre over Orkla*, in *Department of Structural Engineering*. 2015, NTNU.
22. Barli R. and Hakvåg I., *Conceptual Study of Long Arched Timber Bridges - Experimental and Numerical Modeling.*, in *Department of Structural Engineering*. 2013, NTNU.
23. Van De Pontseele K.A.A. and Seides D., *Modelling of Pedestrian Loading on Slender Footbridges*, in *Department of Structural Engineering*. 2015, NTNU.
24. Statens Vegvesen, *Inspeksjonserfaring på trebruer. Learning Experiences from Timber Bridge Inspections*. 2016. p. 61.

25. Elovaara E., et al., *Significance of dermal and respiratory uptake in creosote workers: exposure to polycyclic aromatic hydrocarbons and urinary excretion of 1-hydroxypyrene*. *Occup Environ Med*, 1995. **52**(3): p. 196-203.
26. Norwegian Environment Agency. *Questions and answers about creosote*. [cited 2016 30.05]; Available from: <http://www.miljodirektoratet.no/no/Tjenester-og-verktoy/Sporsmal-og-svar/Sporsmal-og-svar-om-kreosot/>.
27. Norsk Standard, *NS-EN 1993-1-8:2005+NA:2009 Eurocode 3: Design of steel structures - Part 1-8: Design of joints*.
28. Norsk Standard, *NS-EN 1995-1-1:2004+AI:2008+NA:2010 Eurocode 5: Design of timber structures - Part 1-1: General - Common rules and rules for buildings*.
29. Malo K.A., *MSc meeting with the supervisor from the Department of structural engineering at NTNU*. 2016.
30. Stamatopoulou S H. and Malo K.A., *Withdrawal capacity of threaded rods embedded in timber elements*. *Construction and Building Materials*, 2015. **94**: p. 387.
31. DYWIDAG. *DYWIDAG-SYSTEMS*. [cited 2016 25.05]; Available from: <http://www.dywidag-norge.no/wp-content/uploads/2013/09/GEWI-PLUS-bars.pdf>.
32. Statens Vegvesen, *Håndbok N200: Vegbygging*. 2014.
33. NCC. *NCC Topeka 4s*. [cited 2016 20.05]; Available from: http://www.ncc.no/globalassets/produktdatablad_ncc_topeka_4s.pdf.
34. Focus Software. *Focus Konstruksjon*. 2015 [cited 2016 30.05]; Available from: <https://www3.focus.no/produkter/focus/focus-konstruksjon/>.
35. Statens Vegvesen, *Håndbok N101: Rekkverk og vegens sideområder*. 2013.
36. Dahl K. B., *Mechanical properties of clear wood from Norway spruce, Paper II*, in *Department of Structural Engineering*. 2009, NTNU.
37. FATZER AG, *FATZER seilbau structural ropes*. 2016. p. 26.
38. Statens Vegvesen, *Beregningsrapport Steibrua*. 2014.
39. Norsk Standard, *NS-EN 1991-1-5:2003+NA:2008 Eurocode 1: Actions on structures - Part 1-5: General actions - Thermal actions*.
40. Kepp H. and Dyken T., *Thermal Action on Timber Bridges*, in *International Conference Timber Bridges*. 2010: Lillehammer, Norway.
41. Norsk Standard, *NS-EN 1991-1-4:2005+NA:2009 Eurocode 1: Actions on structures - Part 1-4: General actions - Wind actions*.
42. Norsk Standard, *NS-EN 1991-2:2003+NA:2010 Eurocode 1: Actions on structures - Part 2: Traffic loads on bridges*.
43. Norsk Standard, *NS-EN 1998-1:2004+AI:2013+NA2014. Eurocode 8: Design of structures for earthquake resistance. Part 1: General rules, seismic actions and rules for buildings*.
44. Norsk Standard, *NS-EN 1998-2:2005+AI:2009+A2:2011+NA2014. Eurocode 8: Design of structures for earthquake resistance. Part 2: Bridges*.
45. Norsk Standard, *NS-EN 1990:2002/A1:2005+NA2010 Eurocode: Basis of structural design. Amendment A1*.
46. A., K., *Den Nye Driva Bru på Sunndalsøra 1*. 2016, Youtube.
47. Tveit P., et al., *Systematic Thesis on Network Arches*. 2014, University of Agder.

Appendix

Not all the attached material have been presented in the bound copy, some attachments are partly presented in the bound copy and/or presented as data files. It is mainly utilization calculations and design calculations that have been partly presented in the bound copy, only showing one example of every spreadsheet used in the design check.

Explanation of notice:

- (+ *Data*): Parts of the attached material are presented in the bound copy, the remaining parts are given as data files.
- (*Data*): Only given as data files
- (*Confidential*): Sensors only. Data files

Appendix A.....

A.1_Bridge_1_Wind_Calculations

A.2_Bridge_2_Wind_Calculations (Data)

A.3_Bridge_1_Wind_Calculations_14m_Rise.Wind_Calculations (Data).....

Appendix B

B.1_Traffic_Loads

B.2_Load_Combination_ULS_Bridge_1

B.3_Load_Combination_SLS_Bridge_1.....

B.4_Load_Combination_ULS_Bridge_2 (Data)

B.5_Load_Combination_SLS_Bridge_2 (Data)

B.4_Load_Combination_ULS_Bridge_2 (Data).....

B.6_Load_Combination_ULS_Bridge_1_14m_Rise (Data)

B.7_Load_Combination_SLS_Bridge_1_14m_Rise (Data).....

Appendix C

LM1_Load_Placement

Appendix D.....

Earthquake_Calculation.....

Appendix E

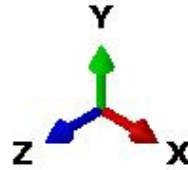
E.1_Stress laminated bridge deck design

E.2_Simplified deck analysis	
Appendix F.....	
F.1_T-Stub_Design Bridge 1	
F.2_T-Stub_Design Bridge 2 (Data)	
F.3_Hangers forces Bridge 1. ULS_LM1_Eq_b (Data)	
F.4_Hangers forces Bridge 2. ULS_LM1_Eq_b (Data)	
Appendix G.....	
G.1_Arch_Design_Check_Bridge 1 (+Data).....	
G.2_Arch_Design_Check_Bridge 2 (+Data).....	
G.3_Arch_Design_Check_Bridge 1. 14m Rise (Data)	
G.4_Arch_Design_Check_Bridge 1. Wind trusses in top (Data)	
Appendix H.....	
H.1_Transverse_Beam_ULS_Design_Check_Focus_Konstruksjon (+Data)	
H.2_Transverse_Beam_SLS_Design_Check_Focus_Konstruksjon (+Data)	
H.3_Transverse_Beam_calculated steel amount, surface and volume (Data)	
Appendix I.....	
I.1_Hanger cost (Confidential).....	
Appendix J.....	
J.1_Abaqus numerical models and output database (Data).....	
Appendix K.....	
K.1_Design Check Tie (+Data).....	
Appendix L.....	
L.1_Design Check Wind Trusses (+Data).....	
Appendix M.....	
M_Asphalt_Design Check.....	
Appendix N.....	
N_Design of Guardrail (Data).....	

Appendix_A: Wind Calculation

Driva bridge 1

Wind parameters



z-direction (transverse direction)
x-direction (longitudinal direction)

Wind class 1 (First natural oscillatory period)

$$T \leq 2 \text{ s}$$

Natural oscillation period, see main report chapter 6.2.2.
[Håndbok N400 5.4.3]

$$v_{b,0} := 27 \frac{\text{m}}{\text{s}}$$

Reference wind speed - Sunndal municipality,
[NS-EN 1991-1-4:2005 tab. NA.4(901.1)]

$$v_0 := 30 \frac{\text{m}}{\text{s}}$$

Limit value,
[NS-EN 1991-1-4:2005 PKT. NA.4.2(2)P (901.1)]

$$v := 15 \cdot 10^{-6} \frac{\text{m}^2}{\text{s}}$$

Kinematic air viscosity,
[NS-EN 1991-1-4 pky. 7.9.1(1)]

$$\rho_{air} := 1.25 \frac{\text{kg}}{\text{m}^3}$$

Air density ,
[NS-EN 1991-1-4:2005/NA:2009, NA.4.5]

$$\psi_0 := 0.7$$

Combination factor wind, accompanying loads, [NS-EN 1990:2002/A1:2005/NA:2010 tab.NAA2.1]

Bridge dimensions

$$l_{Bridge} := 111 \text{ m}$$

Bridge length

$$l_{Arch} := 118.627 \text{ m}$$

Arch length

$$b_{Bridge} := 16.1 \text{ m}$$

Bridge width

$$f_{Arch} := 18 \text{ m}$$

Rising height

$$h_{Traffic} := 2 \text{ m}$$

Height of vehicle

$$h_{Railing} := 1.2 \text{ m}$$

Equivalent height, railings, [NS-EN 1991-1-4:2005 tab. 8.1]

$$h_{Deck} := 800 \text{ mm}$$

Deck height

$$b_{Deck} := 12.95 \text{ m}$$

Deck width

$$h_{Arch} := 850 \text{ mm}$$

Arch cross section height

$$b_{Arch} := 1600 \text{ mm}$$

Arch cross section width

$$d_{Hanger} := 30 \text{ mm}$$

Hanger diameter

$$h_{Tension} := 0 \text{ mm}$$

Tie height

$$z_{free} := 6 \text{ m}$$

The clearance under the bridge (conservative)

$$z_e := z_{free} + 0.5 \cdot (h_{Deck} + h_{Tension})$$

Bridge deck, reference height (from lowest ground level to the center of the deck structure),[NS-EN 1991-1-4:2005 pkt. 7.91(6)]

$$z_e = 6.4 \text{ m}$$

$$z_{e.Arch} := z_{free} + f_{Arch}$$

Arch, reference height (from lowest ground level to top of arch), [NS-EN 1991-1-4:2005 pkt. 7.91(6)]

$$z_{e.Arch} = 24 \text{ m}$$

Dynamic calculations **NOT** required in wind class 1

$$c_s := 1.0$$

size factor (conservative)

$$c_d := 1.0$$

Dynamic factor (conservative)

$$c_s \cdot c_d = 1$$

[NS-EN 1991-1-4:2005+NA:2009 pkt.8.2(1)]

Calculation of basic wind velocity

$$c_{dir} := 1.0$$

Direction factor,
[NS-EN 1991-1-4:2005+NA:2009 pkt. NA.4.2(2)P]

$$c_{season} := 1.0$$

Seasonal factor,
NS-EN 1991-1-4:2005+NA:2009 tab. NA.4.2(2)

$$c_{alt} := 1.0$$

Level factor,
[NS-EN 1991-1-4:2005+NA:2009 tab. NA.4.2(2) P(901.1)]

$$c_{prob} := 1.0$$

Probability factor, Return period 50 year,
[NS-EN 1991-1-4:2005+NA:2009 NA.4.2(2)]

$$v_b := c_{dir} \cdot c_{season} \cdot c_{alt} \cdot c_{prob} \cdot v_{b,0}$$

basic wind velocity,
[NS-EN 1991-1-4:2005+NA:2009 tab. NA.4.2(2)]

$$v_b = 27 \frac{\text{m}}{\text{s}}$$

Calculation of mean wind velocity

$$k_r := 0.19$$

Terrain category II. Terrain categories and terrain parameters [NS-EN 1991-1-4:2005 tab. NA.4.1]

$$z_0 := 0.05 \text{ m}$$

$$z_{min} := 4 \text{ m}$$

$$c_r(z) := \begin{cases} \text{if } z \leq z_{min} \\ \quad \left\| k_r \cdot \ln \left(\frac{z_{min}}{z_0} \right) \right. \\ \text{else} \\ \quad \left\| k_r \cdot \ln \left(\frac{z}{z_0} \right) \right. \end{cases}$$

Terrain roughness, [NS-EN 1991-1-4:2005 Eq. (4.4)]

$$c_r(z_e) = 0.922$$

$$c_r(z_{e.Arch}) = 1.173$$

$$c_0 := 1.0$$

Terrain topography factor, [NS-EN 1991-1-4:2005 kap. 4.3.3]

$$v_m(z) := c_r(z) \cdot c_0 \cdot v_b$$

Mean wind velocity, [NS-EN 1991-1-4:2005 kap. 4.3.1]

$$v_m(z_e) = 24.891 \frac{\text{m}}{\text{s}}$$

$$v_m(z_{e.Arch}) = 31.672 \frac{\text{m}}{\text{s}}$$

Wind turbulence

$$k_I := 1.0$$

Turbulence factor,
[NS-EN 1991-1-4:2005 pkt. NA.4.4(1)]

$$\sigma_v := k_r \cdot v_b \cdot k_I = 5.13 \frac{\text{m}}{\text{s}}$$

Standard deviation,
[NS-EN 1991-1-4:2005 lign. (4.6)]

$$I_v(z) := \begin{cases} \text{if } z \leq z_{min} \\ \quad \left| \frac{\sigma_v}{v_m(z_{min})} \right| \\ \text{else} \\ \quad \left| \frac{\sigma_v}{v_m(z)} \right| \end{cases}$$

Turbulence intensity,
[NS-EN 1991-1-4:2005 lign. (4.7)]

$$I_v(z_e) = 0.206$$

$$I_v(z_{e.Arch}) = 0.162$$

Calculation of wind velocity pressure

$$k_p := 3.5$$

Peak factor

$$v_p(z) := v_m(z) \cdot \sqrt{1 + 2 k_p \cdot I_v(z)}$$

Wind velocity, deck and arch,
[NS-EN 1991-1-4:2005 pkt. NA.4.4(1)]

$$v_p(z_e) = 38.902 \frac{\text{m}}{\text{s}}$$

$$v_p(z_{e.Arch}) = 46.265 \frac{\text{m}}{\text{s}}$$

$$q_b(z) := 0.5 \cdot \rho_{air} \cdot v_b^2 = 0.456 \text{ kPa}$$

Basic velocity pressure,
[NS-EN 1991-1-4:2005 pkt. NA.4.5(1)]

$$q_m(z) := 0.5 \cdot \rho_{air} \cdot v_m(z)^2$$

Location specific basic velocity pressure,
[NS-EN 1991-1-4:2005 lign. (NA.4.8)]

$$q_m(z_e) = 0.387 \text{ kPa}$$

$$q_m(z_{e.Arch}) = 0.627 \text{ kPa}$$

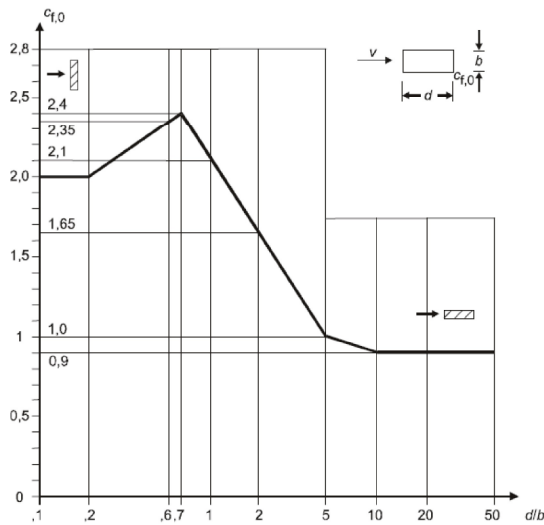
$$q_p(z) := (1 + 2 \cdot k_p \cdot I_v(z)) \cdot q_m(z)$$

$$q_p(z_e) = 0.946 \text{ kPa}$$

$$q_p(z_{e,Arch}) = 1.338 \text{ kPa}$$

The peak velocity pressure,
[NS-EN 1991-1-4:2005 lign. (NA.4.8)]

Force factor on arch



Force coefficients $c_{f,0}$ of rectangular sections with sharp corners and without free end flow ,

[NS-EN 1991-1-4:2005+NA:2009 fig. 7.23]

$$\frac{b_{Arch}}{h_{Arch}} = 1.882$$

$$c_{f,0} := 1.70$$

$$\psi_r := 1.0$$

$$\lambda := \min\left(1.4 \cdot \frac{l_{Arch}}{h_{Arch}}, 70\right) = 70$$

$$\varphi := 1.0$$

$$\psi_\lambda := 1.0$$

$$c_{f,Arch} := c_{f,0} \cdot \psi_r \cdot \psi_\lambda = 1.7$$

Reduction factor ψ_r for a square cross-section with rounded corners. $r=0$

[NS-EN 1991-1-4:2005+NA:2009 fig. 7.24]

Effective slenderness,

[NS-EN 1991-1-4:2005+NA:2009 tab. 7.16]

The solidity ratio,

[NS-EN 1991-1-4:2005+NA:2009 lign. (7.28)]

End-effect factor. $\lambda = 70$ and $\varphi = 1$

[NS-EN 1991-1-4:2005+NA:2009 fig. 7.36]

Force coefficient,

[NS-EN 1991-1-4:2005+NA:2009 Eq. (7.9)]

Force coefficient on hangers

$$c_{f.Hanger} := 1.2$$

Force coefficient for stranded cables,
[NS-EN 1991-1-4:2005+NA:2009 pkt. 7.9.2(3)]

$$c_{f.Hanger} := 2.0$$

To include the wind force on ropes. The rope network is viewed as a flat lattice structure with low solidity ratio

$$\varphi = 0 \text{ [NS-EN 1991-1-4:2005+NA:2009 fig. 7.33]}$$

Force factors on the bridge deck, z-direction (transverse direction)

$$c_{fz.0}(b, d_{tot}) := \begin{cases} \text{if } \frac{b}{d_{tot}} \leq 0.5 \\ \parallel 2.4 \\ \text{else if } 0.5 \leq \frac{b}{d_{tot}} \leq 4 \\ \parallel 2.4 - \frac{1.1}{3.5} \cdot \left(\frac{b}{d_{tot}} - 0.5 \right) \\ \parallel \\ \text{else} \\ \parallel 1.3 \end{cases}$$

Force factor in z-direction,
[NS-EN 1991-1-4:2005 fig. 8.3]

$$\varphi_{inclination} := \text{atan}(3\%) = 1.718 \text{ deg}$$

3% inclination in the transverse direction

$$f_{inclination} := \min\left(1 + 0.03 \cdot \varphi_{inclination} \cdot \frac{360}{2\pi}, 1.25\right)$$

Increasing by 3% per gradient,
[NS-EN 1991-1-4:2005 pkt. 8.3.1(3)]

$$f_{inclination} = 1.052$$

$$c_{fz.0}(b, d_{tot}) := c_{fz.0}(b, d_{tot}) \cdot f_{inclination}$$

Force coefficient, x-direction

$$c_{fx} := 0.5$$

Force coefficient, x-direction. 50% of the wind forces in z-direction,
[NS-EN 1991-1-4:2005 pkt. 8.3.4(1)]

Force coefficient, y-direction (vertical direction)

$$c_{fy} := 0.9$$

Force coefficient in y-direction,
[NS-EN 1991-1-4:2005 pkt. 8.3.3(1)]

Wind force acting on the deck **WITHOUT** traffic

$$d_{tot} := h_{Tension} + h_{Deck} + h_{Railing}$$

$$d_{tot} = 2 \text{ m}$$

$$c_{fz.0}(b_{Deck}, d_{tot}) = 1.367$$

$$q_{z.Deck} := q_p(z_e) \cdot c_{fz.0}(b_{Deck}, d_{tot}) \cdot d_{tot}$$

$$q_{z.Deck} = 2.586 \frac{\text{kN}}{\text{m}}$$

$$q_{y.Deck} := q_p(z_e) \cdot c_{fy} \cdot b_{Deck}$$

$$q_{y.Deck} = 11.024 \frac{\text{kN}}{\text{m}}$$

Calculated performance depth,
NS-EN 1991-1-4:2005 fig. 8.3]

Characteristic horizontal wind load
on deck . Håndbok N400. 5.4.3.4]

Characteristic vertical wind load on deck,
[Håndbok N400. 5.4.3.42]

Wind force acting on the arch **WITHOUT** traffic

$$q_{z.Arch} := q_p(z_{e.Arch}) \cdot c_{f.Arch} \cdot h_{Arch}$$

$$q_{z.Arch} = 1.93306 \frac{\text{kN}}{\text{m}}$$

Characteristic horizontal wind load
on arch

Wind force acting on the hangers **WITHOUT** traffic

$$q_{z.Hanger} := q_p(z_{e.Arch}) \cdot c_{f.Hanger} \cdot d_{Hanger}$$

$$q_{z.Hanger} = 0.080265 \frac{\text{kN}}{\text{m}}$$

Characteristic horizontal wind loads
on hangers

Calculation of wind velocity **WITH** traffic

$$v_{p.*} := 35 \frac{\text{m}}{\text{s}}$$

Maximum gust velocity at the deck,
NS-EN 1991-1-4:2005 pkt. NA8.1(4)]

$$v_{m.*}(z) := \frac{v_{p.*}}{\sqrt[2]{1 + 2 k_p \cdot I_v(z)}}$$

$$v_{m.*}(z_e) = 22.394 \frac{\text{m}}{\text{s}}$$

$$v_{b.*}(z) := \frac{v_{m.*}(z)}{c_r(z) \cdot c_0}$$

$$v_{b.*}(z_e) = 24.292 \frac{\text{m}}{\text{s}}$$

$$v_{b.0.*} := \frac{v_{b.*}(z_e)}{c_{dir} \cdot c_{season} \cdot c_{alt} \cdot c_{prob}} = 24.292 \frac{\text{m}}{\text{s}}$$

(Applies if less than $v_{b.0} = 27 \frac{\text{m}}{\text{s}}$)

$$v_{m.*}(z) := c_r(z) \cdot c_0 \cdot v_{b.*}(z_e)$$

Mean wind velocity, Arch and deck
[NS-EN 1991-1-4:2005 kap. 4.3.1]

$$v_{m.*}(z_e) = 22.394 \frac{\text{m}}{\text{s}}$$

$$v_{m.*}(z_{e.Arch}) = 28.495 \frac{\text{m}}{\text{s}}$$

$$v_{p.*}(z) := v_{m.*}(z) \cdot \sqrt[2]{1 + 2 k_p \cdot I_v(z)}$$

Gust velocity, Arch and deck,
[NS-EN 1991-1-4:2005 pkt. NA.4.4(1)]

$$v_{p.*}(z_e) = 35 \frac{\text{m}}{\text{s}}$$

$$v_{p.*}(z_{e.Arch}) = 41.624 \frac{\text{m}}{\text{s}}$$

$$q_{p.*}(z) := 0.5 \cdot \rho_{air} \cdot v_{p.*}(z)^2$$

The peak velocity pressure,
[NS-EN 1991-1-4:2005+NA:2009 lign. (NA.4.8)]

$$q_{p.*}(z_e) = 0.766 \text{ kPa}$$

$$q_{p.*}(z_{e.Arch}) = 1.083 \text{ kPa}$$

$$q_{p.*.d}(z) := \min(q_{p.*}(z), \psi_0 \cdot q_p(z))$$

Design wind pressure WITH traffic,
[NS-EN 1990:2002/A1:2005+NA:2010 pkt. A2.2(5)]

$$q_{p.*.d}(z_e) = 0.662 \text{ kPa}$$

$$q_{p.*.d}(z_{e.Arch}) = 0.936 \text{ kPa}$$

Wind force acting on the deck WITH traffic

$$d_{tot.*} := h_{Tension} + h_{Deck} + h_{Traffic}$$

Calculated performance depth,
NS-EN 1991-1-4:2005 fig. 8.3]

$$d_{tot.*} = 2.8 \text{ m}$$

$$c_{fz.0}(b_{Deck}, d_{tot.*}) = 1.367$$

$$q_{z.Deck.*} := q_{p.*.d}(z_e) \cdot c_{fz.0}(b_{Deck}, d_{tot.*}) \cdot d_{tot.*}$$

Characteristic horizontal wind loads on deck,
[Håndbok N400, 5.4.3.4]

$$q_{z.Deck.*} = 2.534 \frac{\text{kN}}{\text{m}}$$

$$q_{y.Deck.*} := q_{p.*.d}(z_e) \cdot c_{fy} \cdot b_{Deck}$$

Characteristic vertical wind load on deck,
[Håndbok N400, 5.4.3.4]

$$q_{y.Deck.*} = 7.717 \frac{\text{kN}}{\text{m}}$$

Wind force acting on the arch WITH traffic

Characteristic horizontal wind loads on arch

$$q_{z.Arch.*} := q_{p.*.d}(z_{e.Arch}) \cdot c_{f.Arch} \cdot h_{Arch}$$

$$q_{z.Arch.*} = 1.35314 \frac{\text{kN}}{\text{m}}$$

Wind force acting on the hangers WITH traffic

Characteristic horizontal wind loads on hangers

$$q_{z.Hanger.*} := q_{p.*.d}(z_{e.Arch}) \cdot c_{f.Hanger} \cdot d_{Hanger}$$

$$q_{z.Hanger.*} = 0.056186 \frac{\text{kN}}{\text{m}}$$

Appendix_B.1: Traffic loads

Bridge 1

Geometry

$$w := 12.95 \text{ m}$$

Width deck

$$l_{bru} := 111 \text{ m}$$

Length bridge

$$r := \infty$$

Radius bridge deck

Traffic lane

$$w_l := 3 \text{ m}$$

Width traffic lane,
[NS-EN 1991-2:2003+NA:2010 table. 4.1]

$$n_l := \text{floor} \left(\frac{w}{w_l} \right) = 4$$

Number of lanes,
[NS-EN 1991-2:2003+NA:2010 table. 4.1]

$$w_r := w - n_l \cdot w_l = 0.95 \text{ m}$$

Other area,
[NS-EN 1991-2:2003+NA:2010 table. 4.1]

Vertical load- Load model 1 (LM1)

$$Q_{1k} := 300 \text{ kN}$$

$$q_{1k} := 9 \frac{\text{kN}}{\text{m}^2}$$

Traffic lane 1 - characteristic load value,
[NS-EN 1991-2:2003+NA:2010 table. 4.2]

$$\alpha_{Q1} := 1.0$$

$$\alpha_{q1} := 0.6$$

Traffic lane 1 - correction factors,
[NS-EN 1991-2:2003+NA:2010. NA.4.3.2(3)]

$$Q_{2k} := 200 \text{ kN}$$

$$q_{2k} := 2.5 \frac{\text{kN}}{\text{m}^2}$$

Traffic lane 2 - characteristic load value,
[NS-EN 1991-2:2003+NA:2010 table. 4.2]

$$\alpha_{Q2} := 1.0$$

$$\alpha_{q2} := 1.0$$

Traffic lane 2 - correction factors,
[NS-EN 1991-2:2003+NA:2010. NA.4.3.2(3)]

$$Q_{3k} := 100 \text{ kN}$$

$$q_{3k} := 2.5 \frac{\text{kN}}{\text{m}^2}$$

Traffic lane 3 - characteristic load value,
[NS-EN 1991-2:2003+NA:2010 table. 4.2]

$$\alpha_{Q3} := 1.0$$

$$\alpha_{q3} := 1.0$$

Traffic lane 3 - correction factors,
[NS-EN 1991-2:2003+NA:2010. NA.4.3.2(3)]

$$q_{rk} := 2.5 \frac{\text{kN}}{\text{m}^2}$$

Other area- characteristic load value,
[NS-EN 1991-2:2003+NA:2010 table. 4.2]

$$\alpha_{rk} := 1.0$$

Other areacorrection factors,
[NS-EN 1991-2:2003+NA:2010. NA.4.3.2(3)]

Vertical load- Load model 2 (LM2)

$$Q_{ak} := 400 \text{ kN}$$

Traffic lane i- characteristic load value,
[NS-EN 1991-2:2003+NA:2010.4.3.3(1)]

$$\beta_Q := 1$$

[NS-EN 1991-2:2003+NA:2010 pkt. NA.4.3.3]

Vertical load- Load model 4 (LM4)

$$q_{Crowd} := 5.0 \frac{\text{kN}}{\text{m}^2}$$

Crowd loading- characteristic load
value,
[NS-EN 1991-2:2003+NA:2010. 4.3.5]

Horizontal traffic loads - Braking and acceleration associated with LM1

$$Q_{lk} := 0.6 \cdot \alpha_{Q1} \cdot (2 \cdot Q_{1k}) + 0.1 \cdot \alpha_{q1} \cdot q_{1k} \cdot w_l \cdot l_{bru}$$

Braking load - characteristic load value,
[NS-EN 1991-2:2003+NA:2010 lign. (4.6)]

$$Q_{lk} = 539.82 \text{ kN}$$

$$\text{if } 180 \cdot \alpha_{Q1} \cdot \text{kN} \leq Q_{lk} \leq 900 \text{ kN} \text{ } = \text{“OK”}$$

|| “OK”

else

|| “IKKE OK”

Centrifugal and transverse loads (LM1)

$$Q_{tk} := 0 \text{ kN}$$

No centrifugal forces $r := \infty$,
[NS-EN 1991-2:2003+NA:2010 tab. 4.3]

$$Q_{trk} := 0.25 \cdot Q_{lk} = 134.955 \text{ kN}$$

Skewed braking,
[NS-EN 1991-2:2003+NA:2010 pkt. 4.4.2(4)]

Appendix_B.2: Load Combination

Ultimate Limit State (ULS) Bridge 1

DESIGN VALUE OF ACTIONS (STR/GEO) (Set B)

Persistent and transient design situation	Permanent actions		Leading variable action (*)	Accompanying variable actions
	Unfavourable	Favourable		
(Eq.6.10 a)	$\gamma_{Gj,sup} \cdot G_{kj,sup}$	$\gamma_{Gj,inf} \cdot G_{kj,inf}$	$\gamma_{Q,1} \cdot \psi_{0,1} \cdot Q_{k,1}$	$\gamma_{Q,i} \cdot \psi_{0,i} \cdot Q_{k,i}$
(Eq.6.10 b)	$\gamma_{Gj,sup} \cdot G_{kj,sup}$	$\gamma_{Gj,inf} \cdot G_{kj,inf}$	$\gamma_{Q,1} \cdot Q_{k,1}$	$\gamma_{Q,i} \cdot \psi_{0,i} \cdot Q_{k,i}$

Load factor, γ , can be found in NA.A2(A) and combination factors, ψ , can be found in table NA.A2.1 for road bridges.

ULS STR/GEO-set B	1a	1b	2a	2b	4a	4b	5a	5b	6b
Permanent loads	gr1a	gr1a	gr1b	gr1b	gr4	gr4	Wind without traffic	Wind without traffic	Temp.
Self weight	1,35	1,20	1,35	1,20	1,35	1,20	1,35	1,20	1,20
Variable loads	Variable loads with a favourable effect: 0,0								
Traffic, LM1	0,95	1,35	-	-	-	-	-	-	0,95
Traffic, pedestrian	0,95	1,35	-	-	0,95	1,35	-	-	0,95
Traffic, LM2	-	-	0,95	1,35	-	-	-	-	-
Traffic, LM4	-	-	-	-	0,95	1,35	-	-	-
Traffic, horizontal forces	0,95	1,35	-	-	-	-	-	-	0,95
Wind with traffic	1,12	1,12	1,12	1,12	1,12	1,12	-	-	1,12
Wind without traffic	-	-	-	-	-	-	1,12	1,6	-
Temperature	0,84	0,84	0,84	0,84	0,84	0,84	0,84	0,84	1,2

Table 6.2: UIS STR/GEO- sett B. Values show load factors (γ) multiplied with combination factors (ψ)

Dimension bridge deck. Stress laminated glulam GL24c

$$t_{pedestrian.GL24c} := 800 \text{ mm}$$

Thickness: pedestrian lane

$$t_{roadway.GL24c} := 600 \text{ mm}$$

Thickness: roadway

$$b_{deck} := 12950 \text{ mm}$$

Total width

Wind WITH traffic

$$q_{k,y,deck.wTraffic} := 7.717 \frac{kN}{m}$$

Vertical characteristic wind load on deck, see appendix A

$$q_{k,z,deck.wTraffic} := 2.534 \frac{kN}{m}$$

Horizontal characteristic wind load on deck, see appendix A

$$q_{k,z,Arch.wTraffic} := 1.35314 \frac{kN}{m}$$

Horizontal characteristic wind load arch, see appendix A

Wind WITHOUT traffic

$$q_{k,y,deck.woTraffic} := 11.024 \frac{kN}{m}$$

Vertical characteristic wind load on deck, see appendix A

$$q_{k,z,deck.woTraffic} := 2.586 \frac{kN}{m}$$

Horizontal characteristic wind load on deck, see appendix A

$$q_{k,z,Arch.woTraffic} := 1.93306 \frac{kN}{m}$$

Horizontal characteristic wind load arch, see appendix A

Traffic Load 1a, gr1a (Eq. 6.10a)

$$A_{contact} := 400 \text{ mm} \cdot 400 \text{ mm}$$

Contact area, boggy.
[NS-EN 1991-2:2003/NA:2100, 4.3.2(1)]

$$A_{contact} = (1.6 \cdot 10^5) \text{ mm}^2$$

$$\alpha_{q1} := 0.6$$

Correction factor,
[NS-EN 1991-2:2003/NA:2100, NA.4.3.2(3)]

Lane 1

$$q_{1k} := 0.95 \cdot \alpha_{q1} \cdot 9 \frac{\text{kN}}{\text{m}^2}$$
$$q_{1k} = (5.13 \cdot 10^{-3}) \frac{\text{N}}{\text{mm}^2}$$

Design load value.
[NS-EN 1991-2:2003/NA:2100, Table 4.2]

$$Q_{1k} := \frac{0.95 \cdot 300 \text{ kN}}{2 \cdot A_{contact}}$$
$$Q_{1k} = (8.906 \cdot 10^{-1}) \frac{\text{N}}{\text{mm}^2}$$

Design load value.
[NS-EN 1991-2:2003/NA:2100, Table 4.2]

Lane 2

$$q_{2k} := 0.95 \cdot 2.5 \frac{\text{kN}}{\text{m}^2}$$
$$q_{2k} = (2.375 \cdot 10^{-3}) \frac{\text{N}}{\text{mm}^2}$$

Design load value.
[NS-EN 1991-2:2003/NA:2100, Table 4.2]

$$Q_{2k} := \frac{0.95 \cdot 200 \text{ kN}}{2 \cdot A_{contact}}$$
$$Q_{2k} = (5.938 \cdot 10^{-1}) \frac{\text{N}}{\text{mm}^2}$$

Design load value.
[NS-EN 1991-2:2003/NA:2100, Table 4.2]

Lane 3

$$q_{3k} := 0.95 \cdot 2.5 \frac{\text{kN}}{\text{m}^2}$$
$$q_{3k} = (2.375 \cdot 10^{-3}) \frac{\text{N}}{\text{mm}^2}$$

Design load value.
[NS-EN 1991-2:2003/NA:2100, Tabell 4.2]

$$Q_{3k} := \frac{0.95 \cdot 100 \text{ kN}}{2 \cdot A_{contact}}$$
$$Q_{3k} = (2.969 \cdot 10^{-1}) \frac{\text{N}}{\text{mm}^2}$$

Design load value.
[NS-EN 1991-2:2003/NA:2100, Tabell 4.2]

Remaining area

$$q_{rk} := 0.95 \cdot 2.5 \frac{kN}{m^2}$$
$$q_{rk} = (2.375 \cdot 10^{-3}) \frac{N}{mm^2}$$

Design load value.
[NS-EN 1991-2:2003/NA:2100, Table 4.2]

Wind load WITH traffic

$$q_{d.y.deck.wTraffic} := \frac{1.12 \cdot q_{k.y.deck.wTraffic}}{b_{deck}}$$
$$q_{d.y.deck.wTraffic} = (6.674 \cdot 10^{-4}) \frac{N}{mm^2}$$

Design load value.
Vertical wind load on deck

$$q_{d.z.deck.wTraffic} := 1.12 \cdot q_{k.z.deck.wTraffic}$$
$$q_{d.z.deck.wTraffic} = 2.838 \frac{N}{mm}$$

Design load value.
Horizontal wind load on deck

$$q_{d.z.Arch.wTraffic} := 1.12 \cdot q_{k.z.Arch.wTraffic}$$
$$q_{d.z.Arch.wTraffic} = 1.515517 \frac{kN}{m}$$

Design load value.
Horizontal wind load arch

Longitudinal loads - braking and acceleration associated with LM1

$$Q_{lk} := 0.95 \cdot 539.82 \text{ kN}$$
$$Q_{lk} = 512.829 \text{ kN}$$

Longitudinal design loads - braking and acceleration. see appendix B.1

Centrifugal and transverse loads

$$Q_{tk} := 0 \text{ kN}$$

Centrifugal force, see appendix B.1

$$Q_{trk} := 0.25 \cdot Q_{lk} = (1.282 \cdot 10^2) \text{ kN}$$

Transverse design load - Skew braking, see appendix B.1

Traffic Load 1b, gr1a (Eq. 6.10b)

$$A_{contact} := 400 \text{ mm} \cdot 400 \text{ mm}$$

Contact area, boggy.
[NS-EN 1991-2:2003/NA:2100, 4.3.2(1)]

$$A_{contact} = (1.6 \cdot 10^5) \text{ mm}^2$$

$$\alpha_{q1} := 0.6$$

Correction factor,
[NS-EN 1991-2:2003/NA:2100, NA.4.3.2(3)]

Lane 1

$$q_{1k} := 1.35 \cdot \alpha_{q1} \cdot 9 \frac{\text{kN}}{\text{m}^2}$$
$$q_{1k} = (7.29 \cdot 10^{-3}) \frac{\text{N}}{\text{mm}^2}$$

Design load value.
[NS-EN 1991-2:2003/NA:2100, Table 4.2]

$$Q_{1k} := \frac{1.35 \cdot 300 \text{ kN}}{2 \cdot A_{contact}}$$
$$Q_{1k} = 1.266 \frac{\text{N}}{\text{mm}^2}$$

Design load value.
[NS-EN 1991-2:2003/NA:2100, Table 4.2]

Lane 2

$$q_{2k} := 1.35 \cdot 2.5 \frac{\text{kN}}{\text{m}^2}$$
$$q_{2k} = (3.375 \cdot 10^{-3}) \frac{\text{N}}{\text{mm}^2}$$

Design load value.
[NS-EN 1991-2:2003/NA:2100, Table 4.2]

$$Q_{2k} := \frac{1.35 \cdot 200 \text{ kN}}{2 \cdot A_{contact}}$$
$$Q_{2k} = (8.438 \cdot 10^{-1}) \frac{\text{N}}{\text{mm}^2}$$

Design load value.
[NS-EN 1991-2:2003/NA:2100, Table 4.2]

Lane 3

$$q_{3k} := 1.35 \cdot 2.5 \frac{\text{kN}}{\text{m}^2}$$
$$q_{3k} = (3.375 \cdot 10^{-3}) \frac{\text{N}}{\text{mm}^2}$$

Design load value.
[NS-EN 1991-2:2003/NA:2100, Tabell 4.2]

$$Q_{3k} := \frac{1.35 \cdot 100 \text{ kN}}{2 \cdot A_{contact}}$$

Design load value.
[NS-EN 1991-2:2003/NA:2100, Tabell 4.2]

$$Q_{3k} = (4.219 \cdot 10^{-1}) \frac{\text{N}}{\text{mm}^2}$$

Remaining area

$$q_{rk} := 1.35 \cdot 2.5 \frac{kN}{m^2}$$
$$q_{rk} = (3.375 \cdot 10^{-3}) \frac{N}{mm^2}$$

Design load value.
[NS-EN 1991-2:2003/NA:2100, Table 4.2]

Wind load WITH traffic

$$q_{d.y.deck.wTraffic} := \frac{1.12 \cdot q_{k.y.deck.wTraffic}}{b_{deck}}$$
$$q_{d.y.deck.wTraffic} = (6.674 \cdot 10^{-4}) \frac{N}{mm^2}$$

Design load value.
Vertical wind load on deck

$$q_{d.z.deck.wTraffic} := 1.12 \cdot q_{k.z.deck.wTraffic}$$
$$q_{d.z.deck.wTraffic} = 2.838 \frac{N}{mm}$$

Design load value.
Horizontal wind load on deck

$$q_{d.z.Arch.wTraffic} := 1.12 \cdot q_{k.z.Arch.wTraffic}$$
$$q_{d.z.Arch.wTraffic} = 1.515517 \frac{kN}{m}$$

Design load value.
Horizontal wind load arch

Longitudinal loads - braking and acceleration associated with LM1

$$Q_{lk} := 1.35 \cdot 539.82 \text{ kN}$$

Longitudinal design loads - braking and acceleration. see appendix B.1

$$Q_{lk} = 728.757 \text{ kN}$$

Centrifugal and transverse loads

$$Q_{tk} := 0 \text{ kN}$$

Centrifugal force,
see appendix B.1

$$Q_{trk} := 0.25 \cdot Q_{lk} = (1.822 \cdot 10^2) \text{ kN}$$

Transverse design load - Skew braking, see appendix B.1

Traffic load 2a, gr1b (Eq. 6.10a)

$$A_{contact} := 350 \text{ mm} \cdot 600 \text{ mm}$$

Contact area, single axle.
[NS-EN 1991-2:2003/NA:2100, 4.3.3(4)]

$$A_{contact} = (2.1 \cdot 10^5) \text{ mm}^2$$

$$\beta_Q := 1.0$$

Correction factor,
[NS-EN 1991-2:2003/NA:2100, NA. 4.3.3]

Traffic load

$$Q_{ak} := 0.95 \cdot \beta_Q \cdot \frac{400 \text{ kN}}{2 \cdot A_{contact}}$$

Design load value,
[NS-EN 1991-2:2003/NA:2100, 4.3.3(1)]

$$Q_{ak} = (9.048 \cdot 10^{-1}) \frac{\text{N}}{\text{mm}^2}$$

Wind load WITH traffic

$$q_{d.y.deck.wTraffic} := \frac{1.12 \cdot q_{k.y.deck.wTraffic}}{b_{deck}}$$

Design load value.
Vertical wind load on deck

$$q_{d.y.deck.wTraffic} = (6.674 \cdot 10^{-4}) \frac{\text{N}}{\text{mm}^2}$$

$$q_{d.z.deck.wTraffic} := 1.12 \cdot q_{k.z.deck.wTraffic}$$

Design load value.
Horizontal wind load on deck

$$q_{d.z.deck.wTraffic} = 2.838 \frac{\text{N}}{\text{mm}}$$

$$q_{d.z.Arch.wTraffic} := 1.12 \cdot q_{k.z.Arch.wTraffic}$$

Design load value.
Horizontal wind load arch

$$q_{d.z.Arch.wTraffic} = 1.515517 \frac{\text{kN}}{\text{m}}$$

Traffic Load 2b, gr1b (Eq. 6.10b)

$$A_{contact} := 350 \text{ mm} \cdot 600 \text{ mm}$$

Contact area, single axle.
[NS-EN 1991-2:2003/NA:2100, 4.3.3(4)]

$$A_{contact} = (2.1 \cdot 10^5) \text{ mm}^2$$

$$\beta_Q := 1.0$$

Correction factor,
[NS-EN 1991-2:2003/NA:2100, NA. 4.3.3]

Traffic load

$$Q_{ak} := 1.35 \cdot \beta_Q \cdot \frac{400 \text{ kN}}{2 \cdot A_{contact}}$$

Design load value,
[NS-EN 1991-2:2003/NA:2100, 4.3.3(1)]

$$Q_{ak} = 1.286 \frac{\text{N}}{\text{mm}^2}$$

Wind load WITH traffic

$$q_{d,y,deck.wTraffic} := \frac{1.12 \cdot q_{k,y,deck.wTraffic}}{b_{deck}}$$
$$q_{d,y,deck.wTraffic} = (6.674 \cdot 10^{-4}) \frac{\text{N}}{\text{mm}^2}$$

Design load value.
Vertical wind load on deck

$$q_{d,z,deck.wTraffic} := 1.12 \cdot q_{k,z,deck.wTraffic}$$

Design load value.
Horizontal wind load on deck

$$q_{d,z,deck.wTraffic} = 2.838 \frac{\text{N}}{\text{mm}}$$

$$q_{d,z,Arch.wTraffic} := 1.12 \cdot q_{k,z,Arch.wTraffic}$$

Design load value.
Horizontal wind load arch

$$q_{d,z,Arch.wTraffic} = 1.515517 \frac{\text{kN}}{\text{m}}$$

Traffic load 4a, gr4 (Eq. 6.10a)

$$q_{k.crowd} := 5 \frac{kN}{m^2}$$

Design load value
[NS-EN 1991-2:2003/NA:2100, Table 4.4b]

$$q_{d.crowd} := 0.95 \cdot q_{k.crowd}$$

$$q_{d.crowd} = (4.75 \cdot 10^{-3}) \frac{N}{mm^2}$$

Wind load WITH traffic

$$q_{d.y.deck.wTraffic} := \frac{1.12 \cdot q_{k.y.deck.wTraffic}}{b_{deck}}$$
$$q_{d.y.deck.wTraffic} = (6.674 \cdot 10^{-4}) \frac{N}{mm^2}$$

Design load value.
Vertical wind load on deck

$$q_{d.z.deck.wTraffic} := 1.12 \cdot q_{k.z.deck.wTraffic}$$

$$q_{d.z.deck.wTraffic} = 2.838 \frac{N}{mm}$$

Design load value.
Horizontal wind load on deck

$$q_{d.z.Arch.wTraffic} := 1.12 \cdot q_{k.z.Arch.wTraffic}$$

$$q_{d.z.Arch.wTraffic} = 1.515517 \frac{kN}{m}$$

Design load value.
Horizontal wind load arch

Traffic load 4b, gr4 (Eq. 6.10b)

$$q_{k.crowd} := 5 \frac{kN}{m^2}$$

Design load value
[NS-EN 1991-2:2003/NA:2100, Table 4.4b]

$$q_{d.crowd} := 1.35 \cdot q_{k.crowd}$$

$$q_{d.crowd} = (6.75 \cdot 10^{-3}) \frac{N}{mm^2}$$

Wind load WITH traffic

$$q_{d.y.deck.wTraffic} := \frac{1.12 \cdot q_{k.y.deck.wTraffic}}{b_{deck}}$$
$$q_{d.y.deck.wTraffic} = (6.674 \cdot 10^{-4}) \frac{N}{mm^2}$$

Design load value.
Vertical wind load on deck

$$q_{d.z.deck.wTraffic} := 1.12 \cdot q_{k.z.deck.wTraffic}$$

$$q_{d.z.deck.wTraffic} = 2.838 \frac{N}{mm}$$

Design load value.
Horizontal wind load on deck

$$q_{d.z.Arch.wTraffic} := 1.12 \cdot q_{k.z.Arch.wTraffic}$$

$$q_{d.z.Arch.wTraffic} = 1.515517 \frac{kN}{m}$$

Design load value.
Horizontal wind load arch

Traffic load 5a, Wind without traffic (Eq. 6.10a)

Wind load WITHOUT traffic

$$q_{d,y,deck.woTraffic} := \frac{1.12 \cdot q_{k,y,deck.woTraffic}}{b_{deck}}$$
$$q_{d,y,deck.woTraffic} = (9.534 \cdot 10^{-4}) \frac{N}{mm^2}$$

Design load value.
Vertical wind load on deck

$$q_{d,z,deck.woTraffic} := 1.12 \cdot q_{k,z,deck.woTraffic}$$
$$q_{d,z,deck.woTraffic} = 2.896 \frac{N}{mm}$$

Design load value.
Horizontal wind load on deck

$$q_{d,z,Arch.woTraffic} := 1.12 \cdot q_{k,z,Arch.woTraffic}$$
$$q_{d,z,Arch.woTraffic} = 2.165027 \frac{kN}{m}$$

Design load value.
Horizontal wind load arch

Traffic load 5b, Wind without traffic (Eq. 6.10b)

Wind load WITHOUT traffic

$$q_{d,y,deck.woTraffic} := \frac{1.60 \cdot q_{k,y,deck.woTraffic}}{b_{deck}}$$
$$q_{d,y,deck.woTraffic} = (1.362 \cdot 10^{-3}) \frac{N}{mm^2}$$

Design load value.
Vertical wind load on deck

$$q_{d,z,deck.woTraffic} := 1.60 \cdot q_{k,z,deck.woTraffic}$$
$$q_{d,z,deck.woTraffic} = 4.138 \frac{N}{mm}$$

Design load value.
Horizontal wind load on deck

$$q_{d,z,Arch.woTraffic} := 1.60 \cdot q_{k,z,Arch.woTraffic}$$
$$q_{d,z,Arch.woTraffic} = 3.092896 \frac{kN}{m}$$

Design load value.
Horizontal wind load on arch

Appendix_B.3: Load Combination

Service Limit State (SLS) Bridge 1

NS-EN 1990-NA defines four different load combinations in SLS

- Characteristic
- Infrequent values
- Frequent values
- Quasi-permanent

‘Characteristic’ is used for design check of supports or joint deformations.

‘Infrequent values’ is used for design check of load eccentricities in the case of direct foundation.

‘Frequent values’ is used for design check of deformations and crack width in concrete⁽¹⁾.

‘Quasi-permanent’ is used for design check of long time deformations and crack width in concrete⁽¹⁾.

The combination factors for serviceability state is obtained from NS-EN 1990 table NA.A2.6 og table NA.A2.1. The resulting load factors are shown in Table 6.3.

Combination	Permanent loads G_d		Variable loads Q_d	
	Unfavorable	Favorable	Dominating load	Other loads
Characteristic	$G_{k,j,sup}$	$G_{k,j,inf}$	$Q_{k,1}$	$\psi_{0,i} * Q_{k,i}$
Infrequent values	$G_{k,j,sup}$	$G_{k,j,inf}$	$\psi_{1,infq} * Q_{k,1}$	$\psi_{1,i} * Q_{k,i}$
Frequent values	$G_{k,j,sup}$	$G_{k,j,inf}$	$\psi_{1,1} * Q_{k,2}$	$\psi_{2,i} * Q_{k,i}$
Quasi-permanent	$G_{k,j,sup}$	$G_{k,j,inf}$	$\psi_{2,1} * Q_{k,3}$	$\psi_{2,i} * Q_{k,i}$

Frequent Values

SLS	1	2	3	4	5	6
Frequent	gr1a	gr1b	gr3	Wind without traffic	Wind with traffic	Temp.
Permanent loads						
Self weight	1,00	1,00	1,00	1,00	1,00	1,00
Variable loads	Variable loads with a favourable effect: 0,0					
Traffic, LM1	0,70	-	-	-	0,20	0,20
Trafikk, pedestrian	0,70	-	0,70	-	0,20	0,20
Trafikk, LM2	-	0,70	-	-	-	-
Trafikk, LM4	-	-	0,70	-	-	-
Traffic, horizontal forces	0,70	-	-	-	0,20	0,20
Wind with traffic	0,60	0,60	0,60	-	0,60	0,60
Wind without traffic	-	-	-	0,60	-	-
Temperature	-	-	-	-	-	0,60

Dimension bridge deck. Stresslaminated glulam GL24c

$$t_{pedestrian.GL24c} := 800 \text{ mm}$$

Thickness: pedestrian lane

$$t_{roadway.GL24c} := 600 \text{ mm}$$

Thickness: roadway

$$b_{deck} := 12950 \text{ mm}$$

Total width

Wind WITH traffic

$$q_{k,y,deck.wTraffic} := 7.717 \frac{kN}{m}$$

Vertical characteristic wind load on deck, see appendix A

$$q_{k,z,deck.wTraffic} := 2.534 \frac{kN}{m}$$

Horizontal characteristic wind load on deck, see appendix A

$$q_{k,z,Arch.wTraffic} := 1.35314 \frac{kN}{m}$$

Horizontal characteristic wind load on arch, see appendix A

Wind WITHOUT traffic

$$q_{k,y,deck.woTraffic} := 11.024 \frac{kN}{m}$$

Vertical characteristic wind load on deck, see appendix A

$$q_{k,z,deck.woTraffic} := 2.586 \frac{kN}{m}$$

Horizontal characteristic wind load on deck, see appendix A

$$q_{k,z,Arch.woTraffic} := 1.9330 \frac{kN}{m}$$

Horizontal characteristic wind load on arch, see appendix A

Traffic Load 1, gr1a

$$A_{contact} := 400 \text{ mm} \cdot 400 \text{ mm}$$

Contact area, boggy
[NS-EN 1991-2:2003/NA:2100, 4.3.2(1)]

$$A_{contact} = (1.6 \cdot 10^5) \text{ mm}^2$$

$$\alpha_{q1} := 0.6$$

Correction factor,
[NS-EN 1991-2:2003/NA:2100, NA.4.3.2(3)]

Lane 1

$$q_{1k} := 0.70 \cdot \alpha_{q1} \cdot 9 \frac{\text{kN}}{\text{m}^2}$$

Design load value
[NS-EN 1991-2:2003/NA:2100, Table 4.2]

$$q_{1k} = (3.78 \cdot 10^{-3}) \frac{\text{N}}{\text{mm}^2}$$

$$Q_{1k} := 0.70 \frac{300 \text{ kN}}{2 \cdot A_{contact}}$$

Design load value
[NS-EN 1991-2:2003/NA:2100, Table 4.2]

$$Q_{1k} = (6.563 \cdot 10^{-1}) \frac{\text{N}}{\text{mm}^2}$$

Lane 2

$$q_{2k} := 0.70 \cdot 2.5 \frac{\text{kN}}{\text{m}^2}$$

Design load value
[NS-EN 1991-2:2003/NA:2100, Table 4.2]

$$q_{2k} = (1.75 \cdot 10^{-3}) \frac{\text{N}}{\text{mm}^2}$$

$$Q_{2k} := 0.70 \cdot \frac{200 \text{ kN}}{2 \cdot A_{contact}}$$

Design load value
[NS-EN 1991-2:2003/NA:2100, Table 4.2]

$$Q_{2k} = (4.375 \cdot 10^{-1}) \frac{\text{N}}{\text{mm}^2}$$

Lane 3

$$q_{3k} := 0.70 \cdot 2.5 \frac{\text{kN}}{\text{m}^2}$$

Design load value
[NS-EN 1991-2:2003/NA:2100, Table 4.2]

$$q_{3k} = (1.75 \cdot 10^{-3}) \frac{\text{N}}{\text{mm}^2}$$

$$Q_{3k} := 0.70 \cdot \frac{100 \text{ kN}}{2 \cdot A_{\text{contact}}}$$

Design load value
[NS-EN 1991-2:2003/NA:2100, Table 4.2]

$$Q_{3k} = (2.188 \cdot 10^{-1}) \frac{\text{N}}{\text{mm}^2}$$

Remaining area

$$q_{rk} := 0.70 \cdot 2.5 \frac{\text{kN}}{\text{m}^2}$$

Design load value
[NS-EN 1991-2:2003/NA:2100, Table 4.2]

$$q_{rk} = (1.75 \cdot 10^{-3}) \frac{\text{N}}{\text{mm}^2}$$

Wind load WITH traffic

$$q_{d.y.deck.wTraffic} := \frac{0.60 \cdot q_{k.y.deck.wTraffic}}{b_{\text{deck}}}$$

Design load value.
Vertical wind load on deck

$$q_{d.y.deck.wTraffic} = (3.575 \cdot 10^{-4}) \frac{\text{N}}{\text{mm}^2}$$

$$q_{d.z.deck.wTraffic} := 0.60 \cdot q_{k.z.deck.wTraffic}$$

Design load value.
Horizontal wind load on deck

$$q_{d.z.deck.wTraffic} = 1.52 \frac{\text{N}}{\text{mm}^2}$$

$$q_{d.z.Arch.wTraffic} := 0.60 \cdot q_{k.z.Arch.wTraffic}$$

Design load value.
Horizontal wind load arche

$$q_{d.z.Arch.wTraffic} = 0.811884 \frac{\text{kN}}{\text{m}}$$

Longitudinal loads - braking and acceleration associated with LM1

$$Q_{lk} := 0.70 \cdot 539.82 \text{ kN}$$

Longitudinal design loads - braking and acceleration. See appendix B.1, Traffic loads.

$$Q_{lk} = 377.874 \text{ kN}$$

Centrifugal and transverse loads

$$Q_{tk} := 0 \text{ kN}$$

Centrifugal force, see appendix B.1
Traffic loads

$$Q_{trk} := 0.25 \cdot Q_{lk} = 94.469 \text{ kN}$$

Transverse design loads - Skew
braking. See appendix B.1, Traffic loads

Traffic Load 2, gr1b

$$A_{contact} := 350 \text{ mm} \cdot 600 \text{ mm}$$

Contact area, single axle.
[NS-EN 1991-2:2003/NA:2100, 4.3.3(4)]

$$A_{contact} = (2.1 \cdot 10^5) \text{ mm}^2$$

$$\beta_Q := 1.0$$

Correction factor,
[NS-EN 1991-2:2003/NA:2100, NA. 4.3.3]

Traffic load

$$Q_{ak} := 0.70 \cdot \beta_Q \cdot \frac{400 \text{ kN}}{2 \cdot A_{contact}}$$

Design load value
[NS-EN 1991-2:2003/NA:2100, 4.3.3(1)]

$$Q_{ak} = 0.667 \frac{\text{N}}{\text{mm}^2}$$

Wind load WITH traffic

$$q_{d.y.deck.wTraffic} := \frac{0.60 \cdot q_{k.y.deck.wTraffic}}{b_{deck}}$$
$$q_{d.y.deck.wTraffic} = (3.575 \cdot 10^{-4}) \frac{\text{N}}{\text{mm}^2}$$

Design load value.
Vertical wind load on deck

$$q_{d.z.deck.wTraffic} := 0.60 \cdot q_{k.z.deck.wTraffic}$$

Design load value.
Horizontal wind load on deck

$$q_{d.z.deck.wTraffic} = 1.52 \frac{\text{N}}{\text{mm}}$$

$$q_{d.z.Arch.wTraffic} := 0.60 \cdot q_{k.z.Arch.wTraffic}$$

Design load value.
Horizontal wind load arch

$$q_{d.z.Arch.wTraffic} = (8.11884 \cdot 10^{-1}) \frac{\text{kN}}{\text{m}}$$

Traffic Load 3, gr3

$$q_{k.crowd} := 5 \frac{kN}{m^2}$$

[NS-EN 1991-2:2003/NA:2100, Table 4.4b]

$$q_{d.crowd} := 0.70 \cdot q_{k.crowd}$$

$$q_{d.crowd} = (3.5 \cdot 10^{-3}) \frac{N}{mm^2}$$

Design load value: crowd load

Wind load WITH traffic

$$q_{d.y.deck.wTraffic} := \frac{0.60 \cdot q_{k.y.deck.wTraffic}}{b_{deck}}$$
$$q_{d.y.deck.wTraffic} = (3.575 \cdot 10^{-4}) \frac{N}{mm^2}$$

Design load value.

Vertical wind load on deck

$$q_{d.z.deck.wTraffic} := 0.60 \cdot q_{k.z.deck.wTraffic}$$

$$q_{d.z.deck.wTraffic} = 1.52 \frac{N}{mm}$$

Design load value.

Horizontal wind load on deck

$$q_{d.z.Arch.wTraffic} := 0.60 \cdot q_{k.z.Arch.wTraffic}$$

$$q_{d.z.Arch.wTraffic} = (8.11884 \cdot 10^{-1}) \frac{kN}{m}$$

Design load value.

Horizontal wind load arch

Traffic load 4, wind WITHOUT traffic

$$q_{d,y,deck.woTraffic} := \frac{0.60 \cdot q_{k,y,deck.woTraffic}}{b_{deck}}$$
$$q_{d,y,deck.woTraffic} = 0.000511 \frac{N}{mm^2}$$

Design load value.
Vertical wind load on deck

$$q_{d,z,deck.woTraffic} := 0.60 \cdot q_{k,z,deck.woTraffic}$$
$$q_{d,z,deck.woTraffic} = 1.552 \frac{N}{mm}$$

Design load value.
Horizontal wind load on deck

$$q_{d,z,Arch.woTraffic} := 0.60 \cdot q_{k,z,Arch.woTraffic}$$
$$q_{d,z,Arch.woTraffic} = 1.1598 \frac{kN}{m}$$

Design load value.
Horizontal wind load arch

Traffic load 5, Wind WITH traffic

$$A_{contact} := 400 \text{ mm} \cdot 400 \text{ mm}$$

Contact area, boggy.
[NS-EN 1991-2:2003/NA:2100, 4.3.2(1)]

$$A_{contact} = (1.6 \cdot 10^5) \text{ mm}^2$$

$$\alpha_{q1} := 0.6$$

Correction factor,
[NS-EN 1991-2:2003/NA:2100, NA.4.3.2(3)]

Lane 1

$$q_{1k} := 0.20 \cdot \alpha_{q1} \cdot 9 \frac{kN}{m^2}$$

Design load value
[NS-EN 1991-2:2003/NA:2100, Table 4.2]

$$q_{1k} = 0.00108 \frac{N}{mm^2}$$

$$Q_{1k} := 0.20 \frac{300 \text{ kN}}{2 \cdot A_{contact}}$$

Design load value
[NS-EN 1991-2:2003/NA:2100, Table 4.2]

$$Q_{1k} = 0.188 \frac{N}{mm^2}$$

Lane 2

$$q_{2k} := 0.20 \cdot 2.5 \frac{kN}{m^2}$$

Design load value
[NS-EN 1991-2:2003/NA:2100, Table 4.2]

$$q_{2k} = 0.0005 \frac{N}{mm^2}$$

$$Q_{2k} := 0.20 \cdot \frac{200 kN}{2 \cdot A_{contact}}$$

Design load value
[NS-EN 1991-2:2003/NA:2100, Table 4.2]

$$Q_{2k} = 0.125 \frac{N}{mm^2}$$

Lane 3

$$q_{3k} := 0.20 \cdot 2.5 \frac{kN}{m^2}$$

Design load value
[NS-EN 1991-2:2003/NA:2100, Table 4.2]

$$q_{3k} = (5 \cdot 10^{-4}) \frac{N}{mm^2}$$

$$Q_{3k} := 0.20 \cdot \frac{100 kN}{2 \cdot A_{contact}}$$

Design load value
[NS-EN 1991-2:2003/NA:2100, Table 4.2]

$$Q_{3k} = 0.0625 \frac{N}{mm^2}$$

Remaining area

$$q_{rk} := 0.20 \cdot 2.5 \frac{kN}{m^2}$$

Design load value
[NS-EN 1991-2:2003/NA:2100, Table 4.2]

$$q_{rk} = (5 \cdot 10^{-4}) \frac{N}{mm^2}$$

Wind load WITH traffic

$$q_{d.y.deck.wTraffic} := \frac{0.60 \cdot q_{k.y.deck.wTraffic}}{b_{deck}}$$
$$q_{d.y.deck.wTraffic} = 0.000358 \frac{N}{mm^2}$$

Design load value.
Vertical wind load on deck

$$q_{d.z.deck.wTraffic} := 0.60 \cdot q_{k.z.deck.wTraffic}$$
$$q_{d.z.deck.wTraffic} = 1.52 \frac{N}{mm}$$

Design load value.
Horizontal wind load on deck

$$q_{d.z.Arch.wTraffic} := 0.60 \cdot q_{k.z.Arch.wTraffic}$$
$$q_{d.z.Arch.wTraffic} = 0.811884 \frac{kN}{m}$$

Design load value.
Horizontal wind load arch

Longitudinal loads - braking and acceleration associated with LM1

$$Q_{lk} := 0.20 \cdot 539.82 \text{ kN}$$

Longitudinal design loads - braking and acceleration. See appendix B.1, Traffic loads

$$Q_{lk} = 107.964 \text{ kN}$$

Centrifugal and transverse loads

$$Q_{tk} := 0 \text{ kN}$$

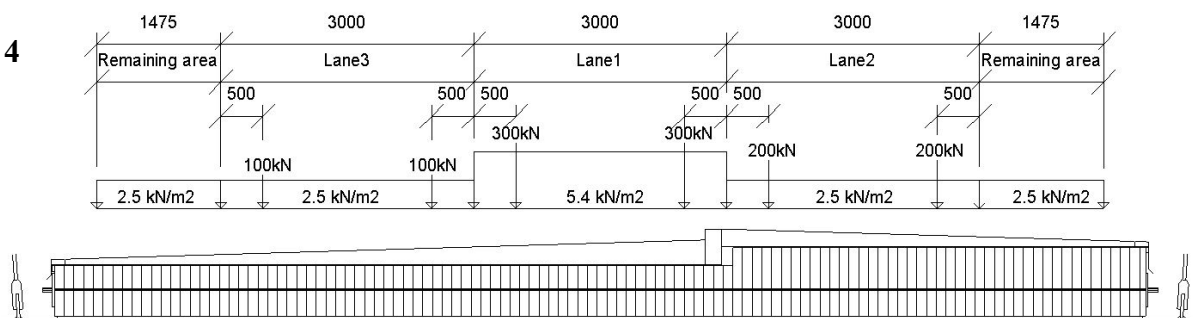
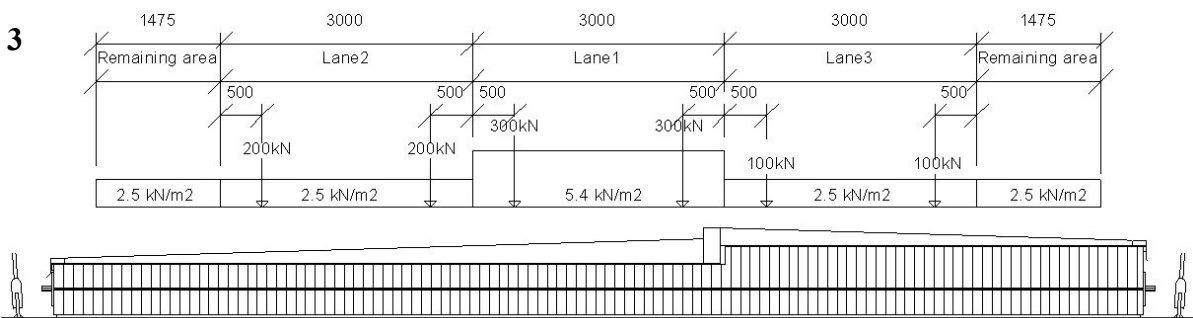
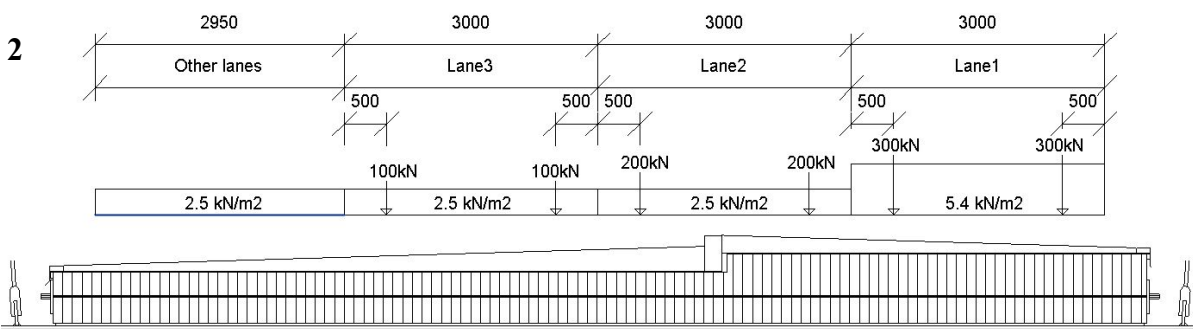
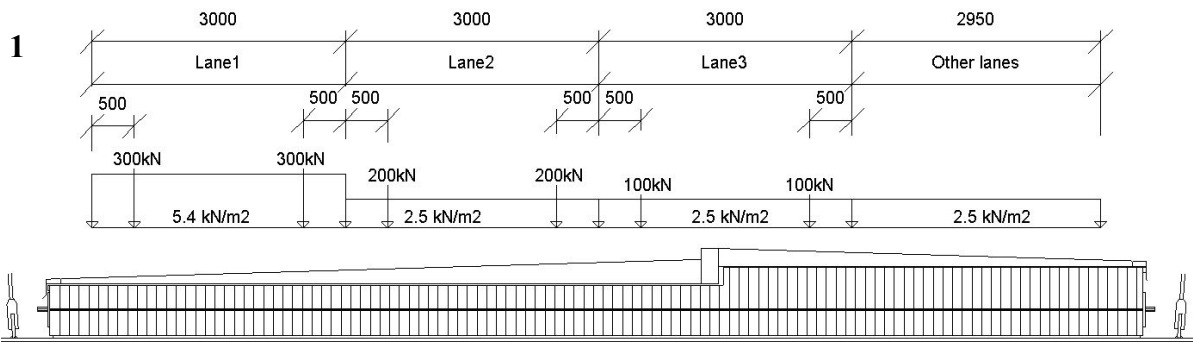
Centrifugal force,
see appendix B.1 Traffic loads

$$Q_{trk} := 0.25 \cdot Q_{lk} = 26.991 \text{ kN}$$

Transverse design load - Skew braking.
See appendix B.1, Traffic loads

Appendix_C: LM1 Load Placement

Placement	Tandem system	Uniformly distributed load
	Axle load Q_{ik} (kN)	q_{ik} (kN/m ²)
Lane 1	300	9
Lane 2	200	2,5
Lane 3	100	2,5
Other lanes	0	2,5
Remaining area	0	2,5



Appendix_D: Earthquake Calculations

Seismic classification : II

Table NA.2(901),
[NS-EN 1998- 2:2005/NA:2014]

$$\gamma_1 := 1.0$$

Seismic factor,
[NS-EN 1998- 2:2005/NA:2014. Table NA.2(903)]

$$a_{g40Hz} := 0.4 \frac{m}{s^2}$$

Ground peak acceleration,
[NS-EN1998-1:2004/NA:2014. Table NA.3(901)]

$$S := 1.4$$

Soil factor,
[NS-EN1998-1:2004/NA:2014, Table NA.3.3]

$$\gamma_1 \cdot (0.8 \cdot a_{g40Hz}) \cdot S = 0.448 \frac{m}{s^2}$$

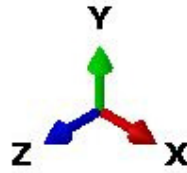
$$0.448 \frac{m}{s^2} \leq 0.49 \frac{m}{s^2}$$

There are no requirements for analytical calculations

Table NA.2(904),
[NS-EN 1998- 2:2005/NA:2009]

Appendix_E.1: Stress laminated bridge deck

Tension force in laminated deck plate



z-direction (transverse direction)
x-direction (longitudinal direction)

$$\varnothing_{Nom} := 28 \text{ mm}$$

Nominal diameter tension system.

$$\varnothing_{Max} := (\varnothing_{Nom} + 4 \text{ mm}) = 32 \text{ mm}$$

$$A_c := \pi \cdot \frac{\varnothing_{Nom}^2}{4} = 615.752 \text{ mm}^2$$

Area

$$f_y := 670 \frac{\text{N}}{\text{mm}^2}$$

Yield strength,
DYWIDAG-SYSTEMS. [21]

$$f_{pk} := 800 \frac{\text{N}}{\text{mm}^2}$$

Ultimate strength,
DYWIDAG-SYSTEMS. [21]

$$F_{p.0.1k} := f_y \cdot A_c = (4.126 \cdot 10^5) \text{ N}$$

Yield load

$$F_{pk} := f_{pk} \cdot A_c = (4.926 \cdot 10^5) \text{ N}$$

Ultimate load

$$P_0 := \min(0.8 \cdot F_{pk}, 0.9 \cdot F_{p.0.1k}) = 371.299 \text{ kN}$$

Maximum pre tension force.
Håndbok N400 9.5.2.2

Sliding between the lamella

$$v_v := 38 \frac{N}{mm}$$

Vertical shear per meter (SF5),
values from abaqus deck model

$$v_H := 0.159 \frac{N}{mm}$$

Horizontal shear per meter (SF3),
values from abaqus deck model

$$M_X := 13560 N \cdot \frac{mm}{mm}$$

Moment about x-axis (SM2),
values from abaqus deck model

$$h := 600 \text{ mm}$$

Lamella height, roadway

$$\mu_{90.d} := 0.30$$

Håndbok N400 Table: 9.4

$$\mu_{0.d} := 0.25$$

Håndbok N400 Table: 9.4

$$\sigma_m := \frac{M_X \cdot 6}{h^2} = 0.226 \frac{N}{mm^2}$$

$$P_{min.m} := \sigma_m \cdot h = 135.6 \frac{N}{mm}$$

$$\sigma_v := \frac{v_v \cdot 1.5}{h \cdot \mu_{90.d}} = 0.317 \frac{N}{mm^2}$$

$$P_{min.v} := \sqrt{\left(\frac{v_v}{\mu_{0.d}}\right)^2 + \left(\frac{v_H}{\mu_{90.d}}\right)^2} = 152.001 \frac{N}{mm}$$

Håndbok N400 9.6.1.3 Eq 9.7

$$P_{min.0} := 0.4 \cdot P_0 = 148.519 \text{ kN}$$

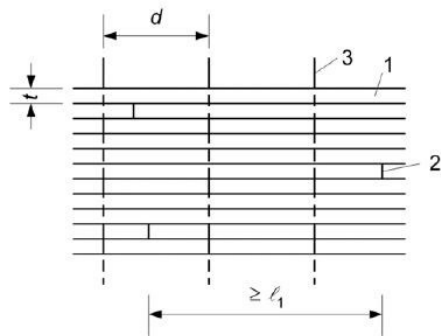
Design tension strenght
Håndbok N400 9.6.1.1,

$$P_{min} := \max\left(80 \frac{kN}{m}, P_{min.m}, P_{min.v}\right) = 152.001 \frac{N}{mm}$$

$$d := \frac{P_{min.0}}{P_{min}} = 0.977 \text{ m}$$

Maximum distance between tendons

System stiffness



Tegnforklaring:

- 1 Lameller
- 2 Buttskjøt
- 3 Forspenningseenhet

NS-EN 1995-2 6.1.2(10)

$$b_{Deck} := 12.95 \text{ m}$$

Width of the deck

$$t_{Lamella} := 115 \text{ mm}$$

lamella thickness

$$n_l := \frac{b_{Deck}}{t_{Lamella}} = 113$$

Number of lamella in the decks with

$$d = 977.096 \text{ mm}$$

Distance between transverse tendons

$$l_1 := \min(2 \cdot d, 25 \cdot t_{Lamella}^{1.2}) = 1.2 \text{ m}$$

The length that can contain n_{max}

NS-EN 1995-2 6.1.2(10)

$$n_{max} := \frac{n_l}{4} = 28.152$$

maximum number of butt joints within the distance l_1 , NS-EN 1995-2 6.1.2(10)

$$n := n_{max}$$

Number of lamella per butt joint in the same cross section

$$k_b := \frac{n}{1+n} = 0.966$$

Empirical butt joint factor for reduced system stiffness, Håndbok N400 9.5.2.3,

Anchoring plate

$$d_p := 500 \text{ mm}$$

Diameter anchor plate

$$k_{c,90} := 1.00$$

NS-EN 1995-1 6.1.5

$$k_{mod,1} := 1.10$$

NS-EN 1995-1 Tabell 3.1, Instant load

$$k_{mod,2} := 0.9$$

NS-EN 1995-1 Tabell 3.1, Short-term load

$$\gamma_m := 1.15$$

NS-EN 1995-1 Tabell NA.2.3, glulam

$$f_{c,90,g,k} := 2.5 \frac{N}{mm^2}$$

Compression strength, GL 24c

$$f_{c,90,g,d1} := k_{mod,1} \cdot \frac{f_{c,90,g,k}}{\gamma_m} = 2.391 \frac{N}{mm^2}$$

Design pressure strength, Instant load

$$f_{c,90,g,d2} := k_{mod,2} \cdot \frac{f_{c,90,g,k}}{\gamma_m} = 1.957 \frac{N}{mm^2}$$

Design pressure strength, Short-term load

$$A_p(x) := \pi \cdot \frac{x^2}{4} - \pi \cdot \frac{\varnothing_{Max}^2}{4}$$

Net area of anchor plate (two plates at the height of beam)

$$A_p(d_p) = (1.955 \cdot 10^5) \text{ mm}^2$$

Instant load

$$P_{d.1} := 1.06 \cdot P_0 = (3.936 \cdot 10^5) \text{ N}$$

Håndbok N400 9.6.1.2 Table: 9.3,
Instant load

$$\sigma_{c.90.d1} := \frac{P_{d.1}}{A_p(d_p)} = 2.013 \frac{\text{N}}{\text{mm}^2}$$

NS-EN 1995-1 6.1.5(1) Eq.6.4.
Design stresses, Instant load

$$\sigma_{c.90.d1} \leq k_{c.90} \cdot f_{c.90.g.d1}$$

NS-EN 1995-1 6.1.5(1) Eq.6.3

$$k_{c.90} \cdot f_{c.90.g.d1} = 2.391 \frac{\text{N}}{\text{mm}^2}$$

if $\sigma_{c.90.d1} \leq k_{c.90} \cdot f_{c.90.g.d1}$ | = "Ok"
|| "Ok"
else
|| "Not ok"

Short-term load

$$P_{d.2} := P_0 = (3.713 \cdot 10^5) \text{ N}$$

Håndbok N400 9.6.1.2 Table: 9.3,
Short-term load

$$\sigma_{c.90.d2} := \frac{P_{d.2}}{A_p(d_p)} = 1.899 \frac{\text{N}}{\text{mm}^2}$$

NS-EN 1995-1 6.1.5(1) Eq.6.4.
Design stresses, Short-term load

$$\sigma_{c.90.d2} \leq k_{c.90} \cdot f_{c.90.g.d2}$$

NS-EN 1995-1 6.1.5(1) Eq.6.3

$$k_{c.90} \cdot f_{c.90.g.d2} = 1.957 \frac{\text{N}}{\text{mm}^2}$$

if $\sigma_{c.90.d2} \leq k_{c.90} \cdot f_{c.90.g.d2}$ | = "Ok"
|| "Ok"
else
|| "Not ok"

Thickness of anchoring plate:

Conservative approach. The anchor plate for the tension system have been calculated as a cantilever with unformal distributed load. Height equal the thickness of the plate, and width (b) equal 1 mm.

$$E := 210000 \frac{N}{mm^2} \quad \text{Modulus of elasticity, S355}$$

$$p_t := 35 \text{ mm} \quad \text{Thickness of anchor plate}$$

$$b := 1 \text{ mm} \quad \text{Calculation width}$$

$$\sigma_{Ed} := \frac{P_{d.1}}{A_p(d_p)} = 2.013 \frac{N}{mm^2} \quad \text{Design value, tension}$$

$$q_{Ed} := \sigma_{Ed} \cdot b = 2.013 \frac{N}{mm} \quad \text{Design load}$$

$$I(x) := b \cdot \frac{(x)^3}{12} \quad \text{Second moment of area}$$

$$I(p_t) = (3.573 \cdot 10^3) \text{ mm}^4$$

$$M_{d.plate} := q_{Ed} \frac{d_p^2}{8} = (6.29 \cdot 10^4) \text{ N} \cdot \text{mm} \quad \text{Max moment}$$

$$W_p(x) := b \cdot \frac{(x)^2}{4} \quad \text{Polar moment of resistance}$$

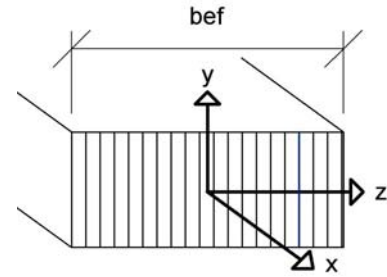
$$W_p(p_t) = 306.25 \text{ mm}^3$$

$$\sigma_P := \frac{M_{d.plate}}{W_p(p_t)} = 205.379 \frac{N}{mm^2} \quad \text{Tension in anchor plate}$$

$$w := \frac{q_{Ed} \cdot \left(\frac{d_p}{2}\right)^4}{8 \cdot E \cdot I(p_t)} = 1.31 \text{ mm} \quad \text{Deflection of anchor plate}$$

Appendix_E.2 Simplified deck analysis

The deck plate may be replaced by one or several beams in the direction of the laminations with the effective width b_{ef} .[EC5-2 5.1.2]



$b_{deck} := 12950 \text{ mm}$	Width of bridge deck
$h_{deck} := 600 \text{ mm}$	Height of bridge deck
$L_{bridge} := 111 \text{ m}$	Length of bridge deck
$k_b := 0.966$	Empirical butt joint factor reduced system stiffness, see Appendix E.1
$b_{lam} := 115 \text{ mm}$	Width of deck lamella
$Q_{Vind} := 2.838 \frac{N}{mm}$	Horizontal design, wind load on deck. ULS_LM1_gr1a_Eq_6.10b. [Appendix B]
$m_{z,d} := 2.154 \cdot 10^5 \text{ N} \cdot \frac{mm}{mm}$	Design Momentum about Z-axis. Abaqus deck model
$M_{y,d} := \frac{Q_{Vind} \cdot L_{bridge}^2}{8} = (4.371 \cdot 10^9) \text{ N} \cdot mm$	Design Momentum about Y-axis.
$N_{x,d} := 1991 \frac{N}{mm}$	Design Axial force X-direction
$v_d := 216.4 \frac{N}{mm}$	Design shear force
$E_{0.9,05} := 9100 \text{ MPa}$	Fifth percentile value of modulus of elasticity
$f_{m,k} := 24 \text{ MPa}$	Characteristic bending strength
$f_{c,0,k} := 21.5 \text{ MPa}$	Characteristic compression strength along grain
$f_{v,k} := 3.5 \text{ MPa}$	Characteristic shear strength
$\rho_k := 365 \frac{kg}{m^3}$	Material density
$k_{mod} := 0.9$	Modification factor for duration of load and moisture content
$k_m := 0.7$	Factor considering re-distribution of bending stresses in a cross-section
$\gamma_m := 1.15$	Partial Factor for material properties
$\beta_c := 0.1$	Straightness factor

$f_{c.0.d} := k_{mod} \cdot \frac{f_{c.0.k}}{\gamma_m} = 16.826 \text{ MPa}$	Design compressive strength along the grain
$f_{m.z.d} := k_{mod} \cdot \frac{f_{m.k}}{\gamma_m} = 18.783 \text{ MPa}$	Design bending strength about the principal z-axis
$f_{m.y.d} := k_{mod} \cdot \frac{f_{m.k}}{\gamma_m} = 18.783 \text{ MPa}$	Design bending strength about the principal x-axis
$f_{v.d} := k_{mod} \cdot \frac{f_{v.k}}{\gamma_m} = 2.739 \text{ MPa}$	Design Shear strength

EC5-2 6.1.1 System strength

$a := 0.3 \text{ m}$	Width depending on structure (Stress-laminated), EC5-2 Table 5.3
$t_{asphalt} := 120 \text{ mm}$	Thickness asphalt
$b_w := 6 \cdot 400 \text{ mm}$	Width of loaded area on the contact surface of the pavement. Conservative LM1 transverse axle-load width
$\beta_1 := 45 \text{ deg}$	Dispersion angle β for pavement
$\beta_2 := 15 \text{ deg}$	Dispersion angle β for laminated timber perpendicular to the grain
$b_{w,middle} := b_w + 2 \cdot \left(\sin(\beta_1) \cdot t_{asphalt} + \sin(\beta_2) \cdot \frac{h_{deck}}{2} \right)$	Width of loaded area at the reference plane in the middle of the deck. EC5-2 5.1.2
$b_{ef} := (b_{w,middle} + a) = 3.025 \text{ m}$	Effective width in direction of the grain, EC5-2 Eq 5.1
$W_z := \frac{b_{ef} \cdot h_{deck}^2}{6} = (1.815 \cdot 10^8) \text{ mm}^3$	Moment of resistance. Z-axis
$W_y := \frac{h_{deck} \cdot b_{ef}^2}{6} = (9.151 \cdot 10^8) \text{ mm}^3$	Moment of resistance. Y-axis
$I_z := \frac{b_{ef} \cdot h_{deck}^3}{12} = (5.445 \cdot 10^{10}) \text{ mm}^4$	Second moment of area. Z-axis
$I_y := \frac{h_{deck} \cdot b_{ef}^3}{12} = (1.384 \cdot 10^{12}) \text{ mm}^4$	Second moment of area. Y-axis
$A_{ef} := b_{ef} \cdot h_{deck} = (1.815 \cdot 10^6) \text{ mm}^2$	Effective Deck cross-sectional area

$$n := \frac{b_{ef}}{b_{lam}} = 26.304$$

For the calculation of k_{sys} , number of loaded lamellas. EC5-2 Eq 6.3

$$k_{sys} := 1.2$$

EC5-1-1 Figure 6.12

The design bending and shear strength of the deck plate should be calculated as:

$$f_{m.d.deck} = k_{sys} \cdot f_{m.d.lam}$$

EC5-2 Eq 6.1

$$f_{m.d.deck.z} := k_{sys} \cdot f_{m.z.d}$$

$$f_{m.d.deck.y} := k_{sys} \cdot f_{m.y.d}$$

$$f_{v.d.deck} = k_{sys} \cdot f_{v.d.lam}$$

EC5-2 Eq 6.2

$$f_{v.d.deck} := k_{sys} \cdot f_{v.d}$$

EC5-1-1 6.2.4 Combined bending and axial compression

$$\sigma_{c.0.d} := \frac{N_{x.d}}{h_{deck}} = 3.318 \frac{N}{mm^2}$$

Design compressive stress along the grain

$$\sigma_{m.z.d} := \frac{m_{z.d} \cdot b_{ef}}{W_z} = 3.59 \frac{N}{mm^2}$$

Design bending stress about the z-axis

$$\sigma_{m.y.d} := \frac{M_{y.d}}{W_y} = 4.777 \frac{N}{mm^2}$$

Design bending stress about the y-axis

$$U_{6.19} := \left(\frac{\sigma_{c.0.d}}{f_{c.0.d}} \right)^2 + \frac{|\sigma_{m.z.d}|}{f_{m.d.deck.z}} + k_m \cdot \frac{|\sigma_{m.y.d}|}{f_{m.d.deck.y}}$$

NS-EN 1995-1-1 6.2.4 Eq.6.19

$$U_{6.19} = 0.347$$

$$U_{6.20} := \left(\frac{\sigma_{c.0.d}}{f_{c.0.d}} \right)^2 + k_m \cdot \frac{|\sigma_{m.z.d}|}{f_{m.d.deck.z}} + \frac{|\sigma_{m.y.d}|}{f_{m.d.deck.y}}$$

NS-EN 1995-1-1 6.2.4 Eq.6.20

$$U_{6.20} = 0.362$$

6.3.2 Columns subjected to combined compression and bending

$l_{k.z} := 5.55 \text{ mm}$	Buckling length, in plane
$l_{k.y} := \frac{L_{bridge}}{2} = 55.5 \text{ m}$	Buckling length, Transverse
$i_z := \sqrt{\frac{I_z}{A_{ef}}} = 173.205 \text{ mm}$	Radius of gyration, z-akse
$i_y := \sqrt{\frac{I_y}{A_{ef}}} = 873.241 \text{ mm}$	Radius of gyration, y-akse
$\lambda_z := \frac{l_{k.z}}{i_z} = 0.032$	Slenderness about z-akse
$\lambda_y := \frac{l_{k.y}}{i_y} = 63.556$	Slenderness about y-akse
$\lambda_{rel.z} := \frac{\lambda_z}{\pi} \cdot \sqrt{\frac{f_{c.0.k}}{k_b \cdot E_{0.g.05}}} = 5.044 \cdot 10^{-4}$	NS-EN 1995-1-1 6.3.2(1) Eq.6.21, Relative slenderness
$\lambda_{rel.y} := \frac{\lambda_y}{\pi} \cdot \sqrt{\frac{f_{c.0.k}}{k_b \cdot E_{0.g.05}}} = 1.001$	NS-EN 1995-1-1 6.3.2(1) Eq.6.21, Relative slenderness
$k_z := 0.5 \left(1 + \beta_c \cdot (\lambda_{rel.z} - 0.3) + (\lambda_{rel.z})^2 \right)$	NS-EN 1995-1-1 6.3.2(3) Eq.6.27
$k_y := 0.5 \left(1 + \beta_c \cdot (\lambda_{rel.y} - 0.3) + (\lambda_{rel.y})^2 \right)$	NS-EN 1995-1-1 6.3.2(3) Eq.6.28
$k_{c.z} := \frac{1}{k_z + \sqrt{k_z^2 - \lambda_{rel.z}^2}} = 1.031$	NS-EN 1995-1-1 6.3.2(3) Eq.6.25
$k_{c.y} := \frac{1}{k_y + \sqrt{k_y^2 - \lambda_{rel.y}^2}} = 0.768$	NS-EN 1995-1-1 6.3.2(3) Eq.6.26
$U_{6.23} := \frac{ \sigma_{c.0.d} }{k_{c.z} \cdot f_{c.0.d}} + \frac{ \sigma_{m.z.d} }{f_{m.d.deck.z}} + k_m \cdot \frac{ \sigma_{m.y.d} }{f_{m.d.deck.y}}$ $U_{6.23} = 0.499$	NS-EN 1995-1-1 6.3.2(3) Eq.6.23
$U_{6.24} := \frac{ \sigma_{c.0.d} }{k_{c.y} \cdot f_{c.0.d}} + k_m \cdot \frac{ \sigma_{m.z.d} }{f_{m.d.deck.z}} + \frac{ \sigma_{m.y.d} }{f_{m.d.deck.y}}$ $U_{6.24} = 0.58$	NS-EN 1995-1-1 6.3.2(3) Eq.6.24

6.1.7 Shear

$$\tau_d \leq f_{v,d}$$

EC5-1-1 Eq 6.13

$$f_{v,d} := f_{v,d,deck} = 3.287 \frac{N}{mm^2}$$

Design shear strength deck plate,
EC5-2 Eq 6.2

$$k_{cr} := 0.67$$

Influence of cracks when bending,
NS-EN 1995-1-1 6.17

$$V_d := v_d \cdot b_{ef}$$

Design shear force

$$\tau_d := \frac{3}{2} \cdot \frac{V_d}{k_{cr} \cdot A_{ef}} = 0.807 \frac{N}{mm^2}$$

Design shear stress

$$U_V := \frac{\tau_d}{f_{v,d,deck}} = 0.246$$

Utilization factors:

$$U_{6.19} = 0.347$$

Combined bending and axial compression

$$U_{6.20} = 0.362$$

Combined bending and axial compression

$$U_{6.23} = 0.499$$

Buckling in-plane

$$U_{6.24} = 0.58$$

Buckling out-of-plane

$$U_V = 0.246$$

Shear

if $\max(U_{6.19}, U_{6.20}, U_{6.23}, U_{6.24}, U_V) < 1$ = "OK!"

|| "OK!"

else

|| "FAILURE"

Appendix_F: Hanger Connection

Bridge 1

- T-stub ULS capacity
- Tensile capacity hanger
- Timber splitting capacity

The data presented is the force in the hangers from load model "ULS_LM1_gr1a_Eq_b" which provides the largest tensile forces in the hangers.

$DATA := \text{READEXCEL}(\text{".\Appendix_F_3_Hangers forces Bridge 1. ULS_LM1_Eq_b.xlsx"}, \text{"Ark1!A2:E39"})$

$Element := DATA^{(0)}$

$i := 0 .. \text{length}(Element) - 1$

$$P_{Hanger_1} := \left(\frac{N}{mm^2} \right) \cdot DATA^{(1)} \quad P_{Hanger_2} := \left(\frac{N}{mm^2} \right) \cdot DATA^{(2)}$$

$$\theta_1 := deg \cdot DATA^{(3)} \quad \theta_2 := deg \cdot DATA^{(4)}$$

Hanger description: FATZER Full Locked Coil Rope (FLC) [28]

$$\emptyset := 30 \text{ mm}$$

Nominal- \emptyset

$$A_{Hanger} := 648 \text{ mm}^2$$

Nom. Metallic cross section

$$F_{Rd.Hanger} := 572 \text{ kN}$$

Design load

$$F_{Uk.Hanger} := 858 \text{ kN}$$

Charact. Breaking Load

Load from hangers

$$F_{Hanger.1_i} := P_{Hanger.1_i} \cdot A_{Hanger}$$

$$F_{Hanger.2_i} := P_{Hanger.2_i} \cdot A_{Hanger}$$

$$F_{y.11_i} := \cos(\theta_{1_i}) \cdot F_{Hanger.1_i}$$

$$F_{y.12_i} := \cos(\theta_{1_i}) \cdot F_{Hanger.2_i}$$

$$F_{y.1_i} := F_{y.11_i} + F_{y.12_i}$$

$$F_{z.1_i} := \sin(\theta_{1_i}) \cdot F_{Hanger.1_i}$$

$$F_{z.2_i} := \sin(\theta_{1_i}) \cdot F_{Hanger.2_i}$$

$$F_{z_i} := |F_{z.1_i} + F_{z.2_i}|$$

$$F_{y.21_i} := \cos(\theta_{2_i}) \cdot F_{y.11_i}$$

$$F_{y.22_i} := \cos(\theta_{2_i}) \cdot F_{y.12_i}$$

$$F_{y.2_i} := F_{y.21_i} + F_{y.22_i}$$

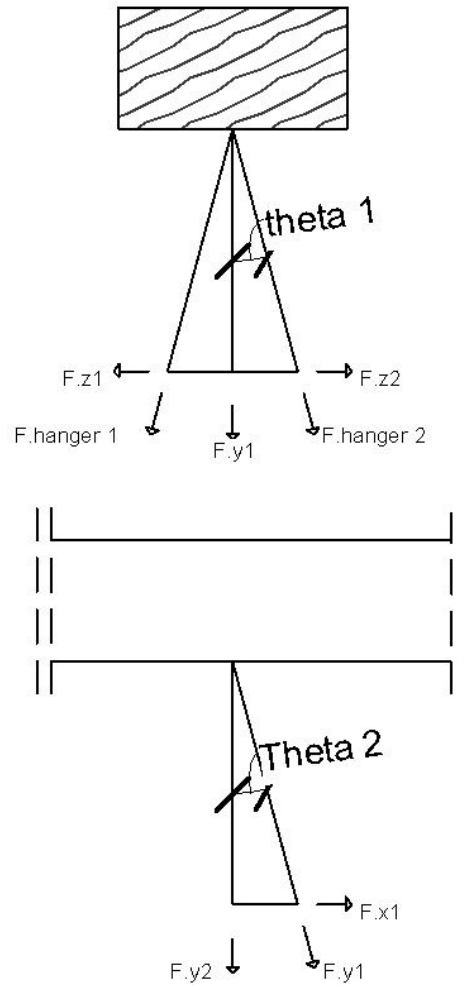
$$F_{x.11_i} := \sin(\theta_{2_i}) \cdot F_{z.1_i}$$

$$F_{x.12_i} := \sin(\theta_{2_i}) \cdot F_{z.2_i}$$

$$F_{x.1_i} := F_{x.11_i} + F_{x.12_i}$$

$$F_{T.Ed_i} := F_{y.2_i}$$

$$F_{V.Ed_i} := \sqrt{F_{z_i}^2 + F_{x.1_i}^2}$$



$t_{g.36.h} := 850 \text{ mm}$	Height arch cross-section
$l_1 := 400 \text{ mm}$	Length, connection bracket (T-stub)
$l_2 := 400 \text{ mm}$	Length, connection transverse beam
$b := 400 \text{ mm}$	Width , connection bracket
$a_w := 15 \text{ mm}$	size of weld
$t_p := 20 \text{ mm}$	Thickness, base plate
$t_{w.1} := 30 \text{ mm}$	T-stub, tension member thickness
$w := 300 \text{ mm}$	Distance between holes in the transverse direction
$d_{rod} := 20 \text{ mm}$	Threaded rod diameter
$d_m := \frac{27 \text{ mm} + 30 \text{ mm}}{2} = 28.5 \text{ mm}$	Nut average width
$n_{rods} := 8$	Number of threaded rods
$f_{y.k} := 355 \text{ MPa}$	steel, characteristic yield strength
$\gamma_{m.0} := 1.1$	partial factor for structural components and cross-sections
$\gamma_{m.1} := 1.05$	partial factor for structural components and cross-sections
$\gamma_{m.2} := 1.25$	partialfaktor for bolts
$E := 210 \text{ GPa}$	Steel, modulus of elasticity
$f_u := 470 \text{ MPa}$	Steel, nominal tensile strength
$f_{u.b} := 800 \text{ MPa}$	Threaded rod, nominal tensile strength
$f_{u.k} := 640 \text{ MPa}$	Threaded rod, characteristic yield strength
$A_s := 0.75 \cdot \frac{\pi \cdot d_{rod}^2}{4} = 235.619 \text{ mm}^2$	Threaded rod net area

Tensile capacity hanger

$$U_{Hanger,i} := \frac{\max(F_{Hanger.1_i}, F_{Hanger.2_i})}{F_{Rd.Hanger}}$$

Utilization hanger

shear capacity Threaded rod

$$\alpha_v := 0.6$$

NS-EN 1993-1-8 Table 3.4

$$F_{V.Rd} := n_{rods} \cdot \frac{\alpha_v \cdot f_{u.b} \cdot A_s}{\gamma_{m.2}} = 723.823 \text{ kN}$$

NS-EN 1993-1-8 Table 3.4

tensile capacity Threaded rod

$$k_2 := 0.9$$

NS-EN 1993-1-8 Table 3.4

$$F_{T.Rd} := n_{rods} \cdot \frac{k_2 \cdot f_{u.b} \cdot A_s}{\gamma_{m.2}} = (1.086 \cdot 10^3) \text{ kN}$$

NS-EN 1993-1-8 Table 3.4

Punching shear capacity, base plate

$$B_{p.Rd} := n_{rods} \cdot 0.6 \cdot \pi \cdot d_m \cdot t_p \cdot \frac{f_u}{\gamma_{m.2}} = 3231.869 \text{ kN}$$

NS-EN 1993-1-8 Table 3.4

$$U_{p.Rd,i} := \frac{F_{T.Ed_i}}{B_{p.Rd}}$$

Utilization punching shear

Weld capacity

$$\beta_w := 0.9$$

correlation factor

$$l_{w.1} := 2 \cdot (l_1 + t_{w.1}) = 860 \text{ mm}$$

Weld length: T-stub

$$l_{w.2} := 2 \cdot (l_2 + t_{w.1}) = 860 \text{ mm}$$

Weld length: Transverse beam connection

$$f_{vwd} := \frac{f_u}{\beta_w \cdot \gamma_{m.2} \cdot \sqrt{3}}$$

NS-EN 1993-1-8, Eq 4.4

$$F_{wRd.f.1} := f_{vwd} \cdot a_w \cdot l_{w.1} = 3111.533 \text{ kN}$$

Weld capacity for T-stub:
NS-EN 1993-1-8, Eq 4.3

$$U_{wRd.f.1_i} := \max\left(\frac{F_{Hanger.1_i}}{F_{wRd.f.1}}, \frac{F_{Hanger.2_i}}{F_{wRd.f.1}}\right)$$

Utilization weld, T-stub

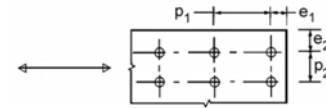
$$F_{wRd.f.2} := f_{vwd} \cdot a_w \cdot l_{w.2} = 3111.533 \text{ kN}$$

Weld capacity for transverse beam connection:
NS-EN 1993-1-8, Eq 4.3

$$U_{wRd.f.2} := \max \left(\frac{F_{Hanger.1_i}}{F_{wRd.f.2}}, \frac{F_{Hanger.2_i}}{F_{wRd.f.2}} \right)$$

Utilization weld, transverse beam

Bearing resistance: Treaded rods T-stub



NS-En 1993-1-8, Figure 3.1

$$e_1 := 50 \text{ mm}$$

End distance, direction of the load

$$e_2 := \frac{b-w}{2} = 50 \text{ mm}$$

Edge distance, transverse

$$d_0 := d_{rod} + 2 \text{ mm} = 22 \text{ mm}$$

hole diameter for the threaded rod

$$p_1 := \frac{l_1 - 2 \cdot e_1}{3} = 100 \text{ mm}$$

spacing between centres of fasteners

$$p_2 := w$$

spacing between adjacent lines of fasteners

$$k_{11} := \min \left(2.8 \cdot \frac{e_2}{d_0} - 1.7, 1.4 \cdot \frac{p_2}{d_0} - 1.7, 2.5 \right) = 2.5$$

NS-EN 1993-1-8 Table 3.4

$$k_{12} := \min \left(1.4 \cdot \frac{p_2}{d_0}, 2.5 \right) = 2.5$$

NS-EN 1993-1-8 Table 3.4

$$k_1 := \min(k_{11}, k_{12}) = 2.5$$

$$\alpha_{d1} := \frac{e_1}{3 \cdot d_0} = 0.758$$

NS-EN 1993-1-8 Table 3.4

$$\alpha_{d2} := \frac{p_1}{3 \cdot d_0} - 0.25 = 1.265$$

NS-EN 1993-1-8 Table 3.4

$$\alpha_d := \min \left(\alpha_{d1}, \alpha_{d2}, \frac{f_{u.b}}{f_u}, 1.0 \right) = 0.758$$

NS-EN 1993-1-8 Table 3.4

$$F_{b.Rd} := n_{rods} \cdot \frac{k_1 \cdot \alpha_d \cdot f_u \cdot d_{rod} \cdot t_p}{\gamma_{m.2}} = 2278.788 \text{ kN}$$

NS-EN 1993-1-8 Table 3.4

$$U_{b.Rd_i} := \frac{F_{V.Ed_i}}{F_{b.Rd}}$$

Utilization, bearing resistance

Design capacity T-stub . (No prying forces)

The mounting lugs for the hangers are viewed as one part, creating a single T-stub

$$t_w := 160 \text{ mm} \quad \text{width, mounting lug}$$

Unstiffened column flange, bolted connection
NS-EN 1993-1-8, 6.2.6.4.1

$$e := \frac{b}{2} - \frac{w}{2} = 50 \text{ mm} \quad e_{min} := e$$

$$m := 0.5 \cdot (w - t_w) - (0.8 \cdot a_w \cdot \sqrt{2}) = 53.029 \text{ mm}$$

$$p_1 := \frac{l_1 - 2 \cdot e_1}{3} = 100 \text{ mm}$$

Inner row of screws: Individually considered

$$l_{eff,cp.11} := (2 \cdot \pi \cdot m) = 333.194 \text{ mm}$$

$$l_{eff,nc.11} := (4 \cdot m + 1.25 \cdot e) = 274.618 \text{ mm}$$

$$l_{eff.11} := \min(l_{eff,cp.11}, l_{eff,nc.11}) = 274.618 \text{ mm}$$

Outer row of screws: Individually considered

$$l_{eff,cp.12} := (2 \cdot \pi \cdot m) = 333.194 \text{ mm}$$

$$l_{eff,nc.12} := (4 \cdot m + 1.25 \cdot e) = 274.618 \text{ mm}$$

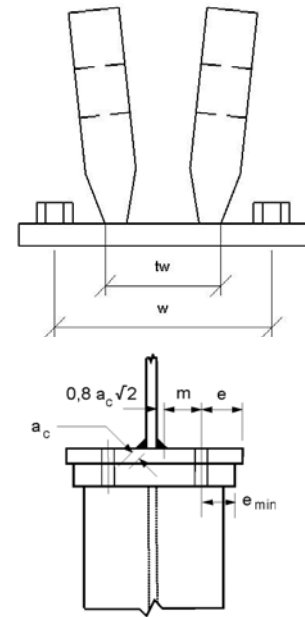
$$l_{eff.12} := \min(l_{eff,cp.12}, l_{eff,nc.12}) = 274.618 \text{ mm}$$

Inner row of screws: : part of a group

$$l_{eff,cp.22} := (2 \cdot p_1) = 200 \text{ mm}$$

$$l_{eff,nc.22} := (p_1) = 100 \text{ mm}$$

$$l_{eff.22} := \min(l_{eff,cp.22}, l_{eff,nc.22}) = 100 \text{ mm}$$



NS-En 1993-1-8, Figure 6.8

NS-EN 1993-1-8, 3.5(2)

NS-EN 1993-1-8 Table 6.4

NS-EN 1993-1-8 Table 6.4

NS-EN 1993-1-8 Table 6.4

Outer row of screws: part of a group

NS-EN 1993-1-8 Table 6.4

$$l_{eff,cp.21} := (\pi \cdot m + p_1) = 266.597 \text{ mm}$$

$$l_{eff,nc.21} := (2 \cdot m + 0.625 \cdot e + 0.5 \cdot p_1) = 187.309 \text{ mm}$$

$$l_{eff.21} := \min(l_{eff,cp.21}, l_{eff,nc.21}) = 187.309 \text{ mm}$$

$$l_{eff.1} := \min(2 \cdot (l_{eff,nc.11} + l_{eff,nc.12}), 2 \cdot (l_{eff,nc.21} + l_{eff,nc.22})) = 574.618 \text{ mm}$$

NS-EN 1993-1-8 Table 6.4

$$l_{eff.2} := \min(2 \cdot (l_{eff.11} + l_{eff.12}), 2 \cdot (l_{eff.21} + l_{eff,nc.22})) = 574.618 \text{ mm}$$

NS-EN 1993-1-8 Table 6.4

Design resistance $F_{T.Rd}$ of a T-stub flange:

$$M_{pl.1.Rd} := \frac{1}{4} \cdot l_{eff.1} \cdot f_{y,k} \cdot \frac{t_p^2}{\gamma_{m.0}} = (1.854 \cdot 10^7) \text{ N} \cdot \text{mm}$$

NS-EN 1993-1-8 Table 6.2

$$M_{pl.2.Rd} := \frac{1}{4} \cdot l_{eff.2} \cdot f_{y,k} \cdot \frac{t_p^2}{\gamma_{m.0}} = (1.854 \cdot 10^4) \text{ kN} \cdot \text{mm}$$

NS-EN 1993-1-8 Table 6.2

No prying forces

$$F_{T.1.2.Rd} := \frac{2 \cdot M_{pl.1.Rd}}{m} = 699.403 \text{ kN}$$

NS-EN 1993-1-8 Table 6.2

$$F_{T.3.Rd} := F_{T.Rd} = (1.086 \cdot 10^3) \text{ kN}$$

NS-EN 1993-1-8 Table 6.2

$$F_{T.Rd} := \min(F_{T.1.2.Rd}, F_{T.3.Rd}) = 699.403 \text{ kN}$$

Tension capacity T-stub

$$F_{V.Rd} = 723.823 \text{ kN}$$

Shear capacity T-stub

$$U_{S.T_i} := \frac{F_{V.Ed_i}}{F_{V.Rd}} + \frac{F_{T.Ed_i}}{1.4 \cdot F_{T.Rd}}$$

Utilization,

Combined shear and tensile forces,

NS-EN 1993-1-8 Table 3.4

Tension in connection plates

Same connection at T-stub and at transverse beam

$$R := 112 \text{ mm}$$

$$t_{w,1} := 30 \text{ mm}$$

$$t_{w,2} := 70 \text{ mm}$$

$$e_{Connect} := 200 \text{ mm}$$

$$A_{Plate} := t_{w,1} \cdot l_2$$

$$I_{x,Web} := \frac{t_{w,1} \cdot l_2^3}{12} = (1.6 \cdot 10^{-4}) \text{ m}^4$$

$$I_{y,Web} := \frac{l_2 \cdot t_{w,1}^3}{12} = (9 \cdot 10^{-7}) \text{ m}^4$$

$$N_{y_i} := \cos(\theta_{2_i}) \cdot \max(F_{y,11_i}, F_{y,12_i})$$

$$N_{x_i} := \sin(\theta_{2_i}) \cdot \max(F_{y,11_i}, F_{y,12_i})$$

$$\gamma_R := 1$$

$$F_{Rd,Connect} := \frac{F_{Uk,Hanger}}{1.5 \cdot \gamma_R}$$

$$N_z := 0.02 \cdot F_{Rd,Connect} = 11.44 \text{ kN}$$

$$M_{z_i} := N_{x_i} \cdot e_{Connect}$$

$$M_{y_i} := N_z \cdot e_{Connect}$$

$$\sigma_{Ed_i} := \frac{N_{y_i}}{A_{Plate}} + \frac{M_{z_i}}{I_{x,Web}} \cdot \frac{l_1}{2} + \frac{M_{y_i}}{I_{y,Web}} \cdot \frac{t_{w,1}}{2}$$

$$\max(\sigma_{Ed}) = 102.559 \text{ MPa}$$

$$U_{Con.Plate} := \frac{\max(\sigma_{Ed})}{\frac{f_{y,k}}{\gamma_{m,0}}} = 0.318$$

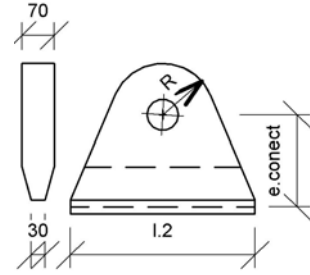


Figure: mounting lug

Area of web at connection

Second moment of area, X-axis

Second moment of area, Y-axis

Vertical force component

Horizontal force component

Partial factor

Design value of tension resistance
EN 1993-1-11, 6.2 (2)

Transverse force component,
(Estimated 2%)

Moment, z-axis

Moment, y-axis

Utilization connection plate
(Mounting lug)

Bearing resistance: mounting lugs for hanger connection

Identical connection at T-stub and at transverse beam

$$d_0 := 68 \text{ mm}$$

Hole diameter

$$e_1 := R - \frac{d_0}{2} = 78 \text{ mm}$$

End/Edge distance

$$e_2 := e_1$$

$$k_1 := \min\left(2.8 \cdot \frac{e_2}{d_0} - 1.7, 2.5\right) = 1.512$$

NS-EN 1993-1-8 Table 3.4

$$\alpha_{d1} := \frac{e_1}{3 \cdot d_0} = 0.382$$

NS-EN 1993-1-8 Table 3.4

$$\alpha_d := \min\left(\alpha_{d1}, \frac{f_{u,b}}{f_u}, 1.0\right) = 0.382$$

NS-EN 1993-1-8 Table 3.4

$$F_{b,Rd} := \frac{k_1 \cdot \alpha_d \cdot f_u \cdot d_0 \cdot t_{w,2}}{\gamma_{m,2}} = 1034.531 \text{ kN}$$

NS-EN 1993-1-8 Table 3.4

$$U_{b,Rd,2_i} := \frac{\max(F_{Hanger,1_i}, F_{Hanger,2_i})}{F_{b,Rd}}$$

$$\max(U_{b,Rd,2}) = 0.358$$

Utilization bearing resistance, mounting lug

Laterally loaded bolts EC5-1-1

$$f_{u,k} := 640$$

Bolt, characteristic tensile strength

$$d_{rod} := 20$$

Bolt diameter

$$\rho_k := 440$$

Characteristic timber density, GL32h

$$\rho_a := 390$$

Characteristic test timber density, GL 30c. [28]

$$\alpha := 0$$

Angle of load to the grain

$$M_{y,Rk} := 0.3 \cdot f_{u,k} \cdot d_{rod}^{2.6}$$

Characteristic yield moment, EC5-1-1 Eq 8.30

$$f_{h,0,k} := 0.082 \cdot (1 - 0.01 \cdot d_{rod}) \cdot \rho_k$$

Characteristic embedment strength parallel to the grain, EC5-1-1 Eq. 8.31

$$k_{90} := 1.35 + 0.015 \cdot d_{rod}$$

EC5-1-1 Eq. 8.33

$$f_{h.\alpha.k} := \frac{f_{h.0.k}}{k_{90} \cdot \sin(\alpha)^2 + \cos(\alpha)^2}$$

Characteristic embedment strenght,
EC5-1-1 Eq. 8.31

Steel-to-timber connection EC5-1-1 8.2.3

$$t_p \geq d + 0.1 d$$

Thick plate

$$t_1 := 600 \quad l_{ef} := t_1$$

Threaded rod Penetration depth,
[28]

$$a_1 := 100$$

Spacing between bolts in grain direction

$$n := 4$$

Number of bolts in the row

$$F_{v.Rk.C} := f_{h.\alpha.k} \cdot t_1 \cdot d_{rod}$$

EC5-1-1 Eq 8.10

$$F_{v.Rk.D} := f_{h.\alpha.k} \cdot t_1 \cdot d_{rod} \cdot \left(\sqrt[2]{2 + \frac{4 \cdot M_{y.Rk}}{f_{h.\alpha.k} \cdot d_{rod} \cdot t_1^2}} - 1 \right)$$

EC5-1-1 Eq 8.10

$$F_{v.Rk.E} := 2.3 \cdot \sqrt{M_{y.Rk} \cdot f_{h.\alpha.k} \cdot d_{rod}}$$

EC5-1-1 Eq 8.10

$$F_{v.Rk.i} := \min(F_{v.Rk.C}, F_{v.Rk.D}, F_{v.Rk.E}) = 3.762 \cdot 10^4$$

Characteristic load-carrying capacity
per shera plane per fastener

$$k_d := \min\left(\frac{d_{rod}}{8}, 1.0\right) = 1$$

EC5-1-1 Eq 8.40

$$f_{ax.k} := 0.52 \cdot d_{rod}^{-0.5} \cdot l_{ef}^{-0.1} \cdot \rho_k^{0.8}$$

EC5-1-1 Eq 8.39

$$n_{ef.1} := n^{0.9} = 3.482$$

EC5-1-1 Eq 8.41

$$\alpha := 90 \text{ deg}$$

Angle to the grain

$$F_{ax.\alpha.Rk} := \frac{n_{ef.1} \cdot f_{ax.k} \cdot d_{rod} \cdot l_{ef} \cdot k_d \cdot \left(\frac{\rho_k}{\rho_a}\right)^{0.8}}{1.2 \cdot \cos(\alpha)^2 + \sin(\alpha)^2} = 3.676 \cdot 10^5$$

Characteristic withdrawal strenght at an
angle to the grain. EC5-1-1 Eq 8.40a

$$Rope_effect := \min\left(\frac{F_{ax.\alpha.Rk}}{4}, F_{v.Rk.i}\right) = 3.762 \cdot 10^4$$

EC5-1-1 8.2.2(2)

$$n_{ef,2} := \min \left(n, n^{0.9} \cdot \sqrt[4]{\frac{a_1}{13 \cdot d_{rod}}} \right)$$

EC5-1-1 Eq 8.34

$$F_{v.Rk} := F_{v.Rk,i} + Rope_effect = 7.524 \cdot 10^4$$

EC5-1-1 Eq 8.10

$$F_{V.ef.Rk} := n_{ef,2} \cdot (F_{v.Rk})$$

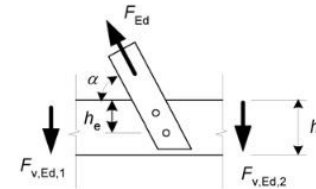
Characteristic load-of one row of fasteners parallel to the grain. EC5-1-1 Eq 8.1

$$U_{8.1_i} := \frac{F_{V.Ed_i}}{2 \cdot F_{V.ef.Rk} \cdot (N)}$$

Utilization, fasteners parallel to the grain

$$\max(U_{8.1}) = 0.346$$

Connection force at angle to the grain EC5-1-1 8.1.4



$$h := 1600$$

Arch width

$$h_e := 950$$

Loaded edge distance to the centre of the most distance fastener

$$b := 850$$

Arch height

$$w := 1$$

EC5-1-1 Eq 8.5

$$k_{mod} := 1.1$$

$$\gamma := 1.3$$

Partialfactor, connections

$$F_{90.Rk} := 14 \cdot b \cdot w \cdot \sqrt{\frac{h_e}{\left(1 - \frac{h_e}{h}\right)}}$$

Characteristic splitting capacity, EC5-1-1 Eq 8.4

$$F_{90.Rd} := F_{90.Rk} \cdot \frac{k_{mod}}{\gamma}$$

Design splitting capacity,

$$U_{8.2_i} := \frac{F_{z_i}}{F_{90.Rd} \cdot (N)}$$

Utilization, splitting perpendicular to the grain

$$\max(U_{8.2}) = 0.289$$

Resulting connection capacity

$$U_{Max} := \max (U_{S_T}, U_{p.Rd}, U_{wRd.f.1}, U_{wRd.f.2}, U_{b.Rd}, U_{Hanger}, U_{Con.Plate}, U_{b.Rd.2}, U_{8.1}, U_{8.2}) = 0.725$$

if $U_{Max} \leq 1$ | = "OK"
|| "OK"
else
|| "NOT OK"

Utilization factors:

$\max (U_{S_T}) = 0.725$	Combined shear and tensile forces, T-stub
$\max (U_{p.Rd}) = 0.179$	Punching shear, T-stub base plate
$\max (U_{wRd.f.1}) = 0.119$	Weld, T-stub/Mounting lug
$\max (U_{wRd.f.2}) = 0.119$	Weld, transverse beam/mounting lug
$\max (U_{b.Rd}) = 0.063$	Bearing resistance T-stub base plate
$\max (U_{Hanger}) = 0.647$	Hanger
$\max (U_{Con.Plate}) = 0.318$	Mounting lug
$\max (U_{b.Rd.2}) = 0.358$	Bearing resistance, mounting lug
$\max (U_{8.1}) = 0.346$	Fasteners parallel to the grain
$\max (U_{8.2}) = 0.289$	Splitting perpendicular to the grain

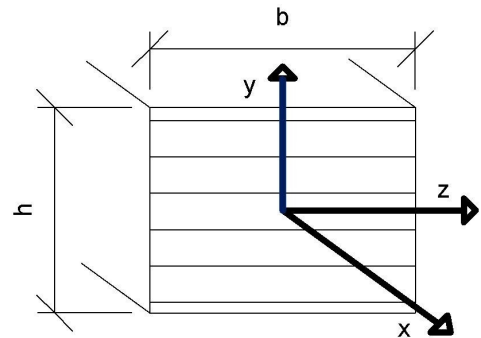
APPENDIX G.1

DESIGN CHECK: Bridge 1, ARCH_2

According to NS-EN 1995-1-1

Load combination: Gravity only

Material Parameters, GL32h



$$b := 1600 \text{ mm}$$

Arch width

$$h := 850 \text{ mm}$$

Arch height

$$\gamma_m := 1.15$$

Partial Factor for material properties

$$k_{mod} := 0.6$$

Modification factor for duration of load and moisture content

$$k_m := 0.7$$

Factor for re-distribution of bending stresses in a cross-section

$$k_{cr} := 0.67$$

Factor for determining effective width

$$k_{shape} := \min\left(1.0 + 0.05 \cdot \frac{h}{b}, 1.3\right) = 1.027$$

Factor depending on the shape of the cross-section

$$\beta_c := 0.1$$

Straightness factor

$$E_{0.05} := 11800 \text{ MPa}$$

Fifth percentile value of modulus of elasticity

$$f_{m,k} := 32 \text{ MPa}$$

Characteristic bending strength

$$f_{c,0,k} := 32 \text{ MPa}$$

Characteristic compression strength along grain

$$f_{t,90,k} := 0.5 \text{ MPa}$$

Characteristic tensile strength perpendicular to the grain

$$f_{v,k} := 3.5 \text{ MPa}$$

Characteristic shear strength

$$\rho_k := 440 \frac{\text{kg}}{\text{m}^3}$$

Material density

INPUT FROM ABAQUS

$$EV_{OP} := 1.476$$

Eigenvalue out of plane

$$EV_{IP} := 6.868$$

Eigenvalue in plane

DATA := READEXCEL (“.\ULS_Gravity_Eq_a.xlsx”, “Ark1!A1221:H2404”)
All forces from Abaqus are printed to excel sheets, that can be found in the digital appendix

$$Element := DATA^{(0)}$$

$$i := 0 .. \text{length}(Element) - 1$$

$$N_{Ed} := DATA^{(2)} \mathbf{N}$$
$$\min(N_{Ed}) = -8.666 \mathbf{MN}$$
$$\max(N_{Ed}) = -8.231 \mathbf{MN}$$

$$V_{y.Ed} := DATA^{(3)} \mathbf{N}$$
$$\min(V_{y.Ed}) = -253.851 \mathbf{kN}$$
$$\max(V_{y.Ed}) = 253.851 \mathbf{kN}$$

$$V_{z.Ed} := DATA^{(4)} \mathbf{N}$$
$$\min(V_{z.Ed}) = -34.47 \mathbf{kN}$$
$$\max(V_{z.Ed}) = 34.47 \mathbf{kN}$$

$$M_{z.Ed} := DATA^{(5)} \mathbf{N \cdot mm}$$
$$\min(M_{z.Ed}) = -278.449 \mathbf{kN \cdot m}$$
$$\max(M_{z.Ed}) = 450.465 \mathbf{kN \cdot m}$$

$$M_{y.Ed} := DATA^{(6)} \mathbf{N \cdot mm}$$
$$\min(M_{y.Ed}) = -10.856 \mathbf{kN \cdot m}$$
$$\max(M_{y.Ed}) = 250.045 \mathbf{kN \cdot m}$$

$$M_{x.Ed} := DATA^{(7)} \mathbf{N \cdot mm}$$
$$\min(M_{x.Ed}) = -9.175 \mathbf{kN \cdot m}$$
$$\max(M_{x.Ed}) = 9.174 \mathbf{kN \cdot m}$$

Cross-section parameters

$$A := b \cdot h = (1.36 \cdot 10^6) \text{ mm}^2$$

Arch cross-sectional area

$$I_z := \frac{b \cdot h^3}{12} = (8.188 \cdot 10^{10}) \text{ mm}^4$$

Second moment of area. Z-axis

$$I_y := \frac{h \cdot b^3}{12} = (2.901 \cdot 10^{11}) \text{ mm}^4$$

Second moment of area. Y-axis

$$W_z := \frac{b \cdot h^2}{6} = (1.927 \cdot 10^8) \text{ mm}^3$$

Moment of resistance. Z-axis

$$W_y := \frac{h \cdot b^2}{6} = (3.627 \cdot 10^8) \text{ mm}^3$$

Moment of resistance. Y-axis

$$W_p := \frac{b \cdot h^2}{3 \cdot \left(1 + 0.6 \cdot \frac{h}{b}\right)} = (2.922 \cdot 10^8) \text{ mm}^3$$

Moment of resistance. polar

$$f_{c.0.d} := k_{mod} \cdot \frac{f_{c.0.k}}{\gamma_m} = 16.696 \text{ MPa}$$

Design compressive strength along the grain

$$f_{m.z.d} := k_{mod} \cdot \frac{f_{m.k}}{\gamma_m} = 16.696 \text{ MPa}$$

Design bending strength about the principal y-axis

$$f_{m.y.d} := k_{mod} \cdot \frac{f_{m.k}}{\gamma_m} = 16.696 \text{ MPa}$$

Design bending strength about the principal z-axis

$$f_{v.d} := k_{mod} \cdot \frac{f_{v.k}}{\gamma_m} = 1.826 \text{ MPa}$$

Design Shear strength

$$f_{t.90.d} := k_{mod} \cdot \frac{f_{t.90.k}}{\gamma_m} = 0.261 \text{ MPa}$$

Design tensile strength perpendicular to the grain

$$\sigma_{c.0.d_i} := \frac{N_{Ed_i}}{A}$$

Design compressive stress along the grain

$$\sigma_{m.z.d_i} := \frac{M_{z.Ed_i}}{W_z}$$

Design bending stress about the z-axis

$$\sigma_{m.y.d_i} := \frac{M_{y.Ed_i}}{W_y}$$

Design bending stress about the y-axis

$$\tau_{tor.d_i} := \frac{M_{x.Ed_i}}{W_p}$$

Design shear stress from torsion

$$\tau_{y.d_i} := \frac{3 \cdot V_{y.Ed_i}}{2 \cdot k_{cr} \cdot A}$$

Design shear stress along y-axis

$$\tau_{z.d_i} := \frac{3 \cdot V_{z.Ed_i}}{2 \cdot k_{cr} \cdot A}$$

Design shear stress along z-axis

6.2.4 Combined bending and axial compression

$$U_{6.19_i} := \left(\frac{|\sigma_{c.0.d_i}|}{f_{c.0.d}} \right)^2 + \frac{|\sigma_{m.z.d_i}|}{f_{m.z.d}} + k_m \cdot \frac{|\sigma_{m.y.d_i}|}{f_{m.y.d}}$$

NS-EN 1995-1-1 6.2.4 Eq.6.19

$$\max(U_{6.19}) = 0.307$$

$$U_{6.20_i} := \left(\frac{|\sigma_{c.0.d_i}|}{f_{c.0.d}} \right)^2 + k_m \cdot \frac{|\sigma_{m.z.d_i}|}{f_{m.z.d}} + \frac{|\sigma_{m.y.d_i}|}{f_{m.y.d}}$$

NS-EN 1995-1-1 6.2.4 Eq.6.20

$$\max(U_{6.20}) = 0.274$$

6.3.2 Columns subjected to combined compression and bending

$$BF_{IP} := EV_{IP} + 1$$

Buckling factor, in plane

$$BF_{OP} := EV_{OP} + 1$$

Buckling factor, out-of-plane

$$l_{k,z} := \sqrt[2]{\frac{\pi^2 \cdot E_{0,g,05} \cdot I_z}{|\min(N_{Ed})| \cdot BF_{IP}}} = 11.827 \text{ m}$$

Buckling length, in plane

$$l_{k,y} := \sqrt[2]{\frac{\pi^2 \cdot E_{0,g,05} \cdot I_y}{|\min(N_{Ed})| \cdot BF_{OP}}} = 39.684 \text{ m}$$

Buckling length, out of plane

$$i_z := \sqrt{\frac{I_z}{A}} = 245.374 \text{ mm}$$

Radius of gyration, z-akse

$$i_y := \sqrt{\frac{I_y}{A}} = 461.88 \text{ mm}$$

Radius of gyration, y-akse

$$\lambda_z := \frac{l_{k,z}}{i_z} = 48.198$$

Slenderness about z-akse

$$\lambda_y := \frac{l_{k,y}}{i_y} = 85.919$$

Slenderness about y-akse

$$\lambda_{rel,z} := \frac{\lambda_z}{\pi} \cdot \sqrt{\frac{f_{c,0,k}}{E_{0,g,05}}} = 0.799$$

NS-EN 1995-1-1 6.3.2(1) Eq.6.21,
Relative slenderness

$$\lambda_{rel,y} := \frac{\lambda_y}{\pi} \cdot \sqrt{\frac{f_{c,0,k}}{E_{0,g,05}}} = 1.424$$

NS-EN 1995-1-1 6.3.2(1) Eq.6.21,
Relative slenderness

$$k_z := 0.5 \left(1 + \beta_c \cdot (\lambda_{rel,z} - 0.3) + (\lambda_{rel,z})^2 \right)$$

NS-EN 1995-1-1 6.3.2(3) Eq.6.27

$$k_y := 0.5 \left(1 + \beta_c \cdot (\lambda_{rel,y} - 0.3) + (\lambda_{rel,y})^2 \right)$$

NS-EN 1995-1-1 6.3.2(3) Eq.6.28

$$k_{c,z} := \frac{1}{k_z + \sqrt{k_z^2 - \lambda_{rel,z}^2}} = 0.896$$

NS-EN 1995-1-1 6.3.2(3) Eq.6.25

$$k_{c,y} := \frac{1}{k_y + \sqrt{k_y^2 - \lambda_{rel,y}^2}} = 0.448$$

NS-EN 1995-1-1 6.3.2(3) Eq.6.26

$$U_{6.23_i} := \frac{|\sigma_{c.0.d_i}|}{k_{c.z} \cdot f_{c.0.d}} + \frac{|\sigma_{m.z.d_i}|}{f_{m.z.d}} + k_m \cdot \frac{|\sigma_{m.y.d_i}|}{f_{m.y.d}}$$

NS-EN 1995-1-1 6.3.2(3) Eq.6.23

$$\max(U_{6.23}) = 0.587$$

$$U_{6.24_i} := \frac{|\sigma_{c.0.d_i}|}{k_{c.y} \cdot f_{c.0.d}} + k_m \cdot \frac{|\sigma_{m.z.d_i}|}{f_{m.z.d}} + \frac{|\sigma_{m.y.d_i}|}{f_{m.y.d}}$$

NS-EN 1995-1-1 6.3.2(3) Eq.6.24

$$\max(U_{6.24}) = 0.98$$

Combined action from shear and torsion

$$U_{V_T_i} := \frac{\sqrt{\left(|\tau_{z.d_i}\right|^2 + \left(|\tau_{y.d_i}\right|^2\right)}}{f_{v.d}} + \frac{|\tau_{tor.d_i}|}{k_{shape} \cdot f_{v.d}}$$

$$\max(U_{V_T}) = 0.234$$

Cambered Beam EC5-1-1 6.4.3

$$l_{Arch} := 118.627 \text{ m}$$

Arch length

$$h_{ap} := h$$

The cross-sectional height of the arch apex
NS-EN 1995-1-1 6.4.3(4),

$$r := 94.563 \text{ m}$$

Center radius

$$r_{in} := r - \frac{h}{2}$$

inner radius of curvature,
NS-EN 1995-1-1 6.4.3(4)

$$\alpha_{ap} := 0 \text{ deg}$$

Angle of inclination in the middle of the apex,
NS-EN 1995-1-1 6.4.3(4),

$$t := 45 \text{ mm}$$

The beams lamellae thickness,
NS-EN 1995-1-1 6.4.3(5)

$$k_1 := 1 + 1.4 \cdot \tan(\alpha_{ap}) + 5.4 \cdot \tan(\alpha_{ap})^2 = 1$$

NS-EN 1995-1-1 6.4.3(4) Eq. 6.44

$$k_2 := 0.35 - 8 \cdot \tan(\alpha_{ap}) = 0.35$$

NS-EN 1995-1-1 6.4.3(4) Eq. 6.45

$$k_3 := 0.6 + 8.3 \cdot \tan(\alpha_{ap}) - 7.8 \cdot \tan(\alpha_{ap})^2 = 0.6$$

NS-EN 1995-1-1 6.4.3(4) Eq. 6.46

$$k_4 := 6 \cdot \tan(\alpha_{ap})^2 = 0$$

NS-EN 1995-1-1 6.4.3(4) Eq. 6.47

$$k_l := k_1 + k_2 \cdot \left(\frac{h_{ap}}{r}\right) + k_3 \cdot \left(\frac{h_{ap}}{r}\right)^2 + k_4 \cdot \left(\frac{h_{ap}}{r}\right)^3 = 1.003$$

NS-EN 1995-1-1 6.4.3(4) Eq. 6.43

$$M_{ap,d} := \left| M_{z,Ed_{592}} \right|$$

Design apex moment,
NS-EN 1995-1-1 6.4.3(4)

$$\sigma_{m,d} := k_l \cdot \frac{6 \cdot M_{ap,d}}{b \cdot h_{ap}^2} = 0.305 \frac{N}{\text{mm}^2}$$

NS-EN 1995-1-1 6.4.3(4) Eq. 6.42

$$k_r := \begin{cases} \text{if } \frac{r_{in}}{t} \geq 240 & \\ \parallel 1 & \\ \text{else} & \\ \parallel 0.76 + 0.001 \cdot \frac{r_{in}}{t} & \end{cases} = 1$$

NS-EN 1995-1-1 6.4.3(5) Eq. 6.49

$$\sigma_{m.d} \leq k_r \cdot f_{m.z.g.d}$$

NS-EN 1995-1-1 6.4.3(3) Eq. 6.41

$$U_{6.41}_{592} := \frac{|\sigma_{m.d}|}{k_r \cdot f_{m.z.d}} = 0.018$$

$$V_b := b \cdot h \cdot l_{Arch} = 161.333 \text{ m}^3$$

Volume of one arch

$$V := \frac{2}{3} \cdot V_b = 107.555 \text{ m}^3$$

NS-EN 1995-1-1 6.4.3(5)

$$V_0 := 0.01 \text{ m}^3$$

NS-EN 1995-1-1 6.4.3(5),
Reference volume

$$k_{vol} := \left(\frac{V_0}{V} \right)^{0.2} = 0.156$$

NS-EN 1995-1-1 6.4.3(5) Eq. 6.51

$$k_{dis} := 1.4$$

NS-EN 1995-1-1 6.4.3(5) Eq. 6.52,
cambered beams

$$k_5 := 0.2 \cdot \tan(\alpha_{ap}) = 0$$

NS-EN 1995-1-1 6.4.3(8) Eq. 6.57

$$k_6 := 0.25 - 1.25 \cdot \tan(\alpha_{ap}) + 2.6 \cdot \tan(\alpha_{ap})^2 = 0.25$$

NS-EN 1995-1-1 6.4.3(8) Eq. 6.58

$$k_7 := 2.1 \cdot \tan(\alpha_{ap}) - 4 \cdot \tan(\alpha_{ap})^2 = 0$$

NS-EN 1995-1-1 6.4.3(8) Eq. 6.59

$$k_p := k_5 + k_6 \cdot \left(\frac{h_{ap}}{r} \right) + k_7 \cdot \left(\frac{h_{ap}}{r} \right)^2 = 0.002$$

NS-EN 1995-1-1 6.4.3(8) Eq. 6.56

$$\sigma_{t.90.d} := k_p \cdot \frac{6 \cdot M_{ap.d}}{b \cdot h_{ap}^2} = (6.827 \cdot 10^{-4}) \frac{N}{\text{mm}^2}$$

NS-EN 1995-1-1 6.4.3(8) Eq. 6.55

$$\frac{\tau_d}{f_{v.d}} + \frac{\sigma_{t.90.d}}{k_{dis} \cdot k_{vol} \cdot f_{t.90.d}} \leq 1$$

NS-EN 1995-1-1 6.4.3(8) Eq. 6.53

$$U_{6.53}_i := \frac{\sqrt{\left(|\tau_{z.d_i}| \right)^2 + \left(|\tau_{y.d_i}| \right)^2}}{f_{v.d}} + \frac{|\sigma_{t.90.d}|}{k_{dis} \cdot k_{vol} \cdot f_{t.90.d}}$$

$$\max(U_{6.53}) = 0.241$$

SUMMARY

Utilization factors:

$$\max \langle U_{6.19} \rangle = 0.307$$

Combined bending and axial compression

$$\max \langle U_{6.20} \rangle = 0.274$$

Combined bending and axial compression

$$\max \langle U_{6.23} \rangle = 0.587$$

Buckling in-plane

$$\max \langle U_{6.24} \rangle = 0.98$$

Buckling out-of-plan

$$\max \langle U_{V_T} \rangle = 0.234$$

Combined shear and torsion

$$\max \langle U_{6.53} \rangle = 0.241$$

Combined tension perpendicular to grain and shear

$$\max \langle U_{6.41} \rangle = 0.018$$

Cambered beam: Apex bending moment

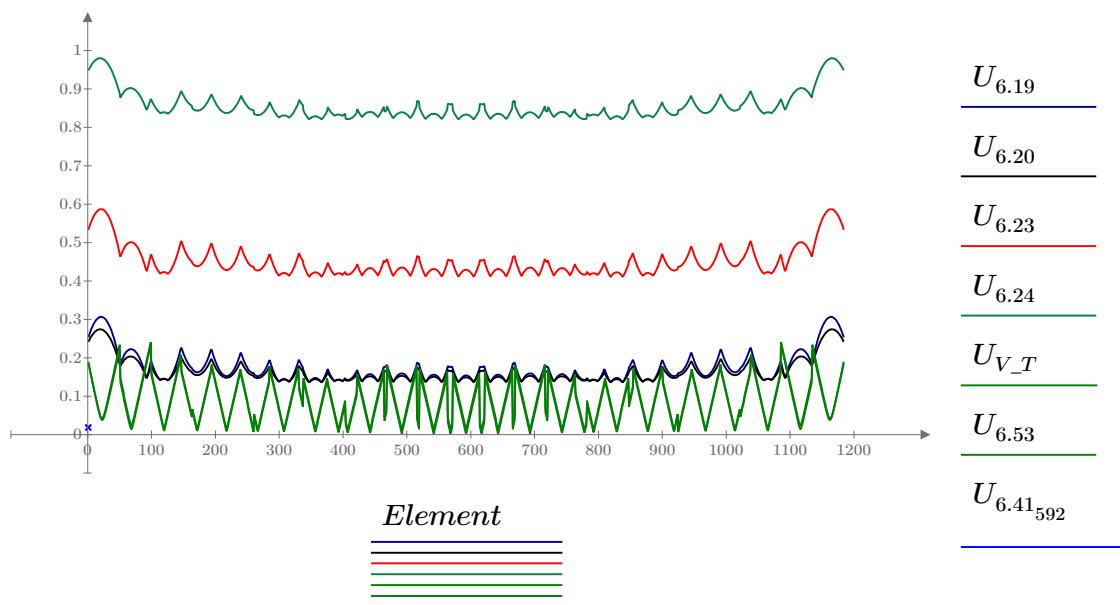
if $\max \langle U_{6.19}, U_{6.20}, U_{6.23}, U_{6.24}, U_{V_T}, U_{6.53}, U_{6.41} \rangle < 1$ = "OK!"

|| "OK!"

else

|| "FAILURE"

Plot of the Arch utilizations:



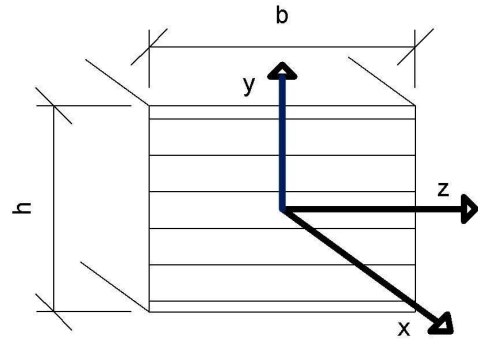
APPENDIX G.2

DESIGN CHECK: Bridge 2, ARCH_1

According to NS-EN 1995-1-1

Load combination: Gravity only

Material Parameters, GL32h



$$\gamma_m := 1.15$$

Partial Factor for material properties

$$k_{mod} := 0.6$$

Modification factor for duration of load and moisture content

$$k_m := 0.7$$

Factor for re-distribution of bending stresses in a cross-section

$$k_{cr} := 0.67$$

Factor for determining effective width

$$\beta_c := 0.1$$

Straightness factor

$$E_{0.05} := 11800 \text{ MPa}$$

Fifth percentile value of modulus of elasticity

$$f_{m,k} := 32 \text{ MPa}$$

Characteristic bending strength

$$f_{c,0,k} := 32 \text{ MPa}$$

Characteristic compression strength along grain

$$f_{t,90,k} := 0.5 \text{ MPa}$$

Characteristic tensile strength perpendicular to the grain

$$f_{v,k} := 3.5 \text{ MPa}$$

Characteristic shear strength

$$\rho_k := 440 \frac{\text{kg}}{\text{m}^3}$$

Material density

INPUT FROM ABAQUS

$$EV_{OP} := 5.6051$$

Eigenvalue out of plane

$$EV_{IP} := 7.3386$$

Eigenvalue in plane

$DATA := \text{READEXCEL}(\text{".\ULS LM1 Gravity Arch1100_850.xlsx"}, \text{"Arch1!A20:J1209"})$

All forces from Abaqus are printed to excel sheets, that can be found in the digital appendix

$$Element := DATA^{(0)}$$

$$i := 0 .. \text{length}(Element) - 1$$

$$b := DATA^{(8)} \text{ mm}$$

Arch width

$$h := DATA^{(9)} \text{ mm}$$

Arch height

$$N_{Ed} := DATA^{(2)} \text{ N}$$

$$\min(N_{Ed}) = -9.384 \text{ MN}$$

$$\max(N_{Ed}) = -8.433 \text{ MN}$$

$$V_{y.Ed} := DATA^{(3)} \text{ N}$$

$$\min(V_{y.Ed}) = -454.036 \text{ kN}$$

$$\max(V_{y.Ed}) = 453.743 \text{ kN}$$

$$V_{z.Ed} := DATA^{(4)} \text{ N}$$

$$\min(V_{z.Ed}) = -25.194 \text{ kN}$$

$$\max(V_{z.Ed}) = 25.198 \text{ kN}$$

$$M_{z.Ed} := DATA^{(5)} \text{ N} \cdot \text{mm}$$

$$\min(M_{z.Ed}) = -894.383 \text{ kN} \cdot \text{m}$$

$$\max(M_{z.Ed}) = 235.468 \text{ kN} \cdot \text{m}$$

$$M_{y.Ed} := DATA^{(6)} \text{ N} \cdot \text{mm}$$

$$\min(M_{y.Ed}) = -68.989 \text{ kN} \cdot \text{m}$$

$$\max(M_{y.Ed}) = 69.948 \text{ kN} \cdot \text{m}$$

$$M_{x.Ed} := DATA^{(7)} \text{ N} \cdot \text{mm}$$

$$\min(M_{x.Ed}) = -17.968 \text{ kN} \cdot \text{m}$$

$$\max(M_{x.Ed}) = 17.985 \text{ kN} \cdot \text{m}$$

Cross-section parameters

$$A_i := b_i \cdot h_i$$

Arch cross-sectional area

$$I_{z_i} := \frac{b_i \cdot h_i^3}{12}$$

Second moment of area. Z-axis

$$I_{y_i} := \frac{h_i \cdot b_i^3}{12}$$

Second moment of area. Y-axis

$$W_{z_i} := \frac{b_i \cdot h_i^2}{6}$$

Moment of resistance. Z-axis

$$W_{y_i} := \frac{h_i \cdot b_i^2}{6}$$

Moment of resistance. Y-axis

$$W_{p_i} := \frac{b_i \cdot h_i^2}{3 \cdot \left(1 + 0.6 \cdot \frac{h_i}{b_i} \right)}$$

Moment of resistance. polar

$$k_{shape_i} := \min \left(1.0 + 0.05 \cdot \frac{h_i}{b_i}, 1.3 \right)$$

Factor depending on the shape of the cross-section

$$f_{c.0.d} := k_{mod} \cdot \frac{f_{c.0.k}}{\gamma_m} = 16.696 \text{ MPa}$$

Design compressive strength along the grain

$$f_{m.z.d} := k_{mod} \cdot \frac{f_{m.k}}{\gamma_m} = 16.696 \text{ MPa}$$

Design bending strength about the principal y-axis

$$f_{m.y.d} := k_{mod} \cdot \frac{f_{m.k}}{\gamma_m} = 16.696 \text{ MPa}$$

Design bending strength about the principal z-axis

$$f_{v.d} := k_{mod} \cdot \frac{f_{v.k}}{\gamma_m} = 1.826 \text{ MPa}$$

Design Shear strength

$$f_{t.90.d} := k_{mod} \cdot \frac{f_{t.90.k}}{\gamma_m} = 0.261 \text{ MPa}$$

Design tensile strength perpendicular to the grain

$$\sigma_{c.0.d_i} := \frac{N_{Ed_i}}{A_i}$$

Design compressive stress along the grain

$$\sigma_{m.z.d_i} := \frac{M_{z.Ed_i}}{W_{z_i}}$$

Design bending stress about the z-axis

$$\sigma_{m.y.d_i} := \frac{M_{y.Ed_i}}{W_{y_i}}$$

Design bending stress about the y-axis

$$\tau_{tor.d_i} := \frac{M_{x.Ed_i}}{W_{p_i}}$$

Design shear stress from torsion

$$\tau_{y.d_i} := \frac{3 \cdot V_{y.Ed_i}}{2 \cdot k_{cr} \cdot A_i}$$

Design shear stress along y-axis

$$\tau_{z.d_i} := \frac{3 \cdot V_{z.Ed_i}}{2 \cdot k_{cr} \cdot A_i}$$

Design shear stress along z-axis

6.2.4 Combined bending and axial compression

$$U_{6.19_i} := \left(\frac{|\sigma_{c.0.d_i}|}{f_{c.0.d}} \right)^2 + \frac{|\sigma_{m.z.d_i}|}{f_{m.z.d}} + k_m \cdot \frac{|\sigma_{m.y.d_i}|}{f_{m.y.d}}$$

NS-EN 1995-1-1 6.2.4 Eq.6.19

$$\max(U_{6.19}) = 0.646$$

$$U_{6.20_i} := \left(\frac{|\sigma_{c.0.d_i}|}{f_{c.0.d}} \right)^2 + k_m \cdot \frac{|\sigma_{m.z.d_i}|}{f_{m.z.d}} + \frac{|\sigma_{m.y.d_i}|}{f_{m.y.d}}$$

NS-EN 1995-1-1 6.2.4 Eq.6.20

$$\max(U_{6.20}) = 0.63$$

6.3.2 Columns subjected to combined compression and bending

$$BF_{IP} := EV_{IP} + 1$$

Buckling factor, in plane

$$BF_{OP} := EV_{OP} + 1$$

Buckling factor, out of plane

$$l_{k,z_i} := \sqrt[2]{\frac{\pi^2 \cdot E_{0.g.05} \cdot I_{z_i}}{|\min(N_{Ed})| \cdot BF_{IP}}}$$

Buckling length, out of plane

$$l_{k,y_i} := \sqrt[2]{\frac{\pi^2 \cdot E_{0.g.05} \cdot I_{y_i}}{|\min(N_{Ed})| \cdot BF_{OP}}}$$

Buckling length, out of plane

$$i_{z_i} := \sqrt{\frac{I_{z_i}}{A_i}}$$

Radius of gyration, z-axis

$$i_{y_i} := \sqrt{\frac{I_{y_i}}{A_i}}$$

Radius of gyration, y-axis

$$\lambda_{z_i} := \frac{l_{k,z_i}}{i_{z_i}}$$

Slenderness about z-axis

$$\lambda_{y_i} := \frac{l_{k,y_i}}{i_{y_i}}$$

Slenderness about y-axis

$$\lambda_{rel,z_i} := \frac{\lambda_{z_i}}{\pi} \cdot \sqrt{\frac{f_{c.0.k}}{E_{0.g.05}}}$$

NS-EN 1995-1-1 6.3.2(1) Eq.6.21,
Relative slenderness

$$\lambda_{rel,y_i} := \frac{\lambda_{y_i}}{\pi} \cdot \sqrt{\frac{f_{c.0.k}}{E_{0.g.05}}}$$

NS-EN 1995-1-1 6.3.2(1) Eq.6.21,
Relative slenderness

$$k_{z_i} := 0.5 \left(1 + \beta_c \cdot (\lambda_{rel,z_i} - 0.3) + (\lambda_{rel,z_i})^2 \right)$$

NS-EN 1995-1-1 6.3.2(3) Eq.6.27

$$k_{y_i} := 0.5 \left(1 + \beta_c \cdot (\lambda_{rel,y_i} - 0.3) + (\lambda_{rel,y_i})^2 \right)$$

NS-EN 1995-1-1 6.3.2(3) Eq.6.28

$$k_{c.z_i} := \frac{1}{k_{z_i} + \sqrt{k_{z_i}^2 - \lambda_{rel.z_i}^2}}$$

NS-EN 1995-1-1 6.3.2(3) Eq.6.25

$$k_{c.y_i} := \frac{1}{k_{y_i} + \sqrt{k_{y_i}^2 - \lambda_{rel.y_i}^2}}$$

NS-EN 1995-1-1 6.3.2(3) Eq.6.26

$$U_{6.23_i} := \frac{|\sigma_{c.0.d_i}|}{k_{c.z_i} \cdot f_{c.0.d}} + \frac{|\sigma_{m.z.d_i}|}{f_{m.z.d}} + k_m \cdot \frac{|\sigma_{m.y.d_i}|}{f_{m.y.d}}$$

$$\max(U_{6.23}) = 0.856$$

NS-EN 1995-1-1 6.3.2(3) Eq.6.23

$$U_{6.24_i} := \frac{|\sigma_{c.0.d_i}|}{k_{c.y_i} \cdot f_{c.0.d}} + k_m \cdot \frac{|\sigma_{m.z.d_i}|}{f_{m.z.d}} + \frac{|\sigma_{m.y.d_i}|}{f_{m.y.d}}$$

$$\max(U_{6.24}) = 0.857$$

NS-EN 1995-1-1 6.3.2(3) Eq.6.24

Combined action from shear and torsion

$$U_{V_T_i} := \frac{\sqrt{\left(|\tau_{z.d_i}\right|^2 + \left(|\tau_{y.d_i}\right|^2\right)}}{f_{v.d}} + \frac{|\tau_{tor.d_i}|}{k_{shape_i} \cdot f_{v.d}}$$

$$\max(U_{V_T}) = 0.492$$

Cambered Beam EC5-1-1 6.4.3

$$l_{Arch} := 118.627 \text{ m}$$

Arch length

$$h_{ap} := h_{595} \quad \text{Element 595 is the top element}$$

The cross-sectional height of the arch apex
NS-EN 1995-1-1 6.4.3(4),

$$r := 94.563 \text{ m}$$

Center radius

$$r_{in} := r - \frac{h_{ap}}{2}$$

Inner radius of curvature,
NS-EN 1995-1-1 6.4.3(4)

$$\alpha_{ap} := 0 \text{ deg}$$

Angle of inclination in the middle of the apex,
NS-EN 1995-1-1 6.4.3(4),

$$t := 45 \text{ mm}$$

The beams lamellae thickness,
NS-EN 1995-1-1 6.4.3(5)

$$k_1 := 1 + 1.4 \cdot \tan(\alpha_{ap}) + 5.4 \cdot \tan(\alpha_{ap})^2 = 1$$

NS-EN 1995-1-1 6.4.3(4) Eq. 6.44

$$k_2 := 0.35 - 8 \cdot \tan(\alpha_{ap}) = 0.35$$

NS-EN 1995-1-1 6.4.3(4) Eq. 6.45

$$k_3 := 0.6 + 8.3 \cdot \tan(\alpha_{ap}) - 7.8 \cdot \tan(\alpha_{ap})^2 = 0.6$$

NS-EN 1995-1-1 6.4.3(4) Eq. 6.46

$$k_4 := 6 \cdot \tan(\alpha_{ap})^2 = 0$$

NS-EN 1995-1-1 6.4.3(4) Eq. 6.47

$$k_l := k_1 + k_2 \cdot \left(\frac{h_{ap}}{r}\right) + k_3 \cdot \left(\frac{h_{ap}}{r}\right)^2 + k_4 \cdot \left(\frac{h_{ap}}{r}\right)^3$$

NS-EN 1995-1-1 6.4.3(4) Eq. 6.43

$$M_{ap,d} := |M_{z,Ed_{595}}|$$

Design apex moment,
NS-EN 1995-1-1 6.4.3(4)

$$\sigma_{m,d} := k_l \cdot \frac{6 \cdot M_{ap,d}}{b_{595} \cdot h_{ap}^2} = 0.095 \frac{N}{mm^2}$$

NS-EN 1995-1-1 6.4.3(4) Eq. 6.42

$$k_r := \begin{cases} \frac{r_{in}}{t} \geq 240 \\ 1 \\ \text{else} \\ 0.76 + 0.001 \cdot \frac{r_{in}}{t} \end{cases} = 1$$

NS-EN 1995-1-1 6.4.3(5) Eq. 6.49

$$\sigma_{m,d} \leq k_r \cdot f_{m.z.d}$$

NS-EN 1995-1-1 6.4.3(3) Eq. 6.41

$$U_{6.41}^{595} := \frac{|\sigma_{m,d}|}{k_r \cdot f_{m.z.d}} = 0.006$$

$$V_b := b_1 \cdot h_1 \cdot l_{Arch} = 143.539 \text{ m}^3$$

Volume of one arch, conservative value:
constant height and width = 1,1m

$$V := \frac{2}{3} \cdot V_b = 95.692 \text{ m}^3$$

NS-EN 1995-1-1 6.4.3(5)

$$V_0 := 0.01 \text{ m}^3$$

NS-EN 1995-1-1 6.4.3(5),
Reference volume

$$k_{vol} := \left(\frac{V_0}{V} \right)^{0.2} = 0.16$$

NS-EN 1995-1-1 6.4.3(5) Eq. 6.51

$$k_{dis} := 1.4$$

NS-EN 1995-1-1 6.4.3(5) Eq. 6.52,
cambered beams

$$k_5 := 0.2 \cdot \tan(\alpha_{ap}) = 0$$

NS-EN 1995-1-1 6.4.3(8) Eq. 6.57

$$k_6 := 0.25 - 1.25 \cdot \tan(\alpha_{ap}) + 2.6 \cdot \tan(\alpha_{ap})^2 = 0.25$$

NS-EN 1995-1-1 6.4.3(8) Eq. 6.58

$$k_7 := 2.1 \cdot \tan(\alpha_{ap}) - 4 \cdot \tan(\alpha_{ap})^2 = 0$$

NS-EN 1995-1-1 6.4.3(8) Eq. 6.59

$$k_p := k_5 + k_6 \cdot \left(\frac{h_{ap}}{r} \right) + k_7 \cdot \left(\frac{h_{ap}}{r} \right)^2 = 0.002$$

NS-EN 1995-1-1 6.4.3(8) Eq. 6.56

$$\sigma_{t.90.d} := k_p \cdot \frac{6 \cdot M_{ap,d}}{b \cdot h_{ap}^2}$$

NS-EN 1995-1-1 6.4.3(8) Eq. 6.55

$$\frac{\tau_d}{f_{v.d}} + \frac{\sigma_{t.90.d}}{k_{dis} \cdot k_{vol} \cdot f_{t.90.d}} \leq 1$$

NS-EN 1995-1-1 6.4.3(8) Eq. 6.53

$$U_{6.53}_i := \frac{\sqrt{\left(|\tau_{z,d_i}| \right)^2 + \left(|\tau_{y,d_i}| \right)^2}}{f_{v.d}} + \frac{|\sigma_{t.90,d}|}{k_{dis} \cdot k_{vol} \cdot f_{t.90,d}}$$

$$\max(U_{6.53}) = 0.577$$

SUMMARY

Utilization factors:

$$\max \langle U_{6.19} \rangle = 0.646$$

Combined bending and axial compression

$$\max \langle U_{6.20} \rangle = 0.63$$

Combined bending and axial compression

$$\max \langle U_{6.23} \rangle = 0.856$$

Buckling in-plane

$$\max \langle U_{6.24} \rangle = 0.857$$

Buckling out-of-plan

$$\max \langle U_{V_T} \rangle = 0.492$$

Combined shear and torsion

$$\max \langle U_{6.53} \rangle = 0.577$$

Combined tension perpendicular to grain and shear

$$\max \langle U_{6.41} \rangle = 0.006$$

Cambered beam: Apex bending moment

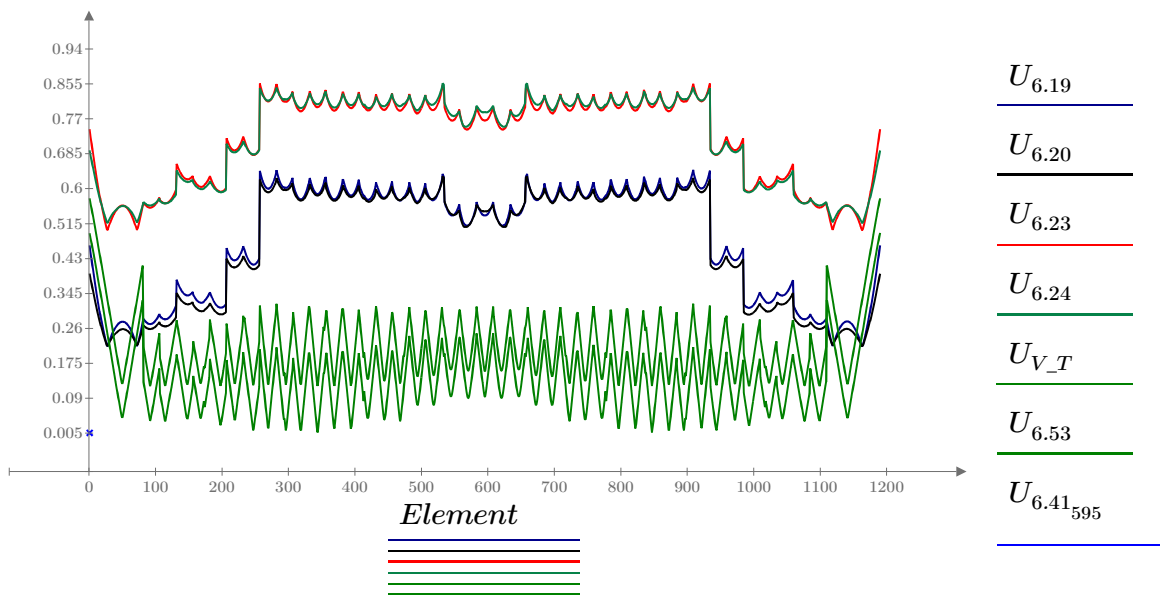
if $\max \langle U_{6.19}, U_{6.20}, U_{6.23}, U_{6.24}, U_{V_T}, U_{6.53}, U_{6.41} \rangle < 1$ = "OK!"

|| "OK!"

else

|| "FAILURE"

Plot of the Arch utilizations:



Appendix H.1 Focus Kostruksjon Design Check

- **ULS_LM1_gr1a_Eq.b_18m**
- **Load placement 3**

Beregning utført: 06.06.2016 22.24.44

Focus Konstruksjon 2016

0. SAMMENDRAG

Modell

Antall segmenter: 17

Antall knutepunkt: 16

Analyse

Antall lastkombinasjoner: 1

Forskyvning / snittkrefter

Største forskyvning: 58,0 mm (Segmentnr. 5)

Største N: 3517,21 kN (Segmentnr. 23)

Største V: -785,26 kN (Segmentnr. 3)

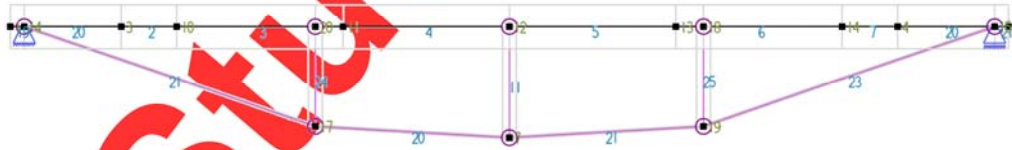
Største M: -2391,46 kN·m (Segmentnr. 5)

Kapazität

Største kapasitetsutnyttelse: 88,19 %

Info: EN 1993-1-1 6.2.3

1. KONSTRUKSJONSMODELL OG LASTER



1.1. KNOTEPUNKTSDATA

Nr.	X [mm]	Z [mm]
1	0	0

2	18000	0
3	2000	0
4	16000	0
7	9000	-2000
10	3000	0
12	9000	0
13	12000	0
14	15000	0
11	6000	0
14	250	0
15	17750	0
17	5500	-1800
18	12500	0
19	12500	-1800
20	5500	0

1.2. TVERRSNITTSDATA

Nr.	Navn	Parametre	
1	Bredflatstål 250x50	A [mm ²] Ix [mm ⁴] Iy [mm ⁴] Iz [mm ⁴] Total vekt [kN]	12500 9,1042e+006 6,5104e+007 2,6042e+006 17,43
2	KFHUP 250x250x6.3	A [mm ²] Ix [mm ⁴] Iy [mm ⁴] Iz [mm ⁴] Total vekt [kN]	6000 9,2900e+007 5,8730e+007 5,8730e+007 2,59
3	Eegendef, 800 mm	A [mm ²] Ix [mm ⁴] Iy [mm ⁴] Iz [mm ⁴] Total vekt [kN]	43400 1,4240e+007 4,8950e+009 3,7450e+008 60,16

1.3. MATERIALDATA

1	S355, Stål	Material: Stål
	Fasthetsklasse: S355	
	Varmeutv.koeff.: 1,20e-005 °C ⁻¹	Tyngdetetthet: 77,01 kN/m ³
	E-modul: 2,1000e+005 N/mm ²	G-modul: 8,1000e+004 N/mm ²
	Total vekt: 80,18 kN	

1.4. SEGMENTDATA

Seg Nr.	Kn.pkt 1	Kn.pkt 2	Tvsn 1	Tvsn 2	Material	Type / Form	Rot. [°]
2	3	10	Eegendef, 800 mm	Eegendef, 800 mm	S355, Stål	Rett bjelke	
4	11	12	Eegendef, 800 mm	Eegendef, 800 mm	S355, Stål	Rett bjelke	

5	12	13	Eegendef, 800 mm	Eegendef, 800 mm	S355, Stål	Rett bjelke	
6	13	14	Eegendef, 800 mm	Eegendef, 800 mm	S355, Stål	Rett bjelke	
7	14	4	Eegendef, 800 mm	Eegendef, 800 mm	S355, Stål	Rett bjelke	
11	7	12	KFHUP 250x250x6.3	KFHUP 250x250x6.3	S355, Stål	Stav	90,0
19	1	14	Eegendef, 800 mm	Eegendef, 800 mm	S355, Stål	Rett bjelke	
20	14	3	Eegendef, 800 mm	Eegendef, 800 mm	S355, Stål	Rett bjelke	
20	4	15	Eegendef, 800 mm	Eegendef, 800 mm	S355, Stål	Rett bjelke	
21	15	2	Eegendef, 800 mm	Eegendef, 800 mm	S355, Stål	Rett bjelke	
21	17	14	Bredflatstål 250x50	Bredflatstål 250x50	S355, Stål	Stav (strekk)	90,0
23	19	15	Bredflatstål 250x50	Bredflatstål 250x50	S355, Stål	Stav (strekk)	90,0
25	19	18	KFHUP 250x250x6.3	KFHUP 250x250x6.3	S355, Stål	Stav	90,0
24	17	20	KFHUP 250x250x6.3	KFHUP 250x250x6.3	S355, Stål	Stav	90,0
3	10	11	Eegendef, 800 mm	Eegendef, 800 mm	S355, Stål	Rett bjelke	
20	17	7	Bredflatstål 250x50	Bredflatstål 250x50	S355, Stål	Stav (strekk)	90,0
21	7	19	Bredflatstål 250x50	Bredflatstål 250x50	S355, Stål	Stav (strekk)	90,0

1.4.1. Segmentdata EN 1993

Seg. nr.	Gamma_M0 (brudd)	Gamma_M1 (brudd)	L_ky [mm]	L_kz [mm]	L_eff [mm]	k	k_w	C1	C2	C2	z_g [mm]	z_j [mm]
2	1,00	1,00	1000	1000	1000	1,00	1,00	1,00	0,00	1,00	0	0
4	1,00	1,00	3000	3000	3000	1,00	1,00	1,00	0,00	1,00	0	0
5	1,00	1,00	3000	3000	3000	1,00	1,00	1,00	0,00	1,00	0	0
6	1,00	1,00	3000	3000	3000	1,00	1,00	1,00	0,00	1,00	0	0
7	1,00	1,00	1000	1000	1000	1,00	1,00	1,00	0,00	1,00	0	0
11	1,00	1,00	2000	2000	2000	1,00	1,00	1,00	0,00	1,00	0	0
19	1,00	1,00	250	250	250	1,00	1,00	1,00	0,00	1,00	0	0
20	1,00	1,00	1750	1750	1750	1,00	1,00	1,00	0,00	1,00	0	0
20	1,00	1,00	1750	1750	1750	1,00	1,00	1,00	0,00	1,00	0	0
21	1,00	1,00	250	250	250	1,00	1,00	1,00	0,00	1,00	0	0
21	1,00	1,00	5550	5550	5550	1,00	1,00	1,00	0,00	1,00	0	0
23	1,00	1,00	5550	5550	5550	1,00	1,00	1,00	0,00	1,00	0	0
25	1,00	1,00	1800	1800	1800	1,00	1,00	1,00	0,00	1,00	0	0
24	1,00	1,00	1800	1800	1800	1,00	1,00	1,00	0,00	1,00	0	0
3	1,00	1,00	3000	3000	3000	1,00	1,00	1,00	0,00	1,00	0	0
20	1,00	1,00	3506	3506	3506	1,00	1,00	1,00	0,00	1,00	0	0
21	1,00	1,00	3506	3506	3506	1,00	1,00	1,00	0,00	1,00	0	0

1.5. RANDBETINGELSER

Seg. Nr.	X [mm]	Z [mm]	Frih.gr. X	Z	RotY	X-vektor	Z-vektor
19	250	0	F	F		[1,00; 0,00]	[0,00; 1,00]
20	17750	0		F		[1,00; 0,00]	[0,00; 1,00]

Forklaring til frihetsgrader: F = fastholdt, (blank) = fri

Tall betyr foreskrevet forskyvning [mm]

1.6. LEDD

Kn.pkt Nr.	Frikoblede frihetsgrader	X-vektor	Z-vektor	Segmenter
7	RotY	[1,00; 0,00]	[0,00; 1,00]	20
7	RotY	[1,00; 0,00]	[0,00; 1,00]	21
12	RotY	[1,00; 0,00]	[0,00; 1,00]	11
14	RotY	[1,00; 0,00]	[0,00; 1,00]	21
15	RotY	[1,00; 0,00]	[0,00; 1,00]	23
17	RotY	[1,00; 0,00]	[0,00; 1,00]	21
17	RotY	[1,00; 0,00]	[0,00; 1,00]	20
18	RotY	[1,00; 0,00]	[0,00; 1,00]	25
19	RotY	[1,00; 0,00]	[0,00; 1,00]	23
19	RotY	[1,00; 0,00]	[0,00; 1,00]	21
20	RotY	[1,00; 0,00]	[0,00; 1,00]	24

1.7. LASTTILFELLER

5 Egenlast, kjørebane

Lasttype:	Annen variabel		
Lastvarighet:	Permanent		
1 Fordelt last	P1 = 20,90 kN/m X1 = 2500 mm P2 = 20,90 kN/m X2 = 3000 mm Retning = [0; -1] Virker på segment: 2	Z1 = 0 mm Z2 = 0 mm	
2 Fordelt last	P1 = 20,90 kN/m X1 = 3000 mm P2 = 20,90 kN/m X2 = 6000 mm Retning = [0; -1] Virker på segment: 3	Z1 = 0 mm Z2 = 0 mm	
3 Fordelt last	P1 = 20,90 kN/m X1 = 6000 mm P2 = 20,90 kN/m X2 = 9000 mm Retning = [0; -1] Virker på segment: 4	Z1 = 0 mm Z2 = 0 mm	
4 Fordelt last	P1 = 20,90 kN/m X1 = 9000 mm P2 = 20,90 kN/m X2 = 10800 mm Retning = [0; -1] Virker på segment: 5	Z1 = 0 mm Z2 = 0 mm	

6 Egenlast, gangfelt

Lasttype:	Annen variabel
Lastvarighet:	Permanent

1 Fordelt last	P1 = 26,13 kN/m X1 = 12000 mm P2 = 26,13 kN/m X2 = 15000 mm Retning = [0; -1] Virker på segment: 6	Z1 = 0 mm Z2 = 0 mm
2 Fordelt last	P1 = 26,13 kN/m X1 = 15000 mm P2 = 26,13 kN/m X2 = 15500 mm Retning = [0; -1] Virker på segment: 7	Z1 = 0 mm Z2 = 0 mm
3 Fordelt last	P1 = 26,13 kN/m X1 = 10800 mm P2 = 26,13 kN/m X2 = 12000 mm Retning = [0; -1] Virker på segment: 5	Z1 = 0 mm Z2 = 0 mm

7 Egenlast, (Rør + Topeka)

Lasttype:	Annen variabel	
Lastvarighet:	Permanent	
1 Fordelt last	P1 = 3,83 kN/m X1 = 3000 mm P2 = 3,83 kN/m X2 = 6000 mm Retning = [0; -1] Virker på segment: 3	Z1 = 0 mm Z2 = 0 mm
2 Fordelt last	P1 = 3,83 kN/m X1 = 6000 mm P2 = 3,83 kN/m X2 = 9000 mm Retning = [0; -1] Virker på segment: 4	Z1 = 0 mm Z2 = 0 mm
3 Fordelt last	P1 = 3,83 kN/m X1 = 9000 mm P2 = 3,83 kN/m X2 = 12000 mm Retning = [0; -1] Virker på segment: 5	Z1 = 0 mm Z2 = 0 mm
4 Fordelt last	P1 = 3,83 kN/m X1 = 12000 mm P2 = 3,83 kN/m X2 = 15000 mm Retning = [0; -1] Virker på segment: 6	Z1 = 0 mm Z2 = 0 mm

8 Nyttelast, q1k

Lasttype:	Annen variabel	
Lastvarighet:	Korttidslast	
1 Fordelt last	P1 = 40,46 kN/m X1 = 7500 mm P2 = 40,46 kN/m X2 = 9000 mm Retning = [0; -1] Virker på segment: 4	Z1 = 0 mm Z2 = 0 mm

2 Fordelt last
 P1 = 40,46 kN/m
 X1 = 9000 mm Z1 = 0 mm
 P2 = 40,46 kN/m
 X2 = 10500 mm Z2 = 0 mm
 Retning = [0; -1]
 Virker på segment: 5

9 Nyttelast, q2k

Lasttype: Annen variabel
 Lastvarighet: Korttidslast
 1 Fordelt last
 P1 = 18,73 kN/m
 X1 = 4500 mm Z1 = 0 mm
 P2 = 18,73 kN/m
 X2 = 6000 mm Z2 = 0 mm
 Retning = [0; -1]
 Virker på segment: 3

2 Fordelt last
 P1 = 18,73 kN/m
 X1 = 6000 mm Z1 = 0 mm
 P2 = 18,73 kN/m
 X2 = 7500 mm Z2 = 0 mm
 Retning = [0; -1]
 Virker på segment: 4

10 Nyttelast, q3k

Lasttype: Annen variabel
 Lastvarighet: Korttidslast
 1 Fordelt last
 P1 = 18,73 kN/m
 X1 = 10500 mm Z1 = 0 mm
 P2 = 18,73 kN/m
 X2 = 12000 mm Z2 = 0 mm
 Retning = [0; -1]
 Virker på segment: 5

2 Fordelt last
 P1 = 18,73 kN/m
 X1 = 12000 mm Z1 = 0 mm
 P2 = 18,73 kN/m
 X2 = 13500 mm Z2 = 0 mm
 Retning = [0; -1]
 Virker på segment: 6

11 Nyttelast, rk

Lasttype: Annen variabel
 Lastvarighet: Korttidslast
 1 Fordelt last
 P1 = 18,73 kN/m
 X1 = 3000 mm Z1 = 0 mm
 P2 = 18,73 kN/m
 X2 = 4500 mm Z2 = 0 mm
 Retning = [0; -1]
 Virker på segment: 3

2 Fordelt last
 P1 = 18,73 kN/m
 X1 = 13500 mm Z1 = 0 mm
 P2 = 18,73 kN/m
 X2 = 15000 mm Z2 = 0 mm
 Retning = [0; -1]
 Virker på segment: 6

12 Vindlast, Med trafikk

Lasttype: Annen variabel
 Lastvarighet: Korttidslast

1 Fordelt last	P1 = 3,73 kN/m X1 = 2500 mm P2 = 3,73 kN/m X2 = 3000 mm Retning = [0; -1] Virker på segment: 2	Z1 = 0 mm Z2 = 0 mm
2 Fordelt last	P1 = 3,73 kN/m X1 = 3000 mm P2 = 3,73 kN/m X2 = 6000 mm Retning = [0; -1] Virker på segment: 3	Z1 = 0 mm Z2 = 0 mm
3 Fordelt last	P1 = 3,73 kN/m X1 = 6000 mm P2 = 3,73 kN/m X2 = 9000 mm Retning = [0; -1] Virker på segment: 4	Z1 = 0 mm Z2 = 0 mm
4 Fordelt last	P1 = 3,73 kN/m X1 = 9000 mm P2 = 3,73 kN/m X2 = 12000 mm Retning = [0; -1] Virker på segment: 5	Z1 = 0 mm Z2 = 0 mm
5 Fordelt last	P1 = 3,73 kN/m X1 = 15000 mm P2 = 3,73 kN/m X2 = 15500 mm Retning = [0; -1] Virker på segment: 7	Z1 = 0 mm Z2 = 0 mm
6 Fordelt last	P1 = 3,73 kN/m X1 = 12000 mm P2 = 3,73 kN/m X2 = 15000 mm Retning = [0; -1] Virker på segment: 6	Z1 = 0 mm Z2 = 0 mm

13 Nyttelast, Q1K

Lasttype:	Annen variabel	
Lastvarighet:	Korttidslast	
1 Fordelt last	P1 = 980,80 kN/m X1 = 7800 mm P2 = 980,80 kN/m X2 = 8200 mm Retning = [0; -1] Virker på segment: 4	Z1 = 0 mm Z2 = 0 mm
2 Fordelt last	P1 = 980,80 kN/m X1 = 9800 mm P2 = 980,80 kN/m X2 = 10200 mm Retning = [0; -1] Virker på segment: 5	Z1 = 0 mm Z2 = 0 mm

14 Nyttelast, Q2k

Lasttype:	Annen variabel
Lastvarighet:	Korttidslast

1 Fordelt last	P1 = 337,52 kN/m X1 = 4800 mm P2 = 337,52 kN/m X2 = 5200 mm Retning = [0; -1] Virker på segment: 3	Z1 = 0 mm Z2 = 0 mm
2 Fordelt last	P1 = 337,52 kN/m X1 = 6800 mm P2 = 337,52 kN/m X2 = 7200 mm Retning = [0; -1] Virker på segment: 4	Z1 = 0 mm Z2 = 0 mm

15 Nyttelast, Qk3

Lasttype:	Annen variabel	
Lastvarighet:	Korttidslast	
1 Fordelt last	P1 = 675,04 kN/m X1 = 10800 mm P2 = 675,04 kN/m X2 = 11200 mm Retning = [0; -1] Virker på segment: 5	Z1 = 0 mm Z2 = 0 mm
2 Fordelt last	P1 = 675,04 kN/m X1 = 12800 mm P2 = 675,04 kN/m X2 = 13200 mm Retning = [0; -1] Virker på segment: 6	Z1 = 0 mm Z2 = 0 mm

16 Rekkverk

Lasttype:	Annen variabel	
Lastvarighet:	Permanent	
1 Fordelt last	P1 = 6,66 kN/m X1 = 2500 mm P2 = 6,66 kN/m X2 = 3000 mm Retning = [0; -1] Virker på segment: 2	Z1 = 0 mm Z2 = 0 mm
2 Fordelt last	P1 = 6,66 kN/m X1 = 15000 mm P2 = 6,66 kN/m X2 = 15500 mm Retning = [0; -1] Virker på segment: 7	Z1 = 0 mm Z2 = 0 mm

17 Egenlast, Astfalt

Lasttype:	Annen variabel	
Lastvarighet:	Permanent	
1 Fordelt last	P1 = 19,99 kN/m X1 = 2500 mm P2 = 22,24 kN/m X2 = 3000 mm Retning = [0; -1] Virker på segment: 2	Z1 = 0 mm Z2 = 0 mm
2 Fordelt last	P1 = 22,24 kN/m X1 = 3000 mm P2 = 35,79 kN/m X2 = 6000 mm Retning = [0; -1] Virker på segment: 3	Z1 = 0 mm Z2 = 0 mm

3 Fordelt last	P1 = 35,79 kN/m X1 = 6000 mm P2 = 49,33 kN/m X2 = 9000 mm Retning = [0; -1] Virker på segment: 4	Z1 = 0 mm Z2 = 0 mm
4 Fordelt last	P1 = 49,33 kN/m X1 = 9000 mm P2 = 57,46 kN/m X2 = 10800 mm Retning = [0; -1] Virker på segment: 5	Z1 = 0 mm Z2 = 0 mm
5 Fordelt last	P1 = 32,31 kN/m X1 = 10800 mm P2 = 28,31 kN/m X2 = 12000 mm Retning = [0; -1] Virker på segment: 5	Z1 = 0 mm Z2 = 0 mm
6 Fordelt last	P1 = 28,31 kN/m X1 = 12000 mm P2 = 18,32 kN/m X2 = 15000 mm Retning = [0; -1] Virker på segment: 6	Z1 = 0 mm Z2 = 0 mm
7 Fordelt last	P1 = 18,32 kN/m X1 = 15000 mm P2 = 16,65 kN/m X2 = 15500 mm Retning = [0; -1] Virker på segment: 7	Z1 = 0 mm Z2 = 0 mm

1.8. LASTKOMBINASJON

Beregning utført for lastkombinasjon

(2) ULS,gr1a Eq.1b

Grensetilstand:	Bruks
Lasttilfeller:	1,00 * <Konstruksjonens tyngde> 1,00 * Egenlast, kjørebane 1,00 * Egenlast, gangfelt 1,00 * Egenlast, (Rør + Topeka) 1,00 * Nyttelast, q1k 1,00 * Nyttelast, q2k 1,00 * Nyttelast, q3k 1,00 * Nyttelast, rk 1,00 * Vindlast, Med trafikk 1,00 * Nyttelast, Q1K 1,00 * Nyttelast, Q2k 1,00 * Nyttelast, Qk3 1,00 * Egenlast, Astfalt

1.9. ANALYSEINFORMASJON

Inkluder skjærdeformasjoner: Ja

2. BEREGNINGER

2.1. KNOTEPUNKTSRESULTATER

2.1.1. Residualkrefter

Nr.	Rx [kN]	Rz [kN]	My [kN·m]
1	0,00	0,00	0,00
2	0,00	0,00	0,00
3	0,00	0,00	0,00
4	0,00	0,00	0,00
7	0,00	376,86	0,00
7	3327,09	-188,43	0,00
7	-3327,09	-188,43	0,00
10	0,00	0,00	0,00
12	0,00	375,94	0,00
12	0,00	-375,94	0,00
13	0,00	0,00	0,00
14	0,00	0,00	0,00
11	0,00	0,00	0,00
14	3327,09	206,06	0,00
14	-3327,09	1143,39	0,00
15	-3327,09	299,45	0,00
15	3327,09	1143,39	0,00
17	0,00	946,24	0,00
17	3327,09	-1138,04	0,00
17	-3327,09	191,81	0,00
18	0,00	945,41	0,00
18	0,00	-945,41	0,00
19	0,00	946,24	0,00
19	-3327,09	-1138,04	0,00
19	3327,09	191,81	0,00
20	0,00	945,41	0,00
20	0,00	-945,41	0,00

2.2. OPPLGGSKREFTER

Seg Nr.	X [mm]	Z [mm]	Rx [kN]	Rz [kN]	My [kN·m]
19	250	0	0,00	1349,45	0,00
20	17750	0	0,00	1442,83	0,00
	Sum		0,00	2792,28	

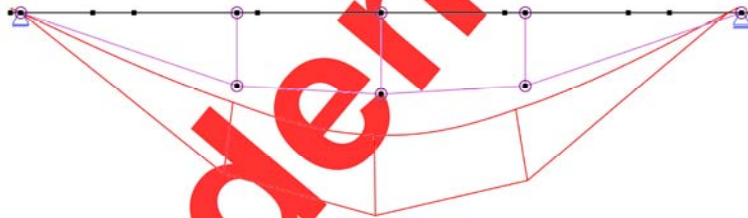
2.3. SEGMENTRESULTATER

Seg Nr.	Snitt mm	My [kN·m]	N [kN]	Vz [kN]	u [mm]	w [mm]
2	1000	-545,73	-3327,09	-174,04	-1,0	-24,1
4	2200	-2230,05	-3327,09	1,53	-2,9	-56,6
5	1050	-2389,81	-3327,09	177,04	-3,6	-57,3

6	0	-1455,09	-3327,09	705,74	-4,3	-49,1
7	0	-802,59	-3327,09	267,03	-5,4	-26,7
11	0	0,00	-376,40	0,00	-2,7	-57,2
19	250	0,13	0,00	0,84	0,0	0,0
20	1750	-353,89	-3327,09	-199,52	-0,6	-15,6
20	0	-517,37	-3327,09	292,91	-5,7	-17,4
21	0	0,08	0,00	-0,70	-6,4	0,0
21	0	0,00	3517,21	0,00	-6,3	-41,2
23	0	0,00	3517,21	0,00	1,0	-44,5
25	0	0,00	-945,82	0,00	1,0	-44,5
24	0	0,00	-945,82	0,00	-6,3	-41,2
3	3000	-1054,16	-3327,09	-746,35	-2,1	-46,0
20	0	0,00	3332,52	0,00	-6,3	-41,2
21	0	0,00	3332,52	0,00	-2,7	-57,2

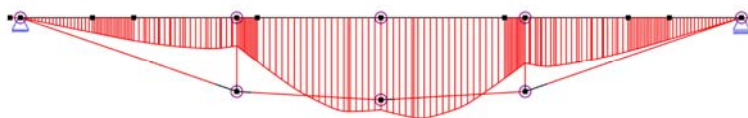
2.4. RESULTATER GRAFISK

2.4.1. Forskyvning



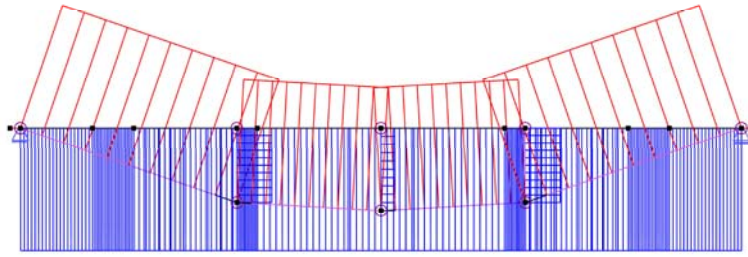
Største forskyvning: 58,0 mm

2.4.2. Moment



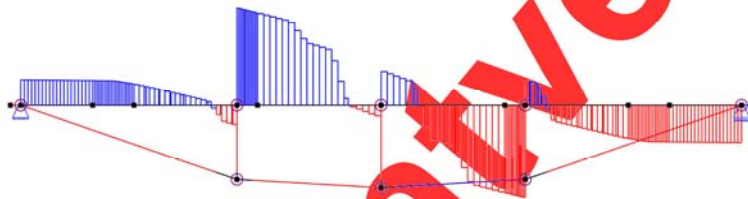
Største moment: 2391,46 kN·m

2.4.3. Aksialkraft

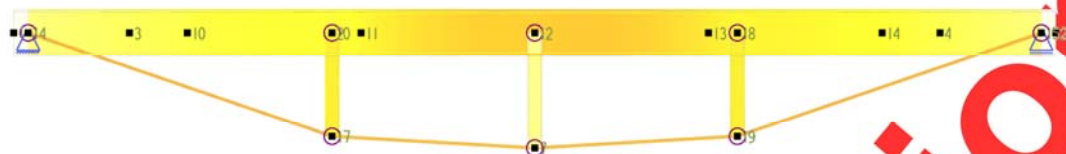


Største aksialkraft: 3517,21 kN

2.4.4. Skjærkraft



Største skjærkraft: 785,26 kN



Studentversjon

Største kapasitetsutnyttelse: 88,19 % (EN 1993-1-1 6.2.3)

Focus Konstruksjon 2016 Versjon 16.4.0.0	Konstruksjon 1	FIL G:\Levering\Appendix\Appendix_H_Transverse_Beam_Design\Ap pendix_H.1_Transverse_Beam_Design_Focus_Konstruksjon\ULS ULS_18m\ULS_gr1a_Eq_6.10b_18m_Load_Placement_3.fkon
--	----------------	---

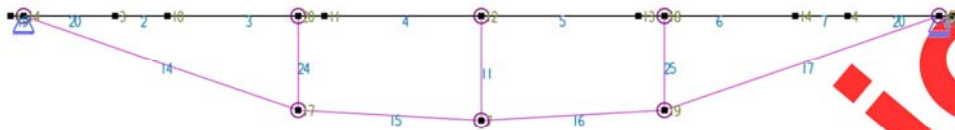
Appendix H.2: Focus Kostruksjon Design Check

- **SLS_LM1_gr1a_18m**
- **Load placement 3**

Beregning utført: 07.06.2016 07.45.41

Focus Konstruksjon 2016

1. KONSTRUKSJONSMODELLOG LASTER



1.1. KNOTEPUNKTSDATA

Nr.	X [mm]	Z [mm]
1	0	0
2	18000	0
3	2000	0
4	16000	0
7	9000	-2000
10	3000	0
12	9000	0
13	12000	0
14	15000	0
11	6000	0
14	250	0
15	17750	0
17	5500	-1800
18	12500	0
19	12500	-1800
20	5500	0

1.2. TVERRSNITTSDATA

Nr.	Navn	Parametre
-----	------	-----------

1	Bredflatstål 250x50	A [mm ²] Ix [mm ⁴] Iy [mm ⁴] Iz [mm ⁴] Total vekt [kN]	12500 9,1042e+006 6,5104e+007 2,6042e+006 17,43
2	KFHUP 250x250x6.3	A [mm ²] Ix [mm ⁴] Iy [mm ⁴] Iz [mm ⁴] Total vekt [kN]	6000 9,2900e+007 5,8730e+007 5,8730e+007 2,59
3	Eegendef, 800 mm	A [mm ²] Ix [mm ⁴] Iy [mm ⁴] Iz [mm ⁴] Total vekt [kN]	43400 1,4240e+007 4,8950e+009 3,7450e+008 60,16

1.3. MATERIALDATA

1 S355, Stål

Material: Stål

Fasthetsklasse: S355

Varmeutv.koeff.: 1,20e-005 °C⁻¹Tyngdetetthet: 77,01 kN/m³E-modul: 2,1000e+005 N/mm²G-modul: 8,1000e+004 N/mm²

Total vekt: 80,18 kN

1.4. SEGMENTDATA

Seg Nr.	Kn.pkt 1	Kn.pkt 2	Tvsn 1	Tvsn 2	Material	Type / Form	Rot. [°]
2	3	10	Eegendef, 800 mm	Eegendef, 800 mm	S355, Stål	Rett bjelke	
4	11	12	Eegendef, 800 mm	Eegendef, 800 mm	S355, Stål	Rett bjelke	
5	12	13	Eegendef, 800 mm	Eegendef, 800 mm	S355, Stål	Rett bjelke	
6	13	14	Eegendef, 800 mm	Eegendef, 800 mm	S355, Stål	Rett bjelke	
7	14	4	Eegendef, 800 mm	Eegendef, 800 mm	S355, Stål	Rett bjelke	
11	7	12	KFHUP 250x250x6.3	KFHUP 250x250x6.3	S355, Stål	Stav	90,0
19	1	14	Eegendef, 800 mm	Eegendef, 800 mm	S355, Stål	Rett bjelke	
20	14	3	Eegendef, 800 mm	Eegendef, 800 mm	S355, Stål	Rett bjelke	
20	4	15	Eegendef, 800 mm	Eegendef, 800 mm	S355, Stål	Rett bjelke	
21	15	2	Eegendef, 800 mm	Eegendef, 800 mm	S355, Stål	Rett bjelke	
25	19	18	KFHUP 250x250x6.3	KFHUP 250x250x6.3	S355, Stål	Stav	90,0
24	17	20	KFHUP 250x250x6.3	KFHUP 250x250x6.3	S355, Stål	Stav	90,0
3	10	11	Eegendef, 800 mm	Eegendef, 800 mm	S355, Stål	Rett bjelke	
15	17	7	Bredflatstål 250x50	Bredflatstål 250x50	S355, Stål	Stav (strekk)	90,0
16	7	19	Bredflatstål 250x50	Bredflatstål 250x50	S355, Stål	Stav (strekk)	90,0
17	19	15	Bredflatstål 250x50	Bredflatstål 250x50	S355, Stål	Stav (strekk)	90,0
14	14	17	Bredflatstål 250x50	Bredflatstål 250x50	S355, Stål	Stav (strekk)	90,0

1.4.1. Segmentdata EN 1993

Seg. nr.	Gamma_M0 (brudd)	Gamma_M1 (brudd)	L_ky [mm]	L_kz [mm]	L_eff [mm]	k	k_w	C1	C2	C2	z_g [mm]	z_j [mm]
2	1,00	1,00	1000	1000	1000	1,00	1,00	1,00	0,00	1,00	0	0
4	1,00	1,00	3000	3000	3000	1,00	1,00	1,00	0,00	1,00	0	0
5	1,00	1,00	3000	3000	3000	1,00	1,00	1,00	0,00	1,00	0	0
6	1,00	1,00	3000	3000	3000	1,00	1,00	1,00	0,00	1,00	0	0
7	1,00	1,00	1000	1000	1000	1,00	1,00	1,00	0,00	1,00	0	0
11	1,00	1,00	2000	2000	2000	1,00	1,00	1,00	0,00	1,00	0	0
19	1,00	1,00	250	250	250	1,00	1,00	1,00	0,00	1,00	0	0
20	1,00	1,00	1750	1750	1750	1,00	1,00	1,00	0,00	1,00	0	0
20	1,00	1,00	1750	1750	1750	1,00	1,00	1,00	0,00	1,00	0	0
21	1,00	1,00	250	250	250	1,00	1,00	1,00	0,00	1,00	0	0
25	1,00	1,00	1800	1800	1800	1,00	1,00	1,00	0,00	1,00	0	0
24	1,00	1,00	1800	1800	1800	1,00	1,00	1,00	0,00	1,00	0	0
3	1,00	1,00	3000	3000	3000	1,00	1,00	1,00	0,00	1,00	0	0
15	1,00	1,00	3506	3506	3506	1,00	1,00	1,00	0,00	1,00	0	0
16	1,00	1,00	3506	3506	3506	1,00	1,00	1,00	0,00	1,00	0	0
17	1,00	1,00	5550	5550	5550	1,00	1,00	1,00	0,00	1,00	0	0
14	1,00	1,00	5550	5550	5550	1,00	1,00	1,00	0,00	1,00	0	0

1.5. RANDBETINGELSER

Seg Nr.	X [mm]	Z [mm]	Frih.gr.		RotY	X-vektor	Z-vektor
			X	Z			
19	250	0	F	F		[1,00; 0,00]	[0,00; 1,00]
20	17750	0		F		[1,00; 0,00]	[0,00; 1,00]

Forklaring til frihetsgrader: F = fastholdt, (blank) = fri

Tall betyr foreskrevet forskyvning [mm]

1.6. LEDD

Kn.pkt Nr.	Frikoblede frihetsgrader	X-vektor	Z-vektor	Segmenter
7	RotY	[1,00; 0,00]	[0,00; 1,00]	15
7	RotY	[1,00; 0,00]	[0,00; 1,00]	16
12	RotY	[1,00; 0,00]	[0,00; 1,00]	11
14	RotY	[1,00; 0,00]	[0,00; 1,00]	14
15	RotY	[1,00; 0,00]	[0,00; 1,00]	17
17	RotY	[1,00; 0,00]	[0,00; 1,00]	14
17	RotY	[1,00; 0,00]	[0,00; 1,00]	15
18	RotY	[1,00; 0,00]	[0,00; 1,00]	25
19	RotY	[1,00; 0,00]	[0,00; 1,00]	16
19	RotY	[1,00; 0,00]	[0,00; 1,00]	17
20	RotY	[1,00; 0,00]	[0,00; 1,00]	24

1.7. LASTTILFELLER

1 Nyttelast

Lasttype:	Annen variabel		
Lastvarighet:	Korttidslast		
1 Fordelt last	P1 = 9,71 kN/m X1 = 6000 mm P2 = 9,71 kN/m X2 = 7500 mm Retning = [0; -1] Virker på segment: 4	Z1 = 0 mm Z2 = 0 mm	
2 Fordelt last	P1 = 9,71 kN/m X1 = 13500 mm P2 = 9,71 kN/m X2 = 15000 mm Retning = [0; -1] Virker på segment: 6	Z1 = 0 mm Z2 = 0 mm	

5 Egenlast, kjørebane

Lasttype:	Annen variabel		
Lastvarighet:	Permanent		
1 Fordelt last	P1 = 17,42 kN/m X1 = 2500 mm P2 = 17,42 kN/m X2 = 3000 mm Retning = [0; -1] Virker på segment: 2	Z1 = 0 mm Z2 = 0 mm	
2 Fordelt last	P1 = 17,42 kN/m X1 = 3000 mm P2 = 17,42 kN/m X2 = 6000 mm Retning = [0; -1] Virker på segment: 3	Z1 = 0 mm Z2 = 0 mm	
3 Fordelt last	P1 = 17,42 kN/m X1 = 6000 mm P2 = 17,42 kN/m X2 = 9000 mm Retning = [0; -1] Virker på segment: 4	Z1 = 0 mm Z2 = 0 mm	
4 Fordelt last	P1 = 17,42 kN/m X1 = 9000 mm P2 = 17,42 kN/m X2 = 10800 mm Retning = [0; -1] Virker på segment: 5	Z1 = 0 mm Z2 = 0 mm	

6 Egenlast, gangfelt

Lasttype:	Annen variabel		
Lastvarighet:	Permanent		
1 Fordelt last	P1 = 21,77 kN/m X1 = 12000 mm P2 = 21,77 kN/m X2 = 15000 mm Retning = [0; -1] Virker på segment: 6	Z1 = 0 mm Z2 = 0 mm	
2 Fordelt last	P1 = 21,77 kN/m X1 = 15000 mm P2 = 21,77 kN/m X2 = 15500 mm Retning = [0; -1] Virker på segment: 7	Z1 = 0 mm Z2 = 0 mm	

3 Fordelt last	P1 = 21,77 kN/m X1 = 10800 mm P2 = 21,77 kN/m X2 = 12000 mm Retning = [0; -1] Virker på segment: 5	Z1 = 0 mm Z2 = 0 mm
----------------	---	------------------------

7 Egenlast, (Rør + Topeka)

Lasttype:	Annen variabel	
Lastvarighet:	Permanent	
1 Fordelt last	P1 = 3,19 kN/m X1 = 3000 mm P2 = 3,19 kN/m X2 = 6000 mm Retning = [0; -1] Virker på segment: 3	Z1 = 0 mm Z2 = 0 mm
2 Fordelt last	P1 = 3,19 kN/m X1 = 6000 mm P2 = 3,19 kN/m X2 = 9000 mm Retning = [0; -1] Virker på segment: 4	Z1 = 0 mm Z2 = 0 mm
3 Fordelt last	P1 = 3,19 kN/m X1 = 9000 mm P2 = 3,19 kN/m X2 = 12000 mm Retning = [0; -1] Virker på segment: 5	Z1 = 0 mm Z2 = 0 mm
4 Fordelt last	P1 = 3,19 kN/m X1 = 12000 mm P2 = 3,19 kN/m X2 = 15000 mm Retning = [0; -1] Virker på segment: 6	Z1 = 0 mm Z2 = 0 mm

8 Nyttelast, q1k

Lasttype:	Annen variabel	
Lastvarighet:	Korttidslast	
1 Fordelt last	P1 = 20,98 kN/m X1 = 7500 mm P2 = 20,98 kN/m X2 = 9000 mm Retning = [0; -1] Virker på segment: 4	Z1 = 0 mm Z2 = 0 mm
2 Fordelt last	P1 = 20,98 kN/m X1 = 9000 mm P2 = 20,98 kN/m X2 = 10500 mm Retning = [0; -1] Virker på segment: 5	Z1 = 0 mm Z2 = 0 mm

9 Nyttelast, q2k

Lasttype:	Annen variabel	
Lastvarighet:	Korttidslast	
1 Fordelt last	P1 = 9,71 kN/m X1 = 4500 mm P2 = 9,71 kN/m X2 = 6000 mm Retning = [0; -1] Virker på segment: 3	Z1 = 0 mm Z2 = 0 mm

10 Nyttelast, q3k

Lasttype:	Annen variabel		
Lastvarighet:	Korttidslast		
1 Fordelt last	P1 = 9,71 kN/m X1 = 10500 mm P2 = 9,71 kN/m X2 = 12000 mm Retning = [0; -1] Virker på segment: 5	Z1 = 0 mm Z2 = 0 mm	
2 Fordelt last	P1 = 9,71 kN/m X1 = 12000 mm P2 = 9,71 kN/m X2 = 13500 mm Retning = [0; -1] Virker på segment: 6	Z1 = 0 mm Z2 = 0 mm	

11 Nyttelast, rk

Lasttype:	Annen variabel		
Lastvarighet:	Korttidslast		
1 Fordelt last	P1 = 9,71 kN/m X1 = 3000 mm P2 = 9,71 kN/m X2 = 4500 mm Retning = [0; -1] Virker på segment: 3	Z1 = 0 mm Z2 = 0 mm	

12 Vindlast, Med trafikk

Lasttype:	Annen variabel		
Lastvarighet:	Korttidslast		
1 Fordelt last	P1 = 2,05 kN/m X1 = 6000 mm P2 = 2,05 kN/m X2 = 9000 mm Retning = [0; -1] Virker på segment: 4	Z1 = 0 mm Z2 = 0 mm	
2 Fordelt last	P1 = 2,05 kN/m X1 = 9000 mm P2 = 2,05 kN/m X2 = 12000 mm Retning = [0; -1] Virker på segment: 5	Z1 = 0 mm Z2 = 0 mm	
3 Fordelt last	P1 = 2,05 kN/m X1 = 12000 mm P2 = 2,05 kN/m X2 = 15000 mm Retning = [0; -1] Virker på segment: 6	Z1 = 0 mm Z2 = 0 mm	
4 Fordelt last	P1 = 2,05 kN/m X1 = 3000 mm P2 = 2,05 kN/m X2 = 6000 mm Retning = [0; -1] Virker på segment: 3	Z1 = 0 mm Z2 = 0 mm	
5 Fordelt last	P1 = 2,05 kN/m X1 = 2500 mm P2 = 2,05 kN/m X2 = 3000 mm Retning = [0; -1] Virker på segment: 2	Z1 = 0 mm Z2 = 0 mm	

6 Fordelt last
 P1 = 2,05 kN/m
 X1 = 15000 mm Z1 = 0 mm
 P2 = 2,05 kN/m
 X2 = 15500 mm Z2 = 0 mm
 Retning = [0; -1]
 Virker på segment: 7

13 Nyttelast, Q1K

Lasttype: Annen variabel
 Lastvarighet: Korttidslast
 1 Fordelt last
 P1 = 524,80 kN/m
 X1 = 7800 mm Z1 = 0 mm
 P2 = 524,80 kN/m
 X2 = 8200 mm Z2 = 0 mm
 Retning = [0; -1]
 Virker på segment: 4

2 Fordelt last
 P1 = 524,80 kN/m
 X1 = 9800 mm Z1 = 0 mm
 P2 = 524,80 kN/m
 X2 = 10200 mm Z2 = 0 mm
 Retning = [0; -1]
 Virker på segment: 5

14 Nyttelast, Q2k

Lasttype: Annen variabel
 Lastvarighet: Korttidslast
 1 Fordelt last
 P1 = 175,20 kN/m
 X1 = 4800 mm Z1 = 0 mm
 P2 = 175,20 kN/m
 X2 = 5200 mm Z2 = 0 mm
 Retning = [0; -1]
 Virker på segment: 3

2 Fordelt last
 P1 = 175,20 kN/m
 X1 = 6800 mm Z1 = 0 mm
 P2 = 175,20 kN/m
 X2 = 7200 mm Z2 = 0 mm
 Retning = [0; -1]
 Virker på segment: 4

15 Nyttelast, Qk3

Lasttype: Annen variabel
 Lastvarighet: Korttidslast
 1 Fordelt last
 P1 = 386,40 kN/m
 X1 = 10800 mm Z1 = 0 mm
 P2 = 386,40 kN/m
 X2 = 11200 mm Z2 = 0 mm
 Retning = [0; -1]
 Virker på segment: 5

2 Fordelt last
 P1 = 386,40 kN/m
 X1 = 12800 mm Z1 = 0 mm
 P2 = 386,40 kN/m
 X2 = 13200 mm Z2 = 0 mm
 Retning = [0; -1]
 Virker på segment: 6

16 Rekkverk

Lasttype: Annen variabel
 Lastvarighet: Permanent

1 Fordelt last	P1 = 5,55 kN/m X1 = 2500 mm P2 = 5,55 kN/m X2 = 3000 mm Retning = [0; -1] Virker på segment: 2	Z1 = 0 mm Z2 = 0 mm
2 Fordelt last	P1 = 5,55 kN/m X1 = 15000 mm P2 = 5,55 kN/m X2 = 15500 mm Retning = [0; -1] Virker på segment: 7	Z1 = 0 mm Z2 = 0 mm

17 Egenlast, Astfalt

Lasttype:	Annen variabel	
Lastvarighet:	Permanent	
1 Fordelt last	P1 = 18,67 kN/m X1 = 3000 mm P2 = 30,76 kN/m X2 = 6000 mm Retning = [0; -1] Virker på segment: 3	Z1 = 0 mm Z2 = 0 mm
2 Fordelt last	P1 = 30,76 kN/m X1 = 6000 mm P2 = 42,85 kN/m X2 = 9000 mm Retning = [0; -1] Virker på segment: 4	Z1 = 0 mm Z2 = 0 mm
3 Fordelt last	P1 = 42,85 kN/m X1 = 9000 mm P2 = 47,88 kN/m X2 = 10800 mm Retning = [0; -1] Virker på segment: 5	Z1 = 0 mm Z2 = 0 mm
4 Fordelt last	P1 = 26,93 kN/m X1 = 10800 mm P2 = 22,58 kN/m X2 = 12000 mm Retning = [0; -1] Virker på segment: 5	Z1 = 0 mm Z2 = 0 mm
5 Fordelt last	P1 = 22,58 kN/m X1 = 12000 mm P2 = 15,12 kN/m X2 = 15000 mm Retning = [0; -1] Virker på segment: 6	Z1 = 0 mm Z2 = 0 mm
6 Fordelt last	P1 = 16,65 kN/m X1 = 2500 mm P2 = 18,67 kN/m X2 = 3000 mm Retning = [0; -1] Virker på segment: 2	Z1 = 0 mm Z2 = 0 mm
7 Fordelt last	P1 = 15,12 kN/m X1 = 15000 mm P2 = 13,88 kN/m X2 = 15500 mm Retning = [0; -1] Virker på segment: 7	Z1 = 0 mm Z2 = 0 mm

1.8. LASTKOMBINASJON

Beregning utført for lastkombinasjon

(2) SLS, Ofte

Grensetilstand:

Bruks

Lasttilfeller:

- 1,00 * <Konstruksjonens tyngde>
- 1,00 * Egenlast, kjørebane
- 1,00 * Egenlast, gangfelt
- 1,00 * Egenlast, (Rør + Topeka)
- 1,00 * Nyttelast, q1k
- 1,00 * Nyttelast, q2k
- 1,00 * Nyttelast, q3k
- 1,00 * Nyttelast, rk
- 1,00 * Vindlast, Med trafikk
- 1,00 * Nyttelast, Q1K
- 1,00 * Nyttelast, Q2k
- 1,00 * Nyttelast, Qk3
- 1,00 * Egenlast, Astfalt

1.9. ANALYSEINFORMASJON

Inkluder skjærdeformasjoner: Ja

2. BEREGNINGER

2.1. KNUTEPUNKTSRESULTATER

2.1.1. Forskyvninger

Nr.	u [mm]	w [mm]	rotY [°]
1	0,0	1,4	0,3
2	-4,0	1,5	-0,4
3	-0,4	-9,8	0,3
4	-3,6	-10,8	-0,3
7	-1,7	-35,3	0,0
7	-1,7	-35,3	0,0
7	-1,7	-35,3	0,0
10	-0,6	-15,1	0,3
12	-2,0	-35,7	0,0
12	-2,0	-35,7	0,0
13	-2,7	-30,4	-0,2
14	-3,3	-16,6	-0,3
11	-1,3	-28,6	0,2
14	0,0	0,0	0,3
14	0,0	0,0	0,0
15	-4,0	0,0	-0,4
15	-4,0	0,0	0,0
17	-3,9	-25,6	0,0
17	-3,9	-25,6	0,0
17	-3,9	-25,6	0,0

18	-2,8	-28,4	-0,2
18	-2,8	-28,4	0,0
19	0,6	-27,6	0,0
19	0,6	-27,6	0,0
19	0,6	-27,6	0,0
20	-1,2	-26,4	0,2
20	-1,2	-26,4	0,0

2.1.2. Residualkrefter

Nr.	Rx [kN]	Rz [kN]	My [kN·m]
1	0,00	0,00	0,00
2	0,00	0,00	0,00
3	0,00	0,00	0,00
4	0,00	0,00	0,00
7	0,00	232,31	0,00
7	2062,25	-116,16	0,00
7	-2062,25	-116,16	0,00
10	0,00	0,00	0,00
12	0,00	231,39	0,00
12	0,00	-231,39	0,00
13	0,00	0,00	0,00
14	0,00	0,00	0,00
11	0,00	0,00	0,00
14	2062,25	140,14	0,00
14	-2062,25	709,73	0,00
15	-2062,25	191,47	0,00
15	2062,25	709,73	0,00
17	0,00	584,85	0,00
17	2062,25	-704,38	0,00
17	-2062,25	119,53	0,00
18	0,00	584,02	0,00
18	0,00	-584,02	0,00
19	0,00	584,85	0,00
19	2062,25	119,53	0,00
19	-2062,25	-704,38	0,00
20	0,00	584,02	0,00
20	0,00	-584,02	0,00

2.2. OPLEGGSKREFTER

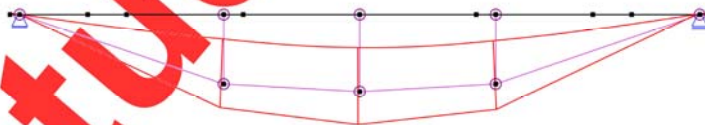
Seg Nr.	X [mm]	Z [mm]	Rx [kN]	Rz [kN]	My [kN·m]
19	250	0	0,00	849,87	0,00
20	17750	0	0,00	901,20	0,00
Sum			0,00	1751,07	

2.3. SEGMENTRESULTATER

Seg Nr.	Snitt mm	My [kN·m]	N [kN]	Vz [kN]	u [mm]	w [mm]
2	1000	-365,57	-2062,25	-112,28	-0,6	-15,1
4	2200	-1359,84	-2062,25	-45,18	-1,8	-35,0
5	900	-1462,18	-2062,25	-72,00	-2,2	-35,6
6	0	-904,90	-2062,25	430,95	-2,7	-30,4
7	0	-506,78	-2062,25	163,34	-3,3	-16,6
11	0	0,00	-231,85	0,00	-1,7	-35,3
19	250	0,13	0,00	0,84	0,0	0,0
20	1750	-238,54	-2062,25	-133,61	-0,4	-9,8
20	0	-328,42	-2062,25	184,93	-3,6	-10,8
21	0	0,08	0,00	-0,70	-4,0	0,0
25	0	0,00	-584,44	0,00	0,6	-27,6
24	0	0,00	-584,44	0,00	-3,9	-25,6
3	3000	-658,56	-2062,25	-445,31	-1,3	-28,6
15	0	0,00	2065,61	0,00	-3,9	-25,6
16	0	0,00	2065,61	0,00	-1,7	-35,3
17	0	0,00	2180,09	0,00	0,6	-27,6
14	0	0,00	2180,09	0,00	0,0	0,0

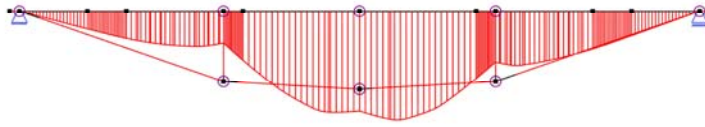
2.4. RESULTATER GRAFISK

2.4.1. Forskyvning



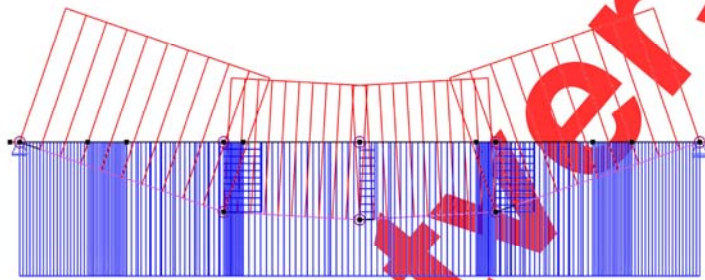
Største forskyvning: 35,9 mm

2.4.2. Moment



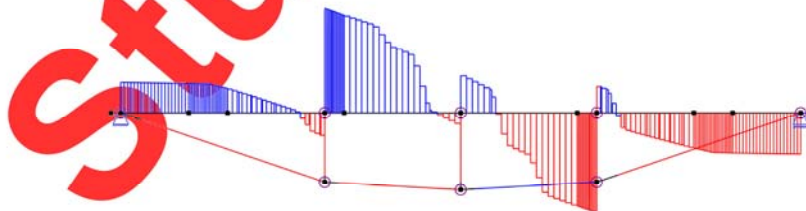
Største moment: 1462,18 kN·m

2.4.3. Aksialkraft



Største aksialkraft: 2180,09 kN

2.4.4. Skjærkraft



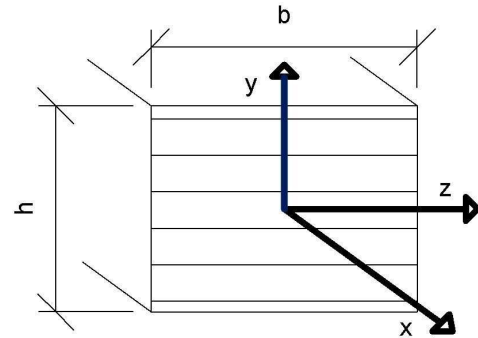
Største skjærkraft: 475,17 kN

APPENDIX K.1

DESIGN CHECK: Bridge 2, DIAGONAL TRUSSES

According to NS-EN 1995-1-1

Load combination: Gravity only



$$b := 400 \text{ mm}$$

Cross-section, width

$$h := 400 \text{ mm}$$

Cross-section, height

$$l_k := 7 \text{ m}$$

Buckling length,
conservative

Material properties, GL32h

$$E_{0.05} := 11800 \text{ MPa}$$

Fifth percentile value of modulus of elasticity

$$f_{m,k} := 32 \text{ MPa}$$

Characteristic bending strength

$$f_{c,0,k} := 32 \text{ MPa}$$

Characteristic compression strength along grain

$$f_{t,90,k} := 0.5 \text{ MPa}$$

Characteristic tensile strength perpendicular to the grain

$$f_{v,k} := 3.5 \text{ MPa}$$

Characteristic shear strength

$$\rho_k := 440 \frac{\text{kg}}{\text{m}^3}$$

Material density

$$\gamma_m := 1.15$$

Partial Factor for material properties

$$k_{mod} := 0.6$$

Modification factor for duration of load and moisture content

$$k_m := 0.7$$

Factor considering re-distribution of bending stresses
in a cross-section

$$k_{cr} := 0.67$$

Factor for determining effective width

$$k_{shape} := \min\left(1.0 + 0.05 \cdot \frac{h}{b}, 1.3\right)$$

Factor depending on the shape of the cross-section

$$\beta_c := 0.1$$

Straightness factor

INPUT FROM ABAQUS

DATA := READEXCEL (“.\ULS_LM1 Gravity Transverse diagonal truss.xlsx”, “Ark1!A20:I2383”)

All forces from Abaqus are printed to excel sheets, that can be found in the digital appendix

$$Element := DATA^{(8)}$$

$$i := 0 .. \text{length}(Element) - 1$$

$$N_{Ed} := DATA^{(2)} N$$
$$\min(N_{Ed}) = -593.69 \text{ kN}$$
$$\max(N_{Ed}) = -1.702 \text{ kN}$$

$$V_{y.Ed} := DATA^{(3)} N$$
$$\min(V_{y.Ed}) = -5.354 \text{ kN}$$
$$\max(V_{y.Ed}) = 6.833 \text{ kN}$$

$$V_{z.Ed} := DATA^{(4)} N$$
$$\min(V_{z.Ed}) = -1.512 \text{ kN}$$
$$\max(V_{z.Ed}) = 1.512 \text{ kN}$$

$$M_{z.Ed} := DATA^{(5)} N \cdot mm$$
$$\min(M_{z.Ed}) = -11.408 \text{ kN} \cdot m$$
$$\max(M_{z.Ed}) = 14.198 \text{ kN} \cdot m$$

$$M_{y.Ed} := DATA^{(6)} N \cdot mm$$
$$\min(M_{y.Ed}) = -5.714 \text{ kN} \cdot m$$
$$\max(M_{y.Ed}) = 5.717 \text{ kN} \cdot m$$

$$M_{x.Ed} := DATA^{(7)} N \cdot mm$$
$$\min(M_{x.Ed}) = -0.799 \text{ kN} \cdot m$$
$$\max(M_{x.Ed}) = 0.799 \text{ kN} \cdot m$$

Cross-section parameters

$$A := b \cdot h = (1.6 \cdot 10^5) \text{ mm}^2$$

Arch cross-sectional area

$$I_z := \frac{b \cdot h^3}{12} = (2.133 \cdot 10^9) \text{ mm}^4$$

Second moment of area. Z-axis

$$I_y := \frac{h \cdot b^3}{12} = (2.133 \cdot 10^9) \text{ mm}^4$$

Second moment of area. Y-axis

$$W_z := \frac{b \cdot h^2}{6} = (1.067 \cdot 10^7) \text{ mm}^3$$

Moment of resistance. Z-axis

$$W_y := \frac{h \cdot b^2}{6} = (1.067 \cdot 10^7) \text{ mm}^3$$

Moment of resistance. Y-axis

$$W_p := \frac{b \cdot h^2}{3 \cdot \left(1 + 0.6 \cdot \frac{h}{b}\right)} = (1.333 \cdot 10^7) \text{ mm}^3$$

Moment of resistance. polar

$$f_{c.0.d} := \frac{f_{c.0.k} \cdot k_{mod}}{\gamma_m} = 16.696 \frac{N}{\text{mm}^2}$$

Design compressive strength along the grain

$$f_{m.z.d} := k_{mod} \cdot \frac{f_{m.k}}{\gamma_m} = 16.696 \frac{N}{\text{mm}^2}$$

Design bending strength about the principal y-axis

$$f_{m.y.d} := k_{mod} \cdot \frac{f_{m.k}}{\gamma_m} = 16.696 \frac{N}{\text{mm}^2}$$

Design bending strength about the principal z-axis

$$f_{v.d} := k_{mod} \cdot \frac{f_{v.k}}{\gamma_m} = 1.826 \text{ MPa}$$

Design Shear strength

$$f_{t.90.d} := k_{mod} \cdot \frac{f_{t.90.k}}{\gamma_m} = 0.261 \text{ MPa}$$

Design tensile strength perpendicular to the grain

$$\sigma_{c.0.d_i} := \frac{N_{Ed_i}}{A}$$

Design compressive stress along the grain

$$\sigma_{m.z.d_i} := \frac{M_{z.Ed_i}}{W_z}$$

Design bending stress about the z-axis

$$\sigma_{m.y.d_i} := \frac{M_{y.Ed_i}}{W_y}$$

Design bending stress about the y-axis

$$\tau_{tor.d_i} := \frac{M_{x.Ed_i}}{W_p}$$

Design shear stress from torsion

$$\tau_{y.d_i} := \frac{3 \cdot V_{y.Ed_i}}{2 \cdot k_{cr} \cdot A}$$

Design shear stress along y-axis

$$\tau_{z.d_i} := \frac{3 \cdot V_{z.Ed_i}}{2 \cdot k_{cr} \cdot A}$$

Design shear stress along z-axis

6.2.4 Combined bending and axial compression

$$U_{6.19_i} := \left(\frac{|\sigma_{c.0.d_i}|}{f_{c.0.d}} \right)^2 + \frac{|\sigma_{m.z.d_i}|}{f_{m.z.d}} + k_m \cdot \frac{|\sigma_{m.y.d_i}|}{f_{m.y.d}}$$

NS-EN 1995-1-1 6.2.4 Eq.6.19

$$\max(U_{6.19}) = 0.151$$

$$U_{6.20_i} := \left(\frac{|\sigma_{c.0.d_i}|}{f_{c.0.d}} \right)^2 + k_m \cdot \frac{|\sigma_{m.z.d_i}|}{f_{m.z.d}} + \frac{|\sigma_{m.y.d_i}|}{f_{m.y.d}}$$

NS-EN 1995-1-1 6.2.4 Eq.6.20

$$\max(U_{6.20}) = 0.136$$

6.3.2 Columns subjected to combined compression and bending

$$i_z = \sqrt{\frac{I_z}{A}}$$

Radius of gyration, z-axis

$$i_y = \sqrt{\frac{I_y}{A}}$$

Radius of gyration, y-axis

$$\lambda_z := \frac{l_k}{\sqrt{\frac{b \cdot h^3}{12 \cdot A}}} = 60.622$$

Slenderness about z-axis

$$\lambda_y := \frac{l_k}{\sqrt{\frac{h \cdot b^3}{12 \cdot A}}} = 60.622$$

Slenderness about y-axis

$$\lambda_{rel.z} := \frac{\lambda_z}{\pi} \cdot \sqrt{\frac{f_{c.0.k}}{E_{0.05}}} = 1.005$$

NS-EN 1995-1-1 6.3.2(1) Eq.6.21, Relative slenderness

$$\lambda_{rel.y} := \frac{\lambda_y}{\pi} \cdot \sqrt{\frac{f_{c.0.k}}{E_{0.05}}} = 1.005$$

NS-EN 1995-1-1 6.3.2(1) Eq.6.21, Relative slenderness

$$k_z := 0.5 \left(1 + \beta_c \cdot (\lambda_{rel.z} - 0.3) + (\lambda_{rel.z})^2 \right)$$

NS-EN 1995-1-1 6.3.2(3) Eq.6.27

$$k_y := 0.5 \left(1 + \beta_c \cdot (\lambda_{rel.y} - 0.3) + (\lambda_{rel.y})^2 \right)$$

NS-EN 1995-1-1 6.3.2(3) Eq.6.28

$$k_{c.z} := \frac{1}{k_z + \sqrt{k_z^2 - \lambda_{rel.z}^2}} = 0.764$$

NS-EN 1995-1-1 6.3.2(3) Eq.6.25

$$k_{c.y} := \frac{1}{k_y + \sqrt{k_y^2 - \lambda_{rel.y}^2}} = 0.764$$

NS-EN 1995-1-1 6.3.2(3) Eq.6.26

$$U_{6.23_i} := \frac{|\sigma_{c.0.d_i}|}{k_{c.z} \cdot f_{c.0.d}} + \frac{|\sigma_{m.z.d_i}|}{f_{m.z.d}} + k_m \cdot \frac{|\sigma_{m.y.d_i}|}{f_{m.y.d}}$$

$$\max(U_{6.23}) = 0.392$$

NS-EN 1995-1-1 6.3.2(3) Eq.6.23

$$U_{6.24_i} := \frac{|\sigma_{c.0.d_i}|}{k_{c.y} \cdot f_{c.0.d}} + k_m \cdot \frac{|\sigma_{m.z.d_i}|}{f_{m.z.d}} + \frac{|\sigma_{m.y.d_i}|}{f_{m.y.d}}$$

$$\max(U_{6.24}) = 0.378$$

NS-EN 1995-1-1 6.3.2(3) Eq.6.24

Combined action from shear and torsion

$$U_{V_T} := \frac{\sqrt{\left(|\tau_{z.d_i}\right|^2 + \left(|\tau_{y.d_i}\right|^2\right)}}{f_{v.d}} + \frac{\left|\tau_{tor.d_i}\right|}{k_{shape} \cdot f_{v.d}}$$

$$\max(U_{V_T}) = 0.067$$

SUMMARY

Utilization factors:

$$\max(U_{6.19}) = 0.151$$

Combined bending and axial compression

$$\max(U_{6.20}) = 0.136$$

Combined bending and axial compression

$$\max(U_{6.23}) = 0.392$$

Buckling in-plane

$$\max(U_{6.24}) = 0.378$$

Buckling out-of-plan

$$\max(U_{V_T}) = 0.067$$

Combined shear and torsion

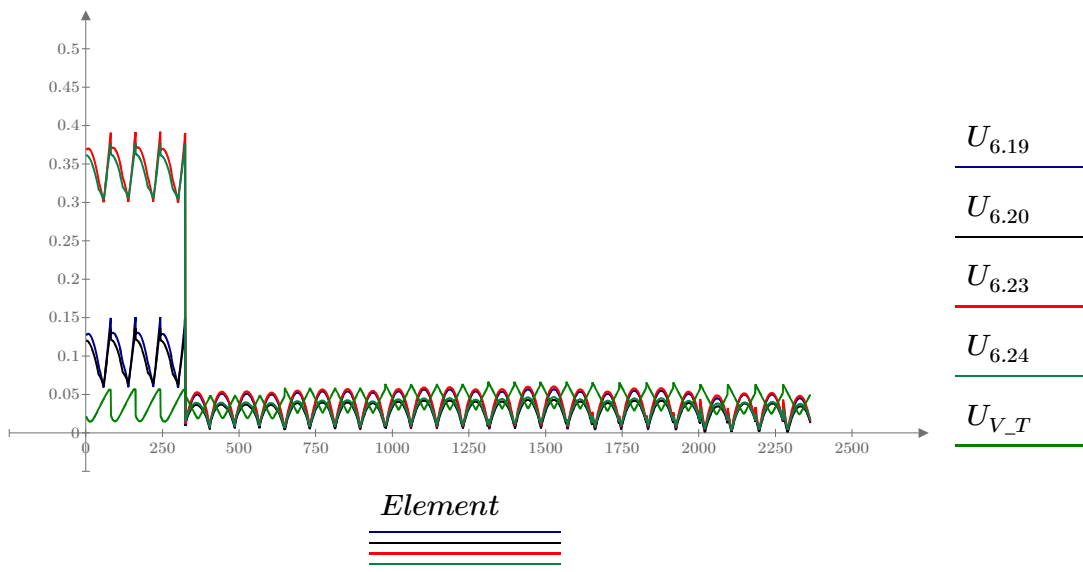
if $\max(U_{6.19}, U_{6.20}, U_{6.23}, U_{6.24}, U_{V_T}) \leq 1$ = "OK!"

|| "OK!"

else

|| "FAILURE"

Utilization plot:



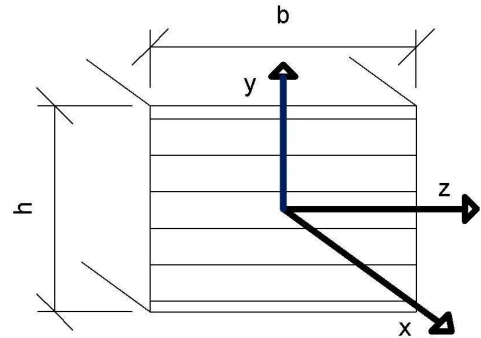
All diagonals trusses are plottet in the graph. The center trusses are furthest to the left, with highest utilization

APPENDIX K.2

DESIGN CHECK: Bridge 2, TRANSVERSE TRUSSES

According to NS-EN 1995-1-1

Load combination: Gravity only



$$b := 300 \text{ mm}$$

Cross-section, width

$$h := 450 \text{ mm}$$

Cross-section, height

$$l_k := 13 \text{ m}$$

Buckling length, conservative

Material properties, GL32h

$$E_{0.05} := 11800 \text{ MPa}$$

Fifth percentile value of modulus of elasticity

$$f_{m,k} := 32 \text{ MPa}$$

Characteristic bending strength

$$f_{c,0,k} := 32 \text{ MPa}$$

Characteristic compression strength along grain

$$f_{t,90,k} := 0.5 \text{ MPa}$$

Characteristic tensile strength perpendicular to the grain

$$f_{t,0,k} := 25.6 \text{ MPa}$$

Characteristic tensile strength parallel to the grain

$$f_{v,k} := 3.5 \text{ MPa}$$

Characteristic shear strength

$$\rho_k := 440 \frac{\text{kg}}{\text{m}^3}$$

Material density

$$\gamma_m := 1.15$$

Partial Factor for material properties

$$k_{mod} := 0.6$$

Modification factor for duration of load and moisture content

$$k_m := 0.7$$

Factor considering re-distribution of bending stresses in a cross-section

$$k_{cr} := 0.67$$

Factor for determining effective width

$$k_{shape} := \min\left(1.0 + 0.05 \cdot \frac{h}{b}, 1.3\right)$$

Factor depending on the shape of the cross-section

$$\beta_c := 0.1$$

Straightness factor

INPUT FROM ABAQUS

DATA := READEXCEL (“.\ULS_LM1 Gravity Transverse truss.xlsx”, “Ark1!A20:I1787”)

All forces from Abaqus are printed to excel sheets, that can be found in the digital appendix

$$Element := DATA^{(8)}$$

$$i := 0 \dots \text{length}(Element) - 1$$

$$N_{Ed} := DATA^{(2)} N$$
$$\min(N_{Ed}) = -12.189 \text{ kN}$$
$$\max(N_{Ed}) = 350.147 \text{ kN}$$

$$V_{y.Ed} := DATA^{(3)} N$$
$$\min(V_{y.Ed}) = -14.53 \text{ kN}$$
$$\max(V_{y.Ed}) = 14.396 \text{ kN}$$

$$V_{z.Ed} := DATA^{(4)} N$$
$$\min(V_{z.Ed}) = -4.405 \text{ kN}$$
$$\max(V_{z.Ed}) = 4.407 \text{ kN}$$

$$M_{z.Ed} := DATA^{(5)} N \cdot mm$$
$$\min(M_{z.Ed}) = -30.309 \text{ kN} \cdot m$$
$$\max(M_{z.Ed}) = 38.281 \text{ kN} \cdot m$$

$$M_{y.Ed} := DATA^{(6)} N \cdot mm$$
$$\min(M_{y.Ed}) = -16.79 \text{ kN} \cdot m$$
$$\max(M_{y.Ed}) = 16.793 \text{ kN} \cdot m$$

$$M_{x.Ed} := DATA^{(7)} N \cdot mm$$
$$\min(M_{x.Ed}) = -0.499 \text{ kN} \cdot m$$
$$\max(M_{x.Ed}) = 0.499 \text{ kN} \cdot m$$

Cross-section parameters

$$A := b \cdot h = (1.35 \cdot 10^5) \text{ mm}^2$$

Arch cross-sectional area

$$I_z := \frac{b \cdot h^3}{12} = (2.278 \cdot 10^9) \text{ mm}^4$$

Second moment of area. Z-axis

$$I_y := \frac{h \cdot b^3}{12} = (1.013 \cdot 10^9) \text{ mm}^4$$

Second moment of area. Y-axis

$$W_z := \frac{b \cdot h^2}{6} = (1.013 \cdot 10^7) \text{ mm}^3$$

Moment of resistance.. Z-axis

$$W_y := \frac{h \cdot b^2}{6} = (6.75 \cdot 10^6) \text{ mm}^3$$

Moment of resistance.. Y-axis

$$W_p := \frac{b \cdot h^2}{3 \cdot \left(1 + 0.6 \cdot \frac{h}{b}\right)} = (1.066 \cdot 10^7) \text{ mm}^3$$

Moment of resistance. polar

$$f_{c.0.d} := \frac{f_{c.0.k} \cdot k_{mod}}{\gamma_m} = 16.696 \frac{N}{mm^2}$$

Design compressive strength along the grain

$$f_{m.z.d} := k_{mod} \cdot \frac{f_{m.k}}{\gamma_m} = 16.696 \frac{N}{mm^2}$$

Design bending strength about the principal y-axis

$$f_{m.y.d} := k_{mod} \cdot \frac{f_{m.k}}{\gamma_m} = 16.696 \frac{N}{mm^2}$$

Design bending strength about the principal z-axis

$$f_{v.d} := k_{mod} \cdot \frac{f_{v.k}}{\gamma_m} = 1.826 \text{ MPa}$$

Design Shear strength

$$f_{t.90.d} := k_{mod} \cdot \frac{f_{t.90.k}}{\gamma_m} = 0.261 \text{ MPa}$$

Design tensile strength perpendicular to the grain

$$f_{t.0.d} := k_{mod} \cdot \frac{f_{t.0.k}}{\gamma_m} = 13.357 \text{ MPa}$$

Design tensile strength parallel to the grain

$$\sigma_{c.0.d_i} := \frac{\begin{array}{l} \text{if } N_{Ed_i} < 0 \\ \quad || N_{Ed_i} \\ \text{else} \\ \quad || 0 \end{array} N}{A}$$

Design compressive stress along the grain

$$\sigma_{t.0.d_i} := \frac{\begin{array}{l} \text{if } N_{Ed_i} > 0 \\ \quad || N_{Ed_i} \\ \text{else} \\ \quad || 0 \end{array} N}{A}$$

Design tensile stress along the grain

$$\sigma_{m.z.d_i} := \frac{M_{z.Ed_i}}{W_z}$$

Design bending stress about the z-axis

$$\sigma_{m.y.d_i} := \frac{M_{y.Ed_i}}{W_y}$$

Design bending stress about the y-axis

$$\tau_{tor.d_i} := \frac{M_{x.Ed_i}}{W_p}$$

Design shear stress from torsion

$$\tau_{y.d_i} := \frac{3 \cdot V_{y.Ed_i}}{2 \cdot k_{cr} \cdot A}$$

Design shear stress along y-axis

$$\tau_{z.d_i} := \frac{3 \cdot V_{z.Ed_i}}{2 \cdot k_{cr} \cdot A}$$

Design shear stress along z-axis

6.2.3 Combined tension and bending

$$U_{6.17_i} := \frac{\sigma_{t.0.d_i}}{f_{t.0.d}} + \frac{|\sigma_{m.z.d_i}|}{f_{m.z.d}} + k_m \cdot \frac{|\sigma_{m.y.d_i}|}{f_{m.y.d}} \quad \text{NS-EN 1995-1-1 6.3.2(3) Eq.6.17}$$

$$\max \langle U_{6.17} \rangle = 0.393$$

$$U_{6.18_i} := \frac{\sigma_{t.0.d_i}}{f_{t.0.d}} + k_m \cdot \frac{|\sigma_{m.z.d_i}|}{f_{m.z.d}} + \frac{|\sigma_{m.y.d_i}|}{f_{m.y.d}} \quad \text{NS-EN 1995-1-1 6.3.2(3) Eq.6.18}$$

$$\max \langle U_{6.18} \rangle = 0.388$$

6.2.4 Combined bending and axial compression

$$U_{6.19_i} := \left(\frac{|\sigma_{c.0.d_i}|}{f_{c.0.d}} \right)^2 + \frac{|\sigma_{m.z.d_i}|}{f_{m.z.d}} + k_m \cdot \frac{|\sigma_{m.y.d_i}|}{f_{m.y.d}} \quad \text{NS-EN 1995-1-1 6.2.4 Eq.6.19}$$

$$\max \langle U_{6.19} \rangle = 0.283$$

$$U_{6.20_i} := \left(\frac{|\sigma_{c.0.d_i}|}{f_{c.0.d}} \right)^2 + k_m \cdot \frac{|\sigma_{m.z.d_i}|}{f_{m.z.d}} + \frac{|\sigma_{m.y.d_i}|}{f_{m.y.d}} \quad \text{NS-EN 1995-1-1 6.2.4 Eq.6.20}$$

$$\max \langle U_{6.20} \rangle = 0.273$$

6.3.2 Columns subjected to combined compression and bending

$$i_z = \sqrt{\frac{I_z}{A}} \quad \text{Radius of gyration, z-axis}$$

$$i_y = \sqrt{\frac{I_y}{A}} \quad \text{Radius of gyration, y-axis}$$

$$\lambda_z := \frac{l_k}{\sqrt{\frac{b \cdot h^3}{12 \cdot A}}} = 100.074 \quad \text{Slenderness about z-axis}$$

$$\lambda_y := \frac{l_k}{\sqrt{\frac{h \cdot b^3}{12 \cdot A}}} = 150.111 \quad \text{Slenderness about y-axis}$$

$$\lambda_{rel.z} := \frac{\lambda_z}{\pi} \cdot \sqrt{\frac{f_{c.0.k}}{E_{0.05}}} = 1.659$$

NS-EN 1995-1-1 6.3.2(1) Eq.6.21, Relative slenderness

$$\lambda_{rel.y} := \frac{\lambda_y}{\pi} \cdot \sqrt{\frac{f_{c.0.k}}{E_{0.05}}} = 2.488$$

NS-EN 1995-1-1 6.3.2(1) Eq.6.21, Relative slenderness

$$k_z := 0.5 \left(1 + \beta_c \cdot (\lambda_{rel.z} - 0.3) + (\lambda_{rel.z})^2 \right)$$

NS-EN 1995-1-1 6.3.2(3) Eq.6.27

$$k_y := 0.5 \left(1 + \beta_c \cdot (\lambda_{rel.y} - 0.3) + (\lambda_{rel.y})^2 \right)$$

NS-EN 1995-1-1 6.3.2(3) Eq.6.28

$$k_{c.z} := \frac{1}{k_z + \sqrt{k_z^2 - \lambda_{rel.z}^2}} = 0.338$$

NS-EN 1995-1-1 6.3.2(3) Eq.6.25

$$k_{c.y} := \frac{1}{k_y + \sqrt{k_y^2 - \lambda_{rel.y}^2}} = 0.155$$

NS-EN 1995-1-1 6.3.2(3) Eq.6.26

$$U_{6.23_i} := \frac{|\sigma_{c.0.d_i}|}{k_{c.z} \cdot f_{c.0.d}} + \frac{|\sigma_{m.z.d_i}|}{f_{m.z.d}} + k_m \cdot \frac{|\sigma_{m.y.d_i}|}{f_{m.y.d}}$$

$$\max(U_{6.23}) = 0.289$$

NS-EN 1995-1-1 6.3.2(3) Eq.6.23

$$U_{6.24_i} := \frac{|\sigma_{c.0.d_i}|}{k_{c.y} \cdot f_{c.0.d}} + k_m \cdot \frac{|\sigma_{m.z.d_i}|}{f_{m.z.d}} + \frac{|\sigma_{m.y.d_i}|}{f_{m.y.d}}$$

$$\max(U_{6.24}) = 0.286$$

NS-EN 1995-1-1 6.3.2(3) Eq.6.24

Combined action from shear and torsion

$$U_{V_T_i} := \frac{\sqrt{\left(|\tau_{z.d_i}\right|^2 + \left(|\tau_{y.d_i}\right|^2\right)}}{f_{v.d}} + \frac{|\tau_{tor.d_i}|}{k_{shape} \cdot f_{v.d}}$$

$$\max(U_{V_T}) = 0.132$$

SUMMARY

Utilization factors:

$$\max \langle U_{6.17} \rangle = 0.393$$

Combined bending and axial tension

$$\max \langle U_{6.18} \rangle = 0.388$$

Combined bending and axial tension

$$\max \langle U_{6.19} \rangle = 0.283$$

Combined bending and axial compression

$$\max \langle U_{6.20} \rangle = 0.273$$

Combined bending and axial compression

$$\max \langle U_{6.23} \rangle = 0.289$$

Buckling in-plane

$$\max \langle U_{6.24} \rangle = 0.286$$

Buckling out-of-plan

$$\max \langle U_{V_T} \rangle = 0.132$$

Combined shear and torsion

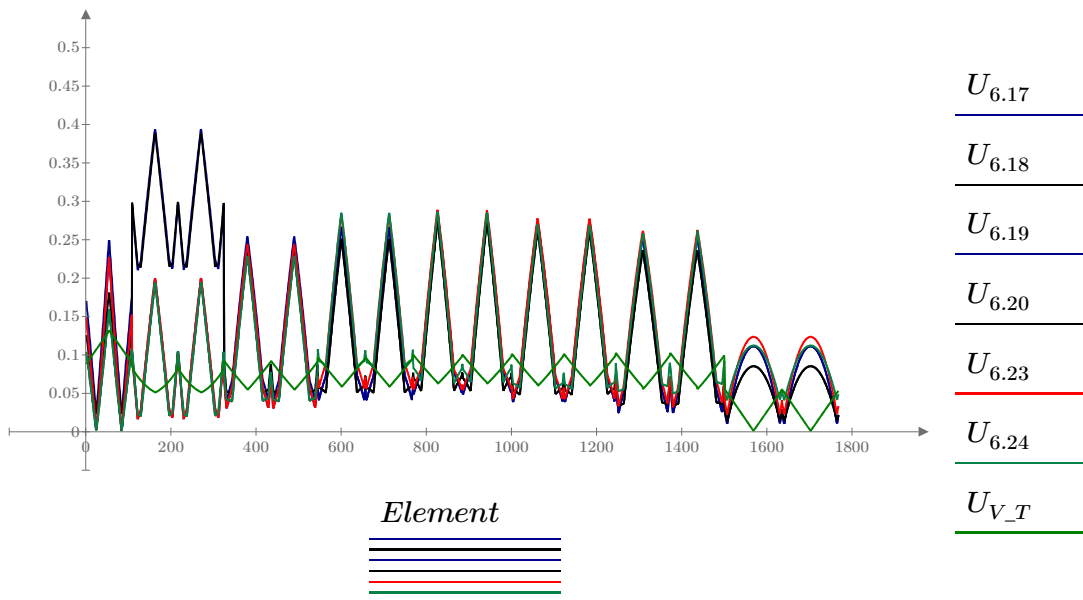
if $\max \langle U_{6.17}, U_{6.18}, U_{6.19}, U_{6.20}, U_{6.23}, U_{6.24}, U_{V_T} \rangle \leq 1$ = "OK!"

|| "OK!"

else

|| "FAILURE"

Utilization plot:



All beams are included in the plot. The number of elements per truss varies from 108 to 134. The trusses closest to the center of the bridge are furthest the left.

APPENDIX L

DESIGN CHECK: Bridge 2, TIE_2

Load combination: LM1 gr1a Eq 1b

Material parameters

$$f_y := 355 \text{ MPa}$$

Yield strenght

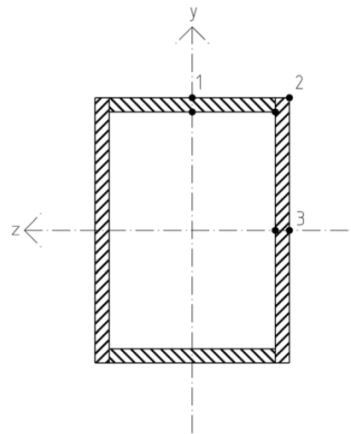
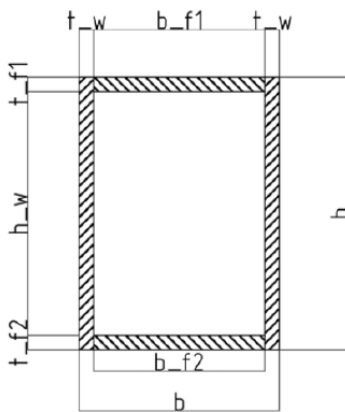
$$\gamma_{M0} := 1.1$$

Partial factor
[NS-EN 1993-2:2006/NA:2009 NA. 6.1(1)P]

$$N_{hanger} := 560 \text{ kN}$$

maximum tension force in hanger

Dimensions, cross-section



$$h := 750 \text{ mm}$$

Hight, cross section

$$b := 550 \text{ mm}$$

Width, cross section

$$h_w := h = 750 \text{ mm}$$

Hight, web

$$t_w := 40 \text{ mm}$$

Thickness, web

$$b_{f2} := b - 2 t_w = 470 \text{ mm}$$

Width, bottom flange

$$t_{f2} := 40 \text{ mm}$$

Thickness, bottom flange

$$b_{f1} := b - 2 t_w = 470 \text{ mm}$$

Width, top flange

$$t_{f1} := 40 \text{ mm}$$

Thickness, top flange

INPUT FROM ABAQUS

$DATA := \text{READEXCEL}(\text{".\ULS_LM1_gr1a_Eq_b Tie.xlsx"}, \text{"Tie2!A20:H1127"})$

All forces from Abaqus are printed to excel sheets, that can be found in the digital appendix

$$Element := DATA^{(0)}$$

$$i := 0 \dots \text{length}(Element) - 1$$

Number of nodes, node index

$$N_{Ed} := DATA^{(2)} N$$

$$\begin{aligned} \min(N_{Ed}) &= (8.326 \cdot 10^3) \text{ kN} \\ \max(N_{Ed}) &= (1.026 \cdot 10^4) \text{ kN} \end{aligned}$$

$$V_{y.Ed} := DATA^{(3)} N$$

$$\begin{aligned} \min(V_{y.Ed}) &= -647.582 \text{ kN} \\ \max(V_{y.Ed}) &= 648.344 \text{ kN} \end{aligned}$$

$$V_{z.Ed} := DATA^{(4)} N$$

$$\begin{aligned} \min(V_{z.Ed}) &= -227.142 \text{ kN} \\ \max(V_{z.Ed}) &= 201.651 \text{ kN} \end{aligned}$$

$$M_{z.Ed} := DATA^{(5)} N \cdot mm$$

$$\begin{aligned} \min(M_{z.Ed}) &= -1.126 \cdot 10^3 \text{ kN} \cdot m \\ \max(M_{z.Ed}) &= (1.365 \cdot 10^3) \text{ kN} \cdot m \end{aligned}$$

$$M_{y.Ed} := DATA^{(6)} N \cdot mm$$

$$\begin{aligned} \min(M_{y.Ed}) &= -572.49 \text{ kN} \cdot m \\ \max(M_{y.Ed}) &= 620.642 \text{ kN} \cdot m \end{aligned}$$

$$M_{x.Ed} := DATA^{(7)} N \cdot mm$$

$$\begin{aligned} \min(M_{x.Ed}) &= -223.208 \text{ kN} \cdot m \\ \max(M_{x.Ed}) &= 223.368 \text{ kN} \cdot m \end{aligned}$$

Cross section parameters

$$A_{f1} := b_{f1} \cdot t_{f1} = (1.88 \cdot 10^4) \text{ mm}^2 \quad \text{Area, top flange}$$

$$A_w := h_w \cdot t_w = (3 \cdot 10^4) \text{ mm}^2 \quad \text{Area, web}$$

$$A_{f2} := b_{f2} \cdot t_{f2} = (1.88 \cdot 10^4) \text{ mm}^2 \quad \text{Area, bottom flange}$$

$$A_{tot} := A_{f1} + 2 \cdot A_w + A_{f2} = (9.76 \cdot 10^4) \text{ mm}^2 \quad \text{Area, cross section}$$

$$a_{y.f1} := \frac{t_{f1}}{2} = 20 \text{ mm} \quad \text{Distance, top cross section - center top flange}$$

$$a_{y.w} := \frac{h_w}{2} = 375 \text{ mm} \quad \text{Distance, top cross section - center web}$$

$$a_{y.f2} := h - \frac{t_{f2}}{2} = 730 \text{ mm} \quad \text{Distance, top cross section - center bottom flange}$$

$$a_{z.f1} := \frac{b_{f1}}{2} + t_w = 275 \text{ mm} \quad \text{Distance, outer web - center top flange}$$

$$a_{z.w1} := \frac{t_w}{2} = 20 \text{ mm} \quad \text{Distance, outer web - center web 1}$$

$$a_{z.w2} := b - \frac{t_w}{2} = 530 \text{ mm} \quad \text{Distance, outer web - center web 2}$$

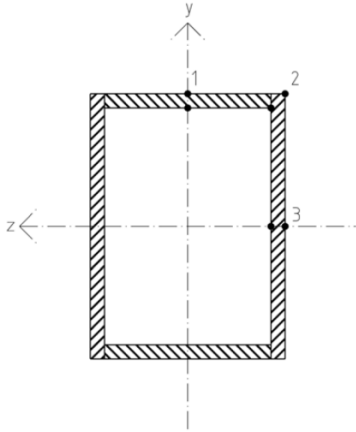
$$a_{z.f2} := t_w + \frac{b_{f2}}{2} = 275 \text{ mm} \quad \text{Distance, outer web - center bottom flange}$$

Center of mass:

$$y_{CM} := \frac{A_{f1} \cdot a_{y.f1} + 2 \cdot A_w \cdot a_{y.w} + A_{f2} \cdot a_{y.f2}}{A_{tot}} = 375 \text{ mm}$$

$$z_{CM} := \frac{A_{f1} \cdot a_{z.f1} + A_w \cdot a_{z.w1} + A_w \cdot a_{z.w2} + A_{f2} \cdot a_{z.f2}}{A_{tot}} = 275 \text{ mm}$$

**First moment of inertia,
in section 1, 2 and 3**



The figure show the three sections controlled for maximum stress

$$S_{y,1} := A_w \cdot \left(z_{CM} - \frac{t_w}{2} \right) + \frac{A_{f1}}{2} \cdot \left(z_{CM} - t_w - \frac{b_{f1}}{4} \right) + \frac{A_{f2}}{2} \cdot \left(z_{CM} - t_w - \frac{b_{f2}}{4} \right)$$

$$S_{y,1} = (9.859 \cdot 10^6) \text{ mm}^3$$

$$S_{y,2} := A_w \cdot \left(z_{CM} - \frac{t_w}{2} \right)$$

$$S_{y,2} = (7.65 \cdot 10^6) \text{ mm}^3$$

$$S_{y,3} := S_{y,2}$$

$$S_{z,1} := b \cdot t_{f1} \cdot \left(y_{CM} - \frac{t_{f1}}{2} \right)$$

$$S_{z,1} = (7.81 \cdot 10^6) \text{ mm}^3$$

$$S_{z,2} := S_{z,1}$$

$$S_{z,3} := A_{f1} \cdot \left(y_{CM} - \frac{t_{f1}}{2} \right) + 2 \cdot \left(\frac{A_w}{2} \cdot \left(y_{CM} - \frac{h_w}{4} \right) \right)$$

$$S_{z,3} = (1.23 \cdot 10^7) \text{ mm}^3$$

Second moment of inertia

$$I_{y.f1} := \frac{b_{f1}^3 \cdot t_{f1}}{12} + A_{f1} \cdot (z_{CM} - a_{z.f1})^2$$

$$I_{y.f1} = (3.461 \cdot 10^{-4}) \text{ m}^4$$

Second moment of area. Y-axis,
top flange

$$I_{y.w1} := \frac{t_w^3 \cdot h_w}{12} + A_w \cdot (z_{CM} - a_{z.w1})^2$$

$$I_{y.w1} = (1.955 \cdot 10^9) \text{ mm}^4$$

Second moment of area. Y-axis,
first web

$$I_{y.w2} := \frac{t_w^3 \cdot h_w}{12} + A_w \cdot (z_{CM} - a_{z.w2})^2$$

$$I_{y.w2} = (1.955 \cdot 10^9) \text{ mm}^4$$

Second moment of area. Y-axis,
second web

$$I_{y.f2} := \frac{b_{f2}^3 \cdot t_{f2}}{12} + A_{f2} \cdot (z_{CM} - a_{z.f2})^2$$

$$I_{y.f2} = (3.461 \cdot 10^8) \text{ mm}^4$$

Second moment of area. Y-axis,
bottom flange

$$I_{y.tot} := I_{y.f1} + I_{y.w1} + I_{y.w2} + I_{y.f2}$$

$$I_{y.tot} = (4.602 \cdot 10^9) \text{ mm}^4$$

Total Second moment of area. Y-axis

$$I_{z.f1} := \frac{b_{f1} \cdot t_{f1}^3}{12} + A_{f1} \cdot (y_{CM} - a_{y.f1})^2$$

$$I_{z.f1} = (2.372 \cdot 10^9) \text{ mm}^4$$

Second moment of area. Y-axis,
top flange

$$I_{z.w} := \frac{t_w \cdot h_w^3}{12} + A_w \cdot (y_{CM} - a_{y.w})^2$$

$$I_{z.w} = (1.406 \cdot 10^9) \text{ mm}^4$$

Second moment of area. Y-axis,
web

$$I_{z.f2} := \frac{b_{f2} \cdot t_{f2}^3}{12} + A_{f2} \cdot (y_{CM} - a_{y.f2})^2$$

$$I_{z.f2} = (2.372 \cdot 10^9) \text{ mm}^4$$

Second moment of area. Y-axis,
bottom flange

$$I_{z.tot} := I_{z.f1} + 2 I_{z.w} + I_{z.f2}$$

$$I_{z.tot} = (7.556 \cdot 10^9) \text{ mm}^4$$

Total Second moment of area. Y-axis

Elastic moment of resistance

$$W_{x.el} := 2 \left(h - \frac{t_{f1}}{2} - \frac{t_{f2}}{2} \right) \cdot (b - t_w) \cdot \min(t_w, t_{f1}, t_{f2})$$

$$W_{x.el} = (2.897 \cdot 10^7) \text{ mm}^3$$

Moment of resistance, x-axis
torsion

$$W_{y.el} := \frac{I_{y.tot}}{z_{CM}}$$

$$W_{y.el} = (1.673 \cdot 10^7) \text{ mm}^3$$

Moment of resistance, y-axis

$$W_{z.el} := \frac{I_{z.tot}}{y_{CM}}$$

$$W_{z.el} = (2.015 \cdot 10^7) \text{ mm}^3$$

Moment of resistance, z-axis

Axial Stress

$$\sigma_{N.Ed_i} := \frac{N_{Ed_i}}{A_{tot}}$$

Design tensile stress

$$\min(\sigma_{N.Ed}) = 85.304 \text{ MPa}$$

$$\max(\sigma_{N.Ed}) = 105.137 \text{ MPa}$$

$$\sigma_{My.Ed_i} := \frac{M_{y.Ed_i}}{W_{y.el}}$$

Design bending stress about the y-axis

$$\min(\sigma_{My.Ed}) = -34.213 \text{ MPa}$$

$$\max(\sigma_{My.Ed}) = 37.09 \text{ MPa}$$

$$\sigma_{Mz.Ed_i} := \frac{M_{z.Ed_i}}{W_{z.el}}$$

Design bending stress about the z-axis

$$\min(\sigma_{Mz.Ed}) = -55.862 \text{ MPa}$$

$$\max(\sigma_{Mz.Ed}) = 67.761 \text{ MPa}$$

$$\sigma_{Ed.1_i} := |\sigma_{N.Ed_i}| + |\sigma_{Mz.Ed_i}|$$

Resulting stress in section 1

$$\sigma_{Ed.2_i} := |\sigma_{N.Ed_i}| + |\sigma_{My.Ed_i}| + |\sigma_{Mz.Ed_i}|$$

Resulting stress in section 2

$$\sigma_{Ed.3_i} := |\sigma_{N.Ed_i}| + |\sigma_{My.Ed_i}|$$

Resulting stress in section 3

$$\min(\sigma_{Ed.1}, \sigma_{Ed.2}, \sigma_{Ed.3}) = 85.359 \text{ MPa}$$

$$\max(\sigma_{Ed.1}, \sigma_{Ed.2}, \sigma_{Ed.3}) = 194.582 \text{ MPa}$$

Shear stress

$$e_{hanger} := \frac{b}{2} = 275 \text{ mm}$$

Eccentricity - hanger connection

$$\tau_{x_i} := \text{if } M_{x.Ed_i} \leq 0 \text{ N} \cdot \text{mm}$$

Design shear stress, x-axis

$$\left\| \begin{array}{l} \frac{M_{x.Ed_i}}{W_{x.el}} - \frac{N_{hanger} \cdot e_{hanger}}{W_{x.el}} \\ \text{else} \\ \frac{M_{x.Ed_i}}{W_{x.el}} + \frac{N_{hanger} \cdot e_{hanger}}{W_{x.el}} \end{array} \right\|$$

$$\min(\tau_x) = -13.022 \text{ MPa}$$

$$\max(\tau_x) = 13.027 \text{ MPa}$$

$$\tau_{y.1_i} := \frac{V_{y.Ed_i} \cdot S_{z.1}}{I_{z.tot} \cdot (2 t_w)}$$

Design shear stress, y-axis
section 1

$$\min(\tau_{y.1}) = -8.367 \text{ MPa}$$

$$\max(\tau_{y.1}) = 8.377 \text{ MPa}$$

$$\tau_{y.2_i} := \frac{V_{y.Ed_i} \cdot S_{z.2}}{I_{z.tot} \cdot (2 t_w)}$$

Design shear stress, y-axis
section 2

$$\min(\tau_{y.2}) = -8.367 \text{ MPa}$$

$$\max(\tau_{y.2}) = 8.377 \text{ MPa}$$

$$\tau_{y.3_i} := \frac{V_{y.Ed_i} \cdot S_{z.3}}{I_{z.tot} \cdot (2 t_w)}$$

Design shear stress, y-axis
section 3

$$\min(\tau_{y.3}) = -13.176 \text{ MPa}$$

$$\max(\tau_{y.3}) = 13.191 \text{ MPa}$$

$$\tau_{z.1_i} := \frac{V_{z.Ed_i} \cdot S_{y.1}}{I_{y.tot} \cdot (t_{f1} + t_{f2})}$$

Design shear stress, z-axis
section 1

$$\min(\tau_{z.1}) = -6.083 \text{ MPa}$$

$$\max(\tau_{z.1}) = 5.4 \text{ MPa}$$

$$\tau_{z.2_i} := \frac{V_{z.Ed_i} \cdot S_{y.2}}{I_{y.tot} \cdot (t_{f1} + t_{f2})}$$

$$\min(\tau_{z.2}) = -4.72 \text{ MPa}$$

$$\max(\tau_{z.2}) = 4.19 \text{ MPa}$$

**Design shear stress, z-axis
section 2**

$$\tau_{z.3_i} := \frac{V_{z.Ed_i} \cdot S_{y.3}}{I_{y.tot} \cdot (t_{f1} + t_{f2})}$$

$$\min(\tau_{z.3}) = -4.72 \text{ MPa}$$

$$\max(\tau_{z.3}) = 4.19 \text{ MPa}$$

**Design shear stress, z-axis
section 3**

Von-mises stresses

$$\sigma_{VM.1_i} := \sqrt{(\sigma_{Ed.1_i})^2 + 3 \left(|\tau_{y.1_i}|^2 + (|\tau_{x_i}| + |\tau_{z.1_i}|)^2 \right)}$$

$$\min(\sigma_{VM.1}) = 86.165 \text{ MPa}$$

$$\max(\sigma_{VM.1}) = 164.125 \text{ MPa}$$

Von-mises stress in section 1

$$\sigma_{VM.2_i} := \sqrt{(\sigma_{Ed.2_i})^2 + 3 \left((|\tau_{y.2_i}| + |\tau_{x_i}|)^2 + |\tau_{z.2_i}|^2 \right)}$$

$$\min(\sigma_{VM.2}) = 89.601 \text{ MPa}$$

$$\max(\sigma_{VM.2}) = 196.934 \text{ MPa}$$

Von-mises stress in section 2

$$\sigma_{VM.3_i} := \sqrt{(\sigma_{Ed.3_i})^2 + 3 \left((|\tau_{y.3_i}| + |\tau_{x_i}|)^2 + |\tau_{z.3_i}|^2 \right)}$$

$$\min(\sigma_{VM.3}) = 88.713 \text{ MPa}$$

$$\max(\sigma_{VM.3}) = 145.754 \text{ MPa}$$

Von-mises stress in section 3

Cross-section class

Class 1 cross-sections are those which can form a plastic hinge with the rotation capacity required from plastic analysis without reduction of the resistance. No danger of local buckling.

Tension is predominant and we use elastic moment of resistance, so it would not be a problem anyway.

$$\frac{\max(h_w - t_{f1} - t_{f2})}{t_w} = 16.75$$

$$\frac{b_{f1}}{t_{f1}} = 11.75$$

$$\varepsilon := \sqrt{\frac{235 \text{ MPa}}{f_y}} = 0.814$$

$$\left(\begin{array}{l} \text{if } \frac{\max(h_w - t_{f1} - t_{f2})}{t_w} \leq 33 \varepsilon \\ \quad \parallel \text{ "Class 1" } \\ \text{else if } 33 \varepsilon < \frac{\max(h_w - t_{f1} - t_{f2})}{t_w} \leq 38 \varepsilon \\ \quad \parallel \text{ "Class 2" } \\ \text{else if } 38 \varepsilon < \frac{\max(h_w - t_{f1} - t_{f2})}{t_w} \leq 42 \varepsilon \\ \quad \parallel \text{ "Class 3" } \\ \text{else} \\ \quad \parallel \text{ "Class 4" } \end{array} \right) = \text{"Class 1"}$$

$$\left(\begin{array}{l} \text{if } \frac{b_{f1}}{t_{f1}} \leq 33 \varepsilon \\ \quad \parallel \text{ "Class 1" } \\ \text{else if } 33 \varepsilon < \frac{b_{f1}}{t_{f1}} \leq 38 \varepsilon \\ \quad \parallel \text{ "Class 2" } \\ \text{else if } 38 \varepsilon < \frac{b_{f1}}{t_{f1}} \leq 42 \varepsilon \\ \quad \parallel \text{ "Class 3" } \\ \text{else} \\ \quad \parallel \text{ "Class 4" } \end{array} \right) = \text{"Class 1"}$$

Elastic capacity, Von-Mises stress

$$U_{VM.1_i} := \frac{\frac{\sigma_{VM.1_i}}{f_y}}{\gamma_{M0}} \quad \text{Utilization section 1}$$

$$U_{VM.2_i} := \frac{\frac{\sigma_{VM.2_i}}{f_y}}{\gamma_{M0}} \quad \text{Utilization section 2}$$

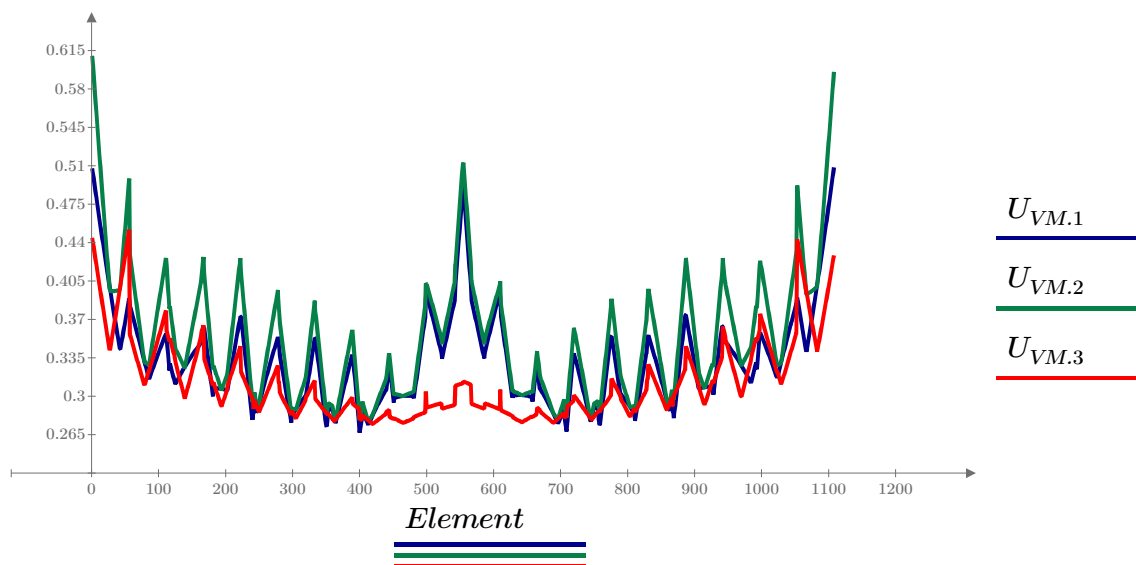
$$U_{VM.3_i} := \frac{\frac{\sigma_{VM.3_i}}{f_y}}{\gamma_{M0}} \quad \text{Utilization section 3}$$

$$\min(U_{VM.1}, U_{VM.2}, U_{VM.3}) = 0.267$$

$$\max(U_{VM.1}, U_{VM.2}, U_{VM.3}) = 0.61$$

$$\left(\begin{array}{l} \text{if } \max(U_{VM.1}, U_{VM.2}, U_{VM.3}) \leq 1.0 \\ \quad \parallel \text{ "OK" } \\ \text{else} \\ \quad \parallel \text{ "NOT OK" } \end{array} \right) = \text{"OK"}$$

PLOT UTILIZATION:



Appendix M_Aspphalt layer design

$$AADT_{2012} := 6000$$

Annual average daily traffic 2012,
NPRA location description.

$$AADT_{2016} := 6000 \cdot 1.02^4 = 6.495 \cdot 10^3$$

Estimated Annual average daily
traffic 2016

$$PercentageHeavy := 12\%$$

Percentage of heavy/commercial vehicle
traffic, NPRA location description

$$AADT_{tung} := AADT_{2016} \cdot PercentageHeavy = 779.351$$

Annual average daily traffic heavy/
commercial vehicle

Traffic group = E

Håndbok N200, Fig 510.2

$$t_{Ac.Roadway} := 60 \text{ mm}$$

Håndbok N200, Fig 512.2, Base courses :
Asphalt concrete (Ac), minimum
thickness

$$t_{AcP.Roadway} := 60 \text{ mm}$$

Håndbok N200, Fig 512.2, Wearing
pavement: Dense graded mix(AcP)
minimum thickness

$$t_{Ac.Pedestrian} := 60 \text{ mm}$$

Håndbok N200, Fig 512.2, Base
courses pedestrian: Asphalt concrete
(Ac) minimum tykkelse

$$t_{AcP.Pedestrian} := 40 \text{ mm}$$

Håndbok N200, Fig 512.2, Wearing
pavement pedestrian: Dense graded
mix(AcP) minimum thickness